MEASUREMENT OF NONLINEARITY IN CHEMICAL PROCESS CONTROL

By

Martin Guay

A thesis submitted to the Department of Chemical Engineering in conformity with the requirements for the degree of Doctor of Philosophy

Queen's University at Kingston
Kingston, Ontario
March 1996

For Bonnie...

Abstract

A framework for the assessment of nonlinearity in controlled processes is developed. Assuming that the process can be represented by a twice differentiable process map, the extent of nonlinearity is measured by evaluating the induced local curvature of the process response. The magnitude of this curvature is assessed with respect to an appropriately chosen scaling region. This approach provides an effective methodology for the development of dimensionless curvature measures that can be used to characterize and quantify the nonlinear behaviour of steady-state and dynamic controlled processes. The impact of steady-state curvature on controller performance is studied using a bioreactor example. A potential application of the measure of dynamic nonlinearity to chemical processes is demonstrated. First and second order sensitivity equations of the output with respect to the inputs are used to evaluate the nonlinearity measures for continuous and batch chemical processes.

Using classical differential geometrical tools, a set of second order identities related to the invertibility of the nonlinear process are developed. Their geometrical interpretation provides a fundamental definition and a new interpretation of the RGA. Application of the identities to the assessment of higher order interaction is shown to be very similar to the analysis of the linear RGA. Higher interaction tables are constructed to measure the contributions of the nonlinear terms to interaction in a closed-loop process.

An analysis of exact linearization of control systems by state-feedback and coordinate transformations is presented. The Gardner and Shadwick (GS) algorithm is used to uncover obstructions to linearizability of classes of models. This provides a systematic way of choosing

appropriate model forms in process model formulation. Extension of this method to dynamic feedback linearization of control-affine processes is also considered. A necessary and sufficient condition for dynamic feedback linearizability of nonlinear control affine systems is developed. The linearizability conditions are based on a filtering of the Pfaffian system associated with a nonlinear system that take account of the presence of a specific precompensator.

ACKNOWLEDGEMENTS

The author would like to thank Professor P.J. McLellan and Professor D.W. Bacon for their help and their excellent supervision. This project has been a great challenge and a wonderful learning experience. Many thanks go out to Professor McLellan for the many fruitful discussions that shaped this thesis. His enthusiasm and constant encouragement have been a true inspiration. The author would also like to thank the faculty, the staff and all the graduate students of the Department of Chemical Engineering for their help. Thanks to Brian, Carl, John, Martin and Steve.

The author gratefully acknowledges the financial support of the "Fonds pour la formation des chercheurs et l'aide à la recherche" of the government of Quebec and of the Natural Sciences and Engineering Council of Canada.

En finissant, l'auteur aimerait remercier sa famille, Raynald, Céline, Nicolas et Isabelle, pour leur support constant. Il remercie du fond du coeur son amie la plus chère, Bonnie, à qui il dédie cette thèse. Merci pour tout...

TABLE OF CONTENTS

List of Figures

Chapter 2

Chapter 3

Chapter 4

List of Tables

Chapter 2

Chapter 4

Chapter 1

Introduction

A wealth of information currently exists describing nonlinear behaviour of processes such as continuous stirred tank reactors (CSTRs), distillation columns, evaporators and biotechnological processes. Nonlinearity in a chemical process may arise from a variety of sources. It may be due to characteristics of the process such as temperature dependence of reaction rates. It may also result from process limitations such as valve limits, leading to input saturation (i.e., flowrate manipulation) or from physical constraints on output variables (e.g., mole fractions of chemical species).

Although nonlinearity of chemical processes is widely recognized in mathematical modelling, design and optimization, chemical process control remains primarily focused on the use of linear controller design techniques. Linear controllers facilitate the development, implementation and operation of control strategies. Even though the gains in controller performance that result from nonlinear control design techniques (e.g. Kravaris and Chung, 1987; Hoo and Kantor, 1986; Bequette, 1990; McLellan *et al.*, 1990) are undisputed, nonlinear controller design procedures may often be avoided in practice. The main impediment is the requirement for mathematical settings that are not easily accessible. Consequently, the loss in performance that results from the use of a linear control strategy is ignored and nonlinear plants are usually controlled with some success using linear control strategies. Many applications have been reported in the chemical engineering literature (see Morari and Zafiriou, 1989) supporting

this approach.

The relative success of linear control strategies for nonlinear processes is surprising. Since the development of a linear controller for a nonlinear process necessarily relies on linearization of that process, its applicability is necessarily of a local nature. This means that reliable performance of the resulting closed-loop system is assumed only within a potentially small operating region. Consequently, serious performance loss, and even instability, may result for processes that deviate beyond that limited range of operation. The reasons for the success of linear controllers in the presence of significant process nonlinearity remain unclear. Although it is possible to design controllers that can provide robust performance in the presence of certain specific classes of nonlinearities, the robustness of linear controllers to *systematic* process nonlinearities is still poorly understood. One reason for this situation is the absence of a methodology to evaluate nonlinearity in controlled processes. Metrics currently used to evaluate process nonlinearity do not reflect the nonlinearity of processes subjected to linear controller strategies.

There are two primary considerations in designing control systems for nonlinear processes. First, the nonlinearity must justify the need for a nonlinear controller. This requires assessment of the nature and magnitude of the nonlinear behaviour. Secondly, the controller must be able to compensate for the effects of nonlinearity. This is normally achieved in practice by using model based approaches that can systematically remove these effects. Predictions of the process response are used to determine appropriate control action. Alternatively, one can apply appropriately chosen coordinate transformations to linearize the process exactly. Using this approach, the linearized process is controlled by application of linear control strategies on the

transformed inputs and outputs. It is also possible to achieve satisfactory controller performance by using collections of linear controllers, each applicable to a specific portion of the operating region. This thesis investigates both of these approaches.

The primary objective of this thesis is to develop a framework for the quantification of process nonlinearity that is applicable to both steady-state and dynamic control of chemical processes. A generic assessment of process nonlinearity is developed that can be used to compare different control strategies for a given process *and* for different processes.

To achieve this result, it is important to identify the types of nonlinearities considered in general terms. Throughout this thesis, processes are represented by differentiable maps of process inputs to outputs. It is assumed that each of these process maps can be expressed as a Taylor series expansion about nominal input values of interest. The nonlinearity of a process is measured as the departure of actual behaviour from its first order Taylor series approximation, and it is estimated by evaluating the contribution of the second order terms of the series relative to the contribution of the first order approximation.

In order to measure the nonlinearity adequately, it is also important to consider the intended range and direction of process operations. This is to ensure that the measure of nonlinearity employed must reflect the anticipated variation in process variables on a meaningful scale. For example, distillation columns typically exhibit moderate nonlinearity. However they can be modeled and controlled using linear models when operated over small ranges. Since the nonlinearity cannot be removed by the controller action, the region of operation and the controller must be chosen such that the effects of the nonlinearity on the closed-loop operation are attenuated.

The proposed methodology is presented in Chapters 2, 3 and 4. In Chapter 2, the framework is developed and applied to the measurement of nonlinearity in steady-state nonlinear processes. Using ideas first introduced by Bates and Watts (1980) in nonlinear regression analysis, the interpretation of the nonlinearity measures is enhanced by providing an orthogonal decomposition that separates the contribution of the nonlinear terms into tangential and normal effects. It is shown that the local effects of nonlinearity can be removed by developing coordinate transformations for the tangential and normal parts.

In Chapter 3, a fundamental approach for assessing nonlinear interaction effects and closed-loop nonlinearity in multivariable processes is presented. This approach is based on a differential geometric interpretation of the relative gain array, which leads naturally to systematic procedures for describing higher order interaction effects and for assessing closed-loop nonlinearity effects in nonlinear processes. Two types of nonlinear effects associated with the behaviour of a process are introduced. Between channel nonlinearity is associated with the nonlinear dependence of an output channel on other input-output pairings. Within channel nonlinearity is used to identify the nonlinear effects that result from the inherent nonlinearity of an individual output channel. The framework developed in Chapter 2 is used to evaluate the significance of local nonlinear effects. Nonlinear interaction measures are derived which provide tools for assessing input-output pairings in a nonlinear process. This approach extends existing standard techniques and provides an estimate of the effect of nonlinearity on closed-loop interactions.

In Chapter 4, the methodology developed in Chapter 2 is extended to the measurement of nonlinearity of dynamic processes using the theory of Fréchet differentiable nonlinear operators

on linear normed spaces. The main result of this extension is a meaningful scale-independent measure of dynamic nonlinearity. The size and orientation of process operations are taken into account to provide an appropriate scaling. This framework is then applied to input-output processes represented by Volterra series expansions. It is shown that the nonlinearity of such systems can be measured using first and second order kernels of the functional expansion. In the more general case, this approach is shown to be equivalent to the solution of a set of ordinary differential equations that provide first and second order derivatives of the process outputs with respect to the inputs. As a demonstration, the methodology is applied to measure the nonlinearity of a chemostat bioreactor and a batch non-isothermal stirred tank reactor.

When a process has been shown to display significant nonlinearity, using methods such as that presented in Chapters 2, 3 and 4, it is important to provide methodologies to remove its effects. Although this can be achieved in a number of ways, most successful methods listed in the literature are based on the use of process models. In this thesis, differential geometrical control techniques are applied to the study of the problem of exact linearization of nonlinear systems by state-feedback and state-space. The analysis is based on an exterior calculus method introduced by Gardner and Shadwick (1992) that can be used to solve the problem of exact linearization by static state-feedback. This method provides a set of necessary and sufficient conditions for exact linearizability and an algorithm, called the GS algorithm, that can be used to calculate linearizing feedback and state-space transformations. More importantly, it gives a framework for studying the general problem of equivalence of nonlinear systems to linear forms. Using this algorithm, Atkins and Shadwick (1993) proved the existence of invariant functions that define, for a class of structurally similar systems, the subclass of linearizable systems. These

functions are curvature-like entities that act as obstructions to linearizability. Because of their invariance under feedback and state-space transformations, these functions can be used as purely geometric outputs that are generic for given classes of system. In this thesis, the GS algorithm is used to compute these invariant structures for a class of nonisothermal continuous stirred tank reactors.

Conditions for linearizability by static state-feedback are often too restrictive and are rarely applied in practice. To widen the scope of application of these methods, considerable work has been done to provide relaxations of these conditions. Exact linearization by dynamic state-feedback, first introduced by Charlet *et al.* (1989, 1991), and the associated concept of flatness of nonlinear systems (Fliess *et al.*, 1994b) have been considered to extend the class of linearizable systems. Necessary conditions and sufficient conditions for dynamic feedback linearizibility have been obtained by various researchers (Charlet *et al.*, 1989, 1991; Shadwick, 1991; Sluis, 1993; Aranda-Bricaire *et al.*, 1995). In this thesis, the geometric framework developed by Gardner and Shadwick (1992) is used to develop a new necessary and sufficient condition for dynamic feedback linearizibility. This exterior calculus setting is shown to provide an effective method to prove dynamic feedback linearizibility and compute the required feedback and coordinate transformations.

CHAPTER 2

Measurement of Nonlinearity In Chemical Process Control Systems:

The Steady State Map

1. Introduction

Most chemical processes are inherently nonlinear in nature. Nevertheless, they are often treated using linear analysis and design techniques in order to simplify the development, implementation and operation of a control strategy. However, the extent of nonlinearity in many chemical processes is such that controller design and analysis methods based on linear process models may no longer be satisfactory. Nonlinearities may arise from chemical process characteristics (e.g., Arrhenius rate expressions), input saturation (e.g., valve limits), and output saturation (physical limits on output variables - e.g., mole fractions). The impact of nonlinearities on controller stability and performance depends on: (i) the degree of nonlinearity of the process, (ii) the intended range and direction of operation and (iii) the choice of controller. For example, distillation columns exhibiting moderate nonlinearity, but operated over a small range, may be adequately modeled and controlled using a linear model, whereas the nonlinear temperature dependence of reaction kinetics may be of great significance in a reactor operated over a wide range of conditions such as in batch operation.

Research in nonlinear process control has been very active in recent years (e.g., Bequette, 1991; Kravaris and Kantor, 1990a; McLellan et al., 1990; Nijmeijer and van der Schaft, 1989; Isidori, 1988) and there is now a wide range of possible control laws using output and state feedback for output tracking, input-state and input-output linearization, and decoupling control.

These nonlinear control laws frequently require substantial additional effort beyond that required by linear methods. From a practitioner's perspective, it is important to be able to assess when a process is sufficiently nonlinear to justify using a nonlinear control law. The development of useful measures of nonlinearity is the focus of this study.

Very few results for assessing the degree of process nonlinearity exist in the chemical engineering literature. Recently, Nikolaou (1993) and Ogunnaike et al. (1993) have proposed operator-based approaches where the process response to a set of input sequences is analyzed. The degree of nonlinearity is viewed either as the departure of actual process performance from an ideal linear approximation (Nikolaou, 1993) or as the change in local gain estimates over the operating region (Ogunnaike et al., 1993). The operator approach offers limited insight into the process structure, and specifically which components (e.g., vapour -liquid equilibria, reaction kinetics) are responsible for the nonlinearity. The local gain estimate approach suffers from sensitivity to the choice of perturbation directions. Both these approaches, and the approach proposed in this study as well, are vulnerable to the effects of process noise.

Koung and MacGregor (1991,1992) studied process nonlinearity by examining the impact on the singular value decomposition (SVD) of local steady-state gain matrices. The SVD is used to obtain a structured description of the uncertainties due to gain mismatch. This mismatch, which is due to the nonlinearity of the process, is measured by the extent of input and output rotation observed in the steady-state gain with respect to the nominal plant. Although this method is useful for the analysis of bivariate processes, its application to multiple inputs- multiple outputs (MIMO) systems of greater dimension is difficult.

In this Chapter, we propose an approach for quantifying process nonlinearity using first

and second derivative information. The approach is based on the methodology developed by Bates and Watts (1980, 1988) in nonlinear least squares regression analysis. The main features of this approach are decomposition of second order information into tangential and normal components and calculation of scale independent measures of nonlinearity. This method quantifies the nonlinearities and identifies their causes. It can also suggest transformations to remove or reduce these effects.

The methods proposed in the following sections deal specifically with the process steady state map, and as such, address the problem of gain nonlinearity in open-loop processes. Extensions to closed-loop and dynamic processes will be described in next two chapters. The current chapter proceeds as follows. A framework for curvature analysis is first proposed, and curvature measures are developed. The problem of scaling is addressed by defining an operating region for the process. The use of curvature arrays for identifying appropriate transformations is described, and the issue of nonlinearity in prediction and control models is discussed. The methodology is illustrated using biochemical and evaporator process examples which exhibit a range of nonlinearities. In particular, we demonstrate how the approach can be used to quantify geometrical properties of the steady-state map of a nonlinear system.

2. Steady-state Measures of Nonlinearity

The assessment of nonlinearity of a process must take into account the extent of nonlinearity of both the process and its inverse in order to obtain an appreciation of the potential effectiveness of predicting and controlling a process using linear techniques. The first aspect of nonlinearity, called *Open-Loop Nonlinearity*, describes the nonlinearity of predictions of the

process variables given the input variables. The second, called *Control-Law Nonlinearity*, directly measures the ability to control a process using linear techniques.

In this study, these two aspects of nonlinearity are assessed by analyzing the extent of nonlinearity of the steady-state process input-output map and its inverse. Although either map can be used to assess both aspects of nonlinearity, it is clear that the extent of open-loop nonlinearity is more directly related to the nonlinearity of the input-output map and that control-law nonlinearity is more directly related to the nonlinearity of the inverse map. In what follows, we present a framework used to measure the extent of nonlinearity of the process input-output map. We first consider the input-state relationship, and then show how the framework can be applied to the input-output map.

Consider an asymptotically stable nonlinear system of the form,

$$\begin{aligned} \dot{\mathbf{x}} &= \mathbf{f}(\mathbf{x}, \mathbf{u}) \\ \mathbf{u} &\in \mathbb{R}^P, \mathbf{x} \in \mathbb{R}^N \end{aligned} \tag{1}$$

where **u** denotes the process inputs, and **x** the states. The linear approximation of the system at a stationary point ($\mathbf{x}_0$, $\mathbf{u}_0$) is given by

$$\dot{\mathbf{x}} = \frac{\partial \mathbf{f}}{\partial \mathbf{x}}(\mathbf{x}_0, \mathbf{u}_0)(\mathbf{x} - \mathbf{x}_0) + \frac{\partial \mathbf{f}}{\partial \mathbf{u}}(\mathbf{x}_0, \mathbf{u}_0)(\mathbf{u} - \mathbf{u}_0) = \mathbf{A}(\mathbf{x} - \mathbf{x}_0) + \mathbf{B}(\mathbf{u} - \mathbf{u}_0) \tag{2}$$

Let the pair (A,B) be controllable with A asymptotically stable and rank(B)=P. For the linearized system, the reachable set from $\mathbf{x}_0$ with constant controls is Range{**B**, **AB**, ..., $\mathbf{A}^{n-1}\mathbf{B}$}. Furthermore, for each constant control there exists a final state **x** such that $(\mathbf{x}-\mathbf{x}_0) \in$ Range{**B**, **AB**, ..., $\mathbf{A}^{n-1}\mathbf{B}$} which satisfies the steady-state relationship $\mathbf{A}(\mathbf{x}-\mathbf{x}_0)+\mathbf{B}(\mathbf{u}-\mathbf{u}_0)=\mathbf{0}$ (note that, naturally,

$\mathbf{x}_0 \in \text{Range}\{\mathbf{B}, \mathbf{AB}, ..., \mathbf{A}^{n-1}\mathbf{B}\}$). Asymptotic stability of the system implies that as $\mathbf{u}$ is changed slowly in a neighbourhood of $\mathbf{u}_0$ given by $|\mathbf{u}-\mathbf{u}_0|<\delta$, the states also change slowly and remain in a small neighbourhood of $\mathbf{x}_0$ given by $|\mathbf{x}-\mathbf{x}_0|<\varepsilon$ where ε and δ are small strictly positive numbers. The consequence is that for each $\mathbf{u}$ in $|\mathbf{u}-\mathbf{u}_0|<\delta$ there exists a steady-state $\mathbf{x}$ in $|\mathbf{x}-\mathbf{x}_0|<\varepsilon$. This means that, locally, there exists a matrix $\mathbf{D}$ such that $(\mathbf{x}-\mathbf{x}_0)=\mathbf{D}(\mathbf{u}-\mathbf{u}_0)$ where ($\mathbf{x}$, $\mathbf{u}$) is another stationary point of the nonlinear system described by Equation (1). Note that since $\mathbf{A}$ is asymptotically stable and rank{$\mathbf{B}$}=P, the matrix $\mathbf{D}$ is given by $-\mathbf{A}^{-1}\mathbf{B}$ and rank{$\mathbf{D}$}=P. Let N_e be a neighbourhood of $\mathbf{x}_0$ for which each of these assumptions holds. It follows that the set of states belonging to N_e reached as $t\to\infty$ depends smoothly on the inputs. Locally, this defines a P-dimensional submanifold of the state space defined by $\mathbf{f}(\mathbf{x},\mathbf{u})=\mathbf{0}$ which is parametrized by the inputs $\mathbf{u}$. Therefore, in a neighbourhood of a point $\mathbf{u}_0 \in \mathbf{U} \subset \mathbb{R}^P$, there exists a nonlinear map $\Xi:\mathbf{U}\to N_e$, which locally defines a P-dimensional manifold in $\mathbb{R}^N$ denoted by $\Xi(\mathbf{U})$. This surface will be referred to as the steady-state locus. The measurement of nonlinearity is performed by analyzing the local geometry of the steady-state locus. Application of the methodology to the input-output relationship is discussed below.

In what follows, we describe a framework for the analysis of the geometry of the steady-state locus of the states. The extent of curvature of this open neighbourhood gives a local assessment of the gain nonlinearity of a process.

The geometry of the steady-state locus can be studied by defining locally a basis for its tangent and normal spaces. In this study, the geometry is described by considering the first and second order derivatives of the steady-state map with respect to the inputs. The first order derivatives, given by

$$\dot{\mathbf{v}}_i = \frac{\partial \boldsymbol{\Xi}(\mathbf{u})}{\partial u_i} \ , \ 1 \le i \le P \ ,$$

span the P-dimensional tangent space of $\Xi(\mathbf{u})$ at a point $\mathbf{u}_0$. These N-dimensional vectors, called velocity vectors, define the steady-state gain matrix $\mathbf{V}=[\dot{\mathbf{v}}_1,..., \dot{\mathbf{v}}_p]$. The extent of departure from linearity of $\Xi(\mathbf{u})$ at any point $\mathbf{u}_0$ is assessed by evaluating the magnitude of the second order derivatives in this basis. For this purpose, we define the acceleration vectors as the P^2 N-dimensional vectors

$$\ddot{\mathbf{v}}_{pq} = \frac{\partial^2 \boldsymbol{\Xi}(\mathbf{u})}{\partial u_p \partial u_q}$$

and assign them to an N by P(P+1)/2 matrix of non-redundant vectors given by

$$\mathbf{W} = \left(\ddot{\mathbf{v}}_{1,1}\ \ddot{\mathbf{v}}_{1,2}\ \ddot{\mathbf{v}}_{2,2} \cdots \ddot{\mathbf{v}}_{1,P} \cdots \ddot{\mathbf{v}}_{P,P}\right).$$

Taking the QR decomposition (Bates and Watts,1988) of the combined matrix [**V,** W], evaluated at a prescribed value of **u**, gives

$$[\mathbf{V},\mathbf{W}] = \mathbf{QR} = \begin{bmatrix} \mathbf{Q}_1^t & \mathbf{Q}_1^n & \mathbf{Q}_2 \end{bmatrix} \begin{bmatrix} \mathbf{R}_1 & \mathbf{A}^t \\ \mathbf{0} & \mathbf{A}^n \\ \mathbf{0} & \mathbf{0} \end{bmatrix} \qquad (3)$$

where **Q** is an N by N orthonormal matrix and **R** is an N by P(P+3)/2 matrix. The first P columns of **Q**, denoted by $\mathbf{Q}_1^t$, span the tangent space of the steady state locus at $\Xi(\mathbf{u}_0)$. The next P^n ($\le$N-P) columns, denoted $\mathbf{Q}_1^n$, span a P^n dimensional subspace of the space normal to $\mathbf{Q}_1^t$. The remaining submatrix, written $\mathbf{Q}_2$, comprises an orthonormal basis of P_2 column vectors spanning the remainder of the state space. The matrix **R** is partitioned into a P by P upper triangular matrix $\mathbf{R}_1$, an (N-P) by P submatrix consisting of zeros, and an N by P(P+1)/2 matrix **A** of

second order derivatives.

The QR decomposition yields an orthonormal basis of $\mathbb{R}^N$ used to decompose higher order derivatives of the steady-state locus with respect to **u** into tangential and normal components. Using the matrix **Q** we can express **W** in the new basis by projection onto the columns of **Q**, yielding the N by P(P+1)/2 acceleration array **A**=**Q´W**. The first P rows of **A**, denoted by $\mathbf{A}^t$, are the projections of **W** onto the first P columns of **Q** which span the tangent space to the steady state locus, and the next P^n rows, denoted by $\mathbf{A}^n$, are the projections of **W** onto the next P^n columns of **Q** which span the normal space. The last P_2(=N-P-P^n) rows yield, by virtue of the QR decomposition, a matrix of zeros. This decomposition of the second order derivatives into tangential and normal components creates a convenient basis for studying various aspects of nonlinearity. These aspects can be illustrated in the following model of a chemostat bioreactor:

$$\frac{dx_1}{dt} = \frac{\mu_{max} x_1 x_2}{1 + x_2 + K_i x_2^2} - k_d x_1 - u_1 x_1$$

$$\frac{dx_2}{dt} = -\frac{\mu_{max} x_1 x_2}{1 + x_2 + K_i x_2^2} + (S_0 - x_2) u_1$$

where x_1 and x_2 are the scaled biomass and substrate concentrations and u_1, the input, is the dilution rate. The model parameters, μ_{max}, S_0, k_d and K_i, are the specific growth rate, inlet scaled substrate concentration, death rate and substrate inhibition constant, respectively.

Figure 2.1 shows the steady-state relationship existing between x_1, x_2 and u_1. The points indicate the parametrization of the steady-state locus resulting from the inputs. These points are the image under the steady-state map of evenly spaced points in the input space.

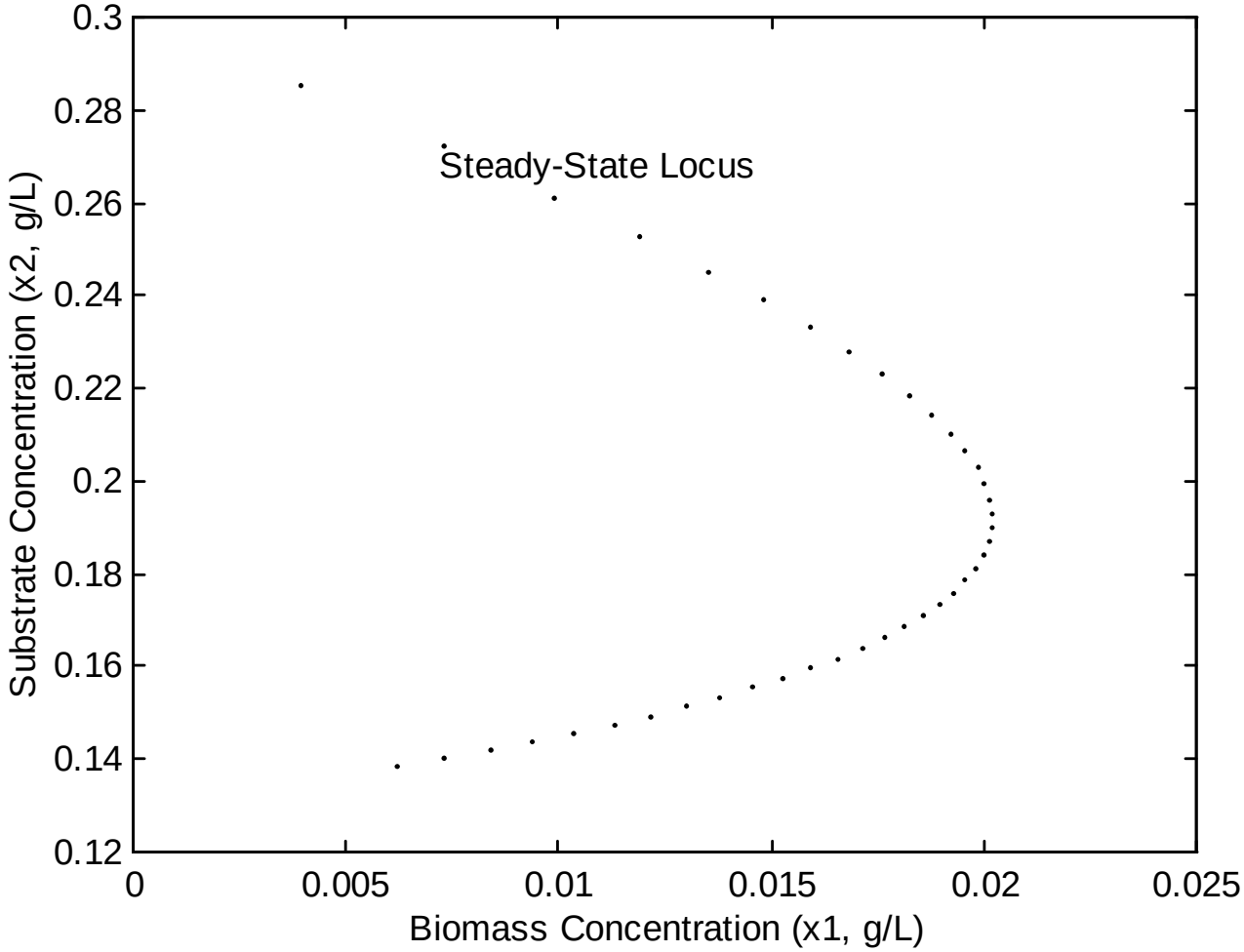

Figure 2.1 Steady-state locus for the chemostat bioreactor model. Biomass and substrate concentration are denoted as x1 and x2 respectively.

As expected, the nonlinearity of the input-output relationship causes an uneven spacing of these points on the steady-state locus. Since this aspect of nonlinearity is related to the change in magnitude and direction of tangent vectors along the steady-state locus, it is called the "tangential component" of nonlinearity. The curvature of the steady-state locus in the surrounding space can also be seen in Figure 2.1. This is related to the change in direction and magnitude

of normal vectors which lie in the space orthogonal to the tangent space along the steady-state locus. This is the so-called "normal component" of nonlinearity.

Having decomposed the components of nonlinearity into normal and tangential parts, we now proceed to define the corresponding measures of nonlinearity.

The curvature experienced along the steady-state locus along a direction **e** defined in the input space (i.e., along the line $\mathbf{u}=\mathbf{u}_0+r\mathbf{e}$) can be expressed as the ratio of the norm of the associated acceleration vector to the tangential velocity vector (Bates and Watts, 1988). Although these quantities can be expressed in terms of the original velocity and acceleration vectors, it is more convenient to express them in terms of their orthogonal basis obtained from the QR decomposition. Multiplying the original quantities by $\mathbf{Q}'$ transforms the original velocity and acceleration vectors into the new basis, preserving the metric on the steady-state locus. The resulting curvature becomes:

$$\frac{\|\mathbf{e}^T\mathbf{A}_r\mathbf{e}\|}{\|\mathbf{R}_1\mathbf{e}\|^2} \tag{4}$$

where $\mathbf{A}_r$ is an N-dimensional array of P by P matrices obtained from the N by P(P+1)/2 matrix **A**. The array $\mathbf{A}_r$ takes the form

$$\mathbf{A_r} = \left[\begin{pmatrix} a_{111} & a_{112} & \cdots & a_{11P} \\ a_{121} & a_{122} & \cdots & a_{12P} \\ . & . & \cdots & . \\ . & . & \cdots & . \\ . & . & \cdots & . \\ a_{1P1} & a_{1P2} & \cdots & a_{1PP} \end{pmatrix}, \begin{pmatrix} a_{211} & a_{212} & \cdots & a_{21P} \\ a_{221} & a_{222} & \cdots & a_{22P} \\ . & . & \cdots & . \\ . & . & \cdots & . \\ . & . & \cdots & . \\ a_{2P1} & a_{2P2} & \cdots & a_{2PP} \end{pmatrix}, \cdots, \begin{pmatrix} a_{N11} & a_{N12} & \cdots & a_{N1P} \\ a_{N21} & a_{N22} & \cdots & a_{N2P} \\ . & . & \cdots & . \\ . & . & \cdots & . \\ . & . & \cdots & . \\ a_{NP1} & a_{NP2} & \cdots & a_{NPP} \end{pmatrix} \right]'$$

where a_{ijk} is partial derivatives with respect to u_j and u_k of the i^{th} coordinate of the rotated state space. This array can be re-arranged, because of symmetry, into the N by P(P+1)/2 matrix **A** written as

$$\mathbf{A} = \begin{pmatrix} a_{111} & a_{112} & a_{122} & \cdots & a_{11P} & a_{12P} & \cdots & a_{1PP} \\ a_{211} & a_{212} & a_{222} & \cdots & a_{21P} & a_{22P} & \cdots & a_{2PP} \\ . & . & . & \cdots & . & . & \cdots & . \\ . & . & . & \cdots & . & . & \cdots & . \\ . & . & . & \cdots & . & . & \cdots & . \\ a_{N11} & a_{N12} & a_{N22} & \cdots & a_{N1P} & a_{N2P} & \cdots & a_{NPP} \end{pmatrix}$$

Pre-multiplication and post-multiplication by **e**, as expressed in Equation (4), is performed on each P by P submatrix (also called face) of $\mathbf{A}_r$. In what follows, the rearrangement of an N by P(P+1)/2 matrix, such as **A**, into an N-dimensional array of P by P matrices will be noted by the subscript r.

We can separate the tangential and normal contributions to the overall curvature by evaluating the curvature for the first P and the next P^n faces of $\mathbf{A}_r$, respectively. Because the magnitude of the acceleration array depends on the scaling of the problem, it is difficult to evaluate uniquely the degree of nonlinearity implied by these measures of curvature. Clearly, scale independent measures of curvature would be more advantageous, and would enable a

"generic" quantification of nonlinearity to be made for any process.

In what follows, we propose a scale independent measure of nonlinearity similar to the one proposed by Bates and Watts (1980, 1988), which takes into account the size of the region of interest in the output space. Such a region of interest will typically be determined by the desired operating region for the process. A combination of the curvature measures and a notion of size in the state space yields a convenient and simple way to evaluate the nonlinearity of the steady-state relationship in a chemical process.

3. Assessing Nonlinearity in Steady-state Relationships

In order to remove the dependence of the curvature on the state variables, we must specify a region in the state space where the assessment of nonlinearity is of particular interest. It may often be possible to define such a region from the extent of variation observed in normal process operations or from the specifications imposed on the process outputs. In what follows, we assume that these regions can be appropriately described by ellipsoidal regions in the state space of the form

$$\Delta\mathbf{x}'(\mathbf{S}'\mathbf{S})\Delta\mathbf{x} = 1 \tag{5}$$

where $\mathbf{S}$ is an invertible matrix and $\Delta\mathbf{x}=\mathbf{x}-\mathbf{x}_0$, where $\mathbf{x}_0$ is an output value at the centre of the region corresponding to $\mathbf{u}_0$. This region can be scaled to a sphere by considering a linear change of coordinates of the form $\mathbf{z}=\mathbf{S}\Delta\mathbf{x}$ and expressing the state region as

$$\mathbf{z}'\mathbf{z} = 1. \tag{6}$$

The nonlinearity of the steady-state map can then be assessed in the region of interest by

evaluating the magnitudes of the second order derivatives expressed in the **z**-coordinates.

We define the velocity vectors and non-redundant set of acceleration vectors in the **z**-coordinates by $\tilde{\mathbf{V}}=\mathbf{SV}$ and $\tilde{\mathbf{W}}=\mathbf{SW}$, respectively, where the overbar ˜ indicates that these arrays have been calculated for the scaled variables. Performing a QR decomposition of the scaled matrix $\tilde{\mathbf{D}}=[\tilde{\mathbf{V}},\tilde{\mathbf{W}}]=\mathbf{QR}$ yields the acceleration array for the scaled output variables, $\tilde{\mathbf{A}}=\mathbf{Q}'\tilde{\mathbf{W}}$. Note that **Q** and **R** are partitioned as before.

We then transform **u** to orthogonal inputs given by

$$\boldsymbol{\phi} = \mathbf{R}_1(\mathbf{u}-\mathbf{u}_0) = \mathbf{R}_1\Delta\mathbf{u}$$

such that the denominator of Equation (4) $\|\mathbf{R}_1\Delta\mathbf{u}\|^2=1$ for any θ (an arbitrary direction in the Φ-space) of unit length. Although this transformation is not unique, it proves to be very advantageous in this case. Such a transformation can be interpreted as removing first order interaction effects, enabling a clear identification and interpretation of effects due to nonlinearity. The velocity and acceleration vectors taken with respect to these new inputs are given by

$$\dot{\mathbf{v}}^{\boldsymbol{\phi}} = \dot{\mathbf{v}}^{\mathbf{u}}\mathbf{K} = \mathbf{QRK} = \mathbf{Q}_1^t$$

and

$$\ddot{\mathbf{v}}_r^{\boldsymbol{\phi}} = \mathbf{K}'(\mathbf{Q}'\ddot{\mathbf{v}}^{\mathbf{u}})_r\mathbf{K} = \mathbf{K}'\tilde{\mathbf{A}}_r\mathbf{K} = \tilde{\mathbf{C}}_r$$

respectively, where $\mathbf{K}=\mathbf{R}_1^{-1}$. $\tilde{\mathbf{C}}_r$ is the "rearranged" relative acceleration array defined for the region prescribed by the elements of **S**. In what follows, the overbar ˜ will be omitted and it will be assumed that all arrays are scaled prior to the analysis.

The following example illustrates these calculations.

Example 2.1

Consider again the two-state, one-input bioreactor model introduced in the preceding section. Figure 2.2 shows the steady-state locus for this example, with points A, B and C as steady-state conditions at which the nonlinearity is to be evaluated. Using the parameter values shown in Table 2.1, the steady-state values for the states and inputs for each point appear in Table 2.2.

Table 2.1

Parameter values for the bioreactor model in Example 2.1.

Model Parameter	Value
μ_{max}	0.5 (min^{-1})
S_0	0.3 (g/L)
k_d	0.05 (min^{-1})
K_i	10.0 (L/g)

At each of the three locations we consider a region of interest defined by the scaling matrix **S** given by

$$\mathbf{S} = \begin{bmatrix} 1/(10^{-5})^{0.5} & 0 \\ 0 & 1/(5\times10^{-4})^{0.5} \end{bmatrix}.$$

The diagonal elements of **S** reflect the expected range of operation of x_1 and x_2, $0.019\pm(10^{-5})^{0.5}$ and $0.18\pm(10^{-4})^{0.5}$ respectively.

Table 2.2

Steady-state conditions and tangential and normal components of the relative curvature array for three points on the steady-state locus for Example 2.1.

Steady-State	u_0	$x_1(u_0)$	$x_2(u_0)$	C^t	C^n
A	0.01	0.019821	0.18107	0.24693	0.86733
B	0.016	0.014841	0.23878	0.33423	-0.07604
C	0.005	0.013453	0.15224	0.17643	0.08855

Table 2.2 also lists the tangential and normal components of the relative curvature array calculated at each point. For point A, the velocity and acceleration vectors are given by

$$[\dot{\mathbf{v}},\ \ddot{\mathbf{v}}] = \begin{bmatrix} 165.23 & -1.0478\times10^{5} \\ 303.01 & 2.3637\times10^{4} \end{bmatrix}.$$

Taking a QR decomposition of this matrix yields

$$\mathbf{Q} = \begin{bmatrix} -0.4788 & -0.8880 \\ -0.8880 & 0.4788 \end{bmatrix},\ \mathbf{R} = \begin{bmatrix} -345.13 & 2.94413\times10^{4} \\ 0.0 & 1.0331\times10^{5} \end{bmatrix}$$

from which the acceleration array,

$$\mathbf{A}_r = \mathbf{A} = \begin{bmatrix} 2.9413\times10^{4} \\ 1.0331\times10^{5} \end{bmatrix}$$

and the relative acceleration array,

$$\mathbf{C}_r = \mathbf{C} = \begin{bmatrix} 0.2469 \\ 0.8673 \end{bmatrix}$$

can be obtained.

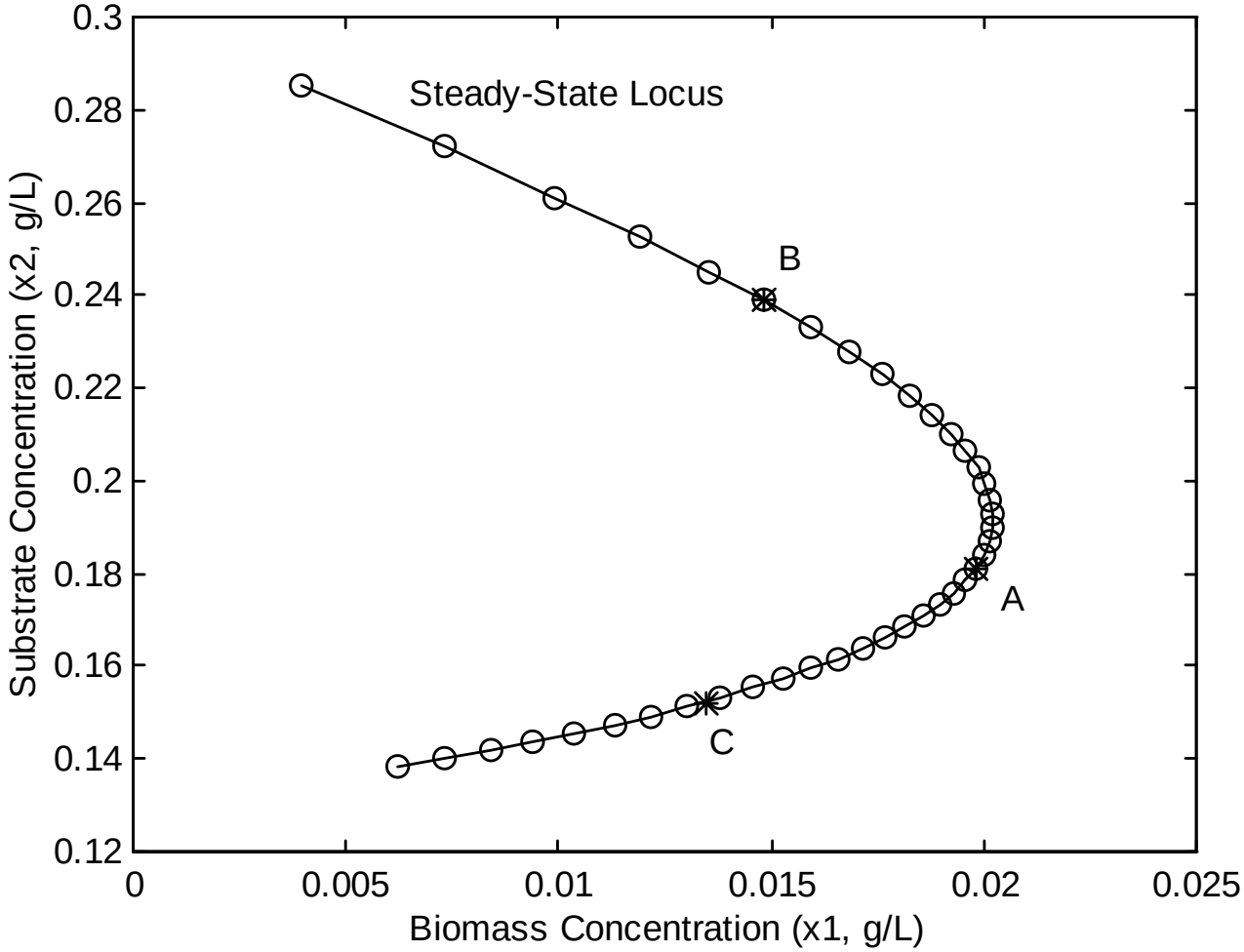

Figure 2.2 Steady-state locus for the bioreactor model of Example 2.1. The nonlinearity measures are obtained at points A, B and C on the steady-state locus.

By relating the results listed in Table 2.2 to the plot of the steady-state locus in Figure 2.2, we can establish the implications of the tangential and normal components. From Figure 2.2 it

can be seen that the steady-state locus exhibits significant curvature with respect to the surrounding coordinates at point A, but not at points B and C. The normal components of the relative acceleration array in Table 2.2 reflect this behaviour as the magnitude of the normal component at point A is ten times larger than at points B and C. As noted in the preceding section, equally spaced inputs used to generate the steady-state locus are unevenly spaced on the locus. This effect tends to be more pronounced at point B. From the results listed in Table 2, this effect is reflected by a larger value of the tangential component at point B relative the values at points A and C.

In summary, measures of nonlinearity which are independent of the scaling of the system can be obtained. For a specified direction in the input space at any point of interest, the tangential and normal components of the relative curvature can be calculated. The magnitude of the normal component measures the degree of curvature in the steady-state locus at that point, while the magnitude of the tangential curvature measures the nonuniformity and nonlinearity of constant input lines on the steady-state locus at that point.

Although this decomposition of second order effects can be used to characterize many aspects of nonlinear behaviour of a process, it is desirable to have one unique measure which can be used by a control engineer as an indicator of the nonlinearity of a process. One overall measure of tangential and normal curvature can be derived by integrating the squared relative curvature in a direction θ,

$$c_{\theta}^{2} = \|\theta' C_r \theta\|^2, \tag{8}$$

over all possible directions. This yields a mean squared measure of curvature

$$c^2 = \frac{1}{A}\int_A \sum_{i=1}^{N} (\theta' \mathbf{C}_{ri} \theta)^2 dA \tag{9}$$

where A is the area of the (P-1)-dimensional sphere described by all unit-norm vectors θ (i.e. vectors satisfying θ′θ=1). Carrying out the integration yields the following result:

$$c^2 = \frac{1}{P(P+2)} \sum_{i=1}^{N} \left[2 \sum_{j=1}^{P} \sum_{k=1}^{P} c_{ijk}^{\ 2} + \left(\sum_{j=1}^{P} c_{ijj} \right)^2 \right] \tag{10}$$

where c_{ijk} is the k^{th} element of the jth row of the i^{th} face of the relative curvature array $\mathbf{C}_r$. Summing over the first P faces gives the tangential mean squared curvature. Correspondingly, summing over the next P′ faces gives the normal mean squared curvature. Note that the choice of integrating over a spherical region is arbitrary. It is also possible to obtain mean squared curvature for arbitrarily shaped regions assuming that the integral can be evaluated.

Figure 2.3 shows how a convenient scale for the root mean squared (RMS) curvature measures c can be obtained. As discussed in Bates and Watts (1980), the steady-state locus can be locally approximated by a sphere of radius 1/c. The magnitude of the RMS curvature can then be related to the extent of deviation between this surface and its tangential approximation at a unit distance from the point of linearization in the scaled input space **z**. That is, the deviation is evaluated at the boundary of the region of interest. The magnitude of the deviation is given by $1/c-(1/c^2-1)^{0.5}$. This is readily compared to the size of the region of interest which is simply unity in the present setting. The percent deviation from the linear approximation expressed in terms of the size of the region of interest is then equal to $100(1/c-(1/c^2-1)^{0.5})$. This provides a convenient scale with which to evaluate the nonlinearity of a process. Table 2.3 gives the percent deviation as a function of the RMS curvature measure.

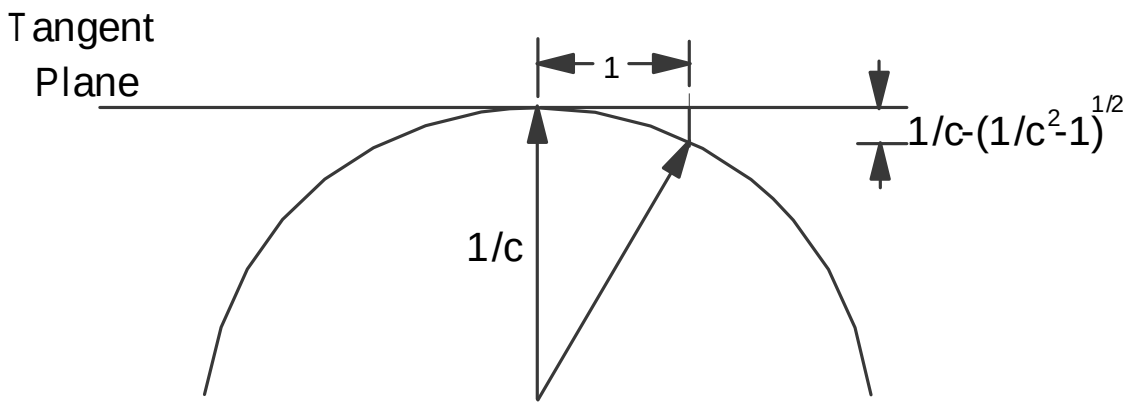

Figure 2.3 Scale for measuring the extent of nonlinearity. The steady-locus is approximated by a surface of constant curvature 1/c where c is the RMS curvature.

Table 2.3

Scale for measuring nonlinearity based on the RMS curvature.

RMS Curvature	%Deviation
0.1	5
0.2	10
0.3	15
0.4	21

Figure 2.4 shows a scaled diagram of surfaces with varying RMS curvatures ranging from 0 to 1.0. This diagram illustrates the degrees of nonlinearity associated with the RMS curvatures.

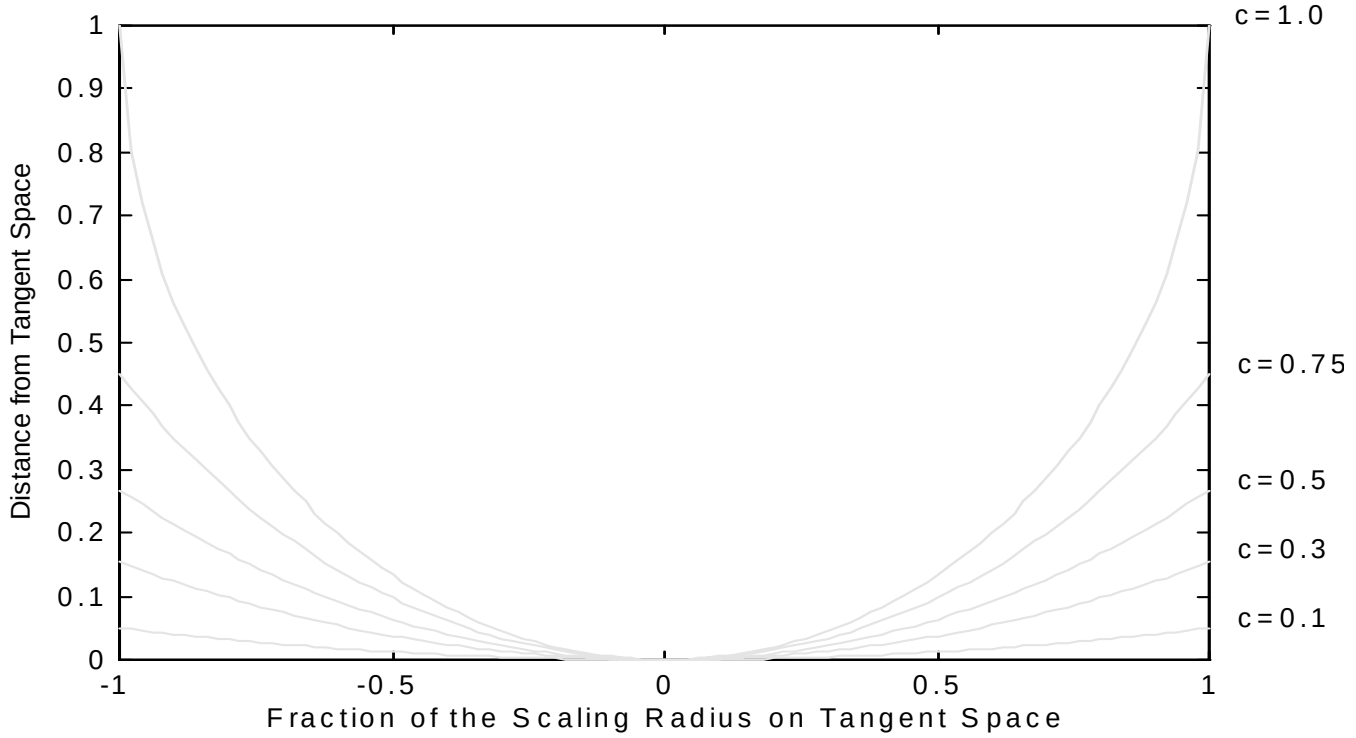

Figure 2.4 Scaled diagram of surfaces with varying RMS curvatures.

Using the values in Table 2.3, the nonlinearity of a process can be evaluated in the neighbourhood of a point of interest as a function of the percent deviation from the linear approximation. As a guideline, a deviation of less than 15%, corresponding to a threshold RMS curvature value of approximately 0.3, may be considered negligible.

For the two-state, one-input bioreactor model, the tangential and normal RMS curvatures at point A are 0.24693 and 0.86733, respectively. From the foregoing discussion, only the normal component is significant in this case. As observed in Figure 2.2, the curvature of the steady-state locus at that point is large with respect to the surrounding space and, as a result, the direction of the open-loop steady-state gain vector quickly changes in this region. However, the negligible

tangential curvature indicates that the magnitude of the steady-state gain vector is nearly constant in this region. The implications for control are that linear controllers would perform adequately in neighbourhoods of points B and C. Controlling about the steady-state point A can be problematic since the direction of the controller action changes in the prescribed region.

The application of the methodology to a MIMO control problem is illustrated in the following example.

Example 2.2

Consider the following two-state, two input bioreactor model:

$$\frac{dx_1}{dt} = \frac{0.5x_1x_2}{1+x_2+10x_2^2} - 0.05x_1 - u_1x_1$$

$$\frac{dx_2}{dt} = -\frac{0.5x_1x_2}{1+x_2+10x_2^2} + (u_2 - x_2)u_1$$

$$y_1 = x_1,\ y_2 = x_2$$

where x_1, x_2 and u_1 are as in Example 2.1 and u_2 is the inlet substrate concentration. The steady-state conditions of interest for this case are $\mathbf{x}_0$=[0.019821, 0.18107]′ and $\mathbf{u}_0$=[0.01, 0.3]′. The region of interest can be described by the scaling matrix

$$\mathbf{S} = \begin{bmatrix} \frac{1}{(1\times10^{-4})^{0.5}} & 0 \\ 0 & \frac{1}{(5\times10^{-4})^{0.5}} \end{bmatrix}.$$

This matrix reflects the expected variations in $\mathbf{x}_1$ and $\mathbf{x}_2$ under normal operating conditions. Figure 2.5 shows the steady-state loci and the superimposed region of interest in the scaled output space. The straight horizontal dashed lines are constant u_1 lines and the curved vertical lines are

constant u_2 lines. The constant u_2 lines exhibit significant curvature but there is no apparent curvature in the constant u_1 lines. This is supported by the relative curvature matrix which is given by

$$\mathbf{C_r} = \left(\begin{bmatrix} -0.18682 & -0.01452 \\ -0.01452 & 0.01056 \end{bmatrix} \begin{bmatrix} 0.38787 & -0.33791 \\ -0.33791 & 0.10501 \end{bmatrix} \right).$$

The RMS curvature is 0.37492, indicating that, overall, the process exhibits significant nonlinearity. Inspection of $\mathbf{C}_r$ shows that the main contributions to nonlinearity are in the second face which is related to variations in the direction of the steady-state gain vector corresponding to the scaled orthogonal input ϕ_2, i.e., in the direction of $\mathbf{Q}^t_{\cdot 2}$, the second column vector of the tangential component of the decomposition. The first diagonal term, 0.38787, demonstrates that there is significant variation in the gain related to ϕ_1 in the direction of $\mathbf{Q}^t_{\cdot 2}$ as ϕ_1 is varied. That is, as one moves along $\mathbf{Q}^t_{\cdot 2}$, the magnitude of $\mathbf{Q}^t_{\cdot 1}$ changes. This indicates that there is significant arcing of the constant ϕ_2 lines in the direction of $\mathbf{Q}^t_{\cdot 2}$. The off-diagonal term (-0.33791) indicates that there is significant variation in the gain related to ϕ_2 in the direction of $\mathbf{Q}^t_{\cdot 2}$ as ϕ_1 is varied (or, alternatively, variation in the gain related to ϕ_1 as ϕ_2 is varied). This indicates that there is a fanning effect in the $\mathbf{Q}^t_{\cdot 2}$ direction of the lines of constant ϕ_2 as ϕ_1 is varied. Both the fanning and the arcing are demonstrated in Figure 2.5. It is interesting to note that the $\mathbf{Q}^t_{\cdot 2}$ direction is essentially parallel to the $\mathbf{z}_1$ axis. This indicates that it is more difficult to predict the gain using a linear approximation when the process moves along the $\mathbf{z}_1$ axis.

4. Accounting for Nonlinearity

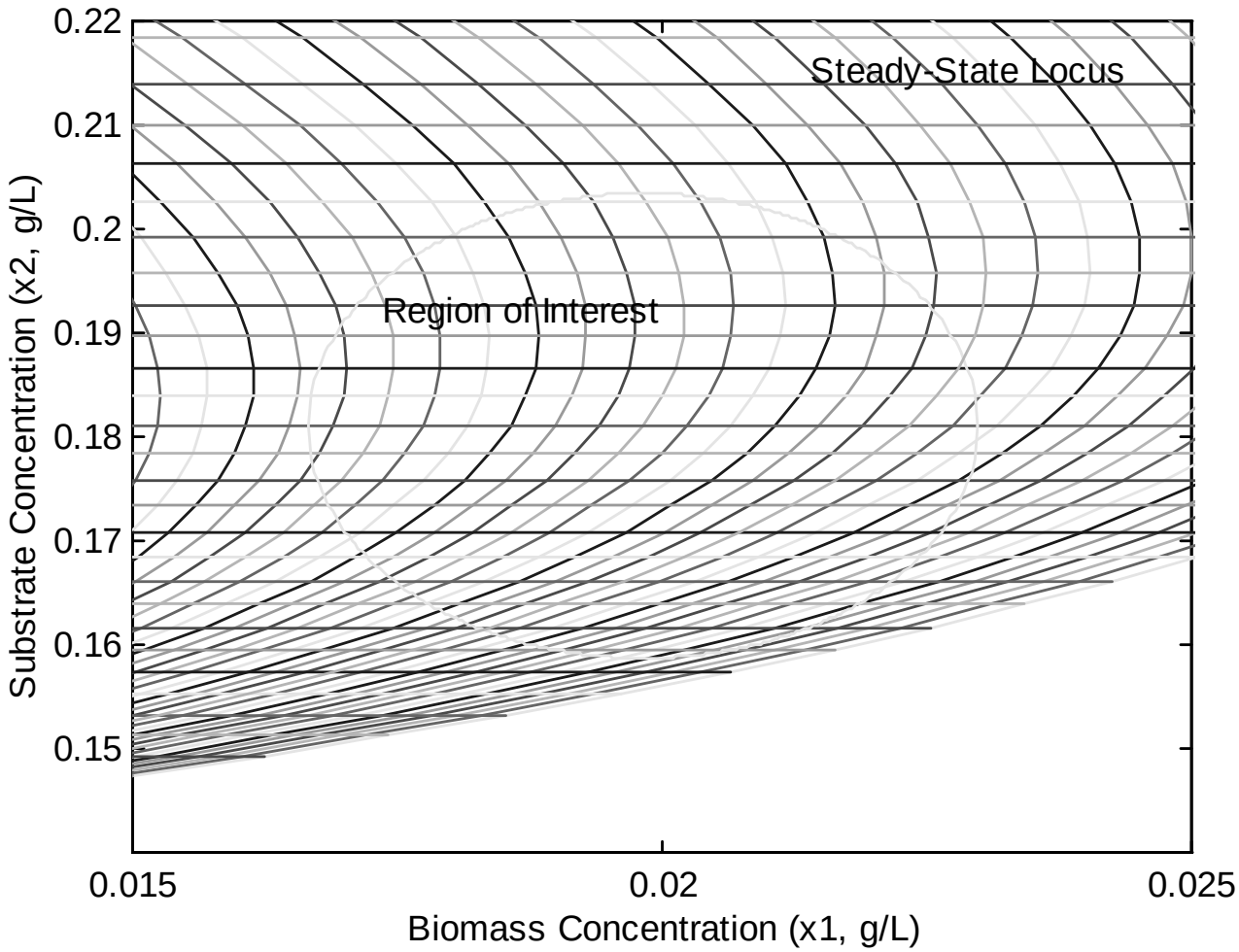

Figure 2.5 Steady-state locus and the region of interest for the model of Example 2.2. Solid lines show the effect of u_1 at constant u_2. Dashed lines show the effect of u_2 at constant u_1.

Local curvatures can be used to determine output or state transformations which reduce the extent of nonlinearity. It is possible to account for the tangential and normal components of nonlinearity by defining appropriate systems of coordinates in the state space. Tangential coordinates of the steady-state locus are simply given by

$$\tau = \mathbf{Q}_1^{t\prime}\mathbf{z}(\mathbf{u}) \tag{11}$$

where, as defined previously, $\mathbf{Q}_1^t$ is the N by P matrix which contains the first P columns of the **Q** matrix. These coordinates are nonlinear functions of the inputs. Note that Equation (11) implies that the τ coordinates are projections of the steady-state locus on the tangent basis defined at $\mathbf{z}(\mathbf{u}_0)$. They can re-written as nonlinear functions of the orthogonal inputs ϕ as $\tau = \mathbf{H}(\phi)$. The map **H** can be approximated by

$$\mathbf{H}(\phi) \approx \phi + \frac{1}{2}\phi'\mathbf{C}_r^t\phi. \tag{12}$$

where $\mathbf{C}_r^t$ is the tangential part of the relative acceleration array. Intuitively, τ coordinates eliminate tangential curvature since the nonuniformity with respect to the basis at $\mathbf{u}_0$ is accommodated.

Similarly, normal coordinates can be obtained. Let $\mathbf{G}(\mathbf{z})$ be a P^n dimensional vector valued function which vanishes as **z** reaches the steady state locus, i.e. $\mathbf{G}(\mathbf{z}_0)=\mathbf{0}$. This vector valued function can be used to describe the geometry of the steady-state locus with respect to the surrounding space. Since $\mathbf{G}(\mathbf{z})\equiv\mathbf{0}$ on the steady-state locus $\mathbf{z}(\mathbf{u})$, the rate of change of **G** with respect to **u** is zero, i.e.,

$$\left(\frac{\partial \mathbf{G}}{\partial \mathbf{z}}\frac{\partial \mathbf{z}}{\partial \mathbf{u}}\right)\Bigg|_{\mathbf{z}_0,\mathbf{u}_0} = \mathbf{0}$$

In a neighbourhood of $\mathbf{z}_0$, the rows of the Jacobian of $\mathbf{G}(\mathbf{z})$ span the space normal to the tangent space. As a result, it can be represented locally by

$$\left.\frac{\partial \mathbf{G}(\mathbf{z})}{\partial \mathbf{z}}\right|_{\mathbf{z}_0,\mathbf{u}_0} = \mathbf{Q}_1^{\mathbf{n}\prime}$$

where $\mathbf{Q}_1^{\mathbf{n}}$ is the N by P^n normal component of **Q**. Differentiating a second time with respect to **u** gives

$$\left\{\frac{\partial \mathbf{z}'}{\partial \mathbf{u}}\frac{\partial^2 \mathbf{G}}{\partial \mathbf{z}\partial \mathbf{z}'}\frac{\partial \mathbf{z}}{\partial \mathbf{u}} + \frac{\partial \mathbf{G}}{\partial \mathbf{z}}\frac{\partial^2 \mathbf{z}}{\partial \mathbf{u}\partial \mathbf{u}'}\right\} = \mathbf{0}$$

where the notational dependence of **G** on **z** has been removed for convenience. Using Equation (11) and the QR decomposition, this expression can be re-written as

$$\mathbf{R}_1'\mathbf{Q}_1^{\mathbf{t}\prime}\frac{\partial^2 \mathbf{G}}{\partial \mathbf{z}\partial \mathbf{z}'}\mathbf{Q}_1^{\mathbf{t}}\mathbf{R}_1 + \mathbf{Q}_1^{\mathbf{n}\prime}\frac{\partial^2 \mathbf{z}}{\partial \mathbf{u}\partial \mathbf{u}'} = \mathbf{0}$$

or

$$\mathbf{R}_1'\mathbf{Q}_1^{\mathbf{t}\prime}\frac{\partial^2 \mathbf{G}}{\partial \mathbf{z}\partial \mathbf{z}'}\mathbf{Q}_1^{\mathbf{t}}\mathbf{R}_1 + \mathbf{A}_{\mathbf{r}}^{\mathbf{n}} = \mathbf{0}$$

in a neighbourhood of $\mathbf{z}_0$ where $\mathbf{A}^{\mathbf{n}}_{\mathbf{r}}$ is the normal part of the acceleration array. Pre-multiplying by **K´** and post-multiplying by **K** yields

$$\mathbf{Q}_1^{\mathbf{t}\prime}\frac{\partial^2 \mathbf{G}}{\partial \mathbf{z}\partial \mathbf{z}^{\mathbf{T}}}\mathbf{Q}_1^{\mathbf{t}} + \mathbf{C}_{\mathbf{r}}^{\mathbf{n}} = \mathbf{0}$$

where $\mathbf{C}_{\mathbf{r}}^{\mathbf{n}}$ is the normal part of the relative acceleration array. This gives

$$\frac{\partial^2 \mathbf{G}}{\partial \mathbf{z}\partial \mathbf{z}'} = -\mathbf{Q}_1^{\mathbf{t}}\mathbf{C}_{\mathbf{r}}^{\mathbf{n}}\mathbf{Q}_1^{\mathbf{t}\prime}. \qquad (13)$$

Equation (13) is important because it establishes that the normal component of the relative

curvature array of the steady-state locus can be obtained from the second order derivatives of some function of **z** with respect to **z**. That is, the presence of normal curvature is attributable to the need for a nonlinear transformation of the **z**-coordinates which can be obtained as **G**(**z**). The vector valued function **G**(**z**) can be replaced by its second order approximation, thereby ensuring that, at $\mathbf{u}_0$, the normal curvature of the steady-state locus is accounted for in the transformation. The second order approximation can be expressed in terms of the normal curvature above, leading to the following coordinates for the state space:

$$\xi = \mathbf{G}(\mathbf{z}) \approx \mathbf{Q}_1^{n\prime}\mathbf{z} - \frac{1}{2}\mathbf{z}'\mathbf{Q}_1^{t}\mathbf{C}_r^{n}\mathbf{Q}_1^{t\prime}\mathbf{z}. \tag{14}$$

The tangential coordinates representation of the steady-state locus provided by Equation (11) can be used to express $\mathbf{z}(\mathbf{u})=\mathbf{Q}_1^{t\prime}(\tau(\mathbf{u}))$. The normal coordinates of the steady locus become

$$\boldsymbol{\xi} = -\frac{1}{2}\boldsymbol{\tau}'\mathbf{C}_r^{n}\boldsymbol{\tau}. \tag{15}$$

To summarize, the steady-state locus in the (τ, ξ) coordinate system given by Equations (11) and (15) yields coordinates in which the steady-state locus has zero local tangential and normal curvature at $\mathbf{u}_0$. As in Hamilton et al. (1982), we separate, in a local fashion, the steady-state input-state map into two maps. First, the input space is mapped onto the tangent space to the steady-state locus by the map $\Xi^t(\mathbf{u})=\mathbf{Q}_1^{t\prime}\mathbf{z}(\mathbf{u})$ defined in Equation (11). We can then combine Equations (11) and (15) to give an approximation of the steady-state locus in terms of τ,

$$\mathbf{z}(\boldsymbol{\tau}) \approx \mathbf{Q}_1^{t}\boldsymbol{\tau} + \frac{1}{2}(\mathbf{Q}_1^{n})(\boldsymbol{\tau}'\mathbf{C}_r^{n}\boldsymbol{\tau}). \tag{16}$$

It is clear that only the tangential coordinates given by Equation (11) depend explicitly

on the form of the steady-state dependence on the inputs. As a result, it is the only component of nonlinearity which can be affected by input transformations of the form $\mathbf{u}=\Phi(\mathbf{v})$ where $\mathbf{v}$ is a transformed input which experiences no tangential curvature. The normal coordinates ξ for the steady-state locus given by Equation (15) reflect the intrinsic geometry of the process and can only be taken into account by nonlinear coordinate transformations and feedback transformations. To justify these observations let us consider a single input nonlinear system of the form of Equation (1). Let the linear approximation of the nonlinear system be such that the required assumptions are fulfilled. Since the (A,B) pair is controllable, there exists a linear change of coordinates of the form $\mathbf{z}=[z_1, z_2, ..., z_N]=\mathbf{P}(\mathbf{x}-\mathbf{x}_0)$ that transforms the single input linearized system to Brunovsky normal form

$$\begin{aligned} \dot{z}_1 &= z_2 \\ \dot{z}_2 &= z_3 \\ &\vdots \\ \dot{z}_{N-1} &= z_N \\ \dot{z}_N &= \mathbf{F}\mathbf{z} + \mathbf{b}u \end{aligned} \tag{17}$$

At steady-state, we impose that, locally, $z_2=z_3=...=z_N=0$. Consequently, we get

$$f_{11}z_1 + b(u-u_0) = 0$$

The steady-state gain vector of the process at $\mathbf{x}_0$ is given by

This clearly identifies the output function z_1 as the tangential, or τ, coordinate of the steady-state

$$\frac{\partial \mathbf{z}}{\partial \mathbf{u}} = \left[-\frac{\mathbf{b}}{\mathbf{f}_{11}}, 0, 0, \ldots, 0 \right]'$$

locus at $\mathbf{x}_0$ and demonstrates that the variables z_2, z_3, ..., z_N act as normal coordinates. In the presence of significant nonlinearity, the system may not be transformable to a Brunovsky normal form. But since the pair {**A**, **B**} from the linear approximation is controllable, the Brunovsky form of the linear system remains. The normal nonlinearity displayed by the system at steady-state in a neighbourhood of $\mathbf{x}_0$ can be expressed as controller mismatch terms for the linear approximation. The transformation of the linear system into a Brunovsky form simplifies the computation of these terms.

As described above, $\mathbf{z}_1$ is taken as an appropriate choice of tangential coordinate (τ) for the steady-state locus. According to Equation (16), the normal nonlinearity displayed by the nonlinear system at steady-state is given by

$$\begin{pmatrix} z_1 \\ z_2 \\ \cdot \\ \cdot \\ \cdot \\ z_N \end{pmatrix} = \mathbf{Q}_1^{\mathbf{t}}\tau + \frac{1}{2}(\mathbf{Q}_1^{\mathbf{n}})(\tau' \mathbf{C}_{\mathbf{r}}^{\mathbf{n}} \tau) = \begin{pmatrix} 1 \\ 0 \\ 0 \\ \cdot \\ \cdot \\ 0 \end{pmatrix} z_1 + \frac{1}{2} \begin{pmatrix} 0 & 0 & 0 & \ldots & 0 \\ 1 & 0 & 0 & \ldots & 0 \\ 0 & 1 & 0 & \ldots & 0 \\ \cdot & \cdot & \cdot & \ldots & \cdot \\ \cdot & \cdot & \cdot & \ldots & \cdot \\ \cdot & \cdot & \cdot & \ldots & \cdot \\ 0 & 0 & 0 & \ldots & 1 \end{pmatrix} \begin{pmatrix} \mathbf{c}^{\mathbf{n}}_{11} z_1^2 \\ \cdot \\ \cdot \\ \cdot \\ \mathbf{c}^{\mathbf{n}}_{(N-1)1} z_1^2 \end{pmatrix}$$

where c^n_{i1} are the elements of the normal component of the relative acceleration array. Note that $\tau = \mathbf{z}_1$ is still due to the Brunovsky normal form of the linearized system.

In a neighbourhood of the steady-state locus, the underlying system must such that Equation (16) holds. The following approximation of the original nonlinear system results in

a neighbourhood of the steady-state locus with slowly changing inputs

$$\dot{z}_1 = z_2 - \frac{1}{2} c^n_{11} z_1^2$$

$$\dot{z}_2 = z_3 - \frac{1}{2} c^n_{21} z_1^2$$

$$\vdots$$

$$\dot{z}_{N-1} = z_N - \frac{1}{2} c^n_{(N-1)1} z_1^2$$

$$\dot{z}_N = \mathbf{Fz} + \mathbf{Gu}$$

It is readily seen that the steady-state behaviour of this system yields the expressions derived from Equation (16). The normal component of curvature enters the process as a mismatch term that can only be taken into account by nonlinear changes of coordinates and nonlinear state-feedback.

In addition, when significant tangential nonlinearity exists, the tangential component must be approximated by

$$\tau = z_1 = \phi + \frac{1}{2} \phi' C^t_r \phi$$

where

$$\phi = -\frac{b}{f_{11}} (u - u_0).$$

Substituting in the last differential equation of Equation (17) gives

$$\dot{\mathbf{z}}_N = \mathbf{F}\mathbf{z} - \mathbf{f}_{11}\boldsymbol{\phi} - \frac{1}{2}\mathbf{f}_{11}\boldsymbol{\phi}'\mathbf{C}_r^t\boldsymbol{\phi}.$$

This demonstrates that the tangential component can be removed by introducing a nonlinear input transformation or a nonlinear state-feedback transformation.

In situations where there is incomplete knowledge of the state space, appreciation of process behaviour is usually restricted to the measured variables. Clearly, there is no specific need to restrict the preceding analysis to the input-state map. All that is required for the application of the framework in the present form is the existence of an injective map from the space of the inputs to the space of the measured variables. Injectivity is required to avoid input multiplicities in the region of interest, such that any steady-state point in this region leads to a unique set of velocity and acceleration vectors. Because injectivity may constitute a serious restriction in a number of situations, the framework must be adapted to account for this problem.

In what follows, we will consider the application of this methodology to the study of the input-output steady-state relationship. In particular, we highlight a simple modification of the framework that alleviates the injectivity restriction.

5. Application to the Input-output Relationship

Note that specific output functions can be incorporated into this framework. To see this, let

$$\mathbf{y} = \mathbf{h}(\mathbf{x}) \tag{18}$$

denote an output function, where $\mathbf{y} \in \mathbb{R}^M$. Let the Jacobian matrix $\partial\mathbf{h}(\mathbf{x})/\partial\mathbf{x}$ have rank M in a neighbourhood $\mathbf{X} \subset \mathbb{R}^N$ of $\mathbf{x}_0$. Assume that the state velocity matrix $\partial\Xi/\partial\mathbf{u}$ evaluated at $\mathbf{u}_0$ has rank

P everywhere on $\mathbf{X}\cap\mathbf{N}_e$ and is such that the input-output gain matrix $\mathbf{k}(\mathbf{x}_0,\mathbf{u}_0)=[(\partial\mathbf{h}(\mathbf{x})/\partial\mathbf{x})(\partial\Xi/\partial\mathbf{u})]_{\mathbf{x}_0,\mathbf{u}_0}$ has constant rank P on $\mathbf{X}\cap\mathbf{N}_e$; then the steady-state input-output map $\mathbf{U}\mapsto\mathbf{h}(\mathbf{X}\cap\mathbf{N}_e)$ is locally injective. Under these assumptions, we can view the local steady-state input-output relationship as a smooth injective map from an open neighbourhood of $\mathbf{u}_0$ in the input space to an open neighbourhood of $\mathbf{h}(\Xi(\mathbf{u}_0))$ in the output space. This ensures that the variation of the input leads to a unique measure of nonlinearity on a given neighbourhood of $\mathbf{x}_0$. As a result, the framework can be directly applied by considering only the dependence of the inputs on the outputs.

If $\mathbf{k}(\mathbf{x}_0,\mathbf{u})$ does not have constant rank as $\mathbf{u}$ is varied in a neighbourhood of $\mathbf{x}_0$, application of the methodology in neighbourhoods of the singular points yields infinite curvature measures. In order to account for this problem, we apply the methodology to the process steady-state graph rather than the steady-state locus in the output space.

The process graph in a neighbourhood U of a point $p\in\mathbb{R}^P$ is viewed as a map $\Gamma_p:U\subset\mathbb{R}^P\rightarrow Y\times U\subset\mathbb{R}^M\times\mathbb{R}^P$ of the form

$$\Gamma_p(\mathbf{u}) = \begin{pmatrix}\mathbf{g}(\mathbf{u})\\ \mathbf{u}\end{pmatrix}$$

where $\mathbf{g}(\mathbf{u})$ denotes the gain matrix in a small neighbourhood of $\mathbf{x}_0$. This alleviates difficulties encountered in rank deficient cases by unfolding the input-output steady-state locus. The methodology can be applied in a straightforward manner to analyze the local geometry of the process graph and measure the nonlinearity of the map Γ_p in a neighbourhood of a steady-state value $\mathbf{u}_0$. We note that this requires scaling in the input and output space simultaneously.

6. Assessment of Control-law Nonlinearity

The analysis performed above was primarily concerned with direct assessment of open-loop nonlinearity by analysis of the process input-state map. However, it is also possible to get a sense of the extent of control-law nonlinearity from this analysis by considering the following. For a linear system, the steady-state gain is constant everywhere and the region of interest described by $\mathbf{z}'\mathbf{z}=1$ is mapped to an ellipsoidal hypersurface in the input space given by

$$\Delta\mathbf{u}'\dot{\mathbf{v}}_S'\dot{\mathbf{v}}_S\Delta\mathbf{u} = 1 \tag{19}$$

which can be written in the ϕ-space as

$$\phi'\phi = 1.$$

For a nonlinear system, similar regions can be constructed by solving $\mathbf{z}(\mathbf{u})'\mathbf{z}(\mathbf{u})=1$ for the inputs $\mathbf{u}$. Because of the nonlinearity of the process, this gives rise to distorted ellipsoids in the input space. The extent of distortion is directly related to the degree of nonlinearity of the inverse map or, alternatively, to the extent of control-law nonlinearity. We can therefore get an appreciation of control-law nonlinearity using this approach.

Equations (11) and (15) can be used to derive an approximation of the model inverse to predict the change in input required to achieve a given point in the output space belonging to a neighbourhood of the point of linearization. Such inverses have been derived by Bates and Watts (1981) and Hamilton *et al.* (1982) to construct improved parameter inference regions for nonlinear regression models. Their analysis is similar in construction to the case where $M \geq P$.

If $N \geq P$, then $\Xi(\mathbf{U})$ is an immersion of $\mathbf{U}$ to $\mathbb{R}^N$. One possibility would be to consider the inverse function, $\mathbf{u}=\mathbf{H}(\tau,\xi)$, where τ and ξ are the tangential and normal coordinates defined by

Equations (11) and (15), respectively. If we assume that the normal component displays negligible nonlinearity, we can let $\xi=\mathbf{0}$ and consider the map $\mathbf{u}=\mathbf{H}(\tau)$. The first order derivatives of $\mathbf{u}$ with respect to τ are given by

$$\frac{\partial \mathbf{u}}{\partial \boldsymbol{\tau}} = \frac{\partial \mathbf{u}}{\partial \mathbf{z}} \mathbf{Q}_1^{t} = \left(\mathbf{Q}_1^{t\prime} \frac{\partial \mathbf{z}}{\partial \mathbf{u}} \right)^{+} = \mathbf{R}_1^{-1} = \mathbf{K} \tag{20}$$

where $\mathbf{Q}_1^{t}$ and $\mathbf{R}_1$ are the tangential components from the QR decomposition of the matrix $\partial\mathbf{z}/\partial\mathbf{u}$, and the superscript $^{+}$ denotes the generalized matrix inverse. Assuming that the matrix $\mathbf{Q}_1^{t}$ does not vary as $\mathbf{z}$ is varied (which is true locally), the second order derivatives are given by

$$\frac{\partial^2 \mathbf{u}}{\partial \boldsymbol{\tau} \partial \boldsymbol{\tau}'} = -(\mathbf{K})\left(\mathbf{K}' \mathbf{A}_r^{t} \mathbf{K}\right) = -(\mathbf{K})\left(\mathbf{C}_r^{t}\right) \tag{21}$$

where $\mathbf{A}_r^{t}$ and $\mathbf{C}_r^{t}$ are the tangential components of the acceleration array and the relative acceleration array, respectively, for the steady-state input-state map. The problem with this approach is that the assumption that $\mathbf{Q}_1^{t}$ does not vary as $\mathbf{z}$ is varied may often be a very poor one. As a result, the inverse calculated from Equations (20) and (21) may be unreliable. Only approximate second-order information about the inverse process map can be obtained from the analysis of the input-state map. Therefore, the extent of control-law nonlinearity cannot be directly assessed by studying the input-state map only. The process inverse map, $\Pi: \mathbf{Y} \subset \mathbb{R}^M \rightarrow \mathbf{U} \subset \mathbb{R}^P$, must be analyzed directly.

To do this, we can repeat the analysis by using derivatives of the inputs with respect to the state space,or output space, to obtain an assessment of the nonlinearity of the inverse map. We first define a region of interest in the input space and use the size of this region to define a scaling matrix to give scaled inputs

$$\mathbf{w} = \mathbf{T}\mathbf{u}.$$

The required derivatives are then given by

$$\dot{\mathbf{r}} = \frac{\partial \mathbf{w}(\mathbf{z})}{\partial \mathbf{z}}$$

for the velocity vectors and

$$\ddot{\mathbf{r}} = \frac{\partial^2 \mathbf{w}(\mathbf{z})}{\partial \mathbf{z} \partial \mathbf{z}'}$$

for the acceleration vectors. We can then proceed to perform the QR decomposition of the velocity and non-redundant acceleration vectors as

$$\left[\dot{\mathbf{r}},\ \ddot{\mathbf{r}}_{11},\ \ddot{\mathbf{r}}_{12},\ \ddot{\mathbf{r}}_{22},\ \ldots,\ \ddot{\mathbf{r}}_{1P},\ \ldots,\ \ddot{\mathbf{r}}_{PP}\right] = \left[\mathbf{Q}_{1i}^{t} | \mathbf{Q}_{1i}^{n} | \mathbf{Q}_{2i}\right] \begin{bmatrix} \mathbf{R}_{1i} & \mathbf{A}_i^{t} \\ 0 & \mathbf{A}_i^{n} \\ 0 & 0 \end{bmatrix} \tag{22}$$

which gives the acceleration array

$$\mathbf{A}_i = \left[\mathbf{Q}_{1i}^{t} | \mathbf{Q}_{1i}^{n}\right]^{T} \left[\ddot{\mathbf{r}}_{11}, \ddot{\mathbf{r}}_{12}, \ddot{\mathbf{r}}_{22}, \ldots, \ddot{\mathbf{r}}_{1N}, \ldots, \ddot{\mathbf{r}}_{NN}\right] \tag{23}$$

and the relative acceleration array

$$\mathbf{C}_{ir} = \mathbf{K}_i' \mathbf{A}_{ir} \mathbf{K}_i. \tag{24}$$

where $\mathbf{K}_i = \mathbf{R}_{1i}^{-1}$. The subscript i indicates that these values have been calculated from the inverse map. The RMS curvatures can then be defined as in Equations (8), (9) and (10). This analysis gives a direct assessment of control-law nonlinearity but it also yields an appreciation of open-loop nonlinearity. The nonlinearity of the input-output map creates distortion in regions in the

output space given by

$$\mathbf{w(z)'w(z)} = 1$$

which are ellipsoidal in the input space. When the extent of nonlinearity is negligible, these regions can be approximated by

$$\Delta \mathbf{z}' \left(\frac{\partial \mathbf{w}}{\partial \mathbf{z}} \right)' \left(\frac{\partial \mathbf{w}}{\partial \mathbf{z}} \right) \Delta \mathbf{z} = 1. \tag{25}$$

Compensation of nonlinear effects can also be performed as described in the previous section. We can define tangential coordinates as

$$\boldsymbol{\tau}_i = \mathbf{Q}_{1i}^{t'} \mathbf{w} \tag{26}$$

and normal coordinates as

$$\boldsymbol{\xi}_i = -\boldsymbol{\tau}_i' \mathbf{C}_{ir}^{n} \boldsymbol{\tau}_i \tag{27}$$

and compute the derivatives of $\mathbf{y}$ with respect to τ as

$$\frac{\partial \mathbf{y}}{\partial \boldsymbol{\tau}_i} = \mathbf{K}_i , \quad \frac{\partial^2 \mathbf{y}}{\partial \boldsymbol{\tau}_i \partial \boldsymbol{\tau}_i'} = -(\mathbf{K}_i)(\mathbf{K}_i' \mathbf{A}_{ir}^{t} \mathbf{K}_i) = -(\mathbf{K}_i)(\mathbf{C}_{ir}^{t}) \tag{28}$$

to obtain an approximate inverse relationship.

As discussed in the previous section, it is possible to consider the input-output behaviour of a process. Since the inverse process gain is frequently rank-deficient, we can also consider the application of the methodology to the inverse process graph. This graph would take the form

$$\Gamma_p^I = \begin{pmatrix} \mathbf{y} \\ \mathbf{g}^I(\mathbf{y}) \end{pmatrix}.$$

As mentioned above, this would require the simultaneous scaling of the inputs and the outputs.

7. Effect of Scaling

An important feature of the methodology presented here is the definition of a region of interest in the output space or in the input space. When considering the nonlinearity of the steady-state locus, we defined a scaling matrix which was used to develop a scale-independent measure of nonlinearity. The main effect of pre-multiplying coordinates by this matrix is the imposition of an orientation which may or may not be inherent to the process. As a result, the nonlinear effects may be enhanced or diminished for directions in the input or output space which do not reflect the actual effects of the process. An appropriate choice of scaling matrix is of great importance in this methodology and should be performed with care to ensure that the true nonlinearity of the process is accurately assessed. In general, this choice will be determined from prior investigations which dictate typical variations and orientation.

It is not necessary, however, to dictate regions of interest in both the input and output spaces, as the choice of a region of interest for one space will dictate an appropriate region for the other through the input-output map. For the case where a region in the input space is specified, the scaling matrix describes an ellipsoidal region in the input space which can be mapped to the output space, where it becomes distorted and rotated. A linear approximation for a specified region in the input space is given by

$$\Delta \mathbf{y}' \left(\frac{\partial \mathbf{w}'}{\partial \mathbf{y}} \frac{\partial \mathbf{w}}{\partial \mathbf{y}} \right) \Delta \mathbf{y} = 1$$

or,

$$\Delta \mathbf{y}' \mathbf{R}_{1i}' \mathbf{R}_{1i} \Delta \mathbf{y} = 1.$$

Therefore we can take $\mathbf{R}_{1i}$ as an appropriate output scaling matrix with which to analyze the nonlinearity of the input-output map. This simple procedure, termed *Input Prescribed Scaling*, ensures that the choice of a region of interest is made with regard to the inherent process orientation. The term "input prescribed scaling" is used to emphasize the fact the scaling is performed with respect to the choice of a region of interest in the input space.

As an illustration, consider the following example due to Newell and Lee (1989). In this example nonlinearity measures are obtained for both input prescribed and output prescribed scalings.

Example 2.3

A diagram of an evaporator system as well as the model equations for the system are given in Figure 2.6. The model consists of three states, three inputs and five disturbances. The states are the liquid level in the separator (L2, m), the product composition (X2, mass %) and the operating pressure (P2, kPa). The inputs are the product flowrate (F2, kg/min), the steam pressure (P100, kPa) and the cooling water flowrate (F200, kg/min). The disturbances are the circulating flowrate (F3, kg/min), the feed flowrate (F1, kg/min), the feed composition (X1, mass%), the feed temperature (T1, °C) and the cooling water temperature (T200, °C). A summary of evaporator variables along with the values used in the simulation is also given in

Tables 2.4 and 2.5, respectively.

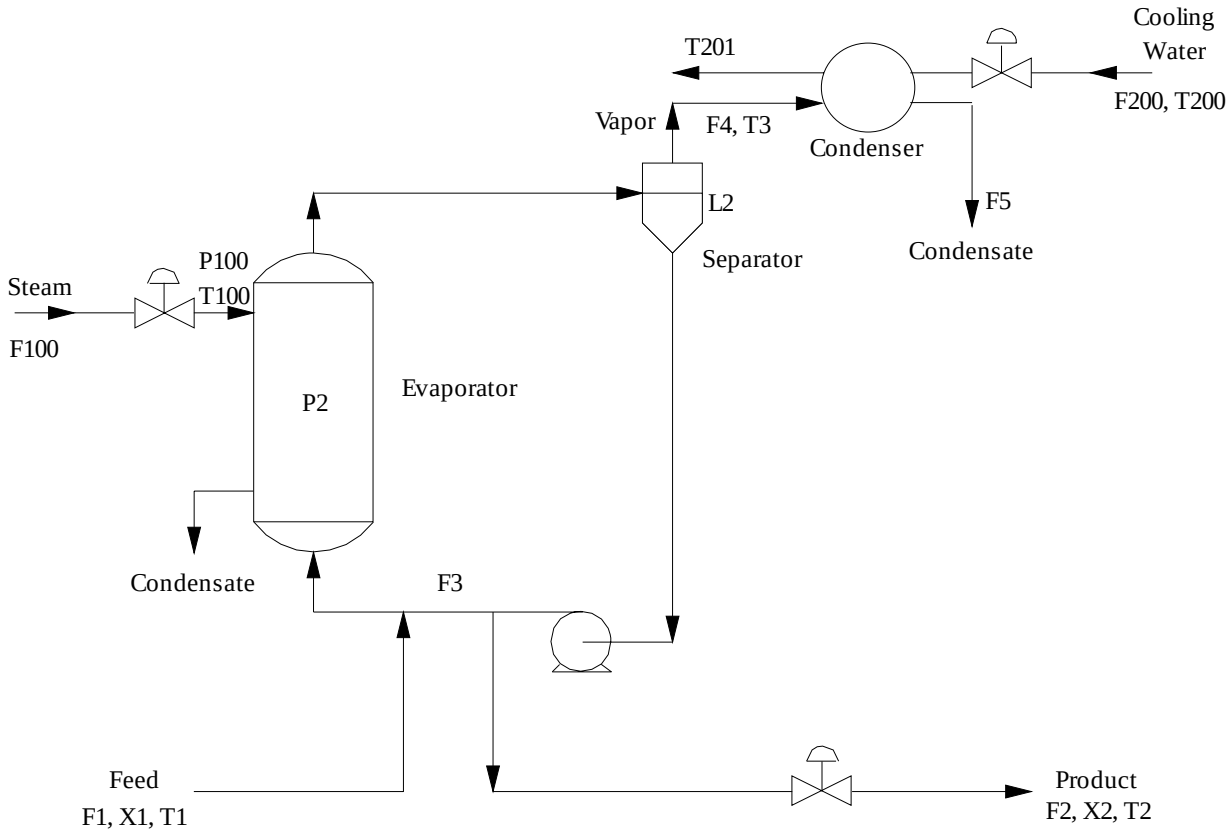

Figure 2.6 Process diagram for the evaporator model of Newell and Lee (1989).

Table 2.4

Description of variables for the evaporator model of Newell and Lee (1989).

Variable	Description	Values	Units
F1	Feed flowrate	10.0	kg/min
F2	Product flowrate	2.0	kg/min
F3	Circulating flowrate	50.0	kg/min
F4	Vapor flowrate	8.0	kg/min
F5	Condensate flowrate	8.0	kg/min
X1	Feed composition	5.0	mass%
X2	Product composition	25.0	mass%
T1	Feed temperature	40.0	°C
T2	Product temperature	84.6	°C
T3	Vapor temperature	80.6	°C
L2	Separator level	1.0	meters
P2	Operating pressure	50.5	kPa
F100	Steam flowrate	9.3	kg/min
T100	Steam temperature	119.9	°C
P100	Steam pressure	194.7	kPa
Q100	Heat duty	339.0	kW
F200	Cooling water flowrate	208.0	kg/min
T200	Cooling water inlet temperature	25.0	°C
T201	Cooling water outlet temperature	46.1	°C
Q200	Condenser duty	307.9	kW

Table 2.5

List of equations of the Newell and Lee evaporator model (1989).

Process Liquid Mass Balance: $$20\,dL2/dt = F1 - F4 - F2$$
Process Liquid Solute Mass Balance: $$20\,dX2/dt = F1X1 - F2X2$$
Process Vapor Mass Balance: $$4\,dP2/dt = F4 - F5$$
Process Liquid Energy Balance: $$T2 = 0.5616P2 + 0.3216X2 + 48.43$$ $$T3 = 0.507P2 + 55.0$$ $$F4 = \frac{Q100 - F1(T2 - T1)0.07}{38.5}$$
Heater Steam Jacket: $$T100 = 0.1538P100 + 90.0$$ $$Q100 = 0.16(F1 + F3)(T100 - T2)$$ $$F100 = Q100/36.6$$
Condenser: $$Q200 = \frac{6.84(T3 - T200)}{1 + 6.84/(2C_pF200)}$$ $$T201 = T200 + Q200/(F200C_p)$$ $$F5 = Q200/38.5$$

Prior to assessing steady-state nonlinearity, the liquid level control loop L2-F2, which is not self-regulatory, was closed using the PI controller settings given by Newell and Lee (1989). The analysis was then performed on the input-output map of the remaining 2 by 2 system.

We are interested in evaluating the nonlinearity of this process in a neighbourhood of the steady-state conditions

$$\mathbf{u} = \begin{bmatrix} \text{P100} \\ \text{F200} \end{bmatrix} = \begin{bmatrix} 194.7 \\ 208.0 \end{bmatrix}, \ \mathbf{y} = \begin{bmatrix} \text{X2} \\ \text{P2} \end{bmatrix} = \begin{bmatrix} 25.0 \\ 50.5 \end{bmatrix}.$$

We first consider assessing nonlinearity using output prescribed scaling. The scaling matrix which describes the region of interest in the output space is given by

$$\mathbf{S} = \begin{bmatrix} 1/(25)^{0.5} & 0 \\ 0 & 1/(49)^{0.5} \end{bmatrix}$$

From the QR decomposition of the scaled matrix of first order and second order derivatives, we obtain

$$\mathbf{R_1} = \begin{bmatrix} -0.029668 & -0.0028219 \\ 0 & -0.011278 \end{bmatrix}, \ \mathbf{C_r}^t = \left(\begin{bmatrix} -0.11498 & -0.09881 \\ -0.09881 & 0.12735 \end{bmatrix} \begin{bmatrix} -0.15293 & -0.15906 \\ -0.15906 & 0.69710 \end{bmatrix} \right).$$

If we use input prescribed scaling with a scaling matrix in the input space given by

$$\mathbf{T} = \begin{bmatrix} 0.016667 & 0 \\ 0 & 0.014286 \end{bmatrix}$$

we obtain a scaling matrix in the output space given by

$$\mathbf{S} = \begin{bmatrix} -0.17164 & 0.10260 \\ 0 & -0.11844 \end{bmatrix}.$$

Performing the QR decomposition on the scaled derivatives yields

$$\mathbf{R_1} = \begin{bmatrix} 0.016667 & 0 \\ 0 & 0.014286 \end{bmatrix}, \quad \mathbf{C_r}^t = \left(\begin{bmatrix} 0.13656 & 0.062590 \\ 0.062590 & 0.028688 \end{bmatrix} \begin{bmatrix} 0.61383 & 0.35125 \\ 0.35125 & -0.47996 \end{bmatrix} \right).$$

Since the matrix $\mathbf{R}_1$ is diagonal, we see that the relative curvature array obtained using input prescribed scaling is directly related to the original inputs. This yields an easier interpretation of the results. The relative curvature array obtained using output prescribed scaling is expressed in terms of the orthogonal inputs obtained with the matrix $\mathbf{R}_1$. It is important to note that a diagonal matrix is obtained whenever the gain matrix has mutually orthogonal columns.

For this example, both approaches suggest that the system displays significant open-loop nonlinearity. From the result obtained using input prescribed scaling, we see that most of the nonlinear behaviour is attributable to large variations in the process gain associated with F200, the cooling water flowrate. This is because only the elements of the second face of the relative curvature array are large. The most prominent element, 0.61383, indicates an increase in the process gain associated with F200 as P100 is increased.

Figure 2.7 shows a portion of the steady-state locus for the process along with the regions of interest obtained with input prescribed scaling and output prescribed scaling. The solid lines are constant P100 lines. The dashed lines are constant F200 lines. As observed above, most of the nonlinearity is attributable to the change in the process gain associated with F200.

The input prescribed scaling region captures the overall orientation of the steady-state process well and this has a significant effect on the extent of nonlinearity observed. Even though the prescribed region covers a larger neighbourhood about the point of linearization in the output space, we observe the same degree of nonlinearity for both choices of scaling region. Output

prescribed scaling does not take into account the orientation of the process. As a result, nonlinear effects and interaction effects are confused.

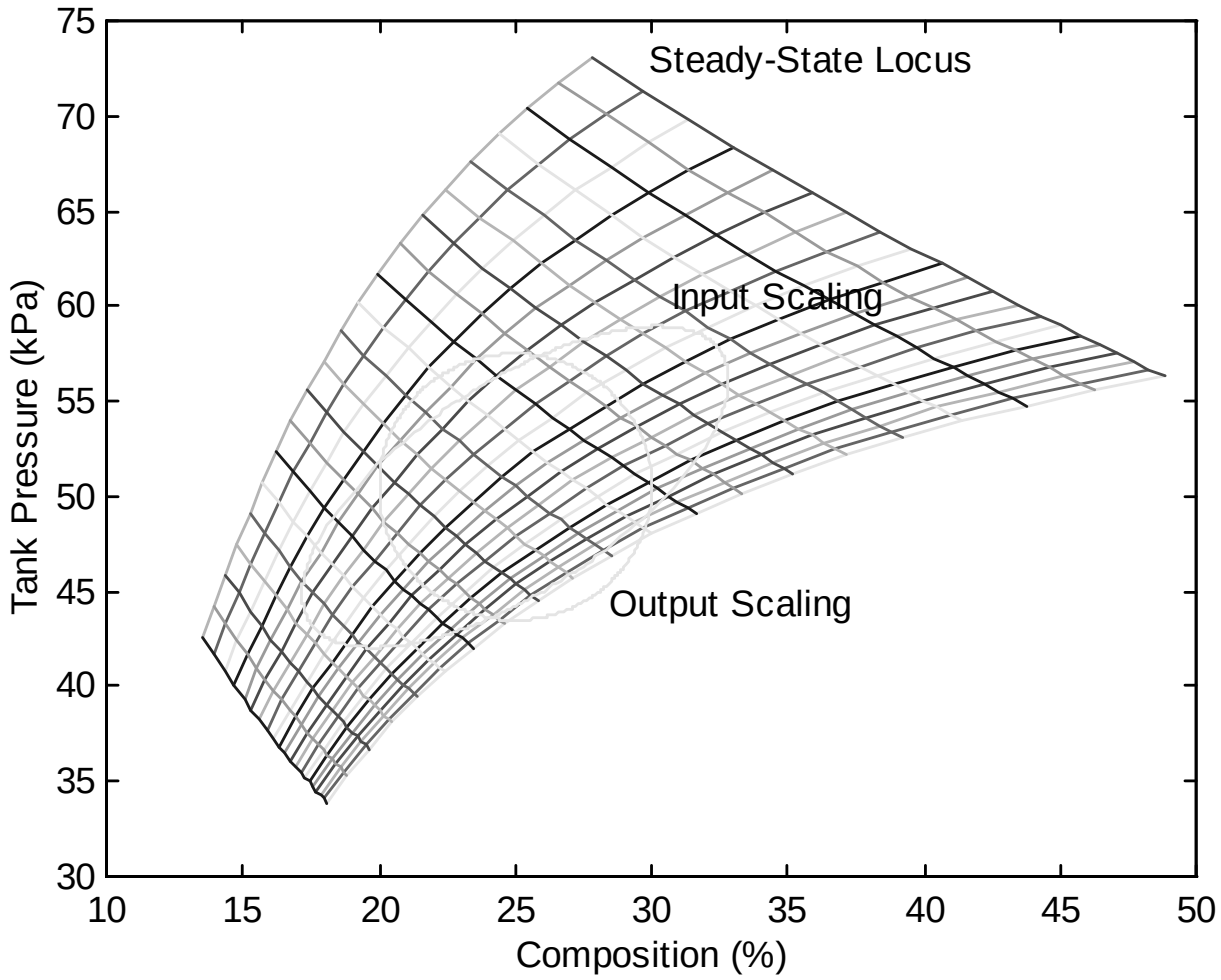

Figure 2.7 Steady-state locus for the evaporator model of Newell and Lee (1989). Solid lines show the effect of variation of F200. Dashed lines give the effect of the variation of P100.

8. Nonlinearity and Performance

In this section we consider the single-input bioreactor introduced in Example 2.1 to study the effect of nonlinearity on controller performance. More precisely, we demonstrate the applicability of the nonlinearity measures in controller design.

The problem considered here is to control the substrate concentration, x_2, by manipulating the dilution rate, u_1, for a constant inlet substrate concentration, S_0=0.3. Substrate is a suitable choice of control variable in this case because of its relative ease of measurement. This allows small measurement times and quick control action. The process is to be operated under the following constraints

$$0.001 \leq u_1 \leq 0.03$$

$$0.15871 \leq x_2 \leq 0.20343.$$

For this range of substrate levels, the RMS steady-state curvature experienced in x_2 at 0.18107 is 0.26. This can be calculated from the velocity and acceleration vectors given in Example 2.1.

Three controllers are considered: a nonlinear input-output linearizing controller with proportional action only, a linear state-feedback controller with proportional-integral action and a proportional-integral controller on the substrate. The linear state-feedback controller was obtained by linearizing the model equations at the nominal operating point. Optimal ITAE tunings were obtained for the three controllers for substrate set-point values of 0.15871 and 0.20343. ITAE was chosen in order to penalize sustained deviation from the set-points.

Optimal tuning parameters and optimal ITAE values for the three controllers are shown in Table 2.6. The impact of nonlinearity on controller performance is assessed by examining the increase in ITAE as set-point changes of larger magnitudes are made. Differences in the rate of

increase between nonlinear and linear controllers are a reflection of the nonlinearity of the process in a neighbourhood of the nominal operating point. Investigations of these trends enables one to attach an interpretation to the nonlinearity measures. Furthermore, for a truly linear process without mismatch, ITAE increases linearly as the size of the set-point change increases. This can be seen by considering the transfer function relating error to set-point. Thus, the impact of nonlinearity can be seen by examining both the relative trends of the controllers and the degree of nonlinearity in the ITAE trends.

Table 2.6

Optimal ITAE tunings for a nonlinear input-output linearizing controller, a linear state-feedback controller, a PI controller and a nonlinear gain PI controller and optimal ITAE

	Nonlinear Controller	Linear Controller	PI Controller	Nonlinear Gain PI Controller
K_c	-0.047867	-0.047866	-0.40250	-0.62132
τ_I	----------	$e^{3.4999}$	$e^{3.1080}$	3.1019
C_c	----------	----------	----------	-19.660
ITAE	19.517	67.262	68.504	41.908

Figure 2.8 compares the performance of the controllers at various fractions of the range of substrate set-points. First, note that the presence of normal curvature requires the use of integral action in the linear controller laws to compensate for mismatch arising from the

Figure 2.8 Optimal ITAE performance for a nonlinear input-output linearizing controller, a linear state-feedback controller and a PID controller for substrate.

nonlinearity. The trends of Figure 2.8 confirm the presence of moderate nonlinearity. The ITAE of the linear controllers increases at a faster rate than that of the nonlinear controller for increasing changes in set-point. The nonlinear control-law provides a better representation of the

nonlinear process behaviour and can provide a compensation which moves the process to a new set-point faster. This is particularly true when the operation shifts significantly away from the nominal operating point, which is the point of linearization. Note that the ITAE profile for the input-output linearizing controller is exactly linear, confirming the linearity of the input-output relationship imposed by the controller. The ITAE profile for the linear controllers both exhibit some nonlinearity, although the nonlinearity is not large. This confirms the moderate nonlinearity implied by the measures. Figure 2.9 gives the resulting responses for the three controllers for set-point changes in substrate from 0.18107 to 0.15871 and 0.20343. The time responses for the biomass concentration (x_1), substrate concentration (x_2) and dilution rate (u_1) are shown. On the left, a set-point decrease in substrate from 0.18107 to 0.15871 is shown and, on the right, a set-point increase from 0.18107 to 0.20343.

The nonlinear controller yields a more favourable performance. In contrast to the response of the linear controllers, there is no oscillatory behaviour. This is due to the absence of integral action in the nonlinear controller. Although there is a noticeable difference between linear and nonlinear controller performance in the trends of Figure 2.8, both linear controllers yield a relatively good performance which reflects the fact that the curvature is relatively low in this case.

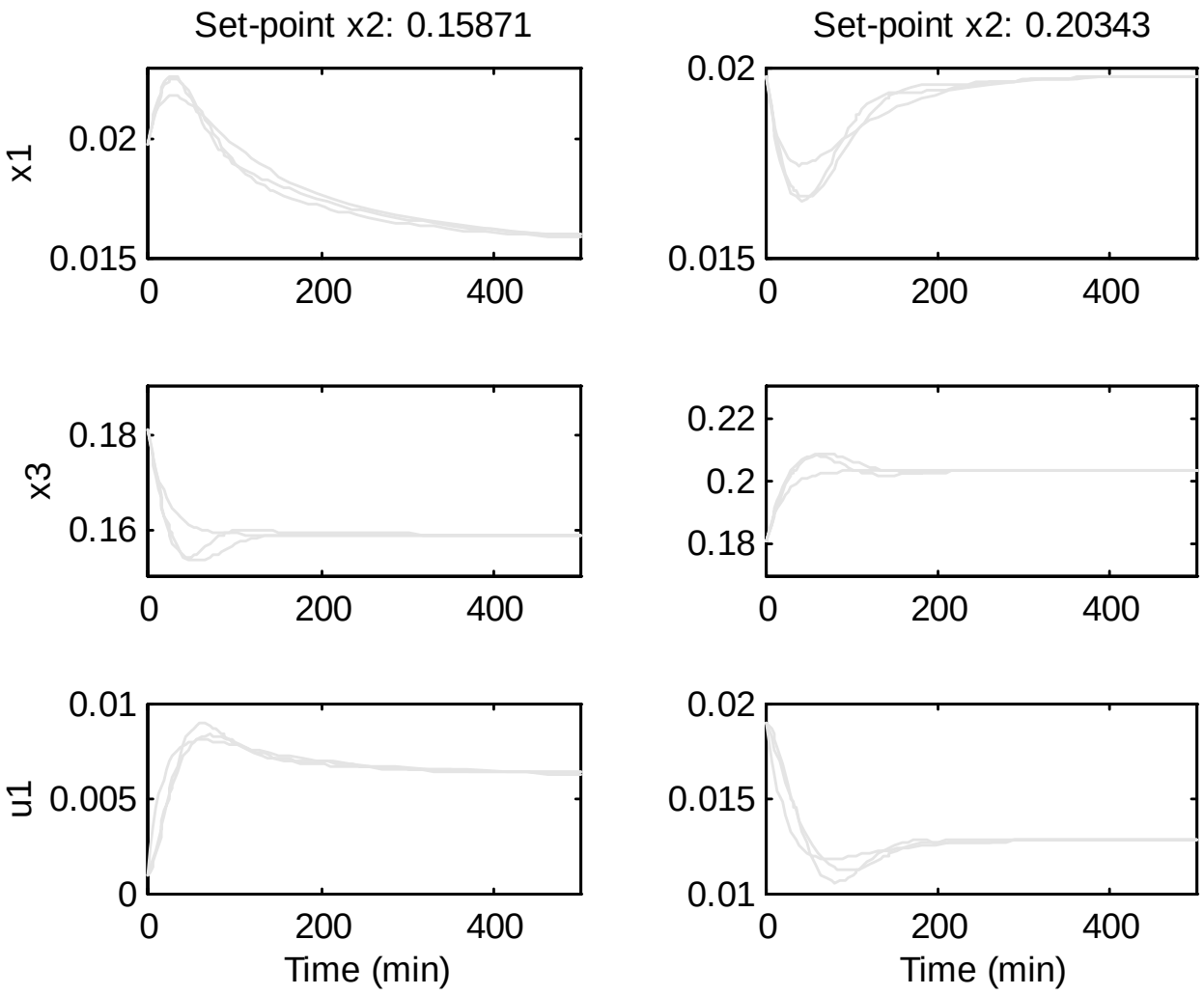

Figure 2.9 Time response for the optimal ITAE tunings of a nonlinear input-output linearizing controller (solid line), a linear state-feedback (dashed line) and a PI controller (dotted line).

We can also design a controller based on the inversion of an expression of Equation (12).

A local estimate of the inverse of this expression is given by

$$\boldsymbol{\phi} = \mathbf{H}^{-1}(\boldsymbol{\tau}) = \boldsymbol{\tau} - \frac{1}{2}\boldsymbol{\tau}'\mathbf{C}_r\boldsymbol{\tau} \tag{29}$$

A SISO PI controller design based on this expression would be of the form

$$\Delta \mathbf{u} = \mathbf{K}_c(\mathbf{y}_{sp} - \mathbf{y}) + (\mathbf{y}_{sp} - \mathbf{y})'\mathbf{C}_c(\mathbf{y}_{sp} - \mathbf{y})' + \frac{1}{\tau_I}\int_0^t (\mathbf{K}_c(\mathbf{y}_{sp} - \mathbf{y}) + (\mathbf{y}_{sp} - \mathbf{y})'\mathbf{C}_c(\mathbf{y}_{sp} - \mathbf{y})')dt$$

where $\mathbf{K}_c$ and τ_I are the usual controller gain and integral time constant and $\mathbf{C}_c$ is the controller curvature. The resulting controller is termed a nonlinear gain PI controller. Using the same tuning procedure as described above, optimal ITAE tuning parameters were calculated for this controller. The values are listed in Table 2.6. The nonlinear gain controller performs better than the two linear controllers but not as well as the nonlinear I-O linearizing controller. If we consider the resulting controller gain and controller curvature and calculate the resulting controller RMS curvature for the region u_1=0.01±0.005, we obtain a value of 0.26. For this case, the resulting nonlinear gain controller reflects the local nonlinearity observed for the process.

9. Conclusions

A framework for the assessment of steady-state process nonlinearity has been developed. It involves evaluating the tangential and normal components of second order information within a prescribed region of interest. The magnitudes of second order derivatives are used to develop a measure of the deviation from linearity of a process in a prescribed region. The tangential component of the second order derivatives is related to variations in the magnitude of the process gain. The normal component is related to variations in the direction of the process gain. The main advantage of this framework is that it allows a generic treatment of nonlinear systems. Although only two-dimensional examples have been presented, the framework is readily extended to higher dimensional systems. Since this analysis deals with steady-state nonlinearity, it can be performed for given input-state or input-output relationships.

Two aspects of nonlinearity have been identified: control-law and open-loop nonlinearity. Open-loop nonlinearity is related to the ability to predict the output of a process given the inputs. It is closely related to the concept of the left inverse of a control system (Hirschorn, 1979). Control-law nonlinearity measures the ability to predict the inputs required to achieve a given output, a notion which is related to the concept of the right inverse of a process.

To assess these aspects of nonlinearity, it has been shown that either the input-output map or its inverse may be considered. However, the extent of open-loop nonlinearity is more directly measured through analysis of the input-output map. The inverse map provides a better assessment of control-law nonlinearity.

The importance of scaling has been highlighted, since the extent of nonlinearity is measured with respect to some prescribed region. The choice of this region, and consequently the choice of scaling, is crucial to successful application of this method. A simple scaling procedure has been proposed which takes into account the inherent orientation of the process.

In this Chapter, a framework was established for the analysis of nonlinearity of steady-state process behaviour. In the following chapters, the framework is applied to the assessment of closed-loop nonlinearity and to dynamic nonlinearity.

Nomenclature

a_{ijk}	partial derivatives with respect to u_j and u_k of the i^{th} coordinate of the rotated state space
A	N by P(P+1)/2 matrix of nonredundant acceleration vectors in orthonormal frame
	N by N Jacobian matrix with respect to the states of a nonlinear system at a particular point
A	Area of a (P-1) dimensional sphere described by P dimensional unit-norm vectors
b	Real number
B	N by P Jacobian matrix with respect to the inputs of a nonlinear system at a particular point
c	Root mean squared curvature measure
C	N by P(P+1)/2 matrix of nonredundant relative acceleration vectors
C_c	Controller derivative action tuning parameter
D	N by P matrix
e	Arbitrary direction in the input space
f	Vector field describing dynamics on the state space
f_{11}	Real number
F	1 by N matrix resulting from transforming a linear system to a linear controllable form
F1	Feed flowrate (kg/min)

F2	Product flowrate (kg/min)
F3	Circulating flowrate (kg/min)
F4	Vapor flowrate (kg/min)
F5	Condensate flowrate (kg/min)
F100	Steam flowrate (kg/min)
F200	Cooling water flowrate (kg/min)
G	Nonlinear transformation describing normal coordinates on steady-state locus
h	State-output map
H	Nonlinear vector valued function from input space to output space expressed in tangential and normal coordinates
k_d	Specific death rate (min^{-1})
K	Matrix inverse of upper left P by P partition of the matrix **R** obtained from the QR decomposition
K_c	Controller proportional action tuning parameter
K_i	Substrate inhibition constant (L/g)
L2	Separator level (meters)
M	Number of output variables
N	Number of state variables
$\mathbf{N}_e$	Set of stationary points of the vector field **f**(**x**,**u**)
P	Number of input variables
P	N by N matrix transforming a linear system to a linear controllable form
P2	Operating pressure (kPa)

P100	Steam pressure (kPa)
Q	Orthogonal matrix obtained from the QR decomposition of a matrix
Q100	Heat duty (kW)
Q200	Condenser duty (kW)
r	Real number $\in$ [0,1]
$\dot{\mathbf{r}}$, $\ddot{\mathbf{r}}$	Velocity and acceleration vectors in the space of inputs
R	Upper triangular factor obtained from the QR decomposition of a matrix
S	Output scaling matrix
S_0	Inlet feed substrate concentration (g/L)
t	Time
T	Input scaling matrix
T1	Feed temperature (°C)
T2	Product temperature (°C)
T3	Vapor temperature (°C)
T100	Steam temperature (°C)
T200	Cooling water inlet temperature (°C)
T201	Cooling water outlet temperature (°C)
u	Vector of input variables
u_1	Dilution Rate (min^{-1})
U	Open neighbourhood of a point $\mathbf{u}_0$ in the input space
$\dot{\mathbf{v}}$, $\ddot{\mathbf{v}}$	Velocity and acceleration vectors in the state (or output) space
V	N by P matrix of velocity vectors

w	Vector of scaled input variables
W	N by P(P+1)/2 matrix of nonredundant acceleration vectors
x	Vector of state variables
x_1	Biomass Concentration (g/L)
x_2	Substrate Concentration (g/L)
x	Vector of time derivatives of state variables
X	Open neighbourhood of a point $\mathbf{x}_0$ in the state space
X1	Feed composition (mass%)
X2	Product composition (mass%)
y	Vector of output variables
z	Vector of scaled state or output variables
z	Vector of states for a linear controllable form

Greek letters

Γ_p	Process graph
Γ_p^I	Inverse process graph
δ	Small positive real number
ε	Small positive real number
θ	Arbitrary direction in the space of orthogonal inputs
μ_{max}	Maximum specific growth rate (min^{-1})
ξ, ξ_i	Vector of normal coordinates from the input-state (or input-output) map and its inverse, respectively
Ξ	Nonlinear map from an open neighbourhood in the input space to an open

neighbourhood in the state (or output) space

Π Nonlinear map from an open neighbourhood in the state (or output) space to an open neighbourhood in the input space

τ, τ_i Vector of tangential coordinates from the input-state (or input-output) map and its inverse, respectively

τ_I Controller integral action tuning parameter

ϕ Vector of orthogonal inputs

Subscripts

0 Specifies steady-state conditions

1, 1i Specifies the component of the **Q** matrix from the QR decomposition which spans the tangential and normal space of the steady-state locus from the input-state (or input-output) map and its inverse, respectively

1,1i Specifies the upper left P by P component of the **R** matrix from the QR decomposition for the analysis of the input-state (or input-output) map and its inverse, respectively

2 Specifies the component of the matrix **Q** which gives the orthogonal complement of $\mathbf{Q}_1$

•2 Specifies the second column of the tangential component of the **Q** matrix from the QR decomposition

i Specifies that the quantity (i.e., τ, ξ, **K**) is evaluated for the inverse relationship

r, ir Specifies the rearrangement of an n by m(m+1)/2 matrix to its corresponding n by m by m three-dimensional array for the analysis of the input-state (or

input-output) map and its inverse, respectively

Superscripts

´	Transpose of a matrix or vector
+	Generalized inverse of a matrix
n	Specifies the normal component of the quantity (i.e., **A**, $\mathbf{Q}_1$, **C**)
t	Specifies the tangential component of the quantity (i.e., **A**, $\mathbf{Q}_1$, **C**)
N,M,P	Indicates the dimension of the space

Overstrikes

~	Indicates that the quantity has been scaled
., ..	Indicates first and second order differentiation of the quantity

Chapter 3

On a Measure of Closed-Loop Nonlinearity and Interaction for Nonlinear Chemical Processes

1. Introduction

The performance of closed-loop multivariable processes can be highly influenced by interactions between individual control loops. For many applications involving linear dynamics, the relative gain array (RGA) (Bristol, 1966) provides an effective tool for the evaluation of potential control loop pairings for multi-loop controller design. Quantitative measures of interaction such as the RGA have been used successfully in the control of linear chemical processes and continue to be of considerable importance, especially with respect to the study of robust stability (Grosdidier and Morari, 1987; Skogestad and Morari, 1987; Morari and Campo, 1994) and performance of ill-conditioned plants (Nett and Manousiouthakis, 1987; Skogestad and Morari, 1987; Skogestad *et al*., 1988).

Since the RGA is basically a first order measure of interaction, its interpretation for nonlinear processes relies heavily on the direction of the input (or output) perturbations used to estimate gains (Koung and MacGregor, 1991). Problems can be encountered in the study of gain-asymmetric processes where interpretation of the RGA may often yield misleading results. Interaction measures which take the gain nonlinearity of the process into account can prove beneficial in overcoming these problems in a number of cases.

Very few measures of interactions for nonlinear processes have been proposed. Daoutidis and Kravaris (1992) used a differential geometric approach to develop a methodology for the evaluation of control configurations in nonlinear control-affine processes. With this approach

various control configurations are evaluated in terms of their corresponding relative order. Input-output pairings are selected by virtue of the most immediately related (or less sluggish) pairs. Assuming the availability of a detailed state space description of the process, this control pairing selection methodology constitutes a very useful strategy for providing insight into the structure of nonlinear systems. However, no information is provided regarding the magnitudes of output changes in response to input changes.

Manousiouthakis and Nikolaou (1989) developed a nonlinear block relative gain array measure using an operator-based approach which elegantly demonstrated the need to consider nonlinear effects in the assessment of interaction in nonlinear plants. This approach, although very general and appealing, can constitute a considerable challenge when applied to complex plants. Other approaches to this problem include that of Mijares *et al.* (1985) who developed a methodology for assessing nonlinear interaction from evaluation of first order gains.

Piette *et al.* (1995) have presented a graphical interpretation of the relative gain array in terms of intersections of constant output contours and the degree of rotation of constant output norm contours. A graphical assessment for nonlinear problems is also proposed which consists of relative gain surfaces and constant output norm contours. Nonlinear effects are identified by deformations in the contours, and by changes in the relative gains over the operating region. This latter approach is consistent with the approaches identified above in which changes in linear approximations are used to identify nonlinearity and nonlinear interactions. The main drawback of graphical methods is their inherent subjectivity and the dependence on the particular graphical representation employed.

The purpose of this chapter is to present an alternative geometric interpretation of the

RGA which extends directly to the treatment of higher (in particular, second) order interactions in nonlinear processes. Furthermore, the problem of interaction is identified fundamentally as the result of input and output coordinate choices. Standard linear techniques such as the relative gain array identify interactions in coordinate choices arising at the first order level. The approach presented is based on the framework proposed in Chapter 2 for the assessment of process nonlinearity of steady-state nonlinear processes. This framework leads to scale-independent measures for the average deviation of the actual behaviour of a nonlinear process from its linear approximation in a neighbourhood of a steady-state, and highlights two perspectives of process nonlinearity: Open-Loop nonlinearity and Control-Law nonlinearity. Open-loop nonlinearity is related to the ability to predict process states and outputs given values of the manipulated variables. It reflects the inherent process nonlinearity. Control-law nonlinearity is the ability to determine the inputs from a particular output or state vector. In the development presented in the current Chapter, methods are proposed for assessing nonlinearity within and between input-output channels. This leads to the definition of a measure of higher order interaction, and also leads to the concept of closed-loop nonlinearity.

For a nonlinear closed-loop process operating at steady-state without offset, it follows that the extent of open-loop nonlinearity, that is, nonlinearity due to input variation, is exactly counterbalanced by the control-law nonlinearity. From a differential geometric perspective, this is because either the inputs or the outputs can be used to parametrize the same space at steady-state. By viewing the inputs and outputs as two coordinate systems on a differentiable manifold, we can establish, through differential geometry, a number of interesting identities which provide local measures of interaction. A direct consequence of this construction is the recognition of a

certain arbitrariness in the choice of coordinates. We do not distinguish, a priori, between input and output variables. Interchangeability of input and output coordinates has been widely discussed by system theorists, particularly with respect to the development of behavioral approaches in the study of dynamical systems (Willems, 1991) and closely related differential algebraic methods (Fliess *et al.*, 1994). In this approach, it becomes more natural to let the underlying structure of the system dictate appropriate choices for the inputs and outputs.

The advantages of interchangeability of coordinate systems is demonstrated here in the development of interaction measures for nonlinear steady-state processes. It is shown that this approach provides a natural rigorous framework for studying interaction effects for both linear and nonlinear systems which provides a fundamental basis for the development of measures of closed-loop nonlinearity and new measures of nonlinear interaction. The result is a set of nonlinear interaction tables that provide easy interpretation of the contribution of nonlinear effects to interaction effects. A CSTR model is used to demonstrate the application of the method.

The format of this Chapter is as follows. In Section 2 the differential geometric basis for this analytical procedure is presented and a number of identities are derived. The application of these identities to the assessment of closed-loop nonlinearity for nonlinear processes is presented in Section 3. In Section 4 a simple chemical reactor example is used to illustrate the application of the measures of nonlinearity. It is shown, in Section 5, how the identities can be used to assess the extent of nonlinearity of closed-loop processes. Nonlinear interaction measures are presented in Section 6. This is followed by two chemical process examples in Section 7 and conclusions in Section 8.

2. Relationship Between Open-Loop and Control-Law Nonlinearity

In this section, classical differential geometric tools (see Boothby, 1975) are used to establish a relationship between open-loop and control-law nonlinearity. Some details pertaining to differential geometrical approaches for process control are provided in Kravaris and Kantor (1991). As will be demonstrated, the resulting relationship yields a nonlinear analogue of the relative gain array (RGA) (Bristol, 1966), an empirical measure of interaction in square linear multi-input multi-output systems.

Formally, the dynamic input-output relationship for a nonlinear process can be described by an implicit relationship of the form

$$\mathbf{G}(\mathbf{x}_0,\mathbf{y},\mathbf{y}^{(1)},\mathbf{y}^{(2)},\ldots,\mathbf{y}^{(N)},\mathbf{u},\mathbf{u}^{(1)},\mathbf{u}^{(2)},\ldots,\mathbf{u}^{(N)}) = \mathbf{0} \tag{1}$$

which, at steady-state, gives a relationship of the form

$$\mathbf{G}(\mathbf{x}_0,\mathbf{y},\mathbf{u}) = \mathbf{0}. \tag{2}$$

The state variables, **x**, evolve on an N-dimensional manifold. The outputs, **y**, and the inputs, **u**, are P-dimensional vectors. The subscript $_0$ denotes initial conditions which specify an initial position in the state space.

Assuming that the state space behaviour of a nonlinear system described by

$$\dot{\mathbf{x}} = \mathbf{f}(\mathbf{x},\mathbf{u})$$

is such that the Jacobian matrix $(\partial\mathbf{f}(\mathbf{x},\mathbf{u})/\partial\mathbf{x})$ evaluated at $(\mathbf{x}_0, \mathbf{u}_0)$ is stable and invertible and the sensitivity matrix $(\partial\mathbf{f}(\mathbf{x},\mathbf{u})/\partial\mathbf{x})$ has rank P in a neighbourhood of $\mathbf{x}_0$, then equation (2) describes a P-dimensional submanifold of $\mathbb{R}^P\times\mathbb{R}^P$, called the steady-state process graph of the input-output relationship in the following way. For a given $\mathbf{x}_0$ it is assumed that the steady-state input-output

relationship, can be described by an expression of the form

$$\mathbf{G}(\mathbf{y},\mathbf{u}) = \mathbf{G}(\mathbf{G}_p(\mathbf{u}),\mathbf{u}) = \mathbf{0} \tag{3}$$

where $\mathbf{y} \in Y \subset \mathbb{R}^P$ and $\mathbf{u} \in U \subset \mathbb{R}^P$ and $\mathbf{G}_p$ is the process steady-state map in the output coordinates. The graph (e.g. Georgiou, 1993) of a steady-state process can be written as a map

$$\mathbf{\Gamma}_p(\mathbf{u}) = \begin{pmatrix} \mathbf{G}_p(\mathbf{u}) \\ \mathbf{u} \end{pmatrix} \tag{4}$$

or, alternatively, as a map

$$\mathbf{\Gamma}_p^I(\mathbf{y}) = \begin{pmatrix} \mathbf{y} \\ \mathbf{G}_c(\mathbf{y}) \end{pmatrix} \tag{5}$$

where the superscript ^{I} is used to denote the inverse steady-state process graph.

Equation (3) defines a P-dimensional manifold, **M**, modeled on $\mathbb{R}^P$. It follows from Equations (3), (4) and (5) that **M** can be locally expressed in either **u** or **y** coordinates. By definition, this implies the existence, for every point p of **M**, of an open neighbourhood diffeomorphic to some open set of $\mathbb{R}^P$ such that **M** is completely covered by the union of such open neighbourhoods. Let u_1, ..., u_P and y_1, ..., y_P represent local coordinate representations in open neighbourhoods **U** and **Y**, respectively, of a point p of **M**. Let $\mathbf{W}=\mathbf{U}\cap\mathbf{Y}\neq\oplus$ be an open set in **M**. By the definition of coordinate neighbourhoods for differentiable manifolds, it follows that there exists a diffeomorphism between the input and output coordinates for every point p of **W.** This diffeomorphism represents the usual process steady-state map in the u and y coordinates. This is shown schematically in Figure 3.1.

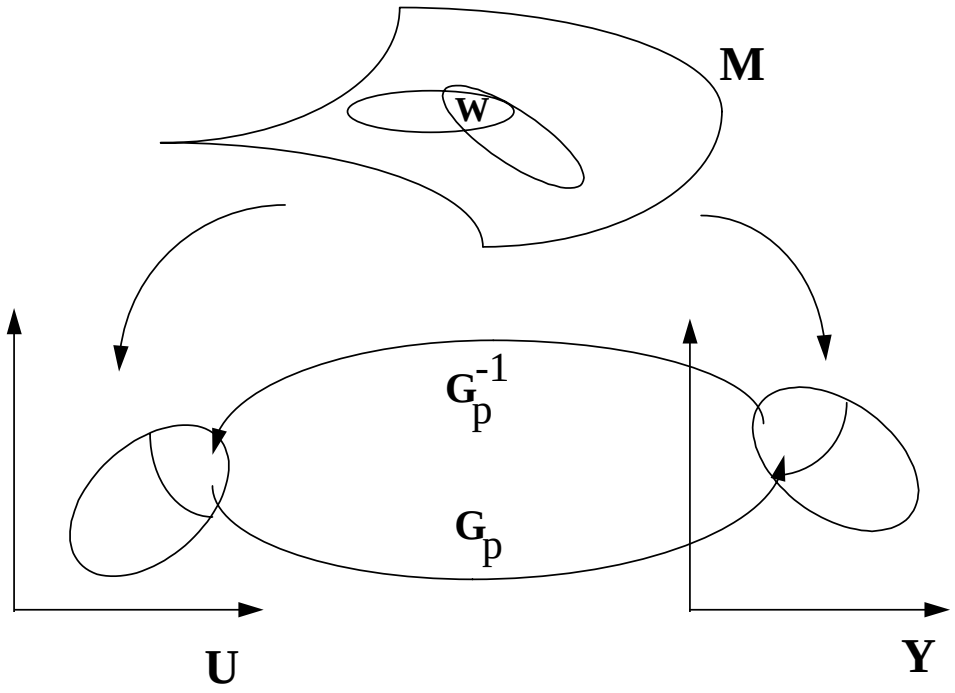

Figure 3.1 Inputs and outputs as coordinate systems on a differentiable manifold.

For every point $p \in \mathbf{W}$, let $\partial/\partial u_i$, $1 \le i \le P$, and $\partial/\partial y_j$, $1 \le j \le P$, represent local bases of $T_p\mathbf{M}$, the tangent space to **M** at p expressed in the u_i and y_j coordinates, respectively. The exchange of bases on T**M** at p, expressed in Einstein summation notation, is given by

$$\frac{\partial}{\partial u_j} = \frac{\partial y^i}{\partial u_j}\frac{\partial}{\partial y_i} \tag{6}$$

in the **y** coordinates, and by

$$\frac{\partial}{\partial y_i} = \frac{\partial u^k}{\partial y_i}\frac{\partial}{\partial u_k} \tag{7}$$

in the **u** coordinates. Note that the Einstein summation notation is used to express summations in the following wayBy this construction, variations in one coordinate system are immediately

$$\frac{\partial u^k}{\partial y_i}\frac{\partial}{\partial u_k} = \sum_{k=1}^{p} \frac{\partial u_k}{\partial y_i}\frac{\partial}{\partial u_k}$$

expressed in the other through the action of a diffeomorphism on **W**. Thus, if one considers a tangent vector in one coordinate system, it is possible to express it in terms of the other coordinate system. Clearly, for consistency, the tangent vector must be recoverable by the inverse mapping to the original coordinate system. To illustrate this, substitute Equation (7) into Equation (6). This gives

$$\frac{\partial}{\partial u_j} = \frac{\partial y^i}{\partial u_j}\frac{\partial u^k}{\partial y_i}\frac{\partial}{\partial u_k}$$

which yields the identities

$$\frac{\partial y^i}{\partial u_j}\frac{\partial u_k}{\partial y_i} = \begin{cases} 0 & , j \neq k \\ 1 & , j = k \end{cases} \tag{8}$$

The usual RGA formula appears within this expression

$$\Lambda_{ij} = \frac{\partial y_i}{\partial u_j}\frac{\partial u_j}{\partial y_i}. \tag{9}$$

The RGA identities of Equation (8) simply reflect the fact that the sum of the RGA elements from the same column is equal to 1. In this setting, the relative gain array adopts a very nice and natural interpretation. The RGA reflects the ability to exchange bases on T**M**. It gives a measure

of how individual components are mapped through the process map and its inverse.

Note that Equation (8) can be written in the standard form

$$\mathbf{\Lambda} = \mathbf{K} \otimes \mathbf{K}^{-T}$$

where **K** is the steady-state gain of the process and ⊗ denotes the Hadamard product of two matrices (see Morari and Zafiriou, 1989). Letting $\mathbf{K}^{-1}=\partial\mathbf{u}/\partial\mathbf{y}$ and $\mathbf{K}=\partial\mathbf{y}/\partial\mathbf{u}$ in (9) automatically yields the standard definition of the RGA.

Summarizing, the RGA condition has been obtained by changing coordinates and then mapping back to the original coordinate system. Consistency of coordinates imposes the RGA condition. This approach forms a basis for deriving additional conditions.

In order to handle nonlinear situations, higher order effects must be considered. First define a metric in either the **y** coordinates

$$g_{ij} = \left\langle \frac{\partial}{\partial y_i}, \frac{\partial}{\partial y_j} \right\rangle \quad , \quad 1 \le i,j \le P,$$

or the **u** coordinates

$$g_{ab} = \left\langle \frac{\partial}{\partial u_a}, \frac{\partial}{\partial u_b} \right\rangle \quad , \quad 1 \le a,b \le P,$$

The metric is a quantity which allows one to define and measure the distance between two points on an abstract manifold. It follows that the metric associated with one system of coordinates can be related to the other coordinate metric by considering

$$g_{ab} = \frac{\partial y^i}{\partial u_a}\frac{\partial y^j}{\partial u_b} g_{ij}$$

and

$$g_{ij} = \frac{\partial u^a}{\partial y_i}\frac{\partial u^b}{\partial y_j} g_{ab}$$

from the exchange of bases. The consistency requirement is imposed by substituting again, yielding

$$g_{ab} = \frac{\partial y^i}{\partial u_a}\frac{\partial y^j}{\partial u_b}\frac{\partial u^c}{\partial y_i}\frac{\partial u^d}{\partial y_j} g_{cd}.$$

This gives a second type of RGA identity of the form

$$\frac{\partial y^i}{\partial u_a}\frac{\partial y^j}{\partial u_b}\frac{\partial u_c}{\partial y_i}\frac{\partial u_d}{\partial y_j} = \begin{cases} 1, & c=a,\ d=b \\ 0, & c\neq a \vee\ d\neq b \end{cases}$$

for $b \geq a$. The identities

$$\frac{\partial y^i}{\partial u_a}\frac{\partial y^j}{\partial u_b}\frac{\partial u_a}{\partial y_i}\frac{\partial u_b}{\partial y_j} = 1$$

can be written in terms of the elements of the RGA matrix, Λ, as

$$\sum_{i=1}^{P}\sum_{j=1}^{P} \Lambda_{ia}\Lambda_{jb} = 1.$$

Having endowed **M** with a metric, it is natural to consider similar identities based on the coefficients of the metric connection. Recall that the connection coefficients give rise to the covariant derivative given by $\nabla_A B$ of a vector field B in the direction of the vector field A. By definition, the connection coefficients are uniquely determined by the covariant derivatives expressed in the basis vector fields. In the current situation, they are given by

$$\Gamma_{abc} = \langle \nabla_{\partial/\partial u_a} \partial/\partial u_b, \partial/\partial u_c \rangle$$

in the input coordinates and by

$$\Gamma_{ijk} = \langle \nabla_{\partial/\partial y_i} \partial/\partial y_j, \partial/\partial y_k \rangle$$

in the output coordinates. The connection coefficients adopted for a coordinate system reflect the fact that the coordinate system is a nonlinear coordinate system. Intuitively, the coefficients Γ_{abc} express the effect of the nonlinear dependence of the b^{th} input component on the a^{th} input component when one moves an infinitesimal distance in the direction of the c^{th} input component of the coordinate basis.

Connection coefficients in the output coordinates can be obtained from the coefficients in the input coordinates from the identity

$$\Gamma_{ijk} = \Gamma_{abc} \frac{\partial u^a}{\partial y_i} \frac{\partial u^b}{\partial y_j} \frac{\partial u^c}{\partial y_k} + \frac{\partial u^a}{\partial y_k} \frac{\partial^2 u^b}{\partial y_i \partial y_j} g_{ab} \tag{10}$$

and, similarly,

$$\Gamma_{abc} = \Gamma_{ijk} \frac{\partial y^i}{\partial u_a} \frac{\partial y^j}{\partial u_b} \frac{\partial y^k}{\partial u_c} + \frac{\partial y^i}{\partial u_c} \frac{\partial^2 y^j}{\partial u_a \partial u_b} g_{ij} \tag{11}$$

The consistency condition is imposed by substituting the expression for Γ_{ijk} from Equation (10) into Equation (11)

$$\Gamma_{abc} = \left\{ \Gamma_{a'b'c'} \frac{\partial u^{a'}}{\partial y_i} \frac{\partial u^{b'}}{\partial y_j} \frac{\partial u^{c'}}{\partial y_k} + \frac{\partial u^{a'}}{\partial y_k} \frac{\partial^2 u^{b'}}{\partial y_i \partial y_j} g_{a'b'} \right\} \frac{\partial y^i}{\partial u_a} \frac{\partial y^j}{\partial u_b} \frac{\partial y^k}{\partial u_c} + \frac{\partial y^i}{\partial u_c} \frac{\partial^2 y^j}{\partial u_a \partial u_b} g_{ij}$$

where a′, b′ and c′ are additional indices. This yields

$$\Gamma_{abc} = \Gamma_{abc} + \frac{\partial u^{a'}}{\partial y_k}\frac{\partial^2 u^{b'}}{\partial y_i \partial y_j} g_{a'b'} \frac{\partial y^i}{\partial u_a}\frac{\partial y^j}{\partial u_b}\frac{\partial y^k}{\partial u_c} + \frac{\partial y^i}{\partial u_c}\frac{\partial^2 y^j}{\partial u_a \partial u_b} g_{ij}$$

Substituting for g_{ij},

$$\Gamma_{abc} = \Gamma_{abc} + \frac{\partial u^{a'}}{\partial y_k}\frac{\partial^2 u^{b'}}{\partial y_i \partial y_j} g_{a'b'} \frac{\partial y^i}{\partial u_a}\frac{\partial y^j}{\partial u_b}\frac{\partial y^k}{\partial u_c} + \frac{\partial y^i}{\partial u_c}\frac{\partial^2 y^j}{\partial u_a \partial u_b}\left\{\frac{\partial u^{a'}}{\partial y_i}\frac{\partial u^{b'}}{\partial y_j} g_{a'b'}\right\}$$

or, upon simplification, using identities (8),

$$\Gamma_{abc} = \Gamma_{abc} + \frac{\partial y^i}{\partial u_a}\frac{\partial^2 u_{b'}}{\partial y_i \partial y_j}\frac{\partial y^j}{\partial u_b} g_{cb'} + \frac{\partial u^{b'}}{\partial y_j}\frac{\partial^2 y^j}{\partial u_a \partial u_b} g_{cb'}$$

The following identity is then obtained:

$$\frac{\partial u_c}{\partial y_j}\frac{\partial^2 y^j}{\partial u_a \partial u_b} + \frac{\partial y^i}{\partial u_a}\frac{\partial^2 u_c}{\partial y_i \partial y_j}\frac{\partial y^j}{\partial u_b} = 0 \qquad (12)$$

which holds for all $1 \le a,b,c \le P$. This is a second order "relative gain type" identity for a nonlinear process.

Under the assumption of perfect control (i.e. integral action), the composition of the process map and its inverse is required to yield the identity map on **W**. Clearly, this implies that Equation (12) must also hold on **W**. Consider the diagram shown in Figure 3.2 in which the process and controller are considered as the sum of a linear part and a nonlinear part.

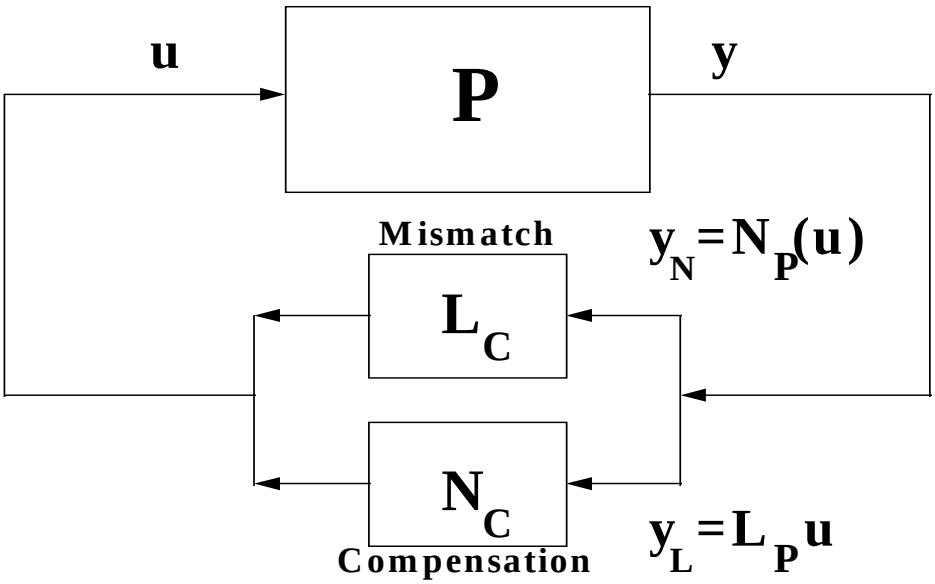

Figure 3.2 Schematic illustration of second order identities for a closed-loop nonlinear process.

This diagram illustrates the implication of the cancellation implied by Equation (12). As we see, the controller is decomposed into a linear gain part (L_c) and a nonlinear gain part (N_c). These components can be represented locally by

$$\mathbf{L_C} = \frac{\partial \mathbf{u}}{\partial \mathbf{y}} \text{ and } \mathbf{N_C} = \frac{\partial^2 \mathbf{u}}{\partial \mathbf{y} \partial \mathbf{y}'}$$

respectively. Similarly, the output response is decomposed into a linear gain part ($\mathbf{L}_p$) and a nonlinear gain part ($\mathbf{N}_p$) represented by

$$\mathbf{L_p} = \frac{\partial \mathbf{y}}{\partial \mathbf{u}} \text{ and } \mathbf{N_p} = \frac{\partial^2 \mathbf{y}}{\partial \mathbf{u} \partial \mathbf{u}'}$$

respectively.

From Figure 3.2, it is seen that, in the absence of a nonlinear gain controller (N_C=0), Equation (12) cannot hold unless the process is linear (N_p=0). When the process is nonlinear, The extent of mismatch experienced by the closed-loop system as a result of the nonlinearity of a process is measured by the first term of Equation (12)

$$\frac{\partial u_c}{\partial y_i}\frac{\partial^2 y^i}{\partial u_a \partial u_b}.$$

This term is called a mismatch term. It is a measure of the input mismatch experienced by a nonlinear process controlled by a linear gain controller.

Consequently, the second term of Equation (12)

$$\frac{\partial y^i}{\partial u_a}\frac{\partial^2 u_c}{\partial y_i \partial y_j}\frac{\partial y^j}{\partial u_b}$$

can be interpreted as a measure of the extent of controller gain nonlinearity required to compensate for that mismatch. It is called the mismatch compensation term.

Note that Equation (12) summarizes the closed-loop nonlinearity of a nonlinear process expressed in terms of the input coordinates. A similar identity can be obtained in the output coordinates:

$$\frac{\partial u^a}{\partial y_i}\frac{\partial^2 y_k}{\partial u_a \partial u_b}\frac{\partial u^b}{\partial y_j} + \frac{\partial y_k}{\partial u_a}\frac{\partial^2 u^a}{\partial y_i \partial y_j} = 0. \qquad (13)$$

The first term of this expression is a measure of the output mismatch experienced by a nonlinear process controlled by a linear gain controller. The second term gives the extent of nonlinearity of a controller which removes the output error.

Following a differential geometric argument, a more precise interpretation can be developed for each of these identities. When considering the geometry of a manifold, the curvature associated with a particular choice of connection indicates the extent of local nonlinearity of the manifold. A connection is said to possess zero curvature if there exists a local coordinate representation for which the corresponding connection coefficients vanish.

To understand the implication of the exchange of bases, suppose that the manifold M admits a connection with zero curvature and that the output coordinates provide a representation in which the connection coefficients vanish ($\Gamma_{ijk}=0$), that is a flat coordinate system of **M**. From Equation (11), the connection coefficients expressed in the input coordinates are given by

$$\Gamma_{abc} = \frac{\partial y^i}{\partial u_c}\frac{\partial^2 y^j}{\partial u_a \partial u_b} g_{ij}$$

Substitution into Equation (10) gives

$$\frac{\partial y^{i'}}{\partial u_c} g_{i'j'} \frac{\partial^2 y^{j'}}{\partial u_a \partial u_b} \frac{\partial u^a}{\partial y_i}\frac{\partial u^b}{\partial y_j}\frac{\partial u^c}{\partial y_k} + \frac{\partial u^a}{\partial y_k}\frac{\partial^2 u^b}{\partial y_i \partial y_j} g_{ab} = 0$$

which yields, upon substitution of the expression of g_{ab} in the output coordinates, the identity

$$\frac{\partial y^{i'}}{\partial u_c} g_{i'j'} \frac{\partial^2 y^{j'}}{\partial u_a \partial u_b} \frac{\partial u^a}{\partial y_i} \frac{\partial u^b}{\partial y_j} \frac{\partial u^c}{\partial y_k} + \frac{\partial u^a}{\partial y_k} \frac{\partial^2 u^b}{\partial y_i \partial y_j} \frac{\partial y^{i'}}{\partial u_a} \frac{\partial y^{j'}}{\partial u_b} g_{i'j'}$$

$$= \frac{\partial^2 y^{j'}}{\partial u_a \partial u_b} \frac{\partial u^a}{\partial y_i} \frac{\partial u^b}{\partial y_j} g_{kj'} + \frac{\partial^2 u^b}{\partial y_i \partial y_j} \frac{\partial y^{j'}}{\partial u_b} g_{kj'} = 0$$

similar to Equation (13). Satisfying this identity is therefore equivalent to requiring that the manifold M admit a connection with zero curvature whose coefficients vanish in the output coordinates. Furthermore, satisfying this identity is independent of the metric employed.

Under the assumption that rank$\{\partial \mathbf{y}/\partial \mathbf{u}\}$=P at every point p of **M,** it can be seen that the geometry of **M** is essentially the geometry of a flat metric space with metric g_{ij}. By letting $g_{ij}=\delta_{ij}$ (where δ_{ij} is the Kronecker delta), **M** can be identified with a subset of $\mathbb{R}^P$ along with coordinates $y_1, ..., y_P$.

These simple identities establish the relationship between the nonlinearity of the input-output map and the nonlinearity of its inverse,that is, between open-loop nonlinearity and control-law nonlinearity. More importantly, they highlight the interaction between linear and nonlinear components of a closed-loop process. As a result, they are very useful in the assessment of nonlinearity of closed-loop nonlinear processes. In the following sections, these identities are used to study nonlinear interaction effects and closed-loop nonlinearity in nonlinear processes.

3. Nonlinearity of Closed-Loop Processes

In this section, the identities (12) and (13) are used to develop a method to assess the nonlinearity of closed-loop processes. This measure of nonlinearity is based on the decompositions of the mismatch term and the compensation term of Equation (12) into their

individual components. This gives an assessment of the contribution of each individual term to the overall mismatch and compensation effects and provides information about the nature of the nonlinear relationship existing between given input-output pairs.

As above, the mismatch from Equation (12) is denoted by

$$\gamma_{abc} = \frac{\partial u_a}{\partial y_i} \frac{\partial^2 y^i}{\partial u_b \partial u_c}$$

where the individual components of the sum are given by

$$\gamma^i_{abc} = \frac{\partial u_a}{\partial y_i} \frac{\partial^2 y_i}{\partial u_b \partial u_c}$$

The term $\gamma^j_{a..}$ is used to denote the P by P matrix associated with the a^{th} input channel and the i^{th} output channel. These terms can be summarized in a table of the following form

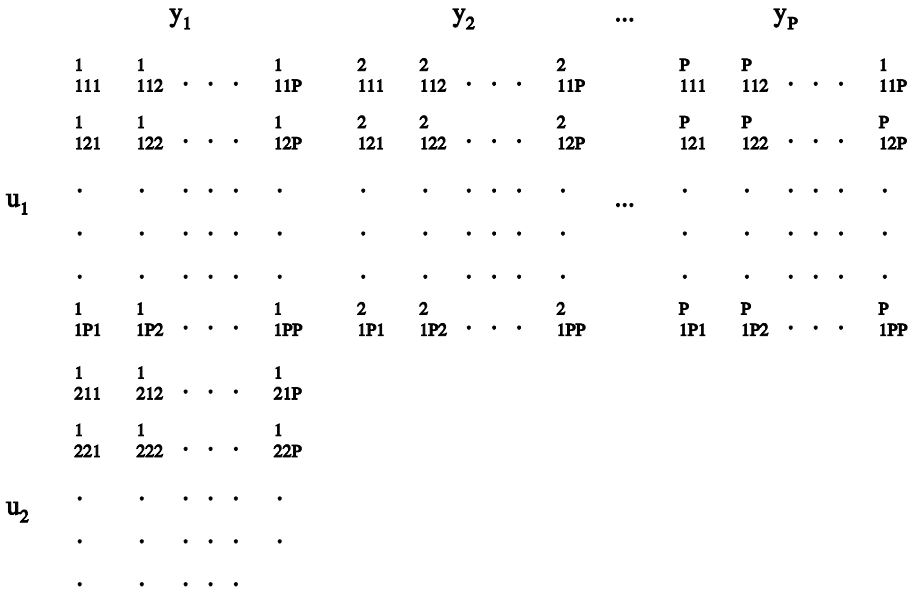

which is called a "mismatch nonlinearity" table.

For each input channel, u_a, the table gives the contribution of each output channel, y_j, $1 \le j \le P$, to the second order effects displayed by the process subject to variations of u_a. For each input-output pair, the P×P submatrix $\gamma^i_{a\bullet\bullet}$ measures the impact of second order effects due to the inputs. For the input-output pair, u_a-y_i, the corresponding $(a,i)^{th}$ submatrix of the mismatch table is a measure of the nonlinearity due to fluctuations of the inputs on this pairing. By construction,

it is related to the nonlinearity experienced by a nonlinear process subject to a linear gain controller. Thus for a given input-output pair, u_a-y_i, each P×P submatrix gives the extent of mismatch of the a^{th} input channel due to the nonlinear effects of the inputs on the i^{th} output channel. This is called *within channel nonlinearity* since it gives the extent of nonlinearity of the inputs on the input mismatch. This type of nonlinearity can be removed without affecting the output channels by introducing nonlinear transformations of the inputs.

If a particular input-output pairing is selected, one must also consider the effect of the other output channels on that pairing. This can be detected by the presence of nonzero submatrices in the entries of the mismatch table corresponding to that input and the remaining output channels. Accordingly, it is called *between channel nonlinearity*. This type of effect is related to the existence of a nonlinear relationship between two output channels. It can only be removed by pairings of the input channels with nonlinear combinations of the output channels. These nonlinearity effects are scale dependent and so their interpretation is subject to the scaling of the system variables. The problem of scaling can be handled as described in Chapter 2. Since the identities expressed in the input coordinates in Equation (12) (or alternatively in the output coordinates in Equation (13)) are invariant under output (or alternatively input) scaling, we need only define a region of interest in the input (or alternatively output) space and re-write the identities (12) (or alternatively (13)) in terms of the scaled coordinates. That is, scaled inputs can be defined as

$$\mathbf{v} = \mathbf{S}(\mathbf{u} - \mathbf{u_0})$$

where **S** is a P by P matrix whose elements define the scaling region in the input space. From Equation (12), it is seen that the scaling of **v** leads to the scaling of each submatrix by post-

multiplying by $\mathbf{S}^{-1}$. In what follows, each scaled submatrix is written as $\hat{\gamma}^{i}_{abc}=\gamma^{i}_{abc}\mathbf{S}^{-1}$. To avoid bias in the measures, each channel is scaled independently by using a diagonal scaling matrix.

A mean squared measure, c_{ai}^{2}, can be associated with each submatrix $\hat{\gamma}^{i}_{a..}$, where

$$c_{ai}^{2} = \int_{A}\left(\sum_{b=1}^{P}\sum_{c=1}^{P}\hat{\gamma}^{i}_{abc}v_{b}v_{c}\right)^{2}dA$$

and A is the area of the unit sphere $\|\mathbf{v}\|^{2}=1$ in the scaled input space. The resulting value is

$$c_{ia}^{2} = \frac{1}{P(P+2)}\left[2\sum_{b=1}^{P}\sum_{c=1}^{P}\left(\hat{\gamma}^{i}_{abc}\right)^{2} + \left(\sum_{d=1}^{P}\hat{\gamma}^{i}_{add}\right)^{2}\right]$$

The root mean squared (RMS) measure, c_{ia}, is then used as a measure of significance of the nonlinear effects. A RMS measure of 0.3 is usually considered to be significant as it leads to a 15% deviation from linearity for every unit step in the scaled input.

When a nonlinear process is controlled using a linear controller, the nonlinearity measures and the table obtained using the procedures described above provide a precise description of the nature of the nonlinear effects in the closed-loop process. If a nonlinear controller is used, it should be designed so that the identities (12) and (13) are satisfied and nonlinear effects are removed. Information about the overall extent of closed-loop nonlinearity can be obtained from the table given above; however, it does not yield information about the local nature of the nonlinear transformations required to remove the between channel nonlinear effects. To provide this information, the above table can be complemented by a second table obtained from mismatch and compensation terms in the identities (12) and (13).

Consider the compensation terms of Equation (12), denoted by

$$\delta_{abc} = \frac{\partial y^i}{\partial u_b}\frac{\partial^2 u^a}{\partial y_i \partial y_j}\frac{\partial y^j}{\partial u_c}$$

The measure of the nonlinearity arising from the control action u_a required to compensate for output changes in y_i and y_j can be locally represented by the individual components of δ_{abc}, given by

$$\delta^{ij}_{abc} = \frac{\partial y_i}{\partial u_b}\frac{\partial^2 u_a}{\partial y_i \partial y_j}\frac{\partial y_j}{\partial u_c}.$$

In analogy with the table given above, these components are arranged in a table of the following form which is called a compensation table:

$$\begin{array}{c|cccc}
 & y_1\,y_1 & y_1\,y_2 & \cdots & y_P\,y_P \\
u_1 & \begin{pmatrix} \delta^{11}_{111} & \delta^{11}_{112} & \cdots & \delta^{11}_{11P} \\ \delta^{11}_{121} & \delta^{11}_{122} & \cdots & \delta^{11}_{12P} \\ \vdots & \vdots & \cdots & \vdots \\ \delta^{11}_{1P1} & \delta^{11}_{1P2} & \cdots & \delta^{11}_{1PP} \end{pmatrix} & \begin{pmatrix} \delta^{12}_{111} & \delta^{12}_{112} & \cdots & \delta^{12}_{11P} \\ \delta^{12}_{121} & \delta^{12}_{122} & \cdots & \delta^{12}_{12P} \\ \vdots & \vdots & \cdots & \vdots \\ \delta^{12}_{1P1} & \delta^{12}_{1P2} & \cdots & \delta^{12}_{1PP} \end{pmatrix} & \cdots & \begin{pmatrix} \delta^{PP}_{111} & \delta^{PP}_{112} & \cdots & \delta^{PP}_{11P} \\ \delta^{PP}_{121} & \delta^{PP}_{122} & \cdots & \delta^{PP}_{12P} \\ \vdots & \vdots & \cdots & \vdots \\ \delta^{PP}_{1P1} & \delta^{PP}_{1P2} & \cdots & \delta^{PP}_{1PP} \end{pmatrix} \\
u_2 & \begin{pmatrix} \delta^{11}_{211} & \delta^{11}_{212} & \cdots & \delta^{11}_{21P} \\ \delta^{11}_{221} & \delta^{11}_{222} & \cdots & \delta^{11}_{22P} \\ \vdots & \vdots & \cdots & \vdots \\ \delta^{11}_{2P1} & \delta^{11}_{2P2} & \cdots & \delta^{11}_{2PP} \end{pmatrix} & \begin{pmatrix} \delta^{12}_{211} & \delta^{12}_{212} & \cdots & \delta^{12}_{21P} \\ \delta^{12}_{221} & \delta^{12}_{222} & \cdots & \delta^{12}_{22P} \\ \vdots & \vdots & \cdots & \vdots \\ \delta^{12}_{2P1} & \delta^{12}_{2P2} & \cdots & \delta^{12}_{2PP} \end{pmatrix} & \cdots & \begin{pmatrix} \delta^{PP}_{211} & \delta^{PP}_{212} & \cdots & \delta^{PP}_{21P} \\ \delta^{PP}_{221} & \delta^{PP}_{222} & \cdots & \delta^{PP}_{22P} \\ \vdots & \vdots & \cdots & \vdots \\ \delta^{PP}_{2P1} & \delta^{PP}_{2P2} & \cdots & \delta^{PP}_{2PP} \end{pmatrix} \\
\vdots & \vdots & \vdots & \cdots & \vdots \\
u_P & \begin{pmatrix} \delta^{11}_{P11} & \delta^{11}_{P12} & \cdots & \delta^{11}_{P1P} \\ \delta^{11}_{P21} & \delta^{11}_{P22} & \cdots & \delta^{11}_{P2P} \\ \vdots & \vdots & \cdots & \vdots \\ \delta^{11}_{PP1} & \delta^{11}_{PP2} & \cdots & \delta^{11}_{PPP} \end{pmatrix} & \begin{pmatrix} \delta^{12}_{P11} & \delta^{12}_{P12} & \cdots & \delta^{12}_{P1P} \\ \delta^{12}_{P21} & \delta^{12}_{P22} & \cdots & \delta^{12}_{P2P} \\ \vdots & \vdots & \cdots & \vdots \\ \delta^{12}_{PP1} & \delta^{12}_{PP2} & \cdots & \delta^{12}_{PPP} \end{pmatrix} & \cdots & \begin{pmatrix} \delta^{PP}_{P11} & \delta^{PP}_{P12} & \cdots & \delta^{PP}_{P1P} \\ \delta^{PP}_{P21} & \delta^{PP}_{P22} & \cdots & \delta^{PP}_{P2P} \\ \vdots & \vdots & \cdots & \vdots \\ \delta^{PP}_{PP1} & \delta^{PP}_{PP2} & \cdots & \delta^{PP}_{PPP} \end{pmatrix}
\end{array}.$$

This table describes in detail the nature of the nonlinear dependencies between the inputs and the various output channels. Interpretation of this table is closely related to that of the

corresponding table for the mismatch terms, γ^{i}_{abc}. It is clear that, by construction, addition of each submatrix δ^{ij}_{abc} of the compensation table with the corresponding entry in the table for the mismatch terms γ^{i}_{abc} for the a^{th} input channel yields a null matrix. Note, however, that only non-redundant terms have been included. As a result, submatrices corresponding to the off-diagonal terms of the form y_i, y_j ($i \neq j$) must be counted twice for the identity (12) to hold.

In considering a given pairing, u_a-y_i, the presence of within channel nonlinear effects can be removed by using a nonlinear input transformation, $v_a=\phi(\mathbf{u})$, which locally eliminates within channel nonlinearity. The corresponding terms of the matrix $\gamma_{a\cdot\cdot}^{\ i}$ given by

$$\gamma^{i}_{abc} = \left(\frac{\partial \Phi_a}{\partial u_a}\frac{\partial u_a}{\partial y_i}\right)\left(\frac{\partial u_b}{\partial \Phi_b}\frac{\partial^2 y_i}{\partial u_b \partial u_c}\frac{\partial u_c}{\partial \Phi_c}\right)$$

vanish locally where

$$\Phi_i = \begin{cases} v_i = u_i \ , & i \neq a \\ v_i = \phi(u_1, \ldots, u_P) \ , & i = a \end{cases}$$

The corresponding compensation terms are given by

$$\delta^{ij}_{abc} = \left(\frac{\partial \Phi_a}{\partial u_a}\right)\left(\frac{\partial u_b}{\partial \Phi_b}\frac{\partial y_i}{\partial u_b}\frac{\partial^2 u_a}{\partial y_i \partial y_j}\frac{\partial y_j}{\partial u_c}\frac{\partial u_c}{\partial \Phi_c}\right)$$

Since this construction implies that the pairing of the new inputs v_a with y_i yields a locally linear response,

$$\frac{\partial^2 v_a}{\partial y_i \partial y_i} = \frac{\partial y_i}{\partial u_b}\frac{\partial^2 v_a}{\partial y_i \partial y_i}\frac{\partial y_i}{\partial u_c} = 0$$

for all b and c. This suggests that the resulting table, re-expressed in terms of v_a, contains a null submatrix in the (y_i, y_i) entry. The remaining non-zero submatrices corresponding to the u_a input channel indicate the nature of the between channel nonlinearity effects. The extent of between channel effects implied by any given pairing, u_a-y_i, is explicitly indicated by the presence of a nonzero submatrix among the (y_k, y_ℓ) entries in the compensation table where $1 \le k, \ell \le P$ with $\ell \neq i$. This second table can be seen to complement the mismatch table by indicating, through the existence of nonzero submatrices, the relationship between a particular input and higher order output terms such as y_k^2 and $y_k y_\ell$.

In the next section, a simple CSTR model is used to illustrate the application of the second order identities in the evaluation of local nonlinear effects in a nonlinear process.

4. An Example

Consider the following model of a CSTR due to Nikolaou (1993),

$$\frac{dx_1}{dt} = -x_1 - Da_1 x_1^2 + 1 + u_1 \ , \quad \frac{dx_2}{dt} = Da_1 x_1^2 - x_2 - Da_2 x_2^{1/2} + u_2$$

with output functions, $y_1=x_1$ and $y_2=x_2$. At steady-state

$$u_1 = y_1 + Da_1 y_1^2 - 1$$

$$u_2 = -Da_1 y_1^2 + y_2 + Da_2 y_2^{1/2}$$

The values of the first and second order inverse gain matrices can be isolated by differentiating

each expression with respect to y_1 and y_2:

$$\frac{\partial \mathbf{u}}{\partial \mathbf{y}} = \begin{pmatrix} 1+2Da_1 y_1 & 0 \\ -2Da_1 y_1 & \frac{1}{2}\frac{2\sqrt{y_2}+Da_2}{\sqrt{y_2}} \end{pmatrix}, \quad \frac{\partial^2 \mathbf{u}}{\partial \mathbf{y} \partial \mathbf{y}^T} = \left\{ \begin{pmatrix} 2Da_1 & 0 \\ 0 & 0 \end{pmatrix} \begin{pmatrix} -2Da_1 & 0 \\ 0 & -\frac{1}{4}\frac{Da_2}{y_2^{3/2}} \end{pmatrix} \right\}.$$

Differentiating with respect to u_1 and u_2 and solving for the required derivatives gives

$$\left.\frac{\partial \mathbf{y}}{\partial \mathbf{u}}\right|_{\mathbf{u}=\boldsymbol{\phi}^{-1}(\mathbf{y})} = \begin{pmatrix} \frac{1}{1+2Da_1 y_1} & 0 \\ \frac{4\sqrt{y_2}Da_1 y_1}{(2\sqrt{y_2}+Da_2)(1+2Da_1 y_1)} & \frac{2\sqrt{y_2}}{2\sqrt{y_2}+Da_2} \end{pmatrix}$$

$$\left.\frac{\partial^2 \mathbf{y}}{\partial \mathbf{u} \partial \mathbf{u}^T}\right|_{\mathbf{u}=\boldsymbol{\phi}^{-1}(\mathbf{y})} = \left\{ \begin{pmatrix} \frac{-2Da_1}{(1+2Da_1 y_1)^3} & 0 \\ 0 & 0 \end{pmatrix} \begin{pmatrix} \frac{4Da_1(2Da_1 y_1^2 Da_2 + 4Da_1^2 y_1^3 Da_2 + 4y_2^{3/2} + 4y_2 Da_2 + \sqrt{y_2}Da_2^2)}{(2\sqrt{y_2}+Da_2)^3(1+2Da_1 y_1)^3} & \frac{4Da_1 y_1 Da_2}{(2\sqrt{y_2}+Da_2)^3(1+2Da_1 y_1)} \\ \frac{4Da_1 y_1 Da_2}{(2\sqrt{y_2}+Da_2)^3(1+2Da_1 y_1)} & \frac{2Da_2}{(2\sqrt{y_2}+Da_2)^3} \end{pmatrix} \right\}.$$

For the steady-state conditions, $\mathbf{y}=\{0.61803399, 0.03085002\}^T$, $\mathbf{u}=\{0,0\}^T$, with $Da_1=1$ and $Da_2=2$,

$$\frac{\partial \mathbf{u}}{\partial \mathbf{y}} = \begin{pmatrix} 2.236 & 0 \\ -1.236 & 6.696 \end{pmatrix}, \quad \frac{\partial^2 \mathbf{u}}{\partial \mathbf{y} \partial \mathbf{y}^T} = \left\{ \begin{pmatrix} 2 & 0 \\ 0 & 0 \end{pmatrix} \begin{pmatrix} -2 & 0 \\ 0 & -92.388 \end{pmatrix} \right\},$$

and

$$\frac{\partial \mathbf{y}}{\partial \mathbf{u}} = \begin{pmatrix} 0.447 & 0 \\ 0.0826 & 0.149 \end{pmatrix}, \quad \frac{\partial^2 \mathbf{y}}{\partial \mathbf{u} \partial \mathbf{u}^T} = \left\{ \begin{pmatrix} -0.179 & 0 \\ 0 & 0 \end{pmatrix} \begin{pmatrix} 0.121 & 0.170 \\ 0.170 & 0.308 \end{pmatrix} \right\}.$$

This gives

$$\frac{\partial \mathbf{u}}{\partial y_i} \frac{\partial^2 y^i}{\partial \mathbf{u} \partial \mathbf{u}^T} = \left\{ \begin{pmatrix} -0.40 & 0 \\ 0 & 0 \end{pmatrix} \begin{pmatrix} 1.0297 & 1.1391 \\ 1.1391 & 2.0607 \end{pmatrix} \right\}^T, \tag{14}$$

and

$$\frac{\partial y^i}{\partial \mathbf{u}} \frac{\partial^2 \mathbf{u}}{\partial y_i y_j} \frac{\partial y^j}{\partial \mathbf{u}} = \left\{ \begin{pmatrix} 0.4 & 0 \\ 0 & 0 \end{pmatrix} \begin{pmatrix} -1.0297 & -1.1391 \\ -1.1391 & -2.0607 \end{pmatrix} \right\}^T. \tag{15}$$

Each term in (14) is obtained by adding over all output channels. The contribution of each output channel can be obtained by isolating the corresponding term of the sum which gives, for example,

$$\frac{\partial u_1}{\partial y_1} \frac{\partial^2 y_1}{\partial u_1^2} = -0.4 , \quad \frac{\partial u_2}{\partial y_1} \frac{\partial^2 y_1}{\partial u_1^2} = 0.2211 ,$$

and so forth. Tabulating these values as described above,

	y_1	y_2
u_1	$\begin{pmatrix} -0.4 & 0 \\ 0 & 0 \end{pmatrix}$	$\begin{pmatrix} 0 & 0 \\ 0 & 0 \end{pmatrix}$
u_2	$\begin{pmatrix} 0.2211 & 0 \\ 0 & 0 \end{pmatrix}$	$\begin{pmatrix} 0.8086 & 1.1391 \\ 1.1391 & 2.0607 \end{pmatrix}$

The latter table demonstrates that the nonlinear behaviour of the process causes both

between and within channel nonlinear effects. The between channel effect arises from the nonlinear effect of y_1 on the u_2-y_2 pairing. The related submatrix contains a non-zero off-diagonal term, 0.2211. The nature of this submatrix with one nonzero entry in the (1,1) position indicates only dependence on y_1 as confirmed from the steady-state relationships. This type of interaction can only be removed by pairing u_2 with a nonlinear function of y_1 and y_2. The null upper right submatrix indicates that there is no nonlinear effect of y_2 on the u_1-y_2 pairing. This is clearly supported by the steady-state expressions for u_1 and u_2 given above. Furthermore, the null sub-matrix also suggests that the linear RGA resulting from input variations in a neighbourhood of the steady-state point will remain an identity matrix. The u_2 steady-state response depends nonlinearly on y_1 and y_2, while u_1 depends only on y_1.

Using the following input scaling,

$$\begin{pmatrix} v_1 \\ v_2 \end{pmatrix} = \begin{pmatrix} 1/0.5 & 0 \\ 0 & 1/0.5 \end{pmatrix} \begin{pmatrix} u_1 \\ u_2 \end{pmatrix}$$

the resulting second order scaled interaction table is given by

$$\begin{array}{cc} & \begin{array}{cc} y_1 & \qquad\qquad y_2 \end{array} \\ \begin{array}{c} v_1 \\ v_2 \end{array} & \begin{pmatrix} -0.2 & 0 \\ 0 & 0 \end{pmatrix} \begin{pmatrix} 0 & 0 \\ 0 & 0 \end{pmatrix} \\ & \begin{pmatrix} 0.1106 & 0 \\ 0 & 0 \end{pmatrix} \begin{pmatrix} 0.4043 & 0.5696 \\ 0.5696 & 1.0304 \end{pmatrix} \end{array}$$

This table can be expressed in terms of RMS measures as

$$\begin{array}{cc} y_1 & y_2 \\ 0.12247 & 0 \\ 0.067728 & 0.85195 \end{array} \begin{array}{l} u_1 \\ u_2 \end{array}$$

For this example, there is no significant between channel nonlinearity effect. The small off-diagonal term 0.067728 indicates a weak nonlinear dependency of the u_2-y_2 pairing on y_1. The larger value 0.85195 shows that there is evidence of strong within channel interaction for the u_2-y_2 pairing. This could be removed by considering pairing the y_2 channel with a nonlinear combination of the inputs.

As discussed above, information about the nature of the nonlinearity is obtained by analysis of the mismatch compensation terms listed in the following table. Consider first the unscaled compensation table given by

$$\begin{array}{c} \\ u_1 \\ u_2 \end{array} \begin{array}{c} y_1,y_1 \\ \begin{pmatrix} 0.40 & 0.0 \\ 0.0 & 0.0 \end{pmatrix} \\ \begin{pmatrix} -0.40 & 0.0 \\ 0.0 & 0.0 \end{pmatrix} \end{array} \begin{array}{c} y_1,y_2 \\ \begin{pmatrix} 0.0 & 0.0 \\ 0.0 & 0.0 \end{pmatrix} \\ \begin{pmatrix} 0.0 & 0.0 \\ 0.0 & 0.0 \end{pmatrix} \end{array} \begin{array}{c} y_2,y_2 \\ \begin{pmatrix} 0.0 & 0.0 \\ 0.0 & 0.0 \end{pmatrix} \\ \begin{pmatrix} -0.6297 & -1.1391 \\ -1.1391 & -2.0607 \end{pmatrix} \end{array}$$

This table provides considerable information about the structure of a nonlinear controller required to decouple this system. It can be seen from the u_1 channel that a simple quadratic transformation involving only y_1 would provide an appropriate controller. The quadratic nature of the relationship is deduced from the presence of the nonzero term 0.4 in the submatrix relating the u_1 channel to the term (y_1,y_1). Since this term is in the upper left corner of this submatrix, it involves only a second order effect related to u_1. This indicates that the second order term of the steady-state relationship expressing the dependence of u_1 on (y_1,y_1) can be written in terms

of a second order term involving u_1 only. This can only happen when u_1 becomes a quadratic function of y_1 at steady-state.

For the interpretation of the u_2 channel, the previous table describing the mismatch can be used. Recall that only the terms in the upper left corner of each submatrix are associated with the between channel interaction. As a result, all other non-zero entries are related to the within channel interactions of the u_2-y_2 pairing, and can be removed by a nonlinear input transformation $v_2=\phi(u_1, u_2)$. From the compensation table, it can be seen that steady-state decoupling can be achieved locally by considering a nonlinear expression in y_1 and y_2. There are no terms of the form y_1y_2, indicating that the expression form required is

$$z_2 = \beta_1(y_1) + \beta_2(y_2)$$

where $\beta_1(y_1)$ is a quadratic function of y_1 and $\beta_2(y_2)$ is a nonlinear function of y_2. This is supported by the model equations given above.

From this example, we see that inspection of the interaction table provides a good description of the nonlinear effects existing in closed-loop nonlinear processes. By using both the mismatch and compensation interaction tables, a good description of the required pairings is obtained. Furthermore, by using the tables along with the RMS curvature measures, we can also provide an accurate description of the steady-state nonlinearity of a process.

In order the assess the importance of these nonlinear effects in the region using the prescribed scaling matrix, we can obtain the following table of RMS measures:

	y_1,y_1	y_1,y_2	y_2,y_2
u_1	0.12247	0	0
u_2	0.12247	0	0.85195

This table indicates that there are no significant nonlinear effects due to u_1. The u_1-y_1 pairing provides an approximately linear steady-state behaviour. Only the y_2,y_2 term has a significantly nonlinear effect on the u_2 channel. A nonlinear transformation of the form

$$z_2 = \beta_2(y_2)$$

would provide an approximately linear steady-state behaviour between u_2 and z_2.

This example illustrates the application of the method presented and the usefulness of the second order identities derived in Section 2. As has been seen, considerable information about the extent and the nature of the nonlinear steady-state behaviour of a closed-loop process can be obtained.

This analysis provides an effective tool for the assessment of nonlinearity in control problems and the extent of nonlinearity that must be addressed by a controller. The necessary second order information about the process can be obtained from a mechanistic process model, numerical simulation experiments in the case of a complex process model (e.g., using a design simulator) or from plant data. A number of possible strategies exist for the assessment of second order properties in steady-state processes. For this purpose, we can consider simple empirical model building approaches, such as response surface methodology, or approximation methods, such as the secant approximation method (Goldberg *et al.* (1983)).

The next two sections discuss the application of Equation (12) for assessment of second order interaction effects.

5. Measurement of Closed-Loop Nonlinearity

In this section, the identities derived in Section 2 are used to measure the extent of the nonlinearity of a process operating under closed-loop.

In the analysis of a nonlinear steady-state process, Equations (4) and (5) can be used to describe the local geometry of the steady-state locus. Clearly, if a process operating under closed-loop has no offset over a given set of output set-point values then we can re-write equation (5) as

$$\Gamma_p^I(\mathbf{r}) = \begin{pmatrix} \mathbf{r} \\ \mathbf{G_c}(\mathbf{r}) \end{pmatrix} \tag{16}$$

where **r** is a reference output signal, or more specifically in this case, an output set-point.

The process dependence on reference signals, as given in equation (16), assumes the existence of a controller which gives zero off-set. For the general case, we assume that both the inputs and the outputs of the closed-loop process are parametrized by the reference signal. That is, we assume that the input-output behaviour of the closed-loop process yields a P-dimensional submanifold of $\mathbb{R}^P \times \mathbb{R}^P$, parametrized by **r**, given by

$$\Gamma_p^C(\mathbf{r}) = \begin{pmatrix} \mathbf{G_c}^C(\mathbf{r}) \\ \mathbf{G_p}^C(\mathbf{r}) \end{pmatrix} \tag{17}$$

where $\mathbf{G}_c{}^C$ and $\mathbf{G}_p{}^C$ are the nonlinear closed-loop relationships between the inputs and the outputs, respectively and the reference signal **r** and where the superscript ^{C} indicates closed-loop process. We now consider the application of the identities obtained in Section 2. First, we derive expressions for the first and second order derivatives of the inputs and the outputs with respect to the reference signal in the closed-loop process. Figure 3.3 shows a standard flow diagram of

a closed-loop process subjected to set-point changes.

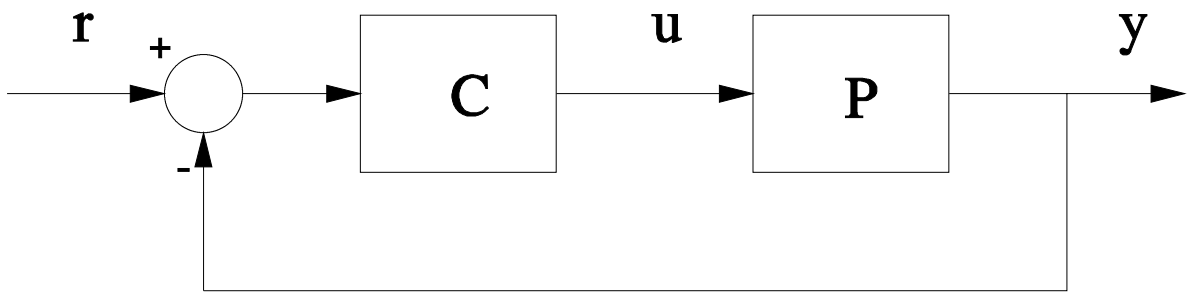

Figure 3.3 Standard flow diagram of a closed-loop process under set-point changes.

For a linear steady-state process, the closed-loop expressions are given by

$$\begin{aligned} \mathbf{u} &= \mathbf{C}(\mathbf{I} + \mathbf{PC})^{-1}\mathbf{r} \\ \mathbf{y} &= \mathbf{PC}(\mathbf{I} + \mathbf{PC})^{-1}\mathbf{r} \end{aligned} \tag{18}$$

where **P** and **C** are P by P matrices corresponding to the process and the controller. For a nonlinear steady-state process, we consider a nonlinear process map and a nonlinear controller map given by

$$\begin{aligned} \mathbf{y} &= \mathbf{G}_p(\mathbf{u}) \\ \mathbf{u} &= \mathbf{G}_c(\mathbf{y}) \end{aligned}$$

Assume that $\mathbf{G}_p$ and $\mathbf{G}_c$ are twice differentiable. Second order approximations of $\mathbf{G}_p$ and $\mathbf{G}_c$ around a stationary point $(\mathbf{y}_0, \mathbf{u}_0)$ are given by

$$\mathbf{G}_p(\mathbf{u}) \approx \frac{\partial \mathbf{G}_p(\mathbf{u}_0)}{\partial \mathbf{u}}(\mathbf{u}-\mathbf{u}_0) + \frac{1}{2}(\mathbf{u}-\mathbf{u}_0)\frac{\partial^2 \mathbf{G}_p(\mathbf{u}_0)}{\partial \mathbf{u}\partial \mathbf{u}'}(\mathbf{u}-\mathbf{u}_0)$$

and

$$\mathbf{G_c(y)} \approx \frac{\partial \mathbf{G_c(y_0)}}{\partial \mathbf{y}}(\mathbf{y}-\mathbf{y_0}) + \frac{1}{2}(\mathbf{y}-\mathbf{y_0})\frac{\partial^2 \mathbf{G_c(y_0)}}{\partial \mathbf{y}\partial \mathbf{y}'}(\mathbf{y}-\mathbf{y_0})$$

As a result, we obtain a second order approximation of the process given by

$$\mathbf{y} = \mathbf{P(u)}(\mathbf{u}-\mathbf{u_0})$$

$$\mathbf{u} = \mathbf{C(y)}(\mathbf{y}-\mathbf{y_0})$$

where

$$\mathbf{P(u)} = \left(\frac{\partial \mathbf{G_p(u_0)}}{\partial \mathbf{u}} + (\mathbf{u}-\mathbf{u_0})\frac{\partial^2 \mathbf{G_p(u_0)}}{\partial \mathbf{u}\partial \mathbf{u}'}\right)$$

and

$$\mathbf{C(y)} = \left(\frac{\partial \mathbf{G_c}}{\partial \mathbf{y}}(\mathbf{y_0}) + (\mathbf{y}-\mathbf{y_0})\frac{\partial^2 \mathbf{G_c}}{\partial \mathbf{y}\partial \mathbf{y}'}(\mathbf{y_0})\right)$$

Substituting for **P**(**u**) and **C**(**y**) in (18), we can obtain expression for the first and second order derivatives of **y** and **u** with respect to **r**. In what follows, we derive the expressions for the case where **C**(**y**) is linear.

For the standard closed-loop diagram, the closed-loop input response is given by solving the implicit nonlinear equation

$$\begin{aligned} \mathbf{u} + \mathbf{C(y)}(\mathbf{I} + \mathbf{P(u)C(y)})^{-1}\mathbf{r} &= \mathbf{0} \\ \mathbf{u} + \frac{\partial \mathbf{G_c}}{\partial \mathbf{y}}\left(\mathbf{I} + \left(\frac{\partial \mathbf{G_p}}{\partial \mathbf{u}} + (\mathbf{u}-\mathbf{u_0})'\frac{\partial^2 \mathbf{G_p}}{\partial \mathbf{u}\partial \mathbf{u}'}\right)\frac{\partial \mathbf{G_c}}{\partial \mathbf{y}}\right)^{-1}\mathbf{r} &= \mathbf{0} \end{aligned} \qquad (19)$$

Similarly, the closed-loop output response is given by solving

$$\mathbf{y} + \mathbf{P}(\mathbf{u})\mathbf{C}(\mathbf{y})(\mathbf{I} + \mathbf{P}(\mathbf{u})\mathbf{C}(\mathbf{y}))^{-1}\mathbf{r} = \mathbf{0}$$

$$\mathbf{y} + \left(\frac{\partial \mathbf{G}_p}{\partial \mathbf{u}} + (\mathbf{u}-\mathbf{u}_0)' \frac{\partial^2 \mathbf{G}_p}{\partial \mathbf{u} \partial \mathbf{u}'}\right) \frac{\partial \mathbf{G}_c}{\partial \mathbf{y}} \left(\mathbf{I} + \left(\frac{\partial \mathbf{G}_p}{\partial u} + (\mathbf{u}-\mathbf{u}_0)' \frac{\partial^2 \mathbf{G}_p}{\partial \mathbf{u} \partial \mathbf{u}'}\right) \frac{\partial \mathbf{G}_c}{\partial \mathbf{y}}\right)^{-1} \mathbf{r} = \mathbf{0} \tag{20}$$

Differentiating (19) with respect **r** gives, at $\mathbf{u}_0$ and $\mathbf{r}_0$=0, the following expressions for the first and second order derivatives of **u** with respect to **r**

$$\left.\frac{\partial \mathbf{u}}{\partial \mathbf{r}}\right|_{\mathbf{u}_0, \mathbf{r}_0} = \frac{\partial \mathbf{G}_c}{\partial \mathbf{y}} \left(\mathbf{I} + \frac{\partial \mathbf{G}_p}{\partial \mathbf{u}} \frac{\partial \mathbf{G}_c}{\partial \mathbf{y}}\right)^{-1}$$

$$\left.\frac{\partial^2 \mathbf{u}}{\partial \mathbf{r} \partial \mathbf{r}'}\right|_{\mathbf{u}_0, \mathbf{r}_0} = \left[\frac{\partial \mathbf{G}_c}{\partial \mathbf{y}} \left(\mathbf{I} + \frac{\partial \mathbf{G}_p}{\partial \mathbf{u}} \frac{\partial \mathbf{G}_c}{\partial \mathbf{y}}\right)^{-1}\right] \left[\left(\mathbf{I} + \frac{\partial \mathbf{G}_p}{\partial \mathbf{u}} \frac{\partial \mathbf{G}_c}{\partial \mathbf{y}}\right)^{-1'} \frac{\partial \mathbf{G}_c'}{\partial \mathbf{y}} \frac{\partial^2 \mathbf{G}_p}{\partial \mathbf{u} \partial \mathbf{u}'} \frac{\partial \mathbf{G}_c}{\partial \mathbf{y}} \left(\mathbf{I} + \frac{\partial \mathbf{G}_p}{\partial \mathbf{u}} \frac{\partial \mathbf{G}_c}{\partial \mathbf{y}}\right)^{-1}\right] \tag{21}$$

Similarly, the corresponding derivatives of the outputs with respect to **r** at $\mathbf{u}=\mathbf{u}_0$ and $\mathbf{r}_0$=0 are given by

$$\left.\frac{\partial \mathbf{y}}{\partial \mathbf{r}}\right|_{\mathbf{u}_0, \mathbf{r}_0} = \frac{\partial \mathbf{G}_p}{\partial \mathbf{u}} \frac{\partial \mathbf{G}_c}{\partial \mathbf{y}} \left(\mathbf{I} + \frac{\partial \mathbf{G}_p}{\partial \mathbf{u}} \frac{\partial \mathbf{G}_c}{\partial \mathbf{y}}\right)^{-1}$$

$$\left.\frac{\partial^2 \mathbf{y}}{\partial \mathbf{r} \partial \mathbf{r}'}\right|_{\mathbf{u}_0, \mathbf{r}_0} = \left(\mathbf{I} - \frac{\partial \mathbf{G}_p}{\partial \mathbf{u}} \frac{\partial \mathbf{G}_c}{\partial \mathbf{y}}\right)^{-1'} \frac{\partial \mathbf{G}_c'}{\partial \mathbf{y}} \frac{\partial^2 \mathbf{G}_p}{\partial \mathbf{u} \partial \mathbf{u}'} \frac{\partial \mathbf{G}_c}{\partial \mathbf{y}} \left(\mathbf{I} + \frac{\partial \mathbf{G}_p}{\partial \mathbf{u}} \frac{\partial \mathbf{G}_c}{\partial \mathbf{y}}\right)^{-1} \tag{22}$$

$$+ \frac{\partial \mathbf{G}_p}{\partial \mathbf{u}} \frac{\partial \mathbf{G}_c}{\partial \mathbf{y}} \left(\mathbf{I} + \frac{\partial \mathbf{G}_p}{\partial \mathbf{u}} \frac{\partial \mathbf{G}_c}{\partial \mathbf{y}}\right)^{-1'} \left[\left(\mathbf{I} + \frac{\partial \mathbf{G}_p}{\partial \mathbf{u}} \frac{\partial \mathbf{G}_c}{\partial \mathbf{y}}\right)^{-1'} \frac{\partial \mathbf{G}_c'}{\partial \mathbf{y}} \frac{\partial^2 \mathbf{G}_p}{\partial \mathbf{u} \partial \mathbf{u}'} \frac{\partial \mathbf{G}_c}{\partial \mathbf{y}} \left(\mathbf{I} + \frac{\partial \mathbf{G}_p}{\partial \mathbf{u}} \frac{\partial \mathbf{G}_c}{\partial \mathbf{y}}\right)^{-1}\right]$$

Equations (21) and (22) are of particular importance in the measurement of local closed-loop nonlinearity for a nonlinear process regulated by a linear controller. They are also closely related to the identities developed in Section 2. In particular, it is readily verified that the right hand side of the expression for the second order derivatives of the outputs with respect to the reference signal in equation (22) is precisely a reformulation of equation (13) of Section 1. To see this, write Equation (13) in terms of **r** and **u** by letting

$$\frac{\partial^2 \mathbf{r}}{\partial \mathbf{u} \partial \mathbf{u}'} = \frac{\partial^2 \mathbf{G_P}}{\partial \mathbf{u} \partial \mathbf{u}'}$$

and substituting Equation (21). We immediately see that, for a nonlinear closed-loop process with no offset, the second order derivatives of **y** with respect to **r** vanish locally. As a result, equation (21) describes the local geometry of the process steady-state locus. It is the control-law nonlinearity of the process as described above.

The following example illustrates this procedure.

Example 3.2

Consider the following model of a chemostat bioreactor:

$$\frac{dx_1}{dt} = \frac{\mu_{max} x_1 x_2}{1 + x_2 + K_i x_2^2} - k_d x_1 - u_1 x_1$$

$$\frac{dx_2}{dt} = -\frac{\mu_{max} x_1 x_2}{1 + x_2 + K_i x_2^2} + (S_0 - x_2) u_1$$

where x_1 and x_2 are the scaled biomass and substrate concentrations and u_1, the input, is the dilution rate. The model parameters, μ_{max}, S_0, k_d and K_i, are the specific growth rate, scaled inlet substrate concentration, death rate and substrate inhibition constant, respectively. These parameters are assigned the values μ_{max}=0.5 min^{-1}, S_0=0.3 g/l, k_d=0.05 min^{-1} and K_i=10 l/g.

The closed-loop steady-state behaviour observed in the control of the substrate concentration by manipulation of the dilution rate is analyzed in the neighbourhood of the steady-state conditions $\mathbf{x}_0$=[0.019821,0.18107], $\mathbf{u}_{10}$=0.01. To illustrate the implications of equations (21) and (22) in the assessment of closed-loop process nonlinearity, we consider the closed-loop response of the process under the action of a feedback controller of the form

$$u_1 = K_c(r - x_2)$$

where K_c=0.1 l g^{-1} min^{-1}. Figure 3.4 shows the resulting closed-loop response of the process along with the actual steady-state locus. As should be expected from this simple proportional controller, the closed-loop process displays a considerable offset at steady-state. Using Equations (21) and (22), we proceed to calculate the contribution of the nonlinear effects to this offset.

At x_2=0.18107, u_1=0.01 we find that

$$\frac{\partial G_p}{\partial u_1} = 6.7754 , \quad \frac{\partial^2 G_p}{\partial u_1 \partial u_1} = 528.54 , \quad \frac{\partial G_c}{\partial x_2} = -0.1.$$

Substitution into equations (21) and (22) gives

$$\frac{\partial u_1}{\partial r} = 0.0596 , \quad \frac{\partial^2 u_1}{\partial r^2} = -0.1120 , \quad \frac{\partial x_2}{\partial r} = 0.4039 , \quad \frac{\partial^2 x_2}{\partial r^2} = 1.1196.$$

The linear approximation of the closed-loop response resulting from these values of the first order derivatives of x_2 and u_1 with respect to r is shown on Figure 3.4. As indicated by the first and second order derivatives of x_2 with respect to r, the closed-loop process deviates from the intended behaviour. We can also calculate the RMS curvature associated with the nonlinearity of the relationship between x_2 and r. For the region of interest given by x_2=0.18107±(5.0×10^{-4}), we obtain an RMS curvature of 0.15. The dependency of x_2 on r is therefore not significantly nonlinear in this region. For the linear controller considered, the closed-loop process behaves in a linear manner in the range of set-point values considered.

Since we are only considering steady-state, or gain, nonlinearity we only consider the implication of nonlinearity in cases where purely proportional linear controllers are used. In order

to consider the implications of implementing other linear controllers such as proportional-integral controllers on nonlinear processes, we need to consider dynamic effects.

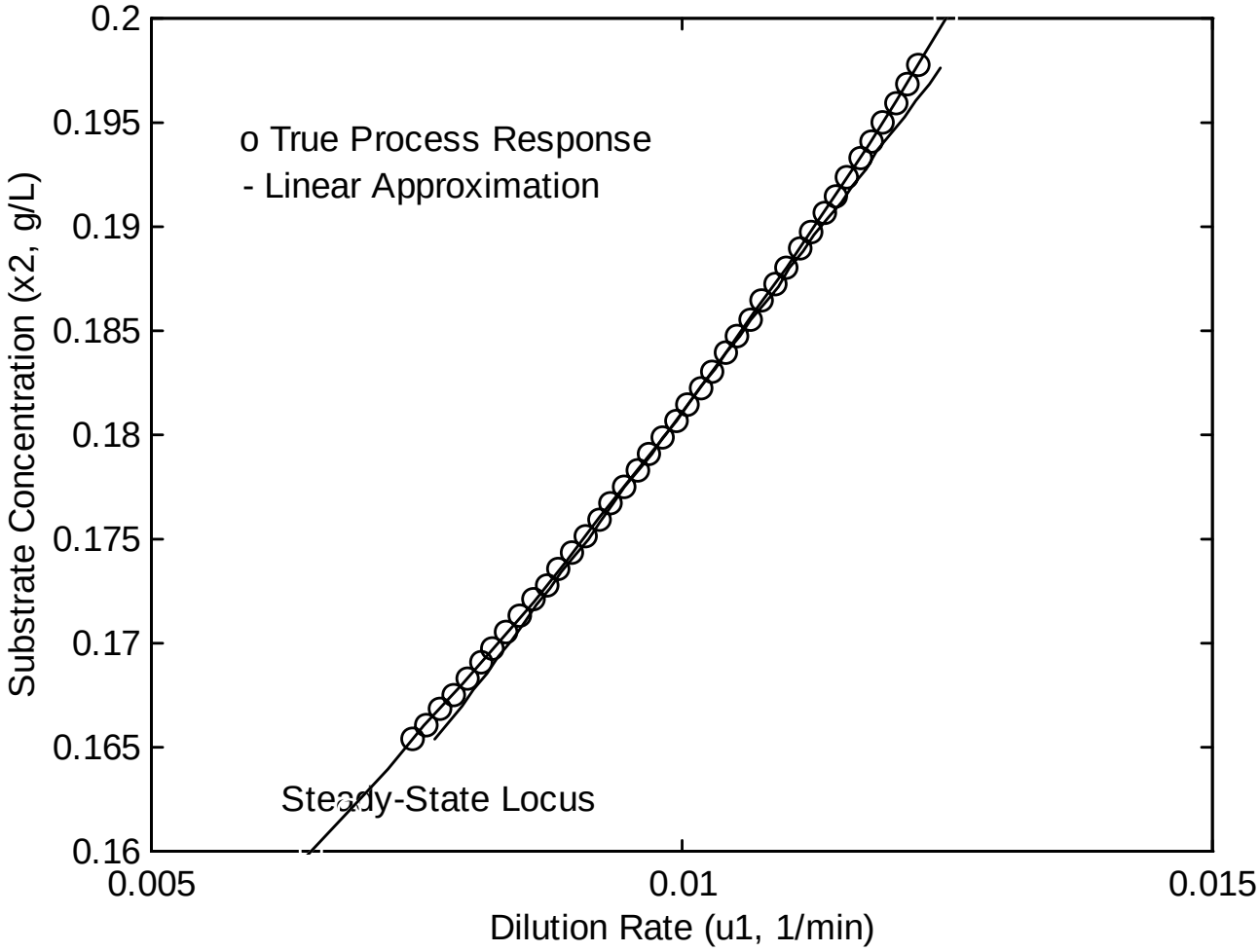

Figure 3.4 Steady-state behaviour of a closed-loop process. The steady-state locus is parametrized by the setpoint signal, **r**.

6. **Nonlinearity and Interaction**

As demonstrated in Section 2, Equations (12) and (13) are closely related to second order interaction effects. Equation (12) defines explicitly the inherent restrictions of input rotation

experienced in a closed-loop nonlinear process. It describes the trade-off that must exist between process nonlinearity and controller nonlinearity, or between the mismatch and the compensation terms in Equation (12). The mismatch term measures the extent of input rotation due to process nonlinearity and the compensation term gives the corresponding rotation that must be supplied by the controller in order to achieve perfect control. Similarly, Equation (13) defines restrictions in output rotation.

Consider the application of Equations (12) and (13) to the measurement of interaction effects in a nonlinear process. From Equation (12), for a given input channel u_a, the following identity is obtained

$$\frac{\partial u_a}{\partial y_i}\frac{\partial^2 y^i}{\partial u_a \partial u_c} + \frac{\partial y^j}{\partial u_c}\frac{\partial^2 u_a}{\partial y_j \partial y_i}\frac{\partial y^i}{\partial u_a} = 0.$$

Note that this identity can also be derived by differentiation of the equation

$$\frac{\partial u_a}{\partial y_i}\frac{\partial y^i}{\partial u_a} = 1$$

with respect to u_c. However, the derivation using the exchange of basis requirements for connection coefficients identifies the coordinate representation issue which is the fundamental basis for interaction.

The second order expression can also be decomposed into i individual terms

$$\gamma^i_{ac} = \frac{\partial u_a}{\partial y_i}\frac{\partial^2 y_i}{\partial u_a \partial u_c} + \frac{\partial y^j}{\partial u_c}\frac{\partial^2 u_a}{\partial y_j \partial y_i}\frac{\partial y_i}{\partial u_a}.$$

The term, γ^i_{ac}, measures the effect of u_c on the u_a-y_i pairing and its magnitude gives an estimate

of the contribution of second order effects to closed-loop interaction effects. These terms can summarized in a table of the following form

	y_1	y_2	...	y_P
u_1	γ_1^1	γ_1^2	...	γ_1^P
u_2	γ_2^1	γ_2^2	...	γ_2^P
.	.	.	...	.
.	.	.	...	.
.	.	.	...	.
u_P	γ_P^1	γ_P^2	...	γ_P^P

where the terms γ_a^i are P dimensional vectors whose elements are $\gamma_{ac}^{\ i}$. By construction, this table is symmetric. Furthermore, to satisfy Equations (12) and (13), the sum of all elements in each row must be a null vector. The sum of the elements of each column must also be a null vector. For a given direction in the input space, this table identifies the contribution of the nonlinearity to the interaction effects.

Using equation (13), the effect of variation of the outputs can also be estimated. As above, for a particular output channel y_i,

$$\frac{\partial u^a}{\partial y_i}\frac{\partial^2 y_i}{\partial u_a \partial u_b}\frac{\partial u^b}{\partial y_j} + \frac{\partial y_i}{\partial u_a}\frac{\partial^2 u^a}{\partial y_i \partial y_j} = 0,$$

which can be easily derived by differentiation of the equation

$$\frac{\partial y_i}{\partial u_a}\frac{\partial u^a}{\partial y_i} = 1$$

with respect to y_j. Individual elements of Equation (13) are given by

$$\delta_{ij}^{a} = \frac{\partial u_a}{\partial y_i}\frac{\partial^2 y_i}{\partial u_a \partial u_b}\frac{\partial u^b}{\partial y_j} + \frac{\partial y_i}{\partial u_a}\frac{\partial^2 u_a}{\partial y_i \partial y_j}.$$

This term measures the effect of y_j on the u_a-y_i pairing. As above, these terms can be arranged in a table of the form

	u_1	u_2	...	u_P
y_1	δ_1^1	δ_1^2	...	δ_1^P
y_2	δ_2^1	δ_2^2	...	δ_2^P
.	.	.	...	.
.	.	.	...	.
.	.	.	...	.
y_P	δ_P^1	δ_P^2	...	δ_P^P

This table displays the same properties as the table corresponding to Equation (12).

Interpretation of these measures of interaction supplements the interpretation of the RGA calculated from the first order gain of the nonlinear process. Of particular importance are the magnitudes of the terms γ_a^i and δ_i^a contained in the tables given above. Since these terms are not scale independent, we must consider appropriate scaling of the original variables. This can be performed as discussed in Section 3. The result is a dimensionless measure of the contribution of the second order terms to the interaction effects in a nonlinear closed-loop process. Naturally, large second order effects within a prescribed region of operation indicates highly nonlinear behaviour and the need for a nonlinear decoupling control strategy.

The choice of input-output pairings may also be affected by the second order measures. For a given input-output pair, the corresponding P-dimensional vector entry from the second order

interaction tables measures the expected variation in interaction due to the second order effects. They therefore provide a method to quantify the interaction effects in nonlinear processes where nonlinearity is the dominant source of interactions. The presence of large negative values in the second order interaction terms associated with an input-output pair indicates large reverse effects due to the nonlinearity, indicating a poor choice of input-output pairing.

As mentioned above, the terms associated with Equations (12) and (13) are related to the extent of input rotation and output rotation, respectively. As a result, significantly large values of γ_a^i (or alternatively, δ_i^a) can be interpreted as an indication of significant variation in input (or alternatively, output) rotation in a prescribed region of operation. This is closely related to the effect of process nonlinearity on the input and output rotation components of the singular value decomposition of the first order gain (Morari and Zafiriou, 1989), as discussed in Koung and MacGregor (1991).

In the next section, two chemical process examples are used to demonstrate the application of the tables discussed above in the assessment of nonlinear interaction effects. The first example is a continuation of the simple CSTR discussed in Section 4. The second example is an evaporator model described by Newell and Lee (1989).

Although both examples are based on process models, it should be understood that the analysis only requires the availability of first and second order gain information in a prescribed region of operation. The models presented in the next section are therefore only used to evaluate the gain information. Other empirical model descriptions such as second order Volterra series (Maner *et al.*, 1994), NARX or NARMAX models (Leontaritis and Billings, 1985) or simple steady-state models may often provide the necessary information.

7. **Chemical Process Examples**

Example 3.3

Let us consider again the simple CSTR discussed in Section 4. As noted previously, this process was shown to display significant nonlinearity in the region of operation described by the scaling matrix

$$\mathbf{S} = \begin{pmatrix} 2 & 0 \\ 0 & 2 \end{pmatrix}$$

The relative gain array of this process at the conditions considered is given by

$$\Lambda = \begin{pmatrix} 1 & 0 \\ 0 & 1 \end{pmatrix}$$

The process displays no first order closed-loop interaction; however, examination of the model equations indicates the presence of one-way interaction from u_1 to y_2. Recall that transmission interaction occurs when the action of one controller on an output is influenced by a path which includes the other controllers. This is the type identified by the linear RGA.

It is reasonable to ask whether the nonlinear effects contribute to transmission interaction effects in the closed-loop process. Using the first and second order gain information given in Section 4, the entries in the interaction tables discussed previously can be evaluated as follows:

γ_1^1

γ

γ

γ

and, similarly, $\gamma_{21}{}^1=\gamma_{22}{}^1=\gamma_{21}{}^2=\gamma_{22}{}^2=0$. The terms corresponding to Equation (13) are

$$\delta_{11}^{1} = \frac{\partial y_1}{\partial u_1}\frac{\partial^2 u_1}{\partial y_1 \partial y_1} + \frac{\partial u_1}{\partial y_1}\frac{\partial^2 y_1}{\partial u_1 \partial u_1}\frac{\partial u_1}{\partial y_1} + \frac{\partial u_2}{\partial y_1}\frac{\partial^2 y_1}{\partial u_2 \partial u_1}\frac{\partial u_1}{\partial y_1}$$

$$= 0.4 + -0.4 + 0.0 = 0$$

$$\delta_{12}^{1} = \frac{\partial y_1}{\partial u_1}\frac{\partial^2 u_1}{\partial y_1 \partial y_2} + \frac{\partial u_1}{\partial y_2}\frac{\partial^2 y_1}{\partial u_1 \partial u_1}\frac{\partial u_1}{\partial y_1} + \frac{\partial u_2}{\partial y_2}\frac{\partial^2 y_1}{\partial u_2 \partial u_1}\frac{\partial u_1}{\partial y_1}$$

$$= 0.0 + 0.0 + 0.0 = 0$$

$$\delta_{11}^{2} = \frac{\partial y_1}{\partial u_2}\frac{\partial^2 u_2}{\partial y_1 \partial y_1} + \frac{\partial u_1}{\partial y_1}\frac{\partial^2 y_1}{\partial u_1 \partial u_2}\frac{\partial u_2}{\partial y_1} + \frac{\partial u_2}{\partial y_1}\frac{\partial^2 y_1}{\partial u_1 \partial u_2}\frac{\partial u_2}{\partial y_1}$$

$$= 0.0 + 0.0 + 0.0 = 0$$

$$\delta_{12}^{2} = \frac{\partial y_1}{\partial u_2}\frac{\partial^2 u_2}{\partial y_1 \partial y_2} + \frac{\partial u_1}{\partial y_2}\frac{\partial^2 y_1}{\partial u_1 \partial u_2}\frac{\partial u_2}{\partial y_1} + \frac{\partial u_2}{\partial y_2}\frac{\partial^2 y_1}{\partial u_1 \partial u_2}\frac{\partial u_2}{\partial y_1}$$

$$= 0.0 + 0.0 + 0.0 = 0$$

It can be easily verified that $\delta_{21}^{1}=\delta_{21}^{2}=\delta_{22}^{1}=\delta_{22}^{2}=0$.

These results indicate that the process nonlinearity does not introduce transmission interaction effects in the closed-loop system. From the steady-state point of view, the u_1-y_1 and u_2-y_2 control loops can be treated independently. However, one-way decoupling may be required to compensate for the action of u_1 on y_2.

Example 3.4

The approach discussed in Section 5 is used to evaluate the extent of interaction in the 2×2 evaporator model of Newell and Lee (1989). In this process, the outlet product mass, y_1 (%), and operating pressure, y_2 (kPa), are controlled using the inlet steam pressure fed to the evaporator, u_1 (kPa), and the cooling water flowrate to an overhead condenser, u_2 (kg/min). In Chapter 2, it was found that this process displays significant nonlinearity at the operating conditions $[y_1, y_2]^T=[25,50.5]^T$ and $[u_1,u_2]^T=[194.7,208.0]^T$. The first and second order gains are

given by

$$\frac{\partial \mathbf{y}}{\partial \mathbf{u}} = \begin{pmatrix} 0.11677 & 0.045585 \\ 0.12807 & -0.049972 \end{pmatrix}$$

and

$$\frac{\partial \mathbf{y}}{\partial \mathbf{u} \partial \mathbf{u}^{\mathrm{T}}} = \left(\begin{bmatrix} 8.1309 \times 10^{-4} & 3.7307 \times 10^{-4} \\ & -2.7355 \times 10^{-4} \end{bmatrix} \right. \\ \left. \begin{bmatrix} -3.0467 \times 10^{-4} & -1.7804 \times 10^{-4} \\ & 3.8670 \times 10^{-4} \end{bmatrix} \right).$$

First and second order inverse gains are given by

$$\frac{\partial \mathbf{u}}{\partial \mathbf{y}} = \begin{pmatrix} 4.2268 & 3.9179 \\ 10.935 & -9.9704 \end{pmatrix}$$

and

$$\frac{\partial^2 \mathbf{u}}{\partial \mathbf{y} \partial \mathbf{y}^{\mathrm{T}}} = \left(\begin{bmatrix} -1.6089 \times 10^{-1} & -1.6163 \times 10^{-6} \\ & -2.6744 \times 10^{-6} \end{bmatrix} \right. \\ \left. \begin{bmatrix} 5.6258 \times 10^{-2} & -9.4865 \times 10^{-1} \\ & 9.5584 \times 10^{-1} \end{bmatrix} \right).$$

The relative gain array is given by

$$\Lambda = \begin{pmatrix} 0.498 & 0.502 \\ 0.502 & 0.498 \end{pmatrix}$$

indicating strong interaction effects. As suggested in Newell and Lee (1989), these results indicate that there is no clearly advantageous choice of input-output pairings in this case.

In order to analyze the second order interaction effects, the first and second order gain information must be appropriately scaled. For the construction of the interaction table corresponding to Equation (12), the inputs can be scaled by the scaling matrix

$$\mathbf{S} = \begin{pmatrix} 0.016667 & 0 \\ 0 & 0.014286 \end{pmatrix}.$$

This matrix scales the inputs with respect to the expected range of variation of both channels during normal operation. The second order interaction table is given by

$$\begin{array}{cc} & \begin{array}{cc} y_1 & y_2 \end{array} \\ \begin{array}{c} u_1 \\ u_2 \end{array} & \begin{pmatrix} 7.1622\times10^{-2} \\ 4.8834\times10^{-2} \end{pmatrix} \quad \begin{pmatrix} -7.1622\times10^{-2} \\ -4.8834\times10^{-2} \end{pmatrix} \\ & \begin{pmatrix} -7.1622\times10^{-2} \\ -4.8834\times10^{-2} \end{pmatrix} \quad \begin{pmatrix} 7.1622\times10^{-2} \\ 4.8834\times10^{-2} \end{pmatrix} \end{array}$$

This indicates that, for the region of operation described by the scaling matrix, the nonlinearity makes a mild contribution to closed-loop interactions. Furthermore, the positive diagonal elements in this table demonstrate a positive interaction effect due to nonlinearity in the u_1-y_1 and u_2-y_2 loop pairings. These loop pairings should therefore be adopted in this region of operation in order to prevent reverse effects due to nonlinearity. Thus this analysis of second order effects complements linear techniques and improves the ability to assign appropriate input-output pairings in a nonlinear process.

Construction of the table from Equation (13) for the output coordinates is now considered. This requires specification of scaling in the output region. As in Chapter 2, consider the region described by the scaling matrix

$$\mathbf{T} = \begin{pmatrix} 0.2 & 0 \\ 0 & 0.14286 \end{pmatrix}.$$

The corresponding interaction table is given by

$$\begin{array}{cc} & \begin{matrix} y_1 \end{matrix} \qquad\qquad \begin{matrix} y_2 \end{matrix} \\ \begin{matrix} u_1 \\ u_2 \end{matrix} & \begin{matrix} \begin{pmatrix} 6.3612\times10^{-2} \\ -1.5953\times10^{-2} \end{pmatrix} & \begin{pmatrix} -6.3612\times10^{-2} \\ 1.5953\times10^{-2} \end{pmatrix} \\ \begin{pmatrix} -6.3612\times10^{-2} \\ 1.5953\times10^{-2} \end{pmatrix} & \begin{pmatrix} 6.3612\times10^{-2} \\ -1.5953\times10^{-2} \end{pmatrix} \end{matrix} \end{array}$$

Again, it can be seen that the nonlinearity of the process contributes significantly to the interaction effect. However, in this case the components of each 2-dimensional vector in the interaction table are of opposite signs, indicating conflicting interaction effects for the closed-loop process due to the nonlinearity.

This situation complicates considerably the task of choosing appropriate input-output pairings. Many strategies can be envisaged. One simple solution is to allocate pairings based on the sign of the larger element in each vector. This is based on the assumption that, on average, the dominant components summarize the interaction effects observed. To facilitate the comparisons, one can normalize each P-dimensional element of the interaction table.

Applying this simple rule in this example, it is seen that the dominant effect of the nonlinearity is given by the term 6.3612×10^{-2}. Since this term appears as a positive term on the diagonal of the interaction table, the u_1-y_1 and u_2-y_2 pairings are selected for this process.

This example highlights the importance of choosing an appropriate scaling region. In this case, two scaling approaches were considered and it was shown that the interpretation of the results generally depend on the choice of scaling region. In the first case, a region defined by

a diagonal matrix was used to evaluate interaction effects in the input coordinates. A direct effect of nonlinearity on closed-loop interactions was observed, which led to a clear choice of input-output pairings. The second analysis, based on the choice of a scaling region in the output coordinates, led to a different appreciation of the extent of nonlinear contributions to the interaction effects, requiring a more cautious interpretation of the results. The relationship between scaling and the orientation of a steady-state process has been in discussed in Chapter 2 where an alternative scaling procedure was proposed.

8. Conclusions

A new approach for assessing closed-loop nonlinearity and interaction in nonlinear processes has been presented. It is based on a differential geometric interpretation of the relative gain array that leads to the derivation of second order identities. These identities can be used to measure the extent and the nature of the nonlinearity of a closed-loop process under linear or nonlinear control. These identities can also be used in the analysis of higher order interaction effects.

Two types of nonlinear closed-loop process behaviour have been introduced. Between channel nonlinearity is associated with the nonlinear dependence of output channels on other input-output pairings. Within channel nonlinearity is used to identify the interaction effects that result from the inherent nonlinearity of each output channel. A root mean squared measure of interaction has been introduced to evaluate the significance of local nonlinearity effects. Application of the approach has been illustrated using a two input two output CSTR model and the method has been shown to yield considerable information about the nature of the nonlinear

behaviour of that process.

An extension of the second order identities to the measurement of nonlinear interaction effects has also been presented. The method yields a second order interaction table which can be expressed in either the input or output coordinates to complement and extend the applicability of the relative gain array to nonlinear processes. Models describing a simple CSTR and an evaporator process have been used to demonstrate the application of the method. The CSTR model was shown to display no first or second order transmission interaction effects. Although this process is shown to display significant nonlinearity, the analysis demonstrates that the RGA captures very accurately the extent of interaction in the closed-loop process. The evaporator model displays both first and second order interaction effects. It has been shown that the choice of input-output pairings may be affected by consideration of the second order effects under different scaling possibilities.

Nomenclature

a,b,c Integer indices of input coordinates

a´,b´,c´ Integer indices of input coordinates

A, B Vector fields

Da_1, Da_2 Kinetic constants

f Vector field describing the dynamics of a process on the state space

g_{ab} Metric on a manifold expressed in the input coordinates

g_{ij} Metric on a manifold expressed in the output coordinates

G Implicit vector valued function of the inputs and the outputs

$\mathbf{G}_c$ Nonlinear process inverse function of the outputs

$\mathbf{G}_p$ Nonlinear process function of the inputs

i,j,k Integer indices of output coordinates

K Steady-state input-output gain of a linear process

M Differentiable manifold arising from the steady-state input-output behaviour

N Dimension of the space of state variables

p A point of manifold **M**

P Number of inputs and outputs

RGA Relative gain array

$\mathbb{R}$ Set of real numbers

S Input scaling matrix

T Output scaling matrix

T**M** Tangent space of the differentiable manifold **M**

$T_p\mathbf{M}$ Tangent space at a point p of a differentiable manifold **M**

u Input vector

$u^{(k)}$ k^{th} time derivative of the input vector

U Open neighbourhood of a point in $\mathbb{R}^P$

v Scaled input vector

W Intersection of two open neighbourhoods of a point p of a manifold **M**

x State variables

$\mathbf{x}_0$ Initial conditions for the state variables

y Vector of outputs

$\mathbf{y}^{(k)}$ k^{th} time derivative of the outputs

Y Open neighbourhood of a point in $\mathbb{R}^P$

z Reparametrization of the outputs

Greek Letters

β_1, β_2 Nonlinear functions of the outputs

γ_{abc} Mismatch terms summed over all outputs

$\hat{\gamma}_{abc}$ Scaled mismatch terms summed over all outputs

$\gamma_{abc}^{\ i}$ Mismatch terms corresponding to y_i

$\gamma_{a\bullet\bullet}^{\ \ i}$ P by P matrix of mismatch terms corresponding to the u_a-y_i pairing

$\gamma_a^{\ i}$ P dimensional vector element of the second order interaction table expressed in the input coordinates

Γ_P Process graph

$\Gamma_P^{\ I}$ Inverse process graph

Γ_{abc} Metric connection coefficients expressed in the input coordinates

Γ_{ijk} Metric connection coefficients expressed in the output coordinates

δ_{abc} Mismatch compensation terms summed over all output combinations

δ_{abc}^{ij} Mismatch compensation term corresponding output combination y_i, y_j

δ_a^i P dimensional vector element of the second order interaction table expressed in the output coordinates

δ_{ij} Kronecker delta

Λ Relative gain array

ϕ Nonlinear vector valued function of the inputs

Φ Nonlinear vector valued function of the inputs

Symbols

$\mathbb{R}^P$ P-dimensional real space

^{T} Transpose of a matrix or vector

$\otimes$ Hadamard product

$\nabla_A B$ Covariant derivative of B in direction of A

<v,w> Inner product of two vector fields v and w

Chapter 4

On a Dynamic Measure of Nonlinearity

1. Introduction

One advantage of the framework developed in Chapters 1 and 2 is that it allows the assessment of the nonlinearity of a steady-state process in a neighbourhood of a point in a systematic fashion. An important aspect of this framework is the recognition of the importance of scaling on the quantification of the nonlinearity, and the development of a methodology to scale the curvature measures obtained to produce generic measures. Although the analysis has been restricted so far to steady-state processes, it is conceivable that this framework could be applied to the analysis of dynamic processes. If one considers a dynamic process to be adequately represented by an operator acting as a mapping between spaces of functions, it is possible to apply the framework in a comprehensive manner using an operator-based approach.

The purpose of this Chapter is to extend the steady-state analysis of nonlinearity to the measurement of dynamic nonlinearity. The methodology is based on an operator description of nonlinear input-output systems. In particular, the application of the input-output formulations described by Zames (1966a, b), Willems (1971), Desoer and Vidyasagar (1975) and, more recently, Georgiou (1993, 1994) to the problem of assessing the extent of dynamic nonlinearity of a continuous nonlinear input-output system is considered. Using these formulations and some other tools, it is shown that the steady-state analysis developed earlier in this thesis extends naturally to the analysis of dynamic processes. Quantification of the nonlinearity of mappings between infinite dimensional normed (Banach) spaces is involved.

The problem of quantifying dynamic nonlinearity of control systems has been an active area of research in chemical engineering (Stack and Doyle III, 1995; Ogunnaike *et al.*, 1993; Nikolaou, 1993). Operator-based settings have also been considered by Nikolaou and Manousiouthakis (1989a, b) for the development of nonlinear measures of interaction and to study hybrid control approaches in chemical engineering. Nikolaou (1993) has also used this formulation to develop a methodology for the measurement of dynamic nonlinearity and has demonstrated its application to a simple two-state nonisothermal CSTR model. The lack of a generic measure, along with the intensive computational requirements of this method, have made it difficult to apply more generally.

Nikolaou (1993) has considered the measurement of dynamic nonlinearity for nonlinear processes using random input sequences of different amplitudes. The approach is based on the calculation of an alternative operator norm of a nonlinear operator. This norm is defined from an inner product in the space of operators from bounded input signals to bounded output signals. Given that a linear approximation of the nonlinear input-output operator exists, the norm of the best linear approximation for a given class of input perturbations can be compared to the true operator norm of the system. Since the linear model approximation is likely to change as the amplitudes of the random sequences are varied, the degree of variation in the parameters of the linear description can be used as a measure of process nonlinearity. Such variations of linear model structures have also been successfully employed by Johansen and Foss (1993) to develop NARMAX (Nonlinear AutoRegressive Moving Average with eXogeneous inputs) models from a collection of ARMAX models which span different operating regions.

The approach of Nikolaou (1993) does not propose a measure of nonlinearity, but rather

a procedure to assess nonlinearity of a process based on variations of linear approximations for various input sequences. Although the framework is generally applicable to a number of situations, its use has been mainly restricted to simulation studies where large numbers of input sequences can be used to assess the nonlinearity of a system.

Recently, Stack and Doyle III (1995) proposed a methodology for the development of control relevant measures of dynamic nonlinearity. An optimal structure is defined which allows description of the input-output dynamic relationship subject to the optimization of a quadratic performance objective. They state that measurement of dynamic nonlinearity subject to the optimal policy provides control relevant measures of nonlinearity that are more informative than open-loop measures nonlinearity. Although this approach is sound and may prove to be useful in a number of applications (including the method proposed in this section), it may be susceptible to the choice of measure of nonlinearity employed. They have used the coherency spectrum (Ljung, 1987; Haber, 1985) to assess nonlinearity. Alternative measures, such as the one proposed in this thesis would also be applicable.

Measurement of nonlinearity has been of considerable importance in nonlinear systems identification. A number of measures have been proposed in the literature (see Haber , 1985 for a complete survey) for testing the presence of nonlinearity in input-output sequences. Such methods can be useful in developing an empirical process model. However, they do not provide generic measures that could be used to compare the extent of nonlinearity of alternate systems. Since they are primarily designed for use in for modelling studies, they do not consider the impact of the nonlinearity on process control.

In this study, the nonlinearity of a process in the neighbourhood of a point is measured

by the contribution of higher order terms of the Taylor series approximation of a nonlinear operator relative to those of the first order terms rather than deviations from the best linear approximation for a given input sequence. This yields a pointwise measure of nonlinearity which is representative of the nonlinearity of the process over a neighbourhood of a point of linearization. By studying the local behaviour of a nonlinear process relative to the behaviour of its linear approximation in the neighbourhood of a point, a local measure of nonlinearity is obtained that becomes an important characteristic of the local behaviour of a nonlinear process. The extent of nonlinearity can be assessed with respect to various scaling strategies.

Although the construction of this measure is intuitive, it provides a scale-independent measure of the magnitudes of the nonlinear effects relative to the linear approximation of a dynamic process in the neighbourhood of an equilibrium point or a nominal trajectory. The ability to define a scale independent measure of nonlinearity is advantageous because it provides a systematic method for evaluating and comparing the nonlinearities of a number of processes. The flexibility of the scaling procedure provides a useful means of comparing the implementations of various stable control structures such as proportional-integral forms, internal model controller (IMC) forms. (Note that the IMCs are closely related to the input prescribed scaling procedure described in Chapter 2).

The method presented here permits the quantification of dynamic nonlinearity effects in nonlinear processes to yield a generic measure of the nonlinearity of a process in the neighbourhood of a stationary point or a nominal trajectory. It is demonstrated that a simple extension of the steady-state measures provides a measure of dynamic nonlinearity. The extension is based on the existence of a continuous twice Fréchet differentiable causal unbiased

operator describing the input-output behaviour of a dynamical control system in a neighbourhood of a stationary point. As in the steady-state analysis, the magnitude of the second order terms of a Taylor series expansion is measured relative to that of the first order terms. The assessment of nonlinearity is performed relative to unit L_2-norm output signals such that interpretation of the curvature measures of the dynamical system is similar to the interpretation of those proposed in the steady-state analysis. Greater flexibility in the scaling of the output signals is possible in the analysis of dynamical systems.

The Chapter proceeds as follows. In section 2, background on the theory of nonlinear differentiable operators is provided. Application of nonlinear operators to the study of dynamical systems is introduced in Section 3. A measure of dynamic nonlinearity is presented in Section 4. The importance of scaling to the development of a meaningful measure is discussed in Section 5. In Section 6, the dynamic measure of nonlinearity is applied to the analyses of two processes. In the first example, a bioreactor is used to demonstrate the application to a continuous chemical processes. The second example involves a non-isothermal batch CSTR.

2. Preliminaries

In this Section, a number of useful definitions and theorems are stated. They provide a brief introduction to basic notions of operator theory (see Khatskevich and Shoiykhet, 1994) and topology, (see Lang, 1985). Although the material discussed in this Section is of technical importance to the development presented in this Chapter, its presentation is not indispensable to the understanding of the following Sections. The reader may therefore wish to skip this Section and proceed to Section 3, referring back as needed.

1) Let $\mathbb{X}$ be a set. A topology on $\mathbb{X}$ is a nonempty family τ of subsets of the set $\mathbb{X}$, satisfy-

ing the following three conditions:

a) the intersection of any two elements of τ is an element of τ;

b) the union of the elements of any subfamily of the family τ belongs to τ;

c) $\mathbb{X} \subseteq \cup\{U_\alpha \mid U_\alpha \in \tau\}$.

The pair $(\mathbb{X}, \tau)$ is called a topological space.

2) Let τ_1 and τ_2 be two topologies on $\mathbb{X}$. It is said that τ_1 is weaker than τ_2, or, alternatively, τ_2 is stronger than τ_1, if $\tau_1 \subseteq \tau_2$.

The topology of a space can be described through convergence. Let $(C, \geq)$ be a directed set. A directedness S on $\mathbb{X}$ is a mapping $S: C \to \mathbb{X}$ defined on the whole C. For example, a sequence is a mapping defined on a set of natural numbers, i.e., where the directed set C is the linearly ordered set $\mathbb{N}=\{1,2,...\}$.

3) **Theorem 1**: A topological space is Hausdorff if and only if no directedness on this space converges to two distinct points.

4) A mapping f from a topological space $(\mathbb{X}, \tau)$ into a topological space $(\mathbb{B}, \beta)$ is called continuous if the preimage of any β-open set in $\mathbb{B}$ is τ-open in $\mathbb{X}$. The composition of continuous mappings is continuous.

5) Let $f: \mathbb{X} \to \mathbb{B}$ be a continuous mapping and $\mathbb{C} \subseteq \mathbb{X}$; then the restriction $f|\mathbb{C}$ is also continuous. It is said to be continuous on $\mathbb{C}$.

6) **Theorem 2**: The following statements are equivalent:

a) The mapping f is continuous.

b) The preimage of any closed set is closed.

c) For each point $x \in \mathbb{X}$, the preimage of any neighbourhood of $f(x)$ is a

neighbourhood of x.

d) For each point $x \in \mathbb{K}$ and any neighbourhood $\mathbb{C}$ of the point $f(x)$, there exists a neighbourhood $\mathbb{B}$ of the point x such that $f(\mathbb{B}) \subseteq \mathbb{C}$.

e) For any directedness S in $\mathbb{K}$, convergent to a point s, the composition $f \circ S$ is convergent to $f(s)$.

7) A homeomorphism f (or a topological isomorphism) of the topological spaces $(\mathbb{K}, \tau)$ and $(\mathbb{B}, \beta)$ is an isomorphism of the sets $\mathbb{K}$ and $\mathbb{B}$ such that both f and f^{-1} are continuous.

8) A family γ of subsets of a topological space is called a cover of a set $\mathbb{B}$ if $\mathbb{B} \subseteq \cup\{B \mid B \in \gamma\}$. A cover γ is called open if each set $B \in \gamma$ is open. A subcover of a cover γ is a subfamily of γ which is itself a cover. A topological space is called compact if every open cover of the space contains a finite subcover.

9) **Theorem 3**: A topological space $\mathbb{K}$ is compact if and only if any directedness in $\mathbb{K}$ has a limit point.

10) A metric on a set $\mathbb{K}$ is a nonnegative real-valued functional d defined in the direct product $\mathbb{K} \times \mathbb{K}$ which satisfies the following conditions:

a) $d(x,y) = d(y,x)$;

b) $d(x,y) + d(y,z) \geq d(x,z)$;

c) $d(x,y) = 0$ if and only if $x=y$.

The pair $(\mathbb{K}, d)$ is called a metric space. The set $\{y \mid d(x,y) < r\}$ is called the open r-ball centred at x. The family of all open balls provides a base for a topology τ on $\mathbb{K}$ called the metric topology.

11) Let $(\mathbb{K}, d)$ be a metric space. A sequence $\{s_n \mid n \in \mathbb{N}\}$ is called Cauchy if $d(s_n, s_m) \to 0$ for

$n,m \to \infty$. A metric space is called complete if all its Cauchy sequences are convergent.

12) **Theorem 4**: In a metric space, any metric convergent sequence is Cauchy. If a Cauchy sequence has a limit point, then it converges to that point.

13) Let $\mathbb{K}$ be a set and let K be the field $\mathbb{R}$ of real numbers or the field $\mathbb{C}$ of complex numbers. The set $\mathbb{K}$ is a linear (or vector) space provided that the operations of addition of two elements and multiplication by a scalar are given which satisfy the following axioms:

Let $x, y, z \in \mathbb{K}$ and $a, b \in K$.

i) $x+y=y+x$

ii) $(x+y)+z=x+(y+z)$

iii) there exists a unique element $0 \in \mathbb{K}$ such that $x+0=x$

iv) for any x there exists a unique element $(-x)$ such that $x+(-x)=0$

v) $a(bx)=(ab)x$

vi) $(a+b)x=ax+bx$, $a(x+y)=ax+ay$

vii) $1 \circ x=x$.

14) The topological space $(\mathbb{K},\tau)$ is said to be a linear topological space if linear operations on the set $\mathbb{K}$ are continuous with respect to the topology τ.

15) A norm on a linear space $\mathbb{K}$ is a real-valued functional, denoted by $\|\|$, which obeys the following conditions

i) $\|x\| \geq 0$; $\|x\|=0$ iff $x=0$,

ii) $\|x+y\| \leq \|x\|+\|y\|$,

iii) $\|ax\| = |a| \bullet \|x\|$.

A linear space $\mathbb{K}$ equipped with a norm is called a normed space. On this space, the for-

mula $\rho(x,y)=\|x-y\|$ defines a metric which induces a topology called the norm topology.

16) Two norms $\|\|_1$, $\|\|_2$ on $\mathbb{X}$ are said to be equivalent if there exists c_1, $c_2>0$ such that $c_1\|x\|_1\leq\|x\|_2\leq c_2\|x\|_1$ for every $x\in\mathbb{X}$..

17) A normed space which is complete in the norm topology is called a Banach space.

18) An operator defines a mapping between normed spaces.

19) An operator $A:\mathbb{X}\rightarrow\mathbb{Y}$ is linear if its domain $D(A)$ is a lineal of $\mathbb{X}$ and $A(\alpha x+\beta y)=\alpha A(x)+\beta A(y)$, $x,y\in D(A)$ and $\alpha,\beta\in\mathbb{R}$. A linear operator is bounded if $\|Ax\|\leq M<\infty$ for every $x\in D(A)$ with $\|x\|=1$.

20) **Theorem 5**: A linear operator is continuous if and only if it is bounded.

21) The set $L(\mathbb{X},\mathbb{Y})$ of all continuous linear operators from the normed space $\mathbb{X}$ into the normed space $\mathbb{Y}$ is a normed space with

i) $(A+B)x = Ax + Bx$,

ii) $(\alpha A)x = \alpha(Ax)$

for $A,B \in L(\mathbb{X},\mathbb{Y})$, $\alpha\in\mathbb{R}$ and the norm

iii) $$\|A\| = \sup_{\|x\| = 1} \|Ax\|.$$

22) Let $\mathbb{X}$ be a normed space. The space of all continuous linear functionals on $\mathbb{X}$ is called the conjugate space of $\mathbb{X}$ and is denoted by $\mathbb{X}^*$. $\mathbb{X}^*=L(\mathbb{X},K)$ where K is $\mathbb{R}$ or $\mathbb{C}$. $\mathbb{X}^*$ is a Banach space. Consider the expression $\langle x,f\rangle$, the value of $f\in\mathbb{X}^*$ at $x\in\mathbb{X}$. which is semilinear in the second argument, i.e., $\langle x,\alpha f_1+\beta f_2\rangle=\bar{\alpha}\langle x,f_1\rangle+\bar{\beta}\langle x,f_2\rangle$, $f_1,f_2\in\mathbb{X}^*$, α, $\beta\in K$, $\bar{\alpha}$ and $\bar{\beta}$ are complex conjuguates.

23) **Theorem 6**: Let $\mathbb{X}$ be a normed space. Consider a set of elements x_i, i=1,...,n, of $\mathbb{X}$

and define the space $\mathbb{X}_i$ obtained by fixing all elements but the i^{th}. An operator $G:\mathbb{X}\to\mathbb{U}$ defined everywhere on $\mathbb{X}$ is called a multilinear (n-linear) continuous operator if G is linear in each of the variables $x_i\in\mathbb{X}_i$, i=1,..,n, and is continuous on $\mathbb{X}$.

24) **Theorem 7**: If an operator $G:\mathbb{X}\to\mathbb{U}$ is linear in each of the variables $x_i\in\mathbb{X}_i$, i=1,...,n, then G is a multilinear continuous operator if and only if

$$\|G\| \le M\|x_1\|...\|x_n\|$$

for all $x=(x_1, ..., x_n)$ where $0\le M<\infty$.

25) If G is a multilinear continuous operator, the norm of G is defined as the smallest number M for which the inequality of Theorem 7 is fulfilled. That is,

$$\|G\| = \sup_{\|x_i'\|\le 1, 1\le i\le n} \|G(x_1,...,x_n)\|.$$

26) An operator H is a homogeneous form of order n if there exists a multilinear operator $G\in L_n(\mathbb{X},\mathbb{U})$ such that

$$H(x) = G(x,x,...,x).$$

27) For a homogeneous form of order n H is such that

$$H(\lambda x) = \lambda^n H(x),$$

for $\lambda\in\mathbb{R}$, $x\in\mathbb{X}$. Also,

$$\|H(x)\| \le \|H\|\|x\|^n.$$

Using this formalism, a methodology for measuring of dynamic nonlinearity will be described in the following sections. It provides a unifying framework in which dynamic and

steady-state processes can be treated using a number of different scenarios. Of particular importance are processes whose states are described by systems of ordinary differential equations.

3. Input-Output Dynamical Systems

Following the formulation of Zames (1966a, b), Willems (1971) and Desoer and Vidyasagar (1975), relevant input and output signals are those of finite magnitude with respect to a certain metric. The magnitude of a signal $x:[0,\infty)\rightarrow\mathbb{R}^N$ is measured by its p norm, defined as

$$\|\mathbf{x}\|_p = \left[\int_0^\infty \|\mathbf{x}(t)\|^p dt\right]^{1/p}$$

where $\|\mathbf{x}(t)\|$ denotes any norm of the vector $\mathbf{x}(t)$. Signals with finite p-norm form an infinite dimensional Banach space L_p^N defined as

$$L_p^N = \left\{\mathbf{x}:[0,\infty)\rightarrow\mathbb{R}^N : \|\mathbf{x}\|_p < \infty\right\}.$$

Physical signals are usually not defined on $[0,\infty)$ but on a finite subset S and are therefore always finite. For a signal defined on $S=[0,\infty)$, $\|\mathbf{x}\|_p=\infty$ if and only if $\|\mathbf{x}(t)\|$ grows without bounds. To prevent this, a physical signal is usually defined as a truncated signal of the form

$$\mathbf{x}_T : t \rightarrow \mathbf{x}_T(t) = \begin{cases} \mathbf{x}(t) & \text{if } t \le T \\ \mathbf{0} & \text{if } t > T \end{cases}$$

This leads to the definition of an extended Banach space L_{pe}^N defined as

$$L_{pe}^N = \left\{\mathbf{x}:[0,\infty)\rightarrow\mathbb{R}^N : \mathbf{x}_T \in L_p^N \ \forall\ T \ge 0\right\}.$$

A nonlinear input-output dynamical system is represented by a nonlinear operator, $\mathbf{G}_p$, acting on certain signals $\mathbf{u}(t)$ belonging to a Banach space $\mathbf{U}=L_{pe}^P$ and producing finite output

signals, **y**(t), also belonging to a Banach space $\mathbf{Y}=L_{pe}^{M}$.

In this study, we consider input-output dynamical systems described by Fréchet differentiable nonlinear operators of the form

$$\mathbf{G_p}:\mathbf{D_p} \rightarrow \mathbf{Y}$$

where $D_p \subseteq \mathbf{U}$ is the domain of G_p (see Georgiou, 1993). We assume that this operator is unbiased, i.e., $\mathbf{0} \in D_p$ and $\mathbf{G}_p(0)=0$. This implies that the analysis is always carried out in terms of deviation variables in the neighbourhood of a stable equilibrium of the process located at the origin.

The dynamic gain associated with the input-output operator $\mathbf{G}_p$ is defined as

$$\|\mathbf{G_p}\| = \sup_{\mathbf{u(T)}} \left\{ \frac{\|\mathbf{G_p(u(T))}\|}{\|\mathbf{u(T)}\|} : \mathbf{u} \in L_p - \mathbf{0}, \mathbf{T} \geq \mathbf{0} \right\}.$$

The dynamic incremental gain is defined as

$$\|\mathbf{G_p}\|_{\Delta} = \sup_{\mathbf{u_1(T)}, \mathbf{u_2(T)}} \left\{ \frac{\|\mathbf{G_p(u_1(T)) - G_p(u_2(T))}\|}{\|\mathbf{u_1(T) - u_2(T)}\|} : \mathbf{u_1}, \mathbf{u_2} \in L_p, \mathbf{u_1} \neq \mathbf{u_2}, \mathbf{T} \geq \mathbf{0} \right\}.$$

The input-output behaviour of a dynamical system described by a continuous operator $\mathbf{G}_p$ is stable if for any bounded input $\mathbf{u} \in \mathbf{U}$ such that $\|\mathbf{u}\| \leq \delta$, there exists a $0 < \gamma \leq \infty$ such that $\|\mathbf{y}\| \leq \gamma \|\mathbf{u}\|$ (Willems, (1971)). A more restrictive definition of stability requires that the operator dynamic gain is bounded, i.e., $\|\mathbf{G}_p\|_p < \infty$. In the following, the former notion of input-output stability is assumed.

4. A Measure of Dynamic Nonlinearity

In this section, a dynamic measure of nonlinearity of a process is considered. This measure is based on the existence of a twice Fréchet differentiable operator representing the input-output behaviour of a nonlinear dynamical system.

The (Fréchet) derivative of $\mathbf{G}_p$ at $\mathbf{u}_0$, denoted by $d\mathbf{G}_p(\mathbf{u}_0)$, is defined as

$$\lim_{\|\mathbf{h}_1\|_p \to 0} \frac{\|\mathbf{G}_p(\mathbf{u}_0 + \mathbf{h}_1) - \mathbf{G}_p(\mathbf{u}_0) - d\mathbf{G}_p(\mathbf{u}_0)\mathbf{h}_1\|_p}{\|\mathbf{h}_1\|_p} = 0.$$

The equality

$$d\mathbf{G}_p(\mathbf{u})\mathbf{h}_1 = \mathbf{H}(\mathbf{u})\mathbf{h}_1$$

maps $\mathbf{u} \in \mathbf{U}$ to the operator $\mathbf{H}(\mathbf{u})$ belonging to the space of linear operators from $\mathbf{U}$ to $\mathbf{Y}$ defined as $L(\mathbf{U}, \mathbf{Y})$. The operator $d\mathbf{G}_p(\mathbf{u}_0)$ is a linear operator from $\mathbf{U}$ to $\mathbf{Y}$. Assuming that the nonlinear operator $\mathbf{H}$ is Fréchet differentiable, its Fréchet derivative is defined as

$$\lim_{\|\mathbf{h}_2\|_p \to 0} \frac{\|\mathbf{H}(\mathbf{u}_0 + \mathbf{h}_2) - \mathbf{H}(\mathbf{u}_0) - \mathbf{K}(\mathbf{u}_0)\mathbf{h}_2\|_p}{\|\mathbf{h}_2\|_p}$$

At an element $\mathbf{h}_1$, the value of $\mathbf{K}(\mathbf{u})\mathbf{h}_2$ is the second Fréchet derivative of $\mathbf{G}_p$ defined as $d^2\mathbf{G}_p(\mathbf{u})(\mathbf{h}_1,\mathbf{h}_2)$. It maps $\mathbf{U}$ into the space of bilinear maps from $\mathbf{U} \otimes \mathbf{U}$ to $\mathbf{Y}$, $L(\mathbf{U}, L(\mathbf{U}, \mathbf{Y})) = L_2(\mathbf{U}, \mathbf{Y})$. The second order Taylor derivative of $\mathbf{G}_p$ evaluated at $\mathbf{u}_0$, $d^2\mathbf{G}_p(\mathbf{u}_0)(\mathbf{h}_1,\mathbf{h}_2)$, is assumed to a be a continuous homogeneous form of order 2 (i.e., symmetric with to its entry $\mathbf{h}$). Correspondingly, it is written as $d^2\mathbf{G}_p(\mathbf{u}_0)(\mathbf{h})$.

Using the first and second order Fréchet derivative of a nonlinear operator, a measure of dynamic nonlinearity analogous to the steady-state measure is constructed. As demonstrated in the following section, the resulting dynamic measure is an extension of the steady-state measure.

Under the assumption that the operator $\mathbf{G}_p$ is Fréchet differentiable up to order 2 on a neighbourhood of $\mathbf{u}_0$, then the expressions

$$\mathbf{G_p(u_0 + h)} \approx \mathbf{G_p(u_0)} + \mathbf{dG_p(u_0)h} + \mathbf{d^2G_p(u_0)(h,h)}\frac{1}{2!} + \boldsymbol{\omega}\mathbf{(u_0,h)}$$

where

$$\|\boldsymbol{\omega}(\mathbf{u_0},\mathbf{h})\|_p \leq \mathbf{M}\|\mathbf{h}\|_p^3.$$

is uniformly valid in $\mathbf{h}$ for $\|\mathbf{h}\|_p \leq \varepsilon$ and the number M is independent of $\mathbf{h}$. In that case, the operator $\mathbf{G}_p$ is called Taylor differentiable and the expressions $d\mathbf{G}_p(\mathbf{u}_0)$ ($\mathbf{h}$) and $d^2\mathbf{G}_p(\mathbf{u}_0)(\mathbf{h}, \mathbf{h})$ are called the first and second order Taylor derivative of $\mathbf{G}_p$ at $\mathbf{u}_0$.

Under this formalism, a measure of the extent of dynamic nonlinearity of a nonlinear process can be defined in a neighbourhood of a point $\mathbf{u}_0$ in D_p by considering the contribution of the second order derivatives of $\mathbf{G}_p$ to the Taylor series approximation of $\mathbf{G}_p$ at $\mathbf{u}_0$. Let the linear and the nonlinear part of the output signal be given by

$$\mathbf{y_L}(t) = \mathbf{dG_P(u_0)(h}(t))$$

and

$$\mathbf{y_N}(t) \approx \mathbf{d^2G_P(u_0)(h}(t)\mathbf{,h}(t))$$

respectively for a given input signal $\mathbf{h}(t)$ about the origin $\mathbf{u}_0$.

By analogy with the steady-state case, the curvature of the nonlinear operator at $\mathbf{u}_0(=\mathbf{0})$ in a direction $\mathbf{h}(t)$ is defined as the ratio

$$c^2(\mathbf{h}(T))\Big|_{0<\|\mathbf{h}(T)\|_2\le\xi} = \frac{\left[\int_0^T \|\mathbf{y}_N(t)\|^2 dt\right]^{1/2}}{\int_0^T \|\mathbf{y}_L(t)\|^2 dt}.$$

This ratio measures the magnitude of the part of the output signal related to the second order effects relative to the signal of the linear approximation of the nonlinear operator. It can be re-written as

$$c^2(\mathbf{h}(t))\Big|_{0<\|\mathbf{h}(t)\|\le\xi} = \frac{\|d^2\mathbf{G}_p(\mathbf{u}_0)(\mathbf{h}(t))\|}{\|d\mathbf{G}_p(\mathbf{u}_0)(\mathbf{h}(t))\|^2}.$$

The following theorem establishes that the measure is bounded for a stable process, $\mathbf{G}_p$.

Theorem 8:

Suppose a dynamical system is described by a stable nonlinear twice Fréchet differentiable continuous operator, $\mathbf{G}_p$:$\mathbf{U}\rightarrow\mathbf{Y}$. Then the measure of nonlinearity c^2 is bounded.

The second order Taylor series of $\mathbf{G}_p$ at $\mathbf{u}_0$ is given by

$$\mathbf{G}_p(\mathbf{h}(t)) = \mathbf{G}_p(\mathbf{u}_0) + d\mathbf{G}_p(\mathbf{u}_0)\mathbf{h}(t) + \frac{1}{2!}d^2\mathbf{G}_p(\mathbf{u}_0)(\mathbf{h}(t)) + \omega(\mathbf{u}_0,\mathbf{h}(t))$$

where

$$\|\omega(\mathbf{u}_0,\mathbf{h}(t))\| \le M\|\mathbf{h}\|^3$$

M is independent of $\mathbf{h}$.

Since $\mathbf{G}_p$ is continuous, then for any $\varepsilon>0$ there exist $r>0$ such for all $\mathbf{h}$ with $\|\mathbf{h}\|<r$, $\|\mathbf{G}_p(\mathbf{u}_0+\rho\mathbf{h})-\mathbf{G}_p(\mathbf{u}_0)\|\le\varepsilon$. Define the functional

$$\phi(\mathbf{u}_0, \rho\mathbf{h}) = \mathbf{G}_p(\mathbf{u}_0+\rho\mathbf{h}) - \mathbf{G}_p(\mathbf{u}_0) - \omega(\mathbf{u}_0,\rho\mathbf{h}).$$

For all ρ, $0\le\rho\le1$,

$$\|\phi(\mathbf{u}_0, \rho\mathbf{h})\| = \|\rho d\mathbf{G}_p(\mathbf{u}_0)\mathbf{h} + \frac{\rho^2}{2}d^2\mathbf{G}_p(\mathbf{u}_0)(\mathbf{h})\| \le \varepsilon + Mr^3 = N.$$

For a linear functional $f\in\mathbf{Y}^*$, the functional

$$\gamma(\rho) = <\phi(\mathbf{u}_0,\rho\mathbf{h},f> = \rho<d\mathbf{G}_p(\mathbf{u}_0)\mathbf{h},f> + \frac{\rho^2}{2}<d^2\mathbf{G}_p(\mathbf{u}_0)(\mathbf{h}),f>$$

is a second order polynomial in ρ. It follows that it satisfies $|\gamma(\rho)|<N$ for all ρ, $0\le\rho\le1$, and all f, $\|f\|\le1$. Then there exists a number $\ell>0$ such that

$$|<d\mathbf{G}_p(\mathbf{u}_0)\mathbf{h},f>| \le N\ell$$

and

$$|<d^2\mathbf{G}_p(\mathbf{u}_0)(\mathbf{h}),f>| \le N\ell.$$

It then follows that

$$\|d\mathbf{G}_p(\mathbf{u}_0)\mathbf{h}\| \le N\ell\ , \quad \|d^2\mathbf{G}_p(\mathbf{u}_0)(\mathbf{h})\| \le N\ell$$

for all $\mathbf{h}$, $\|\mathbf{h}\|\le r$.

Finally, since the operator norms of the first and second order Taylor derivative of $\mathbf{G}_p$ are such that

$$\|d\mathbf{G}_p(\mathbf{u}_0)\mathbf{h}\| \le \|d\mathbf{G}_p(\mathbf{u}_0)\|\|\mathbf{h}\|$$

and

$$\|d^2\mathbf{G}_p(\mathbf{u}_0)(\mathbf{h})\| \leq \|d^2\mathbf{G}_p(\mathbf{u}_0)\|\|\mathbf{h}\|.$$

then the measure is bounded as

$$\frac{\|d^2\mathbf{G}_p(\mathbf{u}_0)(\mathbf{h})\|}{\|d\mathbf{G}_p(\mathbf{u}_0)\|^2\|\mathbf{h}\|^2} \leq c^2(\mathbf{h}) \leq \frac{\|d^2\mathbf{G}_p(\mathbf{u}_0)\|\|\mathbf{h}\|^2}{\|d\mathbf{G}_p(\mathbf{u}_0)(\mathbf{h})\|^2}$$

This completes the proof.

Theorem 8 establishes that for a continuous nonlinear operator, the measure of nonlinearity $c^2(\mathbf{h})$ remains bounded for (L_p) bounded input signals $\mathbf{h} \in \mathbf{U}$. It is a stable property of a nonlinear process. It also establishes that a stable Fréchet differentiable nonlinear operator has stable (finite dynamic gain) first and second order Fréchet derivatives. This extends the results of Willems who established stability of the linearization of a nonlinear differentiable operator.

Conceptually, the application of this measure to the analysis of dynamic processes is similar to the analysis of steady-state processes. We measure the deviation from linearity by the relative magnitude of the second order contribution to the Taylor series expansion of a differentiable mapping in a neighbourhood of a point of interest. In the steady-state case, assessment of the magnitude of the curvature measure was made with respect to an operating region of interest. The average contribution of the second order term of the Taylor series expansion relative to this region interest was then summarized by integrating the measure overall possible directions **h**.

It is clear that application of an average measure of nonlinearity such as the RMS curvature measure may constitute a very difficult task in the dynamic case. Because this implies conducting a search over an infinite dimensional space, it may be impossible to obtain such a

measure. Although it is conceptually possible to consider overall measures of nonlinearity such as a mean squared measure analogous to the steady-state measure (which would require the solution of an abstract integral over a bounded set of input signals in L_2), one is always restricted, in practice, to specific classes of input signals.

As a result, the dynamic measure $c^2(\mathbf{h})$ is to be computed for various input signals **h** in a neighbourhood of the origin. Its magnitude must be assessed relative to a region of interest defined in the L_p space, **Y**, where the first and second order derivative of the nonlinear operator $\mathbf{G}_p$ take their value. The problem of defining such a region is discussed in the next section.

4. Scaling of the Dynamic Measures

The measure c^2 does not constitute by itself an absolute measure of process nonlinearity. It is subject to the scaling of the outputs and the size of the time horizon considered. Its magnitude alone does not provide a meaningful measure. An appropriate scaling of the output signals must then be considered. In this section, we consider the problem of scaling in the assessment of dynamic nonlinearity. The approach relies on the operator approach highlighted in the previous section. Certain ramifications of this strategy are discussed.

The main feature of the measure of curvature proposed for steady-state processes is that it provides a scale-independent measure of nonlinearity. Provided that the output scaling employed appropriately designated the process operating region, the steady-state measure was a good reflection of the extent of nonlinearity within this region. Recall that by specifying a region of interest, we considered a change of coordinates

mapping output perturbations to a dimensionless unit normal perturbation, **z**. The scaled

$$\mathbf{z}(t) = \mathbf{S}(\mathbf{y}(t) - \mathbf{y_0})$$

measures of nonlinearity were then gauged with respect to this region of unit norm. For dynamic processes, the magnitude of output signals is measured by their L_p-norm. It then becomes natural to measure nonlinearity and, consequently, to scale the output signals with respect to this norm. A natural approach to scaling of the output response of a dynamic process is through an invertible linear operator $\mathbf{S}:\mathbf{D}_S \subset \mathbf{Y} \rightarrow \mathbf{Y}$ that defines a linear time varying output transformation of the form

$$\mathbf{z}(t) = \mathbf{S}(\mathbf{y}(t) - \mathbf{y_0})$$

The operator **S** is chosen to describe a subset of output signals of interest expressed in terms of a dimensionless, unit L_p-normal signal **z**(t). Care must be taken when choosing an appropriate scaling operator. It must be such that the composition $\mathbf{SG}_P(\mathbf{u}_0)$ is stable. This is equivalent to the requirement that the operator $\mathbf{G}_p(\mathbf{u}_0)$ is stabilizable by a linear controller. This is to ensure that the scaled curvature measure remains bounded.

In this setting, scaling with respect to structures such as integrals and derivatives of the output signal can easily be accommodated. For example, the nonlinearity of a system subject to a linear control strategy with integral action can be assessed by scaling the output response with respect to a region of the form

$$\mathbf{z}(T) = \mathbf{K_C}(\mathbf{y_0} - \mathbf{y}(t)) + \frac{\mathbf{K_C}}{\boldsymbol{\tau_I}} \int_0^T (\mathbf{y_0} - \mathbf{y}(t))dt.$$

The resulting measure of curvature gives an indication of the degree of nonlinearity of the system subject to a region describing the behaviour of a linear proportional-integral controller

compensation.* A number of situations exist where highly nonlinear plants are adequately controlled by linear control strategies. The approach proposed here could be used to evaluate the nonlinearity of such plants with respect to a linear control structure expressed as a scaling operator **S**. This provides great flexibility in the interpretation and application of the measures of curvature.

The interpretation of the curvature measure established for the analysis of steady-state processes is directly applicable in the dynamic case. The scaled measure is related to the curvature of a "surface" of radius 1/c. An output signal with a curvature of 0.3 displays, on average, a 15% deviation from the linear approximation in terms of its L_p norm.

The main difficulty is the requirement to remove the dependence on output and time scalings. To demonstrate this explicitly, let the output signals (belonging to L_2) of a system be scaled such that

$$\mathbf{z}(t) = \mathbf{S}(\mathbf{y}(t) - \mathbf{y}_0).$$

where **S** is a constant invertible matrix. As in the steady-state case, the time dependent scaling region is described by $\|z(\cdot)\|^2=1$. The L_2-norm of an output signal remaining on the boundary of the time dependent scaling region is given by

Adjustment of the time scale through division of the norm by T yields $L_2(\mathbf{z}(\sigma))=1$. Thus,

*Note that, in this case, the norm of **z**(t)

$$\|\mathbf{z}(t)\|^P = \int_0^T \|\mathbf{z}(t)\|^P dt \quad , \; P < \infty$$

and, consequently, the curvature measure depend on the size of the time interval [0,T). This must usually be accounted for in the analysis.

$$L_2(\mathbf{z}(t)) = \left[\int_0^T \|\mathbf{z}(t)\|^2 dt\right]^{1/2} = T^{1/2}.$$

combination of output and time scaling results in a curvature measure given with respect to a region of unit norm signals. For a given input signal, the scaled measure of dynamic nonlinearity proposed here gives a measure of the magnitude of the second order terms when the linear approximation of the operator generates an output signal of unit L_2-norm.

A more general approach to scaling is to provide a weight operator for both the inputs and the outputs. Recall that, in the steady-state case, this was achieved through the manipulation of the **Q** and **R** factors of the QR decomposition of the first order gain matrix and a scaling matrix **S**. In the dynamic case, it is not practical (although it is conceivable) to develop a counterpart of the QR decomposition for linear operators. We must use a more generic procedure defined as follows.

Suppose there exists a pair of stable invertible linear operators $\mathbf{Q}\in L(\mathbf{Y},\mathbf{Y})$ and $\mathbf{R}\in L(\mathbf{U},\mathbf{U})$ such that for $\mathbf{h}=\mathbf{Ra}$, $\|\mathbf{Q}d\mathbf{G}_p(\mathbf{u}_0)\mathbf{R}(\mathbf{a})\|=1$ with $\|\mathbf{a}\|=1$. The measure is redefined with respect to **a** as

$$c^2(\mathbf{a}) = \|\mathbf{Q}d^2\mathbf{G}_p(\mathbf{u}_0)(\mathbf{Ra})\| = \|\mathbf{A}(\mathbf{a})\|$$

where $\mathbf{A}(\mathbf{a})=\mathbf{Q}d^2\mathbf{G}_p(\mathbf{u}_0)$ $(\mathbf{Ra})$. We identify with a particular trajectory, **a**, a family of linear invertible operators with the specified property. This gives

$$c^2(\mathbf{a}) \le \|\mathbf{A}\|\|\mathbf{a}\|^2 = \|\mathbf{A}\|.$$

By definition, the operator norm $\|\mathbf{A}\|$ is the maximum value of the measure experienced by the system in the region $\|\mathbf{a}\|\le 1$. Since

$$\|\mathbf{Q}d\mathbf{G}_p(\mathbf{u}_0)\mathbf{R}\mathbf{a}\| = 1 \leq \|\mathbf{Q}d\mathbf{G}_p(\mathbf{u}_0)\mathbf{R}\|\|\mathbf{a}\|^2 = \|\mathbf{Q}d\mathbf{G}_p(\mathbf{u}_0)\mathbf{R}\|$$

it follows that there exists a positive nonzero real number $0 \leq \rho \leq 1$ such that

$$\rho c^2(\mathbf{a}) \leq c^2(\mathbf{a}) \leq \|\mathbf{A}\|.$$

The parallel with the steady-state analysis is obvious. The operators **Q** and **R** are identified with the matrices $\mathbf{Q}'$ and $\mathbf{R}_1^{-1}$ from the QR decomposition of the scaled first order steady-state gain matrix. In the dynamic case, the operators **Q** and **R** are interpreted as weighting (or scaling) operators for the output and input spaces, respectively. The operator **Q** describes the dynamic region of interest for the assessment of nonlinearity. The operator **R** is such that $\mathbf{h}=\mathbf{R}\mathbf{a}$ provides a typical input signal for the process. Note this approach is similar in nature to the procedure described in Morari and Zafirou (1988) for the assessment of process robustness. In fact, the development of weighting factors prescribed by these authors is directly applicable to the current problem.

The main obstacle in the application of the framework presented above is the actual computation of the second order derivatives of the operators at $\mathbf{u}_0$. Naturally if a nonlinear process model exists then it is possible to calculate such measures and evaluate the need for nonlinear control directly. A number of situations exist where this is not possible. Since the measure of nonlinearity provides a scale, a more pragmatic approach would be to use the measure as a gauge of the anticipated nonlinearity of a process control configuration. Assuming a certain of degree of nonlinearity (e.g. $c \approx 0.3$ for mildly nonlinear and $c \approx 1.0$ for highly nonlinear) and an appropriately chosen pair of weighting operators **Q** and **R**, one could conceivably construct an estimate of the contribution of the higher order effects to the output response and design a robust

linear controller that achieves a specified performance. It would then be reasonable to assume that, as the extent of nonlinearity is increased, the search for an acceptable linear controller would become more difficult, justifying the need for a nonlinear controller. Such an implementation of the proposed curvature measure and its extact relation to robust performance remain to be demonstrated. This will not be attempted in this study. It is of considerable interest however in light of the current analysis.

In the following section, the curvature measure is used to assess the nonlinearity of a continuous chemostat bioreactor model and a batch non-isothermal CSTR model. The first and second order sensitivity coefficients of the process outputs with respect to the process inputs are computed explicitly from the process models to obtain the curvature measure. The main objective is to highlight the potential advantages of assessing nonlinearity in a controlled process.

5. An Application of the Nonlinearity Measure

In this section, we consider the application of the measure of nonlinearity to time invariant state-space realizations of time-invariant nonlinear operators. It is assumed that a time invariant realization of a dynamical input-output nonlinear operator of the form

$$\dot{\mathbf{x}}(t) = \mathbf{f}(\mathbf{x}(t), \mathbf{u}(t))$$
$$\mathbf{y}(t) = \mathbf{h}(\mathbf{x}(t)).$$

exists.

In the following, we demonstrate how one can evaluate the curvature of a dynamic process expressed in this state-space form by calculating the first and second order sensitivity coefficients of the process outputs with respect to the inputs in a neighbourhood of a nominal point $u(t) \in U$. To motivate this, we consider the calculation of curvature of a Volterra series

expansion of a nonlinear system.

Suppose the nonlinear input-output operator is expressed as a Volterra series expansion of the form

$$\mathbf{y}(t) = \mathbf{w_0}(t) + \sum_{k=1}^{\infty} \sum_{i_k \ldots i_1=1}^{P} \int_0^t \int_0^{\tau_k} \ldots \int_0^{\tau_2} \mathbf{w}_{i_k \ldots i_1}(t, \tau_k, \ldots, \tau_1) \mathbf{u}_{i_k}(\tau_k) \ldots \mathbf{u}_{i_1}(\tau_1) d\tau_1 \ldots d\tau_k$$

where i_1, ..., i_k are integers between 1 and P, inclusively. The functions $\mathbf{w}_0$, $\mathbf{w}_{i_k \ldots i_1}$ are analytic functions called the kernels of the Volterra series expansion. The first and second order Taylor Fréchet derivative of the Volterra operator are easily computed at an equilibrium point of the system ($\mathbf{u}_0$, $\mathbf{y}_0$, $\mathbf{x}_0$). Assume that the input and output variables have been translated to the origins of **U** and **Y**, respectively, by using deviation variables about a point of interest[**]. The first order derivative at the origin $\mathbf{u}_0 = \mathbf{0}$ is simply given by

$$\mathbf{dG_p(u_0)h}(t) = \int_0^t \mathbf{w_1}(t, \tau_1) \mathbf{h}(\tau_1) d\tau_1.$$

The second order derivative is given by

$$\mathbf{d^2G_p(u_0)(h}(t)) = \int_0^t \int_0^{\tau_2} \mathbf{w_2}(t, \tau_1, \tau_2) \mathbf{h}(\tau_1) \mathbf{h}(\tau_2) d\tau_1 d\tau_2.$$

Now, consider the response of the process to constant input functions. This can be written as where the inputs are simply taken out of the integral. Differentiation of y(t) with respect to the

[**]In the case where the Volterra series is realized by a nonlinear time invariant system, it is known that achieving this translation requires a new state-space coordinatisation and a feedback transformation.

$$\mathbf{y}(t) = \mathbf{w_0}(t) + \sum_{k=1}^{\infty} \sum_{i_k \ldots i_1=1}^{P} \int_0^t \int_0^{\tau_k} \cdots \int_0^{\tau_2} \mathbf{w}_{i_k \ldots i_1}(t, \tau_k, \ldots, \tau_1) d\tau_1 \ldots d\tau_k u_{i_k} \ldots u_{i_1}$$

inputs yields the kernel representations of the first and second order gains. That is,

$$\frac{\partial \mathbf{y}}{\partial u_i}(t) = \int_0^t \mathbf{w}_i(t, \tau_1) d\tau_1$$

and

$$\frac{\partial^2 \mathbf{y}}{\partial u_i \partial u_j}(t) = \int_0^t \int_0^{\tau_2} \mathbf{w}_{ij}(t, \tau_2, \tau_1) d\tau_1 d\tau_2.$$

The first and second order instantaneous gains evaluated at a stationary point ($\mathbf{u}_0$, $\mathbf{y}_0$, $\mathbf{x}_0$) are identified with the unit impulse response of the first and second order kernels of the Volterra series expansion.

In general, process models expressed in state-space form are employed rather than their Volterra series expansion. One must therefore rely on the model equations to calculate the required derivatives. It is well known that the solution of a system of the form (1) in which $\mathbf{f}(\mathbf{x},\mathbf{u}) = \mathbf{f}(\mathbf{x})+\mathbf{g}(\mathbf{x})\mathbf{u}$ with initial condition $\mathbf{x}(0)=\mathbf{x}_0$ can be expressed in terms of a Volterra series functional expansion. Convergence of the Volterra series is ensured for small input signals, $\|\mathbf{u}(t)\| \leq \delta$ for $t \in [0,T]$. Because of the close connection between Volterra series and their state-space realizations, we can justify the calculation of the first and second order sensitivity coefficients of the process directly from the state-space models with the understanding that these coefficients are related to the first and second order Fréchet derivatives of the underlying input-output nonlinear operator.

The coefficients can be evaluated by solving the set of ordinary differential equations

$$\frac{d}{dt}\frac{\partial \mathbf{x}}{\partial \mathbf{u}} = \frac{\partial \mathbf{f}(\mathbf{x}_0, \mathbf{u}_0)}{\partial \mathbf{x}}\frac{\partial \mathbf{x}}{\partial \mathbf{u}} + \frac{\partial \mathbf{f}(\mathbf{x}_0, \mathbf{u}_0)}{\partial \mathbf{u}}$$

$$\frac{d}{dt}\frac{\partial^2 \mathbf{x}}{\partial \mathbf{u}\partial \mathbf{u}'} = \frac{\partial \mathbf{x}'}{\partial \mathbf{u}}\frac{\partial^2 \mathbf{f}(\mathbf{x}_0, \mathbf{u}_0)}{\partial \mathbf{x}\partial \mathbf{x}}\frac{\partial \mathbf{x}}{\partial \mathbf{u}} + \frac{\partial \mathbf{f}(\mathbf{x}_0, \mathbf{u}_0)}{\partial \mathbf{x}}\frac{\partial^2 \mathbf{x}}{\partial \mathbf{u}\partial \mathbf{u}'} + \frac{\partial \mathbf{x}'}{\partial \mathbf{u}}\frac{\partial^2 \mathbf{f}(\mathbf{x}_0, \mathbf{u}_0)}{\partial \mathbf{x}\partial \mathbf{u}'}$$

$$+ \frac{\partial^2 \mathbf{f}(\mathbf{x}_0, \mathbf{u}_0)}{\partial \mathbf{u}\partial \mathbf{x}'}\frac{\partial \mathbf{x}}{\partial \mathbf{u}} + \frac{\partial^2 \mathbf{f}(\mathbf{x}_0, \mathbf{u}_0)}{\partial \mathbf{u}\partial \mathbf{u}'}$$

$$\frac{\partial \mathbf{y}}{\partial \mathbf{u}} = \frac{\partial \mathbf{h}(\mathbf{x}_0)}{\partial \mathbf{x}}\frac{\partial \mathbf{x}}{\partial \mathbf{u}}$$

$$\frac{\partial^2 \mathbf{y}}{\partial \mathbf{u}\partial \mathbf{u}'} = \frac{\partial \mathbf{x}'}{\partial \mathbf{u}}\frac{\partial^2 \mathbf{h}(\mathbf{x}_0)}{\partial \mathbf{x}\partial \mathbf{x}'}\frac{\partial \mathbf{x}}{\partial \mathbf{u}} + \frac{\partial \mathbf{h}(\mathbf{x}_0)}{\partial \mathbf{x}}\frac{\partial^2 \mathbf{x}}{\partial \mathbf{u}\partial \mathbf{u}'}$$

These equations, called sensitivity equations, are obtained by differentiating the equations of system (1) with respect to **u**.

In what follows, the nonlinearity of nonlinear dynamical process expressed in state-space form is assessed by solution the sensitivity equations. A bioreactor model is considered in the first example to demonstrate the application of the dynamic measure of nonlinearity to continuous dynamical processes.

Example 4.1

Consider the two-state, one-input bioreator model

$$\frac{dx_1}{dt} = \mu x_1 - k_d x_1 - u_1 x_1$$

$$\frac{dx_2}{dt} = -\mu x_1 + (S_0 - x_2)u_1$$

where x_1 and x_2 are the biomass and substrate concentrations (g/l), u_1 is the reactor dilution rate (min^{-1}) and μ is specific growth rate given by

$$\mu = \frac{\mu_{max} x_2}{1 + x_2 + \frac{x_2^2}{K_i}}.$$

The model parameters are the maximum specific growth rate, μ_{max} (min^{-1}), the specific death rate, k_d (min^{-1}), the substrate inhibition constant, K_i (g/l) and the inlet substrate concentration, S_0 (g/l). Nominal values of these variables are given in Table 4.1.

Table 4.1

Nominal operating conditions of two-state one-input bioreactor model

Variables	Nominal Values
x_1	0.019821
x_2	0.18107
u_1	0.01
μ_{max}	0.5
k_d	0.05
S_0	0.3
K_i	10.0

Figure 4.1 shows the first and second order instantaneous gains of this process evaluated at the nominal conditions shown in Table 4.1.

We first consider scaling of the derivatives with respect to static regions of the state space. The scaling matrix

$$\mathbf{S} = \begin{bmatrix} 1/1.0\times10^{-5} & 0 \\ 0 & 1/5.0\times10^{-4} \end{bmatrix}$$

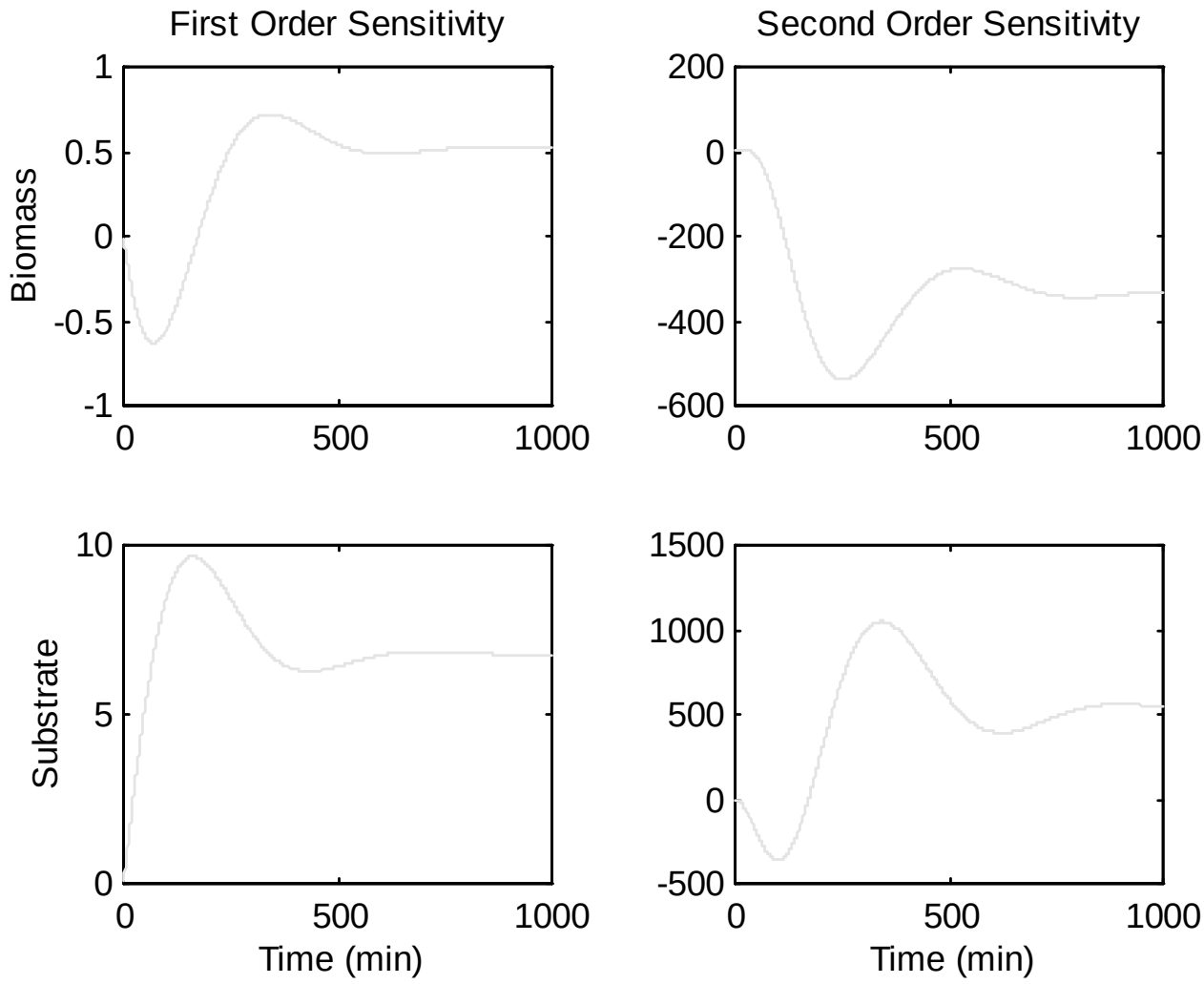

Figure 4.1 First and second order instantaneous gains of the bioreactor at the nominal conditions listed in Table 4.1.

provides a time independent scaling region of the state space about the stationary point $\mathbf{x}' = [x_1, x_2]' = [0.019821, 0.18107]'$. The L_2 curvature measure is given by

$$c(T) = \frac{\int_0^T \left\| \mathbf{S}\frac{\partial^2 \mathbf{x}}{\partial u_1^2} \right\|^2 dt}{\int_0^T \left\| \mathbf{S}\frac{\partial \mathbf{x}}{\partial u_1} \right\|^2 dt}^{1/2} = \frac{\int_0^T \left\| \frac{\partial^2 \mathbf{z}}{\partial u_1^2} \right\|^2 dt}{\int_0^T \left\| \frac{\partial \mathbf{z}}{\partial u_1} \right\|^2 dt}^{1/2}$$

The impact of time scaling on the resulting value of c(T) is removed by dividing the integrals of the numerator and the denominator by T(=1000). The contribution of x_1 and x_2 are given by

$$c^2(T) = \frac{\left(\int_0^T \left\| \frac{\partial^2 z_1}{\partial u_1^2} \right\|^2 dt\right)^{1/2}}{\int_0^T \left\| \frac{\partial \mathbf{z}}{\partial u_1} \right\|^2 dt} + \frac{\left(\int_0^T \left\| \frac{\partial^2 z_2}{\partial u_1^2} \right\|^2 dt\right)^{1/2}}{\int_0^T \left\| \frac{\partial \mathbf{z}}{\partial u_1} \right\|^2 dt}$$

For this choice of scaling region, the dynamic measure of nonlinearity is evaluated at 0.88. Therefore, the process can be said to display a highly nonlinear behaviour in a neighbourhood of the stationary point. The biomass contributes to 94.55% (=0.73) of the total squared curvature (=0.77).

In example 4.1, the assessment of nonlinearity was performed by solution of the sensitivity equations about a stationary point. In the same manner, we can also assess the extent of nonlinearity of a nonlinear system about a nominal trajectory, $\mathbf{y}_0(t)$, corresponding to a nominal input signal $\mathbf{u}_0(t)$. We can assign to each input trajectory $\mathbf{u}_0(t)$ a unique state trajectory $\mathbf{x}_0(t)$ with initial condition $\mathbf{x}(0)=\mathbf{x}_0$ which is mapped to $\mathbf{y}_0(t)$. The effect of perturbations of the inputs about its nominal trajectory can be assessed from the first and second instantaneous gains evaluated at a point ($\mathbf{u}_0(t)$, $\mathbf{x}_0(t)$). These are obtained by solving the equations

$$\dot{\mathbf{x}}_0(t) = \mathbf{f}(\mathbf{x}_0(t), \mathbf{u}_0(t))$$

$$\frac{d}{dt}\frac{\partial \mathbf{x}(t)}{\partial \mathbf{u}} = \frac{\partial \mathbf{f}}{\partial \mathbf{x}}(\mathbf{x}_0(t), \mathbf{u}_0(t))\frac{\partial \mathbf{x}(t)}{\partial \mathbf{u}} + \frac{\partial \mathbf{f}}{\partial \mathbf{u}}(\mathbf{x}_0(t), \mathbf{u}_0(t))$$

$$\frac{d}{dt}\frac{\partial^2 \mathbf{x}(t)}{\partial \mathbf{u}\partial \mathbf{u}'} = \frac{\partial \mathbf{f}}{\partial \mathbf{x}}(\mathbf{x}_0(t), \mathbf{u}_0(t))\frac{\partial^2 \mathbf{x}}{\partial \mathbf{u}\partial \mathbf{u}'} + \frac{\partial \mathbf{x}'(t)}{\partial \mathbf{u}}\frac{\partial^2 \mathbf{f}}{\partial \mathbf{x}\partial \mathbf{x}'}\frac{\partial \mathbf{x}(t)}{\partial \mathbf{u}} +$$

$$\frac{\partial \mathbf{x}'(t)}{\partial \mathbf{u}}\frac{\partial^2 \mathbf{f}}{\partial \mathbf{x}\partial \mathbf{u}'}(\mathbf{x}_0(t), \mathbf{u}_0(t)) + \frac{\partial^2 \mathbf{f}}{\partial \mathbf{u}\partial \mathbf{x}'}(\mathbf{x}_0(t), \mathbf{u}_0(t))\frac{\partial \mathbf{x}(t)}{\partial \mathbf{u}} + \frac{\partial^2 \mathbf{f}}{\partial \mathbf{u}\partial \mathbf{u}'}(\mathbf{x}_0(t), \mathbf{u}_0(t)).$$

As discussed above, the first and second order coefficients evaluated at a given nominal input trajectory $\mathbf{u}_0(t)$ can be associated with the first and second Fréchet derivatives, i.e., $d\mathbf{G}_p(\mathbf{u}_0(t))\mathbf{h}(t)$ and $d^2\mathbf{G}_p(\mathbf{u}_0(t))(\mathbf{h}(t))$, of the underlying nonlinear operator $\mathbf{G}_p:\mathbf{U}\rightarrow\mathbf{Y}$ in the direction of constant input perturbations, $\mathbf{h}(t)=\mathbf{c}$. These derivatives can be used to assess the nonlinearity of a nonlinear process about a nominal time-varying trajectory. In chemical engineering, this can be applied to batch processes operating in the neighbourhood of an optimal output trajectory. In the following example, this approach is used to assess the nonlinearity of the batch isothermal CSTR model discussed by Kravaris and Chung (1987).

Example 4.2

The problem addressed by Kravaris and Chung (1987) was the temperature tracking problem of a batch reactor where the simple reaction scheme

$$A \xrightarrow{k_1} B \xrightarrow{k_2} C$$

takes place. The first reaction is assumed to be of second order. The second reaction is first order. Let x_1, x_2 and x_3 represent the concentration of A, concentration of B and the reactor temperature then the process model can be expressed as

$$\frac{dx_1}{dt} = -k_1(x_3)x_1^2$$

$$\frac{dx_2}{dt} = k_1(x_3)x_1^2 - k_2(x_3)x_2$$

$$\frac{dx_3}{dt} = \gamma_1 k_1(x_3)x_1^2 + \gamma_2 k_2(x_3)x_2 + (a_1 + a_2 x_3) + (b_1 + b_2 x_3)u_1$$

where

$$k_1(x_3) = A_{10} e^{-\frac{E_1}{RT}}$$

$$k_2(x_3) = A_{20} e^{-\frac{E_2}{RT}}$$

The input u_1 is chosen such that the steam temperature T_s and the reactor heat transfer coefficient U_c are given by

$$T_s = (T_{s,max} - T_{s,min})u_1 + T_{s,min}$$

$$U_c = (U_{c,max} - U_{c,min})u_1 + U_{c,min}$$

The input u_1 must remain between 0 and 1 in order to meet the system limitations in steam temperature and cooling rate. The following process parameters have been defined

$$\gamma_1 = (-\Delta H_1)/\rho C_p$$

$$\gamma_2 = (-\Delta H_2)/\rho C_p$$

$$a_1 = (U_j A_j T_{s,min} + U_{c,max} A_c T_c)/\rho C_p V$$

$$a_2 = -(U_j A_j + U_{c,max} A_c)/\rho C_p V$$

$$b_1 = [U_j A_j (T_{s,max} - T_{s,min}) - (U_{c,max} - U_{c,min}) A_c T_c]/\rho C + pV$$

$$b_2 = (U_{c,max} - U_{c,min})/\rho C_p V$$

The parameters of the model are described in Table 4.2 along with the values used for the simulations.

Table 4.2
Process parameter descriptions and values

Process Parameter	Description	Value
A_{10}	Frequency factor of Rx 1	1.1 (m^3 $kmol^{-1}s^{-1}$)
A_{20}	Frequency factor of Rx 2	172.2 (s^{-1})
E_1	Activation energy of Rx 1	2.09×10^4 (kJ $kmol^{-1}$ K^{-1})
E_2	Activation energy of Rx 2	4.18×10^4 (kJ $kmol^{-1}$ K^{-1})
R	Ideal gas constant	8.314 (kJ $kmol^{-1}$ K^{-1})
T_s	Steam Temperature	[70,150] (∘C)
U_c	Overall heat transfer coeffi-cient of cooling coil	[1.39,4.42] (kJ m^{-2} ∘$C^{-1}s^{-1}$)
ρ	density	1000 (kg m^{-3})
C_p	Heat capacity	1 (kJ kg^{-1} ∘C^{-1})
$-\Delta H_1$	Heat of reaction 1	4.18×10^4 (kJ $kmol^{-1}$)
$-\Delta H_2$	Heat of reaction 2	8.36×10^4 (kJ $kmol^{-1}$)
A_c/V	Heat transfer area of cooling coil per unit volume	30 (m^{-1})
A_j/V	Heat transfer area of heating jacket per unit volume	17 (m^{-1})
T_c	Coolant Temperature	25 (∘C)
U_j	Overall heat transfer of heating jacket	1.16 (kJ m^{-2}∘$C^{-1}s^{-1}$)

The reactor temperature is to follow an optimal trajectory given by

$$T_d(t) = 54 + 71e^{-2.5\times10^{-3}t}$$

This trajectory maximizes the yield of B for a batch time of one hour. Two controllers are to

be used for this tracking problem. The first controller is a input-output linearizing controller of the form

$$u_1 = \frac{v - \beta_0 - \beta_1[\gamma_1 k_1(x_3)x_1^2 + \gamma_2 k_2(x_3)x_2 + (a_1 + a_2 x_3)]}{\beta_1(b_1 + b_2 x_3)}$$

where β_0 and β_1 are controller tuning parameters. This controller is such that the new input, v, acts linearly on the temperature. Control is achieved by manipulating v according to a PI controller of the form

$$v(t) = K_c(T_d(t) - x_3(t)) + \frac{K_c}{\tau_i}\int_0^t (T_d(\sigma) - x_3(\sigma))d\sigma$$

where K_c and τ_I are the controller gain and time constant. The tuning parameter values suggested by Kravaris and Chung (1987) are β_0=1, β_1=1000, K_c=0.1 and τ_I=3600. The second controller is a simple PI controller

$$u_1(t) = K_c(T_d(t) - x_3(t)) + \frac{K_c}{\tau_i}\int_0^t (T_d(\sigma) - x_3(\sigma))d\sigma.$$

where, as suggested by Kravaris and Chung (1987), K_c=0.1 and τ_I=3600.

Using the nonlinear controller to calculate the required input trajectory, $u_1(t)$, the first and second order sensitivity coefficients were evaluated by solving the corresponding time-varying sensitivity equations. The initial conditions $x_1(0)$=1, $x_2(0)$=0 and $x_3(0)$=25, were used. First and second order sensitivity coefficients of the output signal to perturbations in u_1 about its nominal trajectory $u_1(t)$ are plotted in Figure 4.2. The curvature measure is simply given as the ratio

$$c = \frac{\left(\int_0^T \left\| \frac{\partial^2 x_3(t)}{\partial u_1^2} \right\|^2 dt \right)^{1/2}}{\int_0^T \left\| \frac{\partial x_3(t)}{\partial u_1} \right\|^2 dt}$$

Two scaling strategies were used to evaluate the nonlinearity of the process. First, the first and second order sensitivity coefficients were scaled with respect to a 5 degree window about the nominal output trajectory. Scaling is simply performed as in the steady-state case by dividing the coefficients by 5.

Since nonlinearity is evaluated for the entire batch, the integrals used in the estimation of c are simply divided by 3600 seconds to remove the time dependence. Alternatively, we could scale by expressing the time t in terms of batch units of time. In this case, expressing t in terms of hours would have removed the dependence of the curvature measure on the size of the time interval used. The resulting curvature measure is 0.12. This process is therefore nearly linear. On average, perturbations of the input about its nominal trajectory do not contribute to the nonlinearity of the batch process.

According to the simulations performed by Kravaris and Chung (1987), it would seem that this conclusion is contradictory. In their work, the performance of the nonlinear and linear PI controllers were compared on the basis of their response to noise temperature measurement. They observed that the linear controller was very sensitive to this measurement error whereas the nonlinear controller performed very well. Although this can only be due to the presence of nonlinearity in the closed-loop system which is not accounted for by the linear controller, the current analysis indicates that this nonlinearity is not inherited by the process dynamics. This

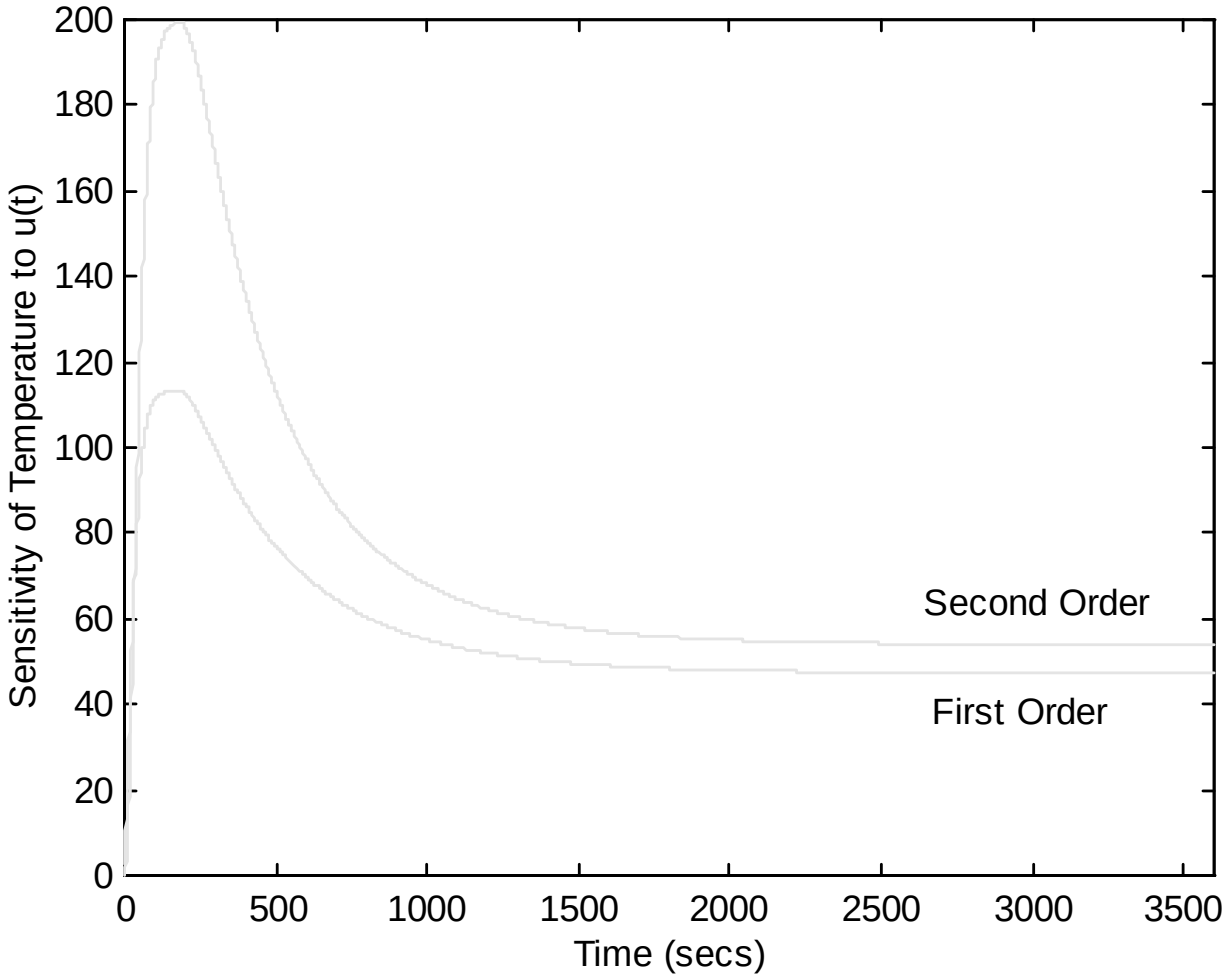

Figure 4.2 First and second order sensitivity coefficients evaluated at the nominal trajectory generated by the nonlinear controller given by Kravaris and Chung (1987).

also suggests that the scaling procedure employed for this analysis was not appropriate. The simple scaling approach employed does not provide a measure of nonlinearity with respect to the regions of the output space where nonlinearity is manifested.

An alternative scaling approach consists of filtering the output signal by an integral operator

$$z(t) = k_s(T_d(t) - x_3(t)) + \frac{k_s}{\tau_s}\int_0^t (T_d(\sigma) - x_3(\sigma))d\sigma.$$

The nonlinearity associated with perturbations of the inputs on the scaled output z(t) is assessed by evaluation of the first and second order sensitivity coefficients of z(t) with respect to the inputs. This scaling procedure transforms the problem of assessing the nonlinearity of the process output subject to input perturbations to the evaluation of the nonlinearity of the controller output subject to the same perturbations. Consequently, we can simply choose k_c and τ_s to be the parameters (K_c and τ_I, respectively) of the linear PI controller suggested by Kravaris and Chung (1987). Figure 4.3 shows the response of the scaled output, z(t), generated by the closed-loop process subject to linear PI control.

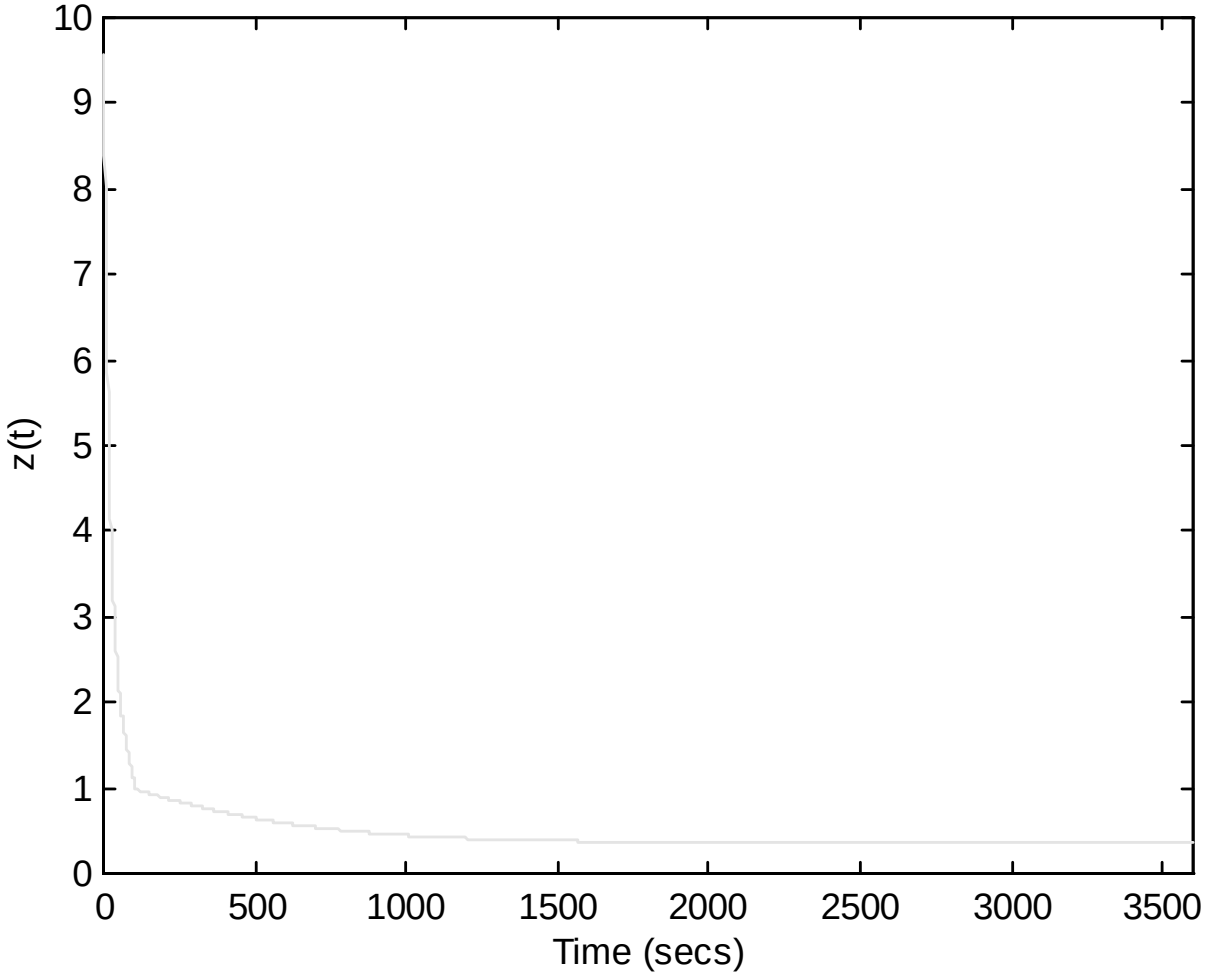

Figure 4.3 Scaled output signal for the closed-loop response of the batch reactor under linear PI control.

The initial condition, z(0), is dictated by the controller equation, i.e., z(0)=0.1(51+74-25)=10. The first and second order sensitivity coefficients are shown in Figure 4.4.

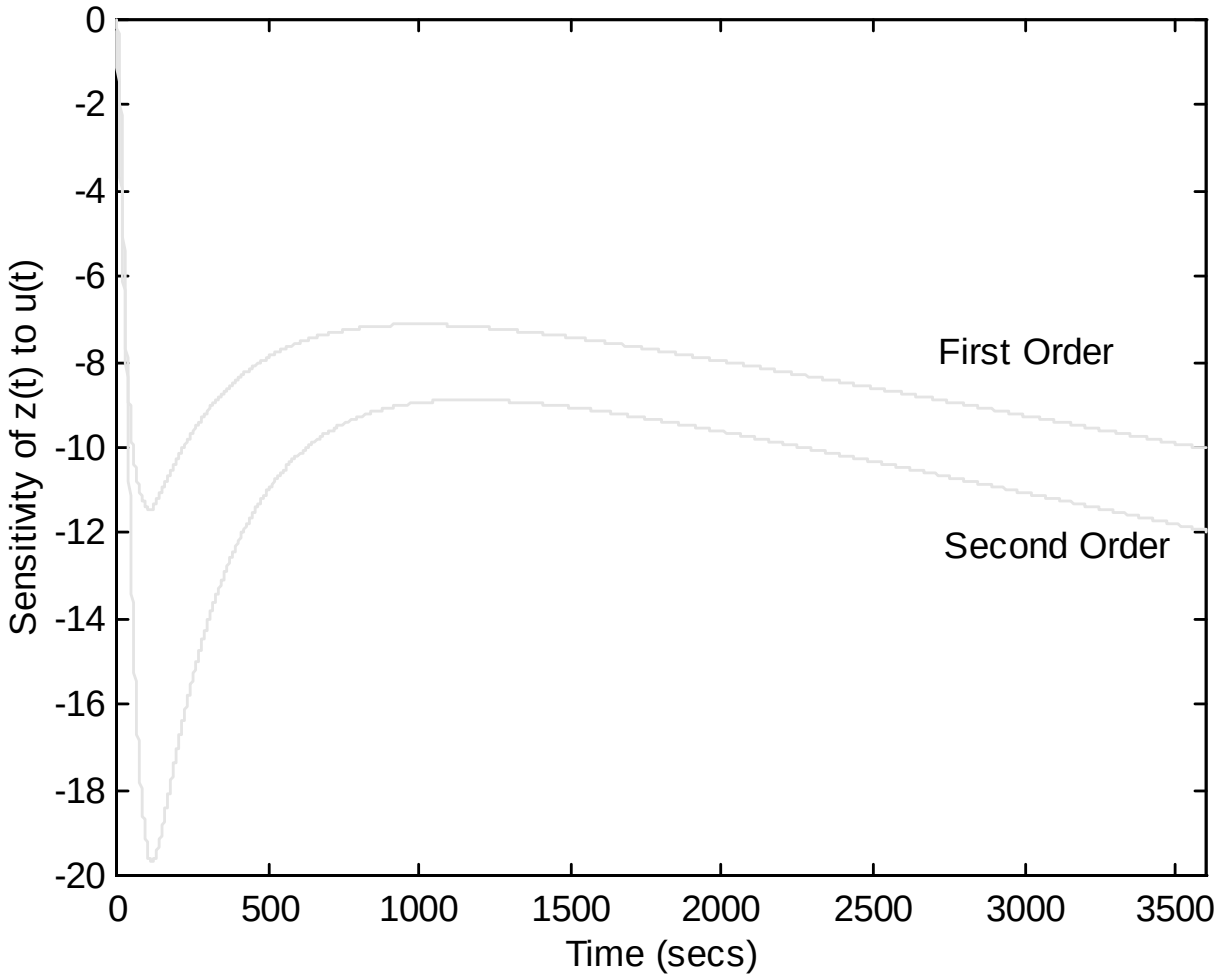

Figure 4.4 First and second order sensitivity coefficients of the scaled output z(t) evaluated at the nominal trajectory of the linear PI controlled batch reactor.

Since the controller output must be constrained between 0 and 1, we simply divide the sensitivity coefficients by 10 to convert the controller output to input units. Upon averaging the numerator and denominator integral by 3600 seconds to remove the impact of the time scale, the curvature measure is evaluated at 0.38. This suggests that the closed-loop system is nonlinear and that its nonlinearity originates from saturation of the input. Inspection of the simulation performed by Kravaris and Chung (1987) confirms this observation. The response of the process under linear

PI controller subjected to noisy temperature measurements results in fast fluctuations of the input between 0 and 1. Although the nonlinearity of the process to fluctuations of the inputs is small, the linear PI controller amplifies its magnitude through saturation of the input. The large input changes required for the controller output to fulfil the saturation bounds introduce nonlinearity in the closed-loop system.

6. Conclusions

In this chapter, a measure of dynamic nonlinearity was introduced. The measure reflects the importance of the contribution of the second order Taylor derivative of Fréchet differentiable time invariant unbiased operator describing the dynamic input-output behaviour of a nonlinear system.

Development of the dynamic measure of nonlinearity comes as a result of a simple extension of the steady-state measure. In the steady-state case, the contribution of the second order terms to the second Taylor series expansion of a differentiable map is measured relative to the Euclidean norm. The dynamic extension requires the evaluation of the contribution of the second order terms relative to the L_p-norm of the process output signals. As in the steady-state case, scaling must be provided to remove the dependence of the curvature measure to output scaling. Scaling must be provided in order to measure curvature relative to a region of unit norm. This can be done in a number of ways. The general approach is to define a scaling operator that maps a bounded set of the space of output signals to a unit norm bounded set of scaled output signals. This approach to scaling provides great flexibility in the analysis allowing, for example, to measure nonlinearity of a process relative to sets described by linear controller structures.

The application of the curvature measure was demonstrated using two chemical process

examples. A bioreactor example was used to demonstrate the application of the measure to continuous processes. The nonlinearity of the batch CSTR example presented by Kravaris and Chung (1987) was also calculated. The latter example clearly demonstrated the benefits of measuring process nonlinearity in the analysis of a nonlinear chemical process. Since the process did not display significant nonlinearity about the nominal trajectory, nonlinear control, as performed by Kravaris and Chung (1987), was not necessary. Using an alternative scaling procedure, it was shown that the nonlinearity of the closed-loop process was due to large input saturation effects that could have been removed by appropriate linear controller design.

The ability to measure the extent of nonlinear of a process is a powerful in controller design. It is interpreted as a justification for nonlinear controller design which comes as a result of restrictions of the performance of linear controller imposed by the nonlinearity. In that sense, the nonlinearity measure could be used as a tool of analysis for developing robust linear controller of nonlinear plants. Elucidating the relationship between robust performance of a linear controller and the nonlinearity measure may prove to be an essential component in the implementation of the framework presented in this Chapter.

Nomenclature

A Linear operator

a Real number

B Subset of a topological space

b Real number

C Directed set

c Root squared curvature

d Metric on a topological space

d Fréchet differential of a nonlinear operator

D Domain of an operator

D_p Domain of the input-output operator

f Mapping

f Vector field describing dynamics on the state space

$\mathbf{G}_p$ Differentiable Input-output nonlinear operator

g Vector field describing input-driven dynamic on the state space of a control-affine nonlinear system

H Homogeneous form

h State-output map

K Field

K_C Controller gain

$L(\mathbf{U},\mathbf{Y})$ Space of linear operators between topological spaces **U** and **Y**

L_P^N Banach space of p-integrable functions taking values in $\mathbb{R}^N$

M	Real number
$\mathbf{Q}$	Linear operator
$\mathbf{R}$	Linear operator
r	Real number
S	Directedness on a topological space
$\mathbf{S}$	Linear operator
s	Sequence in a topological space
T	Final integration time
t	Time
$\mathbf{U}$	Banach space of p-integrable input trajectories
$\mathbf{u}$	Input trajectory
$\mathbf{u}_0$	Nominal input trajectory
$\mathbf{w}$	Wiener-Volterra kernel
x	Point in a topological space
$\mathbf{x}$	State trajectory
$\mathbf{x}_0$	Nominal state trajectory
$\mathbf{Y}$	Banach space of p-integrable output trajectories
y	Point in a topological space
$\mathbf{y}$	Output trajectory
$\mathbf{y}_0$	Nominal output trajectory
$\mathbf{y}_\mathbf{L}$	Linear part of output trajectory
$\mathbf{y}_\mathbf{N}$	Nonlinear part of output trajectory

z Point in a topological space

Greek Letters

α Real number

β Real number

β Topology

γ Cover of a topological space

δ Real number

ε Real number

ξ Real number

$\rho(\ ,\ )$ Metric of a normed space

ρ Real number

τ Topology

τ_I Controller time constant

ϕ Functional

ω Functional

Symbols

$\mathbb{B}$ Topological space

$\mathbb{Ж}$ Topological space

$\mathbb{Ж}^*$ Conjugate space of $\mathbb{Ж}$

$\mathbb{И}$ Topological space

$\mathbb{Ц}$ Topological space

$\mathbb{C}$ Set of complex numbers

ℓ	Real number
$\mathbb{N}$	Set of natural numbers
$\mathbb{R}$	Set of real numbers

Chapter 5

Linearizability of Nonlinear Control Processes

1. Introduction

The focus of this thesis, as demonstrated in Chapters 2, 3 and 4, is to provide a methodology for measuring nonlinearity in controlled processes. It is important to provide a systematic way to account for nonlinearity in order to achieve adequate controller designs. For steady-state processes, as shown in Chapters 2 and 3, curvature measures can be used to derive transformations that remove the local effects of gain nonlinearity. For dynamic processes, the approach presented in Chapter 4 provides a methodology for the measurement of process nonlinearity. However, the problem of finding coordinate transformations that remove nonlinearity cannot be addressed empirically. More fundamental approaches must be considered.

Of primary interest in this chapter is the problem of exact linearization of nonlinear systems by coordinate transformations and feedback. The exact (and the approximate) linearization problem has been an active area of research over the last 20 years in the systems theoretic literature. The most powerful approaches involving rigorous treatment of this problem have used differential geometric techniques (Brockett, 1978; Brockett *et al.* , 1983; Hunt, Su and Meyer, 1983a, 1983b; also see Nijmeijer and van der Schaft, 1989 and Isidori, 1989 for a comprehensive development of differential geometric methods). These techniques have been used extensively in the study of the equivalence of nonlinear systems to linear systems by state space transformations and feedback. The ability to linearize nonlinear control systems exactly currently forms the basis for most engineering applications of nonlinear control techniques (see Hoo and

Kantor, 1986, Henson and Seborg, 1990 and McLellan *et al.*, 1990, for chemical engineering applications).

It is generally recognized, however, that linearizability is not a generic property of nonlinear control systems (Atkins and Shadwick, 1994; Shadwick, 1993). By this we mean that the class of feedback linearizable nonlinear systems forms a subset of the set of all nonlinear systems with infinite co-dimensions. The occurrence of feedback linearizable systems is therefore extremely rare in practice. To overcome this problem, approximation techniques are often used to linearize systems approximately that cannot be exactly transformed by feedback and state-space transformations to a linear system. This situation introduces another aspect of the nonlinearity of a process, namely its linearizability.

Two types of linearization are usually considered: 1) exact linearization of a nonlinear dynamical system by feedback and state space transformation and 2) exact linearization of an input-output response by feedback and state-space transformation where feedback transformations can be either static or dynamic.

The problem of linearization by state feedback has been considered by a number of researchers. In the differential geometric setting, two approaches have been used to solve this problem. Originally, the problem of formal linearization of Lie algebras of vector fields (Hermann, 1968) was applied to the problem of linearization by state feedback. This led to the development of necessary and sufficient conditions for linearization (Jakubzcyk and Respondek, 1980; Hunt, Su and Meyer, 1983a) and to the development of procedures for multi-input nonlinear systems (Hunt, Su and Meyer, 1983b). The second approach to the solution of this problem was motivated by the study of Cartan's method of equivalence of Pfaffian systems

(Gardner , 1967, 1989; Hermann, 1982). Gardner and Shadwick (1990, 1992) used this setting to develop an algorithm which is essentially the exterior differential counterpart of the method of Hunt, Su and Meyer (1983b). However, this algorithm is more general in construction and is considerably easier to implement using computer algebra software such as MAPLE® or MATHEMATICA®.

It is obvious that the linearizability of a nonlinear system by state feedback and state space transformation is a truly non-generic property. But since linearizability is such an important feature of controller design using differential geometrical control techniques, a great deal of effort has been devoted to extending the applicability of linearization methods of nonlinear systems. Dynamic feedback transformations, first introduced by Charlet *et al* (1989), have been used to linearize nonlinear systems which are more intrinsically nonlinear. Their development, later supported by Shadwick (1991), considered dynamic feedback linearization of single-input systems using a simple dynamic compensator obtained by differentiating the input channel with respect to time. Charlet *et al.* (1989) and Shadwick (1991) showed that, for this specific class of compensators, a nonlinear system can be linearized by dynamic feedback if and only if it can be linearized by state feedback. Thus the use of dynamic feedback does not broaden the class of SISO systems that can be linearized. Their result demonstrated that the use of dynamic feedback is essentially reserved to multi-input systems since it cannot be used to extend the class of systems that are linearizable by state feedback. Recently, Tchoń (1994) demonstrated the non-genericity of multi-input control-affine systems which are linearizable by dynamic feedback using linear compensators. This work showed that most control-affine systems cannot be linearized by dynamic feedback and the ability to do so is not an inherent property of MIMO nonlinear

systems. Rouchon (1994) and Sluis (1993) developed necessary conditions for the linearizability of multi-input general nonlinear systems. In particular, Rouchon (1994) showed that these necessary conditions imply the non-genericity of dynamic feedback linearization in general nonlinear systems.

It is significant that these results have been developed in the absence of a condition for dynamic feedback linearizibility which is both necessary and sufficient. Non-genericity, as discussed by Rouchon (1994) and Tchoń (1994), is deduced from topological considerations which can be argued to be too general and poorly adapted to the problem at hand. This point was discussed by Rouchon (1994), who noted the paradox posed by the apparent genericity of dynamic feedback linearizability in practical applications.

Another approach to the problem of linearization by state feedback is to implement feedback and state space transformations which approximately linearize a nonlinear system. This problem was first treated by Krener (1984). It essentially consists of finding feedback and state-space transformations which are polynomials of order ρ in the states and ρ-1 in the inputs, such that a nonlinear system can be linearized up to order ρ. Krener *et al.* (1987, 1988) and Krener and Wang (1990) demonstrated the benefits of using approximate linearization techniques to simplify the design of nonlinear controllers for single-input systems. Guzzella and Isidori (1993) and Hunt and Turi (1993) extended the approach presented by Krener *et al.* (1987) to multi-input systems using simplified approaches. Banaszuk and Hauser (1994) used a heuristic approach based on the homotopy operator to solve the approximate linearization problem for single-input systems. Using these techniques, it is relatively easy to find coordinate transformations and feedbacks which approximately linearize a system. Although not an issue in most of these

developments, such techniques are approximate and the validity of the approximations must be checked. Doyle III and Morari (1990) demonstrated the robustness of controller designs based on the approximate linearization approach of Krener *et al.* (1987, 1988). In their approach, the higher order terms neglected by approximate linearization are treated as residual nonlinearity. The structured singular value was used to demonstrate the robustness of approximate linearizing controllers to the effect of higher order terms for a chemical reactor.

When a system is not linearizable, it is important to know how far it is from being linearizable or how well it can be approximated by a linearizable system. Atkins and Shadwick (1993) and Shadwick (1993) considered this question and used the Gardner and Shadwick (GS) algorithm (1992) and the group reduction technique of Cartan (see Gardner, 1989) to identify invariant functions which must vanish in order for a system to be linearizable. Using a class of models from air flight control, Shadwick (1993) demonstrated how these invariant functions can be used in design to uncover natural geometrical outputs and how they can be used to parametrize subclasses of linearizable systems.

Another design alternative which has been considered in differential geometrical control is the exact linearization of the input-output response (Isidori, 1989; Nijmeijer and van der Schaft, 1990). This technique is often preferred in practice because the regularity conditions which are used to prove necessity and sufficiency (Isidori, 1989) are generally less restrictive than the conditions for exact linearization by state feedback. Input-output exact linearization with dynamic feedback has also been considered in a differential geometrical setting by Isidori *et al.* (1986). Approximate input-output linearization has recently been considered by Kang (1994).

Differential algebraic techniques (Fliess, 1987; Di Benedetto *et al.*, 1989) have been used

to complete or improve results obtained in the differential geometric setting. Of particular importance is the concept of differential flatness of a nonlinear system. This concept, introduced by Fliess *et al*. (1993), generalizes the concept of linearizing outputs of a nonlinear system using a differential algebraic framework which does not differentiate between state, input and output variables. This approach is consistent with the behavioral methodology of Willems (1991). Sufficient conditions for differential flatness have been formulated in geometrical terms by Martin (1993). In the differential geometrical context, flatness is a property displayed by linearizable systems. It is not, however, restricted to this class of systems.

It is obvious that, from a system theoretic point of view, the nonlinear behaviour of a system should be handled with appropriate techniques. In this framework, the "true" nonlinearity of a process reflects the impossibility of linearizing it exactly using coordinate and feedback transformations. This aspect of the nonlinearity of a process is considered in this Chapter.

The primary tool of the analysis presented here is the exterior calculus setting employed by Gardner and Shadwick (1992), Sluis (1993), Martin (1994) and Aranda-Bricaire *et al.* (1995). This setting is summarized in Section 2. In Section 3, we present the GS algorithm for the linearization of nonlinear systems. In Section 4, this algorithm is used to uncover invariant functions which are curvature-like quantities acting as geometric obstructions to the linearizability of classes of chemical processes. A simple CSTR model is used to illustrate the ideas. In section 5, the GS algorithm is adapted to provide a solution to the problem of dynamic feedback linearization of nonlinear systems by endogenous feedback. A new necessary and sufficient condition for dynamic feedback linearizability is presented which also provides a systematic way to obtain linearizing dynamic precompensators.

2. Exterior Calculus Setting

Before engaging in a discussion of the application of the exterior calculus setting in control theory, a brief review of exterior algebra and exterior calculus will be presented.

a) Exterior algebra

Let V be an n-dimensional vector space[***] of the field of real numbers $\mathbb{R}$.

The wedge product between two vectors $v,w \in V$ is a non-commutative product which is

i) distributive,

$$(\alpha v_1 + \beta v_2) \wedge w = \alpha(v_1 \wedge w) + \beta(v_2 \wedge w)$$

ii) bilinear,

$$v \wedge (\alpha w_1 + \beta w_2) = \alpha(v \wedge w_1) + \beta(v \wedge w_2)$$

iii) skew-commutative

$$v \wedge w = -w \wedge v.$$

Note that property (iii) $\Rightarrow v \wedge v \equiv 0$.

The result of the wedge product of two (one-)vectors is called a two-vector. The space of two-vectors on V, $\Lambda^2(V)$, is given by the set of all wedge products of the form

$$\sum_i \alpha_i (v_i \wedge w_i) \ , \ v_i, w_i \in V \text{ and } \alpha_i \in \mathbb{R}.$$

Let $\{e_1, ..., e_n\}$ be a basis for V. The n(n-1)/2 elements

[***]A vector space is a space made up of elements called vectors along with the operations of addition and multiplication by scalars.

$$\{e_i \wedge e_j \mid i<j\}$$

form a basis for $\Lambda^2(V)$. The space $\Lambda^2(V)$ is a linear space of dimension n(n-1)/2.

We can also define a p-vector as the result of the wedge product of p (one-) vectors. Let $\omega(=v_1 \wedge \ldots \wedge v_p) \in \Lambda^p(V)$ with $v_1, .., v_p \in V$. It is clear that $\omega=0$ if any $v_i=v_j$, $i \neq j$. Because of the skew-commutativity property (iii) above, the sign of ω is changed when any two (one-) vectors v_i, v_j are exchanged in the wedge product $v_1 \wedge \ldots \wedge v_p$. The space $\Lambda^p(V)$ has dimension $n!/p!(n-p)!={}_nC_p$.

Let $\omega \in \Lambda^p$, $\upsilon \in \Lambda^q$. The wedge product of ω and υ is given by

$$\omega \wedge v = (-1)^{pq} v \wedge \omega.$$

The vectors $v_1, \ldots, v_p \in V$ are linearly dependent if and only if $v_1 \wedge \ldots \wedge v_p=0$. In other words, for any w, $v_i \in V$, we see that if $w \wedge v_1 \wedge \ldots \wedge v_p=0$ then there exist $\alpha_i \in \mathbb{R}$ such that

$$w = \sum_{i=1}^{p} \alpha_i v_i.$$

Let V^* be the covector space of V, where a covector maps $v \in V$ to $\mathbb{R}$. V^* is also known as the dual space of V. By defining an exterior algebra on V^*, the space of p-covectors given by $\Omega^p(V)=\Lambda^p(V^*)$ is defined. If $\{e_1^*, \ldots, e_n^*\}$ is a basis for V^*, then $\{e_{i_1} \wedge \ldots \wedge e_{i_p}\}$, $1 \leq i_1<\ldots<i_p \leq n$, is a basis of $\Omega^p(V)$, the exterior algebra on the covector space of V.

By definition, covectors $w^*:V \rightarrow \mathbb{R}$ are linear functions on V. If $w^*=\sum_i w_i e_i^* \in V^*$ and $v=\sum_i v_i e_i \in V$, then $w^*(v)=\sum_i w_i v_i$. Similarly, two-covectors $\omega \in \Omega^2(V)$ are skew bilinear maps $\omega:V \times V \rightarrow \mathbb{R}$. For any $\omega=\sum_{ij} \omega_{ij} e_i^* \wedge e_j^*$, $i<j$ and $v, w \in V$, then

$$\omega(v,w) = \sum_{1 \le i < j \le n} (\omega_{ij} v_i w_j - \omega_{ij} v_j w_i).$$

b) Differentiable manifolds

An n-dimensional differentiable manifold M is an abstract set of points with the following properties:

1) The notion of a continuous function is defined on M (i.e., M is Hausdorff with countable base).

2) M is the union of a collection of open sets U_i. $M \subset \cup_i U_i$, $i \in A$, where A is an indexing set.

3) For each $i \in A$, there exists a continuous equivalence between U_i and $\mathbb{R}^n$. More precisely, there exists a diffeomorphism $\phi_i: U_i \rightarrow \mathbb{R}^n$ called a coordinate chart of M.

4) For any two intersecting coordinate charts $U_i \cap U_j$, the change of coordinate map expressed as the composition $\phi_i \circ \phi_j^{-1}$ is a smoothly differentiable map.

The collection $\{(U_i, \phi_i) \mid i \in A\}$ is called an atlas of charts on the manifold M.

Conceptually, a differentiable manifold is an abstract space that locally looks like a Euclidean space. Using local coordinate representations, familiar operations from differential calculus can be applied directly to abstract manifolds.

At each point $p \in M$, a tangent space can be attached to M. This tangent space is denoted as T_pM. The differentiable structure (property 4) allows the concept of a tangent space on a manifold to be related to the familiar concept of a tangent space in $\mathbb{R}^n$.

For a point $x \in \mathbb{R}^n$, the tangent space $T_x\mathbb{R}^n$ at x is the set of tangent vectors to $\mathbb{R}^n$ at x. $T_x\mathbb{R}^n$ is in fact a copy of $\mathbb{R}^n$. The natural basis of $T_x\mathbb{R}^n$ is denoted by

$$\left\{\frac{\partial}{\partial x_1}\Big|_x, \ldots, \frac{\partial}{\partial x_n}\Big|_x\right\}.$$

A corresponding basis for T_pM can be identified as follows. Consider a manifold of dimension n and let $p \in M$. Let (U,ϕ) be a coordinate chart in a neighbourhood of p. For $v \in T_{\phi(p)}\mathbb{R}^n$, define

$$\phi_*(p)v = \frac{\partial \phi^{-1}}{\partial x}(\phi(p))v.$$

The expression $\phi_*(p)v$ is the image of v in T_pM via the local coordinate representation. The tangent space T_pM at p is defined as

$$T_pM = \text{span}_{C^\infty(M)}\left\{\phi_*(p)\frac{\partial}{\partial x_k}\Big|_{\phi(p)} \Big| k = 1, \ldots, n\right\}$$

The elements of T_pM are called tangent vectors at p. Since ϕ is a diffeomorphism, the mapping $\phi_*(p):T_{\phi(p)}\mathbb{R}^n \to T_pM$ is a linear isomorphism. Hence the vectors

$$\frac{\partial}{\partial \phi_k}\Big|_p = \phi_*(p)\frac{\partial}{\partial x_k}\Big|_{\phi(p)}, \quad k = 1, \ldots, n$$

form a basis of T_pM. The set $TM=\{(p,v) \mid p \in M, v \in T_pM\}$ is called the tangent bundle of M.

Note that this definition of T_pM coincides with the intuitive notion of the tangent space to a surface in $\mathbb{R}^n$. It is also independent of the choice of local coordinates.

A vector field v on M is a mapping that assigns a tangent vector $v(p) \in T_pM$ to each $p \in M$. A vector field is smooth if for each $p \in M$ there exists a coordinate chart (U,ϕ) around p and smooth functions $v_1, \ldots, v_n$ on M such that for all $\bar{p} \in U$, $v(\bar{p}) = \sum_{i=1}^{n} v_i(\bar{p})\partial/\partial\phi_i \mid_{\bar{p}}$, i.e., v can be expressed in terms of the basis vector fields with smooth coefficient functions.

A distribution Δ of M is a mapping that assigns to each $p \in M$ a linear subspace of T_pM.

Δ is called a smooth distribution if for each $p \in M$ there exists a neighbourhood $U \subset M$ of p and a set of vector fields v_1, ..., v_i, $i \in I$, with I some (possibly infinite) index set, such that for all $\bar{p} \in U$, $\Delta(\bar{p}) = \text{span}\{v_i(\bar{p}) \mid i \in I\}$.

c) Differential forms

The cotangent space, T_p^*M, of M at p is defined as the space of linear mappings of T_pM. Its elements are linear maps $\omega: T_pM \to \mathbb{R}$. The elements of T_p^*M are called cotangent vectors at p. If $\omega \in T_p^*M$, the value of ω at $v \in T_pM$ is denoted by $\omega(v)$.

Let $\{v_1, ..., v_n\}$ be a basis of T_pM at p. The unique basis $\{\omega_1, ..., \omega_n\}$ which satisfies $\omega_i(v_j) = \delta_{ij}$, $1 \le i,j \le n$, is called the dual basis of T_p^*M with respect to $\{v_1, ..., v_n\}$.

Given a coordinate chart (U,ϕ) around p, the dual basis to

$$\left\{ \frac{\partial}{\partial \phi_1}\Big|_p, \ldots, \frac{\partial}{\partial \phi_n}\Big|_p \right\}$$

is given by

$$\{ d\phi_1|_p, \ldots, d\phi_n|_p \}.$$

The cotangent bundle is the set

$$T^*M = \{ (p,\omega) \mid m \in M, \omega \in T_p^*M \}.$$

A differential one-form (or covector field) ω on M is a mapping that assigns to each $p \in M$ a cotangent vector $\omega(p) \in T_p^*M$. A differential one-form is smooth if for each $p \in M$ there exists a coordinate chart (U,ϕ) around p and smooth functions ω_1, ..., ω_n on M such that for all $\bar{p} \in U$, $\omega(\bar{p}) = \sum_{i=1}^{n} \omega_i(\bar{p}) d\phi_i|_{\bar{p}}$.

The cotangent space (space of one-forms on M) is denoted by $\Omega^1(M)$ or simply $\Omega(M)$.

Similarly, a k-form on M at p is a mapping ω that assigns to each point $p \in M$ a k-covector $\omega(p) \in \Lambda^k(T_p^*M) = \Omega^k(T_pM)$.

A codistribution Θ of M is a mapping that assigns to each $p \in M$ a linear subspace of T_p^*M. Θ is called a smooth codistribution if for each $p \in M$ there exists a neighbourhood $U \subset M$ of p and a set of one-forms $\omega_1, ..., \omega_i$, $i \in I$, with I some (possibly infinite) index set, such that for all $\bar{p} \in U$, $\Theta(\bar{p}) = \text{span}\{\omega_i(\bar{p}) \mid i \in I\}$.

d) Exterior derivative

Let

$$\omega = \sum_{i_1<...<i_p} a_{i_1...i_p} dx_{i_1} \wedge ... \wedge dx_{i_p}$$

be a smooth p-form on M where $a_{i_1...i_p}$ are smooth functions of x_{i_j}. The exterior derivative of ω is the (p+1)-form

$$d\omega = \sum_{i_1<...<i_p} da_{i_1...i_p} \wedge dx_{i_1} \wedge ... \wedge dx_{i_p}.$$

Note that

$$da_{i_1...i_p} = \sum_{i=1}^{n} \frac{\partial a_{i_1...i_p}}{\partial x_i} dx_i$$

The operator d has the following properties:

i) Linearity

$$d(\omega_1 + \omega_2) = d\omega_1 + d\omega_2,$$

ii) Action on wedge products

$$d(\omega \wedge \nu) = (d\omega \wedge \nu) + (-1)^p(\omega \wedge d\nu),$$

iii) Poincaré Lemma

$$d(d\omega) = 0.$$

d) Integrability of forms

A codistribution $I \subset T^*M$ of constant dimension k is integrable if there exist k functions h_1, ..., h_k such that $I=\text{span}\{h_1, ..., h_k\}$.

Theorem 1 (Frobenius) A k-dimensional codistribution $I=\text{span}\{\omega_1, ..., \omega_k\}$ is locally integrable if and only if there exist one-forms θ_{ij} such that

$$d\omega_i = \sum_{j=1}^{k} \theta_{ij} \wedge \omega_j.$$

A closed one-form is such that $d\omega=0$. A one-form is said to be exact is there exists a function h such that $\omega=dh$. Theorem 1 asserts that all closed one-forms are exact.

e) Exterior differential systems

An exterior differential system is given by a homogeneous ideal $I \subset \Omega(M)$ that is closed under exterior differentiation. More specifically, I satisfies

(i) $\alpha \in I, \beta \in \Omega(M) \Rightarrow \alpha \wedge \beta \in I$

(ii) $\alpha \in I, \alpha = \sum_i \alpha_i \omega_i, \omega_i \in \Omega(M) \Rightarrow \omega_i \in I$

(iii) $\alpha \in I \Rightarrow d\alpha \in I.$

f) Pfaffian systems

An algebra *V* is called a ring if and only if the following conditions are satisfied

(i) $\forall \mathbf{v}_1, \mathbf{v}_2 \in V$, $\mathbf{v}_1 + \mathbf{v}_2 = \mathbf{v}_2 + \mathbf{v}_1$

(ii) $\forall \mathbf{v}_1, \mathbf{v}_2, \mathbf{v}_3 \in V$, $\mathbf{v}_1 + (\mathbf{v}_2 + \mathbf{v}_3) = (\mathbf{v}_1 + \mathbf{v}_2) + \mathbf{v}_3$

(iii) $\exists \mathbf{0} \in V \mid \forall \mathbf{v} \in V, \mathbf{v} + \mathbf{0} = \mathbf{v}$

(iv) $\forall \mathbf{v} \in V, \exists -\mathbf{v} \in V \mid \mathbf{v} + (-\mathbf{v}) = \mathbf{0}$

(v) $\forall \mathbf{v}_1, \mathbf{v}_2, \mathbf{v}_3 \in V, \mathbf{v}_1(\mathbf{v}_2\mathbf{v}_3) = (\mathbf{v}_1\mathbf{v}_2)\mathbf{v}_3$.

A commutative ring is such that

(vi) $\forall \mathbf{v}_1, \mathbf{v}_2 \in V, \mathbf{v}_1\mathbf{v}_2 = \mathbf{v}_2\mathbf{v}_1$.

A module for the algebra *V* is a vector space W over the field K along with a binary product $V \times W$ into W mapping (υ, w), $\upsilon \in V$, $w \in W$ to $\upsilon w \in W$ such that

(i) $\nu(\mathbf{w}_1 + \mathbf{w}_2) = \nu\mathbf{w}_1 + \nu\mathbf{w}_2$, $(\nu_1 + \nu_2)\mathbf{w} = \nu_1\mathbf{w} + \nu_2\mathbf{w}$

(ii) $\alpha(\nu\mathbf{w}) = (\alpha\nu)\mathbf{w} = \nu(\alpha\mathbf{w})$,

(iii) $(\nu_1\nu_2)\mathbf{w} = \nu_1(\nu_2\mathbf{w})$

$\forall \nu \in V$, $\forall w \in W$ and $\forall \alpha \in K$.

A submodule U of a module W is a subspace closed under the composition by elements of the algebra.

A Pfaffian system, *P*, is a submodule of the module of differential one-forms $\Omega(M)$ over the commutative ring of smooth functions $C^\infty(M)$. Locally, a Pfaffian system is represented by a set of one-forms $\{\omega_1, ..., \omega_n\}$ and

$$P = \left\{ \sum_i \alpha_i \omega_i \mid \alpha_i \in C^\infty(M) \right\}.$$

A Pfaffian system defines an exterior differential system

$$I = \langle \{P, dP\} \rangle = \text{Ideal generated by } P, dP.$$

A control system of the form

$$\dot{\mathbf{x}} = \mathbf{f}(\mathbf{x}, \mathbf{u})$$

where $\mathbf{x} \in M \subset \mathbb{R}^n$, $\mathbf{u} \in \mathbb{R}^p$, defines a Pfaffian system on the manifold $M^* = M \times \mathbb{R}^p \times \mathbb{R}$ with local coordinates ($\mathbf{x}$, $\mathbf{u}$, t) generated by the one-forms

$$P = \{\omega_1, \ldots, \omega_N\} = \{dx_1 - f_1(\mathbf{x}, \mathbf{u})dt, \ldots, dx_n - f_n(\mathbf{x}, \mathbf{u})dt\}.$$

The integral curves $c(s) \in M^*$ of the control system are the solutions of

$$\omega(c(s))c'(s) = 0 \quad , \forall \omega \in P$$

where $c'(s)$ is the velocity vector tangent to c(s).

f) Congruence

Let $I = \{\omega_1, \ldots, \omega_k\}$ be an exterior differential system. Two forms, ω and $\xi \in \Omega(M)$, are congruent modulo I, written

$$\omega \equiv \xi \mod I$$

if there exists $\mu \in I$ such that $\omega = \xi + \mu$.

If I is a Pfaffian system then

$$\eta \equiv \xi \mod I \Leftrightarrow \eta = \xi + \sum_i \theta_i \wedge \omega_i$$

for $\theta_i \in \Omega(M)$.

It follows that

$$\eta \equiv 0 \bmod I \Leftrightarrow \eta \wedge \omega_1 \wedge \ldots \wedge \omega_k = 0.$$

As a result, we see from the Frobenius theorem that a Pfaffian system *I* is integrable if and only if

$$d\omega_i \equiv 0 \bmod I.$$

3. The Gardner-Shadwick (GS) Algorithm

The algorithm of Gardner and Shadwick (1992) is presented in this section. More precisely, we consider the necessary and sufficient condition for linearizibility of nonlinear systems utilized in the development of their approach.

We consider systems with n states and p inputs of the general form

$$\dot{\mathbf{x}} = \mathbf{f}(\mathbf{x}, \mathbf{u}) \tag{1}$$

Associated with a system of this form is a Pfaffian system given by

$$\mathbf{I} = \{dx_1 - f_1(\mathbf{x}, \mathbf{u})dt, \ldots, dx_N - f_N(\mathbf{x}, \mathbf{u})dt\} \tag{2}$$

which is called the associated Pfaffian system (Hermann, 1986). Of primary importance in the GS algorithm is an invariant filtering of the associated Pfaffian system, called the derived flag.

This flag is composed of a sequence of Pfaffian systems called derived systems. Let γ be a collection of differential one-forms which define the original system **I**. The first derived system, $\mathbf{I}^{(1)}$, of **I** is a collection of one-forms, δ, which satisfy the Frobenius condition, $d\delta \equiv 0 \bmod \mathbf{I}$. The second derived system, $\mathbf{I}^{(2)}$, is generated by forms which satisfy $d\delta \equiv 0 \bmod \mathbf{I}^{(1)}$. This

procedure can be continued inductively until a derived system is reached for which $\mathbf{I}^{(N)}=\mathbf{I}^{(N+1)}$. N is called the derived length. The derived system $\mathbf{I}^{(N)}$ is the largest completely integrable system contained in **I**.

For a system in Brunowsky normal form, there exist Kronecker indexes $k_1 \geq k_2 \geq ... \geq k_P$ and independent functions, t, $y_{1,1}$, ..., y_{1,k_1}, $y_{2,1}$,..., $y_{2,k2}$,..., $y_{P,1}$,..., y_{P,k_P}, v_1, v_2,..., v_P which give the following generators for its associated Pfaffian system:

$$\begin{aligned}
&w_{1,1} = dy_{1,1} - y_{1,2}dt,\ w_{1,2} = dy_{1,2} - y_{1,3}dt, \\
&\qquad\qquad ...,\ w_{1,k_1} = dy_{1,k_1} - v_1 dt \\
&w_{2,1} = dy_{2,1} - y_{2,2}dt,\ w_{2,2} = dy_{2,2} - y_{2,3}dt, \\
&\qquad\qquad ...,\ w_{2,k_2} = dy_{2,k_2} - v_2 dt \\
&\qquad ... \\
&w_{P,1} = dy_{P,1} - y_{P,2}dt,\ w_{P,2} = dy_{P,2} - y_{P,3}dt, \\
&\qquad\qquad ...,\ w_{P,k_P} = dy_{P,k_P} - v_P dt.
\end{aligned}$$

The structure equations for these generators thus become

$$\begin{aligned}
dw_{1,1} &= dt \wedge dy_{1,2} \\
&= dt \wedge (dy_{1,2} - y_{1,3}dt) \\
&= dt \wedge w_{1,2}
\end{aligned}$$

such that for i=1...P, j=1...k_i-1,

$$dw_{i,j} = dt \wedge w_{i,j+1} \tag{3}$$

and

$$\mathbf{dw_{i,k_i} = dt \wedge dv_i.} \tag{4}$$

This yields the following structure for the derived flag of this Pfaffian system,

$$\begin{array}{cccccccccc}
w_{1,1} & w_{1,2} & \cdots & w_{1,k_1} & \cdots & \cdots & w_{p,1} & w_{p,2} & \cdots & w_{p,k_p} \\
\cdot & & & & & & \cdot & & & \\
\cdot & & & & & & \cdot & & & \\
\cdot & & & & & & \cdot & & & \\
\cdot & & & & & & w_{p,1} & & & \\
\cdot & & & & & & & & & \\
w_{1,1} & w_{1,2} & & & & & & & & \\
w_{1,1} & & & & & & & & &
\end{array}$$

where the first row is formed by the generators of the system **I** and each subsequent row j is formed by the generators of the corresponding j^{th} derived system $\mathbf{I}^{(j)}$. Each input generates a tower of the form

$$\begin{array}{cccc}
w_{j,1} & w_{j,2} & \cdots & w_{j,k_j} \\
 & \cdot & & \\
 & \cdot & & \\
 & \cdot & & \\
w_{j,1} & w_{j,2} & w_{j,3} & \\
w_{j,1} & w_{j,2} & & \\
w_{j,1} & & &
\end{array}$$

One can construct such a structure if the equalities (3) are met. Clearly, this condition will not be satisfied for a control system in general. Although the derived systems are feedback invariant, their bases are not, and these equalities must be replaced by congruences modulo the appropriate derived system. That is, the generators of $\mathbf{I}^{(j)}$ must satisfy the following conditions:

$$\begin{aligned}
\mathbf{dw_{1,k_1-j}} &\equiv \mathbf{dt \wedge w_{1,k_1-j+1}} \\
&\cdots \qquad\qquad \text{mod } I^{(j+1)} \\
\mathbf{dw_{m_j,k_{m_j}-j}} &\equiv \mathbf{dt \wedge w_{m_j,k_{m_j}-j+1}}
\end{aligned} \tag{5}$$

where m_j is the number of towers with at least j+1 rows.

Once the congruences have been established, it is possible to find new generators, $\bar{w}_{i,j}$,

which transform them to equalities. This is easily done by employing the procedure developed by Gardner and Shadwick (1992).

One of the main advantages of the GS algorithm is that it guarantees a minimum number of integrations. Assuming that there are ℓ distinct Kronecker indexes with multiplicities $\nu_1,...,\nu_\ell$, it was proven by Gardner and Shadwick (1992) that integration of ℓ decoupled completely integrable systems of dimensions $\nu_1,...,\nu_\ell$ is required. In the case that each Kronecker index has multiplicity one, the integration of P one-dimensional systems is required in order to find generators of the form $w_{j,1}=\eta_{j,1}-b_{j,1}dt$, where $\eta_{j,1}$ are differential forms on the state space which are independent of t, and $b_{j,1}$ are functions defined on the state space, j=1,...,P. As a result, there exist functions defined on the state space, $y_{j,1}$, which satisfy

$$\eta_{j,1} = \mu_{j,1}dy_{j,1}.$$

This then yields new generators

$$\bar{w}_{j,1} = \frac{w_{j,1}}{\mu_{j,1}} = dy_{j,1} - y_{j,2}dt$$

where $y_{j,2}=b_{j,1}/\mu_{j,1}$. When multiple Kronecker indexes occur, similar manipulations, expressed in matrix form, are required.

Using the above generators as initiators of the towers, one can proceed with the Gardner and Shadwick procedure (Gardner and Shadwick, 1992) to obtain the new generators. The linearizing coordinates are simply obtained as the functions multiplying dt in each generator. This procedure is illustrated in Example 5.1.

Example 5.1. Linearization by Static State Feedback using the GS Algorithm

Consider the following model of a mixed culture bioreactor developed by Hoo and Kantor (1986):

$$\frac{dx_1}{dt} = \mu_1 x_1 - u_1 x_1$$

$$\frac{dx_2}{dt} = \mu_2 x_2 - u_1 x_2$$

$$\frac{dx_3}{dt} = -p x_1 x_3 - u_1 x_3 + u_2$$

where x_1, x_2 and x_3 are the concentrations of inhibitor resistant cells, inhibitor sensitive cells and inhibitor, respectively, and

$$\mu_1 = \frac{\mu_{max1} S}{K + S}$$

$$\mu_2 = \frac{\mu_{max2} S}{K + S} \frac{K_I}{K_I + I}$$

$$S = S_f - x_1/Y_1 - x_2/Y_2.$$

The generators for this system are given by

$$w_1 = dx_1 - (\mu_1 x_1 - u_1 x_1)dt$$

$$w_2 = dx_2 - (\mu_2 x_2 - u_1 x_2)dt$$

$$w_3 = dx_3 - (-p x_1 x_3 - u_1 x_3 + u_2)dt$$

These are generators of the Pfaffian system **I**={w_1,w_2,w_3} which give structure equations of the form

$$dw_1 = -x_1 dt \wedge du_1$$

$$dw_2 = -x_2 dt \wedge du_1 \qquad \text{ĂĐú É}$$

$$dw_3 = -x_3 dt \wedge du_1 + dt \wedge du_2$$

The dependence of w_1 and w_2 on u_1 can be removed by defining

$$w_4 = \frac{w_1}{x_1} - \frac{w_2}{x_2}$$

such that $dw_4 \equiv 0 \bmod \mathbf{I}$. w_4 generates the first derived system which terminates the derived flag in this case. The system has Kronecker indexes $k_1=1$, $k_2=2$.

The tower structure is then easily constructed by taking $w_{2,1}=w_4$. Differentiating yields

$$\begin{aligned} d(w_{2,1}) &= dt \wedge \\ &\left[\left(\frac{\partial \mu_1}{\partial x_1} - \frac{\partial \mu_2}{\partial x_1}\right)dx_1 + \left(\frac{\partial \mu_1}{\partial x_2} - \frac{\partial \mu_2}{\partial x_2}\right)dx_2 - \frac{\partial \mu_2}{\partial x_3}dx_3\right] \\ &\equiv dt \wedge \\ &\left[\left(\frac{\partial \mu_1}{\partial x_1} - \frac{\partial \mu_2}{\partial x_1} + \frac{x_2}{x_1}\left(\frac{\partial \mu_1}{\partial x_2} - \frac{\partial \mu_2}{\partial x_2}\right)\right)dx_1 - \frac{\partial \mu_2}{\partial x_3}dx_3\right] \bmod \boldsymbol{I}^{(1)} \\ &\equiv dt \wedge \\ &\left[\left(\frac{\partial \mu_1}{\partial x_1} - \frac{\partial \mu_2}{\partial x_1} + \frac{x_2}{x_1}\left(\frac{\partial \mu_1}{\partial x_2} - \frac{\partial \mu_2}{\partial x_2}\right)\right)w_1 - \frac{\partial \mu_2}{\partial x_3}w_3\right] \bmod \boldsymbol{I}^{(1)} \end{aligned} \tag{6}$$

such that

$$w_{2,2} = \left(\frac{\partial \mu_1}{\partial x_1} - \frac{\partial \mu_2}{\partial x_2} + \frac{x2}{x1}\left(\frac{\partial \mu_1}{\partial x_1} - \frac{\partial \mu_2}{\partial x_2}\right)\right)w_1 - \frac{\partial \mu_2}{\partial x_3}w_3.$$

The second tower is simply composed of $w_{1,1}$ which is equal to w_1. The following tower

structure thus results

$$w_{1,1} \qquad w_{2,1} \qquad w_{2,2}$$

$$w_{2,1}$$

This problem is relatively simple in that only one congruence appears. $w_{1,1}$ and $w_{2,1}$ do not need to be transformed. $w_{2,2}$ must be transformed in order to satisfy the congruence (6). This is done by taking

$$\bar{w}_{2,2} = w_{2,2} - x_2\left(\frac{\partial \mu_1}{\partial x_2} - \frac{\partial \mu_2}{\partial x_2}\right)w_{2,1}.$$

The linearizing coordinates can then be easily obtained. The coordinate transformation $y_{2,1}$ is obtained by integrating the equation

$$\frac{dy_{2,1}}{x_1} - \frac{dy_{2,1}}{x_2} = 0$$

which gives $y_{2,1}=\ln(x_1/x_2)$. $y_{2,2}$ is the function multiplying dt in $w_{2,1}$. This gives

$$y_{2,2} = \mu_1 - \mu_2.$$

The linearizing feedback transformation, v_2, is the function multiplying dt in $w_{2,2}$. That is,

$$v_2 = \left(\frac{\partial \mu_1}{\partial x_1} - \frac{\partial \mu_2}{\partial x_1}\right)(\mu_1 x_1 - u_1 x_1) + \left(\frac{\partial \mu_1}{\partial x_2} - \frac{\partial \mu_2}{\partial x_2}\right)(\mu_2 x_2 - u_1 x_2)$$
$$-\left(\frac{\partial \mu_2}{\partial x_3}\right)(-p x_1 x_3 - x_1 u_1 + u_2).$$

The remaining coordinates are obtained from the second tower. They are simply

$$y_{1,1} = x_1$$

$$v_1 = \mu_1 x_1 - u_1 x_1.$$

It can be verified that these coordinates are similar to those calculated by Hoo and Kantor (1986).

4. Linearizability Conditions for Classes of Chemical Processes

When a system is not linearizable, the structure equations of its corresponding Pfaffian system contain terms which fail to be congruent to zero. The coefficients of these terms are curvature-like quantities which represent obstructions to linearity. When these quantities vanish, the GS algorithm can be used to obtain the linearizing state and feedback transformations.

In this section, we follow an analysis performed by Shadwick (1993) on a class of air flight control models and demonstrate how the GS algorithm can be used to uncover obstructions to linearizations using the batch reactor example of Kravaris and Chung (1987). The model is based on the reaction

$$A \xrightarrow{k_1} B \xrightarrow{k_2} C$$

where it is assumed that the first reaction has second order kinetics, whereas the second reaction has first order kinetics. The model form used by Kravaris and Chung (1987) is

$$\frac{dx_1}{dt} = -k_1(x_3)x_1^2$$

$$\frac{dx_2}{dt} = k_1(x_3)x_1^2 - k_2(x_3)x_2$$

$$\frac{dx_3}{dt} = \gamma_1 k_1(x_3)x_1^2 + \gamma_2 k_2(x_3)x_2 + a_1 + a_2 x_3 + (b_1 + b_2 x_3)u$$

where x_1, x_2 and x_3 are the molar concentrations of A and B and the temperature of the reactor, respectively. The rate constants, $k_1(x_3)$ and $k_2(x_3)$, are treated as *arbitrary functions* of temperature. The manipulated variable, u, is as defined by Kravaris and Chung (1987). It is chosen to be a balance between cooling and heating of the system (i.e., a split range manipulated variable). The parameters γ_1, γ_2, a_1, a_2, b_1 and b_2 are constants.

It is shown by Kravaris and Chung (1987) that this system is not linearizable by state feedback when the standard Arrhenius relationships are assumed for the temperature dependencies of the rate constants. Using the GS algorithm, we will show how the set of linearizable models of this form can be characterized.

The model yields a Pfaffian system of the form

$$\begin{aligned} I &= [w_1, w_2, w_3] \\ &= [dx_1 - (-k_1(x_3)x_1^2)dt, \\ &\quad dx_2 - (k_1(x_3)x_1^2 - k_2(x_3)x_2)dt, \\ &\quad dx_3 - (\gamma_1 k_1(x_3)x_1^2 + \gamma_2 k_2(x_3)x_2 + a_1 + a_2 x_3 + (b_1 + b_2 x_3)u)dt]. \end{aligned}$$

Following the GS algorithm, we calculate the structure equations. They can be written in vector form as

$$d\begin{pmatrix} w_1 \\ w_2 \\ w_3 \end{pmatrix} = dt \wedge \begin{pmatrix} 0 \\ 0 \\ b_1 + b_2 x_3 \end{pmatrix} du \mod I.$$

The first derived system, $I^{(1)}=[w_1, w_2]$, is

$$d\begin{pmatrix} w_1 \\ w_2 \end{pmatrix} = dt \wedge \begin{pmatrix} -\frac{\partial k_1(x_3)}{\partial x_3} x_1^2 \\ \frac{\partial k_1(x_3)}{\partial x_3} x_1^2 - \frac{\partial k_2(x_3)}{\partial x_3} x_2 \end{pmatrix} dx_3 \mod I^{(1)}.$$

Next, we construct the generator

$$w_4 = \left(-\frac{\partial k_1(x_3)}{\partial x_3} x_1^2 + \frac{\partial k_2(x_3)}{\partial x_3} x_2 \right) w_1 - \left(\frac{\partial k_1(x_3)}{\partial x_3} x_1^2 \right) w_2$$

which is such that

$$dw_4 \equiv 0 \mod I^{(1)}.$$

We then see that this system is linearizable if we can find $k_1(x_3)$ and $k_2(x_3)$ such that

$$dw_4 \equiv dt \wedge A(x) dx \mod w_4.$$

where $\mathbf{A(x)}$ is matrix of functions of the states only. It can be confirmed that

$$dw_4 \equiv dt \wedge A_1(x) dx_1 + dt \wedge A_2(x) dx_3 + \left(\frac{\partial^2 k_1(x_3)}{\partial x_3} x_1^2 - \frac{\partial^2 k_2(x_3)}{\partial x_3^2} x_2 - \frac{\frac{\partial^2 k_1(x_3)}{\partial x_3^2} \left(\frac{\partial k_1(x_3)}{\partial x_3} x_1^2 - \frac{\partial k_2(x_3)}{\partial x_3} x_2 \right)}{\frac{\partial k_1(x_3)}{\partial x_3}} \right) dx_1 \wedge dx_3.$$

The coefficient of $dx_1 \wedge dx_3$ is an example of the curvature-like quantities which act as obstructions

to linearizability. For this example, we can rearrange this term to obtain the following sufficient condition for linearizability of this class of models:

$$x_2 \frac{\left(\frac{\partial k_1(x_3)}{\partial x_3} \frac{\partial^2 k_2(x_3)}{\partial x_3^2} - \frac{\partial k_2(x_3)}{\partial x_3} \frac{\partial^2 k_1(x_3)}{\partial x_3^2} \right)}{\frac{\partial k_1(x_3)}{\partial x_3}} = 0.$$

Assuming that the first rate constant depends on the temperature, we finally obtain the condition

$$\frac{\partial k_1(x_3)}{\partial x_3} \frac{\partial^2 k_2(x_3)}{\partial x_3^2} - \frac{\partial^2 k_1(x_3)}{\partial x_3^2} \frac{\partial k_2(x_3)}{\partial x_3} = 0 \qquad (7)$$

which parametrizes the class of linearizable systems in terms of the temperature dependencies of the rate constants. For this case, a simple linear temperature dependence for the rate constants is sufficient to ensure feedback linearizability of the model.

Assuming Equation (8) is fulfilled, we can state that the differential one-form

$$dx_4 = \left(-\frac{\partial k_1(x_3)}{\partial x_3} x_1^2 + \frac{\partial k_2(x_3)}{\partial x_3} x_2 \right) dx_1 - \left(\frac{\partial k_1(x_3)}{\partial x_3} x_1^2 \right) dx_2$$

is approximately exact. As a result, the generator $\mathbf{w}_4$ provides, through exterior differentiation, a normal form that approximates the original system. When the functions $k_1(x_3)$ and $k_2(x_3)$ are known, the condition for linearizibility given by Equation (7) provides a measure of the departure of this approximation from the original model that is, by construction, *invariant under state-feedback and state-space transformations*. These invariant obstructions to linearizibility provide geometric outputs for this class of nonisothermal CSTRs.

5. A Necessary and Sufficient Condition for Dynamic Feedback Linearization of Control-Affine Systems

A comprehensive framework for the problem of dynamic feedback linearizability of control-affine systems was first proposed by Charlet *et al.* (1989, 1991). Using a standard Lie-algebraic differential geometric framework, necessary conditions and sufficient conditions were obtained. Other differential geometric techniques based on exterior calculus have also been used to study this problem. Shadwick (1991) demonstrated the application of Cartan prolongations to the problem of dynamic feedback linearization in single input systems. Sluis (1993) also considered the implication of Cartan's ideas for the problem of dynamic feedback linearization and developed a necessary condition for dynamic feedback linearization.

There have been a number of research efforts aimed at extending and generalizing the framework of Charlet *et al.* (1989, 1991). Among the most useful generalizations is the concept of differential flatness introduced by Fliess *et al.* (1992, 1994a, 1994b). The close relationship between flatness and dynamic feedback linearization has been established by Rouchon (1994) and Martin (1993) who also emphasized the importance of differential geometric techniques based on the ideas of Cartan employed by Gardner and Shadwick (1992), Martin (1993) and Shadwick (1990).

Aranda-Bricaire *et al.* (1993, 1995) have recently developed a linear algebraic framework for the study of dynamic feedback linearization for control affine systems. In their approach, an infinitesimal Brunovsky form is identified which generalizes the Brunovsky canonical forms to dynamically feedback linearizable systems. It is shown that, as in the GS algorithm, dynamic linearizability requires the existence of exact differential forms.

In this section, a necessary and sufficient condition for dynamic feedback linearizability of control-affine nonlinear systems by endogenous feedback is presented. The conditions extend the approach considered by Shadwick (1990) to multi-input systems. They are based on a modified derived flag of a Pfaffian system associated with a control system which takes into account the presence of a precompensator. Similar to the results of Gardner and Shadwick (1992), it is shown that the generators associated with this modified derived flag must satisfy a number of congruences. The congruences ensure that the conditions stated by Gardner and Shadwick (1992) are satisfied for the prolongated system, and thus provide an algorithm to calculate the required feedback and state space transformations via the Gardner and Shadwick algorithm (1992). As in Gardner and Shadwick (1992), a tower structure is identified with respect to a set of indices corresponding to the infinitesimal Brunovsky form of Aranda-Bricaire *et al.* (1995).

Furthermore, using these conditions, a bound related to the extent of precompensation of each input channel is identified, and it is shown how linearizing outputs can be obtained by studying the derived flag of the Pfaffian system associated with a nonlinear system.

The development proceeds as follows. Preliminary considerations related to feedback linearizability of nonlinear systems are presented in Section 5.1. The conditions for dynamic feedback linearizability are presented in Section 5.2. Examples are presented in Section 5.3.

5.1. Preliminary Considerations

Consider a smooth nonlinear system of the form

$$\dot{\mathbf{x}} = \mathbf{f}(\mathbf{x}) + \mathbf{g}(\mathbf{x})\mathbf{u} \tag{8}$$

where $x \in \mathbb{R}^N$, $u \in \mathbb{R}^P$. The problem of dynamic feedback linearization of systems of this form in the

sense of Charlet *et al.* (1989, 1991) is now considered. The existence of a regular dynamic precompensator

$$\begin{aligned} \dot{\mathbf{z}} &= \mathbf{a}(\mathbf{x},\mathbf{z}) + \mathbf{b}(\mathbf{x},\mathbf{z})\mathbf{v} \\ \mathbf{u} &= \mathbf{c}(\mathbf{x},\mathbf{z}) + \mathbf{d}(\mathbf{x},\mathbf{z})\mathbf{v} \end{aligned} \tag{9}$$

is sought where $\mathbf{v} \in \mathbb{R}^m$ and $z \in \mathbb{R}^q$, along with a nonlinear state transformation

$$\xi = \phi(\mathbf{x},\mathbf{z}) \tag{10}$$

such that the combined system

$$\begin{aligned} \dot{\mathbf{x}} &= \mathbf{f}(\mathbf{x}) + \mathbf{g}(\mathbf{x})\mathbf{c}(\mathbf{x},\mathbf{z}) + \mathbf{g}(\mathbf{x})\mathbf{d}(\mathbf{x},\mathbf{z})\mathbf{v} \\ \dot{\mathbf{z}} &= \mathbf{a}(\mathbf{x},\mathbf{z}) + \mathbf{b}(\mathbf{x},\mathbf{z})\mathbf{v} \end{aligned} \tag{11}$$

is equivalent to a controllable linear system

$$\dot{\xi} = \mathbf{A}\xi + \mathbf{B}\mathbf{v}.$$

This system can be put in Brunovsky canonical form by a static state feedback and a linear invertible transformation $y=T\xi$ such that

$$\begin{aligned} y_1^{(\nu_1)} &= v_1 \\ &\vdots \\ y_M^{(\nu_M)} &= v_M \end{aligned} \tag{12}$$

where $\nu_1, \nu_2, \ldots, \nu_M$ are the controllability indices of the extended system.

The Pfaffian system associated with (11) is given by

$$\Sigma = [dx_1 - (f_1(x,z) + g_1(x,z)v)dt, \ldots, dx_N - (f_N(x,z) + g_N(x,z)v)dt, \\ dz_1 - (a_1(x,z) + b_1(x,z)v)dt, \ldots, dz_q - (a_q(x,z) - b_q(x,z)v)dt] \tag{13}$$

or

$$\Sigma = [w_1, \ldots, w_N, \zeta_1, \ldots, \zeta_q]$$

in terms of generators where

$$f_i(x,z) = f_i(x) + g_i(x)c(x,z), \text{ and } g_i(x,z) = g_i(x)d_i(x,z)$$

for $1 \le i \le N$, and

$$f_i(x,z) = a_i(x,z), \quad g_i(x,z) = b_i(x,z)$$

for $N+1 \le i \le N+q$.

Following the approach of Gardner and Shadwick (1992), feedback linearizability of the extended system implies the existence of a set of generators which fulfil the congruences

$$dw_i^{\nu_i - j} \equiv dt \wedge w_i^{\nu_i - j + 1} \mod \Sigma^{(j+1)} \tag{14}$$

where $1 \le i \le m_j$, $m_j = \dim\{\Sigma^{(j)}/\Sigma^{(j+1)}\}$, $1 \le j \le \nu_1$ and

$$dw_i^{\nu_i} \equiv dt \wedge dv_i \mod \Sigma^{(1)}. \tag{15}$$

$\Sigma^{(j)}$ is the j^{th} derived system of Σ as defined in Section 3.

If we consider dynamic feedback linearizability in the sense of Charlet *et al.* (1991), we see that the Pfaffian system associated with system (11) is equivalent to the Pfaffian system $\Sigma = \{S, P\}$ where

$$S = \left[dx_1 - (f_1(x) + g_1(x)u)dt, \ldots, dx_N - (f_N(x) + g_N(x)u)dt\right] \tag{16}$$

and

$$\begin{aligned} P &= [du_1 - u_1^{(1)}dt, \ldots, du_1^{(\alpha_1)} - u_1^{(\alpha_1)}dt, \ldots, du_P - u_P^{(1)}dt, \ldots, du_P^{(\alpha_P)} - u_P^{(\alpha_P+1)}dt] \\ &= [\eta_1^{(1)}, \ldots, \eta_1^{(\alpha_1+1)}, \ldots, \eta_P^{(1)}, \ldots, \eta_P^{(\alpha_P+1)}]. \end{aligned} \tag{17}$$

Denote the set of integers $\{\alpha_1, \alpha_2, ..., \alpha_p\}$ as the degree of precompensation of the system. Other types of precompensators have been discussed in the literature. Sluis (1993) considered a class of precompensators in which the prolongated channels u_1, ..., u_P are possibly taken as state-feedback transformations of the original variables. This provides a relaxation of the conditions stated by Charlet *et al.* (1991). In the most general case, the coordinates z of the precompensators are functions of x, u, $u^{(1)}$, ..., $u^{(\alpha)}$, where α is finite. This approach is associated with the notion of differential flatness Fliess *et al.* (1992).

It is clear that, for any type of precompensator, the resulting Pfaffian system Σ must always be equivalent to the Pfaffian system associated with (12), and the indices $\{\alpha_1,..., \alpha_P\}$ and $\{\nu_1, ..., \nu_p\}$ must always satisfy $\alpha_1+...+\alpha_p=q$ and $\nu_1+...+\nu_P=N+q$. We now consider the equivalence of Pfaffian systems of the form (16), (17) to linear controllable forms. In particular, we analyze conditions that describe the geometrical properties of a nonlinear system required for feedback linearizability of the extended system (16), (17).

5.2 Conditions for dynamic feedback linearizability

In this section, geometric conditions for dynamic feedback linearizability of nonlinear control systems are presented. First, a filtering of the Pfaffian system associated with a nonlinear system which takes into account the presence of prolongated input channels is defined.

Definition 1

Consider a control-affine system with N states and P inputs and a precompensator with indices $\{\alpha_1, ..., \alpha_p\}$, $\alpha_1 \geq ... \geq \alpha_p$, with multiplicities $\{s_1, ..., s_m\}$ and corresponding indices $\{k_1, ..., k_1, ..., k_m, ..., k_m\}$ ($k_1=\alpha_P$, ..., $k_m=\alpha_1$). As in (16), let S be the Pfaffian system associated with the nonlinear system. The *first derived system associated with the precompensator* is given by the set of forms which satisfy

$$dw^{(1)} \equiv 0 \mod S, du_1, ..., du_{P-s_1}$$

The *second derived system associated with the precompensator* is given by the set of forms, $\mathbf{w}^{(1)}$, which satisfy

$$dw^{(2)} \equiv 0 \mod w^{(1)}, du_1, ..., du_{P-s_1-s_1} \text{ if } k_2-k_1>1$$

or

$$dw^{(2)} \equiv 0 \mod w^{(1)}, du_1, ..., du_{P-s_1-s_2} \text{ if } k_2-k_1=1$$

Generally, we write the following defining relationship for the derived systems associated with the precompensator:

$$dw^{(k_i-k_1+j)} \equiv 0 \mod w^{(k_i-k_1+j-1)}, du_1, ..., du_{P-s_1...-s_i}$$

for $1 \leq j \leq k_{i+1}-k_i$, $1 \leq i \leq m-1$. If there exists a number Q for which $w^{(Q+1)}=w^{(Q)}$, it is called the derived length associated with the precompensator.

Note that for this class of systems, this derived flag is invariant under feedback and state space transformations. It does, however, depend on the choice of precompensator and may therefore be subject to the presence of differential algebraic constraints.

Note also that this filtering of the Pfaffian system associated with the nonlinear system (8) relates to a more general setting. One can easily see that the linear constraints imposed by the differential forms du_i given in the definition can be replaced by nonlinear algebraic constraints dz_i, $1 \le i \le q$, where z_i are functions of x and u.

In what follows, conditions based on the derived flag associated with a precompensator are presented. They are shown to be necessary and sufficient conditions for dynamic feedback linearizability in the sense of Sluis (1993). First it is shown that the possible sets of indices which are applicable for dynamic feedback linearizability are restricted.

Lemma 1:

Consider a control-affine system with N states and P inputs and define a precompensator by ordering the inputs $\{u_1, ..., u_p\}$ according to the indices $\{k_1, ..., k_m\}$ with multiplicities $\{s_1, ..., s_m\}$ such that $k_m \ge ... \ge k_1$. If the system is dynamic feedback linearizable in the sense of Sluis (1993), then the class of admissible precompensators is defined by

$$N - (k_2 - k_1)s_1 - ... - (k_m - k_{m-1})(s_1 + ... + s_{m-1}) > 0$$

Proof:

Consider the Pfaffian system associated with (16), (17),

$$\Sigma = [w_1, ..., w_{N-P}, w_{N-P+1}, ..., w_N, \eta_1^{(1)}, ..., \eta_1^{(k_m+1)}, ..., \eta_P^{(1)}, ..., \eta_P^{(k_1+1)}]$$

which contains N+q generators. The first derived system is generated by

$$\Sigma^{(1)} = [w_1, ..., w_{N-P}, w_{N-P+1}, ..., w_N, \eta_1^{(1)}, ..., \eta_1^{(k_m)}, ..., \eta_P^{(1)}, ..., \eta_P^{(k_1)}]$$

Inductively, the (k_1)-th derived system is given by

$$\Sigma^{(k_1)} = [w_1,\ldots,w_{N-P},w_{N-P+1},\ldots,w_N,\eta_1^{(1)},\ldots,\eta_1^{(k_m-k_1+1)},\ldots,\eta_{P-s_1}^{(1)},\ldots,\eta_{P-s_1}^{(k_2-k_1+1)},\eta_{P-s_1+1}^{(1)},\ldots,\eta_P^{(1)}]$$

and

$$\Sigma^{(k_1+1)} = [w_1,\ldots,w_{N-P},w_{N-P+1},\ldots,w_N,\eta_1^{(1)},\ldots,\eta_1^{(k_m-k_1)},\ldots,\eta_{P-s_1}^{(1)},\ldots,\eta_{P-s_1}^{(k_2-k_1)}]$$

At this point, s_1 of the input channels are not precompensated. Exterior differentiation of this set of generators yields $s_2+...+s_m$ generators from the precompensated channels which are necessarily non-zero modulo this derived system. This leaves s_1 generators which must be removed from the Pfaffian system associated with the original system. Fulfilment of the congruences (14) for the extended system first implies that there exists a set, $w^{(1)}$, of $N-s_1$ generators which are such that

$$dw^{(1)} \equiv 0 \mod \Sigma^{(k_1+1)}$$

This is clearly equivalent to

$$dw^{(1)} \equiv 0 \mod S, du_1,\ldots,du_{P-s_1}$$

which also implies that *the set of generators $w^{(1)}$ forms the first derived system associated with the precompensator*. The system can always be feedback transformed to

$$\begin{aligned} S &= [dx_1 - (f_1(x) + g_1(x)u)dt,\ldots,dx_{N-P} - (f_{N-P}(x) + g_{N-P}(x)u)dt, \\ &\qquad dx_{N-P+1} - u_1dt,\ldots,dx_N - u_Pdt] \\ &= [w_1,\ldots,w_{N-P},w_{N-P+1},\ldots,w_N]. \end{aligned}$$

If we write the original Pfaffian system as

$$S = [w^{(1)}, w_{N-s_1+1}, \ldots, w_N]$$

feedback linearizability of the prolongated system requires that these generators fulfil

$$dw^{(1)} \equiv dt \wedge \Omega(x,u) \begin{pmatrix} w_{N-s_1+1} \\ \cdot \\ \cdot \\ \cdot \\ w_N \end{pmatrix} \mod \Sigma^{(k_1+1)}$$

This is equivalent to the statement

$$dw^{(1)} \equiv dt \wedge \Omega(x,u_1,\ldots,u_{P-s_1}) \begin{pmatrix} w_{N-s_1+1} \\ \cdot \\ \cdot \\ \cdot \\ w_N \end{pmatrix} \mod w^{(1)}, du_1, \ldots, du_{P-s_1}$$

which are simply the congruences expressed in terms of the derived flag associated with the precompensator. The derived system

$$\Sigma^{(k_1+2)} = [w^{(1)}, \eta_1^{(1)}, \ldots, \eta_1^{(k_m-k_1-1)}, \ldots, \eta_{P-s_1}^{(1)}, \ldots, \eta_{P-s_1}^{(k_2-k_1-1)}]$$

is obtained. Similarly, the next derived system implies the existence of a set of $N-s_1-s_1$ generators, $w^{(2)}$, which are such that

$$dw^{(2)} \equiv 0 \mod w^{(1)}, du_1, \ldots, du_{P-s_1}$$

Again rewriting the generators such that

$$w^{(1)} \equiv [w^{(2)}, w_{N-s_1-s_1+1}^{(1)}, \ldots, w_{N-s_1}^{(1)}]$$

the congruences to be fulfilled can be written as

$$dw^{(2)} \equiv dt \wedge K^{(1)} \begin{pmatrix} w^{(1)}_{N-s_1-s_1+1} \\ . \\ . \\ . \\ w^{(1)}_{N-s_1} \end{pmatrix} \mod w^{(2)}, du_1, \ldots, du_{P-s_1}$$

The next derived system is generated by

$$\Sigma^{(k_1+3)} = [w^{(2)}, \eta_1^{(1)}, \ldots, \eta_1^{(k_m-k_1-2)}, \ldots, \eta^{(1)}_{P-s_1}, \ldots, \eta^{(k_2-k_1-2)}_{P-s_1}].$$

Proceeding further, it is found, by induction, that

$$\Sigma^{(k_2)} = [w^{(k_2-k_1-1)}, \eta_1^{(1)}, \ldots, \eta_1^{(k_m-k_2+1)}, \ldots, \eta^{(1)}_{P-s_1-s_2}, \ldots, \eta^{(k_3-k_2+1)}_{P-s_1-s_2}, \eta^{(1)}_{P-s_1-s_2+1}, \ldots, \eta^{(1)}_{P-s_1}]$$

and

$$\Sigma^{(k_2+1)} = [w^{(k_2-k_1)}, \eta_1^{(1)}, \ldots, \eta_1^{(k_m-k_2)}, \ldots, \eta^{(1)}_{P-s_1-s_2}, \ldots, \eta^{(k_3-k_2)}_{P-s_1-s_2}].$$

As above, we find that s_1+s_2 input channels are not precompensated. The existence of a set of $N-(k_2-k_1)s_1-s_2$ generators,

$$dw^{(k_2-k_1+1)} \equiv 0 \mod w^{(k_2-k_1)}, du_1, \ldots, du_{P-s_1-s_2}$$

is required. Congruences (14) imply that the generators can be re-written as

$$w^{(k_2-k_1)} = [w^{(k_2-k_1+1)}, w^{(k_2-k_1)}_{N-(k_2-k_1)s_1-s_2+1}, \ldots, w^{(k_2-k_1)}_{N-(k_2-k_1)s_1}]$$

such that

$$dw^{(k_2-k_1+1)} \equiv dt \wedge K^{(k_2-k_1)} \begin{pmatrix} w^{(k_2-k_1)}_{N-(k_2-k_1)s_1-s_2+1} \\ \cdot \\ \cdot \\ \cdot \\ w^{(k_2-k_1)}_{N-(k_2-k_1)s_1} \end{pmatrix} \mod w^{(k_2-k_1+1)}, du_1, \ldots, du_{P-s_1-s_2}.$$

This yields

$$\Sigma^{(k_2+2)} = [w^{(k_2-k_1+1)}, \eta_1^{(1)}, \ldots, \eta_1^{(k_m-k_2-1)}, \ldots, \eta^{(1)}_{P-s_1-s_2}, \ldots, \eta^{(k_3-k_2-1)}_{P-s_1-s_2}]$$

Finally, the derived system

$$\Sigma^{(k_m)} = [w^{(k_m-k_1+1)}, \eta_1^{(1)}, \ldots, \eta^{(1)}_{P-s_1-\ldots-s_{m-1}}]$$

is obtained by induction. For the next step, feedback linearizability implies the existence of a set of $N-(k_2-k_1)s_1-\ldots-(k_m-k_{m-1})(s_1+\ldots+s_{m-1})$ generators which satisfy

$$dw^{(k_m-k_1)} \equiv 0 \mod \Sigma^{(k_m)}$$

and, consequently,

$$dw^{(k_m-k_1)} \equiv 0 \mod w^{(k_m-k_1-1)}, du_1, \ldots, du_{P-s_1-\ldots-s_{m-1}}$$

As above, the set of generators

$$w^{(k_m-k_1-1)} = [w^{(k_m-k_1)}, w^{(k_m-k_1-1)}_{N-(k_2-k_1)s_1-\ldots-(k_m-k_{m-1})(s_1+\ldots+s_{m-1})+1}, \ldots, w^{(k_m-k_1-1)}_{N-(k_2-k_1)s_1-\ldots-(k_m-k_{m-1}-1)(s_1+\ldots+s_{m-1}}]$$

is obtained. Fulfilment of the congruences (14) for the extended system implies that

$$dw^{(k_m-k_1)} \equiv dt \wedge K^{(k_m-k_1-1)} \begin{pmatrix} W_{N-(k_2-k_1)s_1-\ldots-(k_m-k_{m-1})(s_1+\ldots+s_{m-1})+1}^{(k_m-k_1-1)} \\ \vdots \\ W_{N-(k_2-k_1)s_1-\ldots-(k_m-k_{m-1}-1)(s_1+\ldots+s_{m-1})} \end{pmatrix} \mod w^{(k_m-k_1)}, du_1, \ldots, du_{P-s_1-\ldots-s_{m-1}}$$

Finally, the derived system is

$$\Sigma^{(k_m+1)} = [w^{(k_m-k_1)}]$$

which must contain $N-(k_2-k_1)s_1-\ldots-(k_m-k_{m-1})(s_1+\ldots+s_{m-1})$ generators.

It is obviously necessary that $(k_2-k_1)s_1-\ldots-(k_m-k_{m-1})(s_1+\ldots+s_{m-1})<N$; otherwise, some of the required linearizing outputs will be directly identified with certain input channels.

It possible to refine the bounds on the set of possible precompensators. First consider the situation where the precompensator required for dynamic feedback linearization is such that $N-(k_2-k_1)s_1-\ldots-(k_m-k_{m-1})(s_1+\ldots+s_{m-1})\leq P$. Since feedback linearizability implies that the derived flag stabilizes at this point, it follows that the class of admissible precompensators is described by

$$N-P \leq (k_2-k_1)s_1+\ldots+(k_m-k_{m-1})(s_1+\ldots+s_{m-1}) < N$$

This completes the proof.

The bounds on the possible compensators can be improved by studying the derived flag of the original system *a priori*. Assume that there is a certain number, $\ell \leq P$, of generators $\{\omega_1^1, \ldots, \omega_\ell^1\}$ belonging to the k^{th} derived system of the Pfaffian system associated with the nonlinear system which fulfil congruences of the form

$$d\omega_i^1 \equiv dt \wedge \omega_i^2 \mod \omega_1^1, \ldots, \omega_\ell^1$$

such that

$$d\omega_i^2 \equiv dt \wedge \omega_i^3 \mod \omega_1^1, \ldots, \omega_\ell^1, \omega_1^2, \ldots, \omega_\ell^2, \omega_{\ell+1}^1, \ldots, \omega_P^1$$

and, finally,

$$d\omega_i^k \equiv dt \wedge \omega_i^{k+1} \mod \omega_1^1, \ldots, \omega_1^k, \ldots, \omega_\ell^1, \ldots, \omega_\ell^k, \ldots, \omega_P^1, \ldots, \omega_P^{k-1}.$$

The Pfaffian system $\{\omega_1^1, \ldots, \omega_1^{k+1}, \ldots, \omega_\ell^1, \ldots, \omega_\ell^{k+1}, \ldots, \omega_P^1, \ldots, \omega_P^k\} = w^{(k_m - k_1)}$ forms a subsystem of the original system. By construction, it follows that these congruences must also be observed for the derived system associated with a precompensator. Consequently, for every $k \geq 0$, the class of precompensators is defined by

$$N-(k+1)P \leq (k_2 - k_1)s_1 + \ldots + (k_m - k_{m-1})(s_1 + \ldots + s_{m-1}) < N-kP. \tag{18}$$

Finally, since the conditions imply that the extended system with the precompensator defined by the set of indices $\{\alpha_1, \ldots, \alpha_p\}$ fulfils the feedback linearization conditions (14) for the extended system, it is possible, by the GS algorithm, to find linearizing transformations which transform the congruences to equalities.

Lemma 1 indicates that a dynamic feedback linearizable system has a filtering of the derived flag associated with a precompensator of the form

$$\left[w^{(1)}, \ldots, w^{(k_m - k_1)}, \ldots, w^{(k_m - k_1 + k + 1)}\right] \tag{19}$$

containing $\{N-s_1, \ldots, N-(k_2-k_1)s_1, N-(k_2-k_1)s_1-(s_1+s_2), \ldots, N-(k_2-k_1)s_1-(k_3-k_2)(s_1+s_2), \ldots, N-(k_2-k_1)s_1-(k_3-k_2)(s_1+s_2)-\ldots-(k_m-k_{m-1})(s_1+\ldots+s_{m-1}), .., N-(k_2-k_1)s_1-(k_3-k_2)(s_1+s_2)-\ldots-(k_m-k_{m-1})(s_1+\ldots+s_{m-1})-(k)P\}$ or, similarly, $\{N-s_1, \ldots, N-(k_2-k_1)s_1, \ldots, N-(k_2-k_1)s_1-(k_3-k_2)s_2, \ldots, N-(k_2-_1)s_1-\ldots-(k_m-k_{m-1})s_{m-1}, \ldots, N-(k_2-k_1+k)s_1-\ldots-(k_m-k_{m-1}+k)s_{m-1}-(k)s_m\}$ generators. Depending on the number of generators, ℓ, remaining in $w^{(k_m-k_1+k+1)}$, we require that either

$$N-(k_2-k_1+k)s_1-...-(k_{i+1}-k_i+k)s_i-(k_i-k_{i-1}+k+1)s_{i-1}-...-(k_m-k_{m-1}+1)s_{m-1}-(k+1)s_m=0 \text{ if } \ell<P$$

or

$$N-(k_2-k_1+k+1)s_1-...-(k_m-k_{m-1}+k+1)s_{m-1}-(k+1)s_m=0 \text{ if } \ell=P.$$

Define P integers, ν_i, $1\le i\le P$ as

$$\begin{aligned}
\nu_i &= k+1 \quad , \ 1\le i\le s_m \\
\nu_i &= (k_m-k_{m-1}+k+1) \quad , \ s_m+1\le i\le s_m+s_{m-1} \\
&\ \ \vdots \\
\nu_i &= (k_q-k_{q-1}+k+1) \quad , \ s_m+...+s_q+1\le i\le s_m+...+s_{q-1}(=\ell) \\
\nu_i &= (k_{q-1}-k_{q-2}+k) \quad , \ s_m+...+s_{q-1}+1\le i\le s_m+...+s_{q-2} \\
&\ \ \vdots \\
\nu_i &= (k_2-k_1+k) \quad , \ P-s_1+1\le i\le P.
\end{aligned} \tag{20}$$

such that $\Sigma_i\nu_i=N$. Then a set of P integers is obtained with multiplicities $\{s_m, ..., s_1\}$ which act as generalized Kronecker indices of the nonlinear system.

The generators of each successive derived system of the derived flag associated with the precompensator are such that they fulfil the congruences of the GS algorithm for the prolongated Pfaffian system. Lemma 1 also establishes the correspondence between the fulfilment of these congruences and the fulfilment of the congruences related to the derived flag associated with a precompensator. As shown in the proof of Lemma 1, these congruences take the form

$$dw^{(k_i-k_1+j)} \equiv dt\wedge K^{(k_i-k_1+j-1)}w^{(k_i=k_1+j-1)} \ \text{mod} \ \ w^{(k_i-k_1+j)},du_1,...,du_{P-s_1-...-s_i} \tag{21}$$

for $1\le j\le k_{i+1}-k_i$, $1\le i\le m-1$ and

$$dw^{(k_m-k_1+p)} \equiv dt\wedge K^{(k_m-k_1+p-1)}w^{(k_m-k_1+p-1)} \mod w^{(k_m-k_1+p)} \tag{22}$$

for $1\leq p\leq\delta$, where the matrices $\mathbf{K}^{(\ell)}$ are such that

$$dw^{(k_i-k_1+j)} \equiv 0 \mod w^{(k_i-k_1+j-1)}, du_1, \ldots, du_{P-s_1-\ldots-s_i}$$

and

$$dw^{(k_m-k_1+p)} \equiv 0 \mod w^{(k_m-k_1+p-1)}.$$

Using the generalized Kronecker indices obtained above, we can re-express these conditions in a more generic fashion. By analogy to the GS algorithm, the generalized Kronecker indices give the following set of generators of the Pfaffian system associated with the original system:

$$S = \left[\omega_1^1, \ldots, \omega_1^{\nu_1}, \ldots, \omega_P^1, \ldots, \omega_P^{\nu_P}\right].$$

The last set of generators of the filtering is defined as

$$w^{(k_m-k_1+k+1)} = \left[\omega_1^1, \ldots, \omega_\ell^1\right].$$

Fulfilment of the congruences (22) can be expressed as

$$d\omega_i^1 \equiv dt\wedge\omega_i^2 \mod \left\{\omega_1^1, \ldots, \omega_\ell^1\right\}$$

for $1\leq i\leq\ell$. As a result of (22), the set

$$w^{(k_m-k_1+k)} = \left[\omega_1^1, \omega_1^2, \ldots, \omega_\ell^1, \omega_\ell^2, \omega_{\ell+1}^1, \ldots, \omega_P^1\right]$$

is obtained and, inductively,

$$w^{(k_m-k_1)} = [\omega_1^1,\ldots,\omega_1^{k+1},\ldots,\omega_{s_m}^1,\ldots,\omega_{s_m}^{k+1},\omega_{s_m+1}^1,\ldots,$$
$$\omega_{s_m+1}^k,\ldots,\omega_\ell^1,\ldots,\omega_\ell^{k+1},\ldots,\omega_P^1,\ldots,\omega_P^k]$$

Only the first s_m channels depend on u_1, ..., u_{s_m}, and the fulfilment of the congruences (21) can be expressed as

$$d\omega_i^{k+1} \equiv dt\wedge\omega_i^{k+2} \bmod w^{(k_m-k_1)}, du_1,..,du_{s_m} \quad , s_m+1\le i\le \ell.$$

and

$$d\omega_i^{k} \equiv dt\wedge\omega_i^{k+1} \bmod w^{(k_m-k_1)}, du_1,..,du_{s_m} \quad , \ell+1\le i\le P.$$

Proceeding k_m-k_{m-1} steps,

$$w^{(k_{m-1}-k_1)} = [\omega_1^1,\ldots,\omega_1^{k+1},\ldots,\omega_{s_m}^1,\ldots,\omega_{s_m}^{k+1},\omega_{s_m+1}^1,\ldots,\omega_{s_m+1}^{k_m-k_{m-1}+k+1}$$
$$,\ldots,\omega_\ell^1,\ldots,\omega_\ell^{k_m-k_{m-1}+k+1},\ldots,\omega_P^1,\ldots,\omega_P^{k_m-k_{m-1}+k}]$$

or

$$w^{(k_{m-1}-k_1)} = [\omega_1^1,\ldots,\omega_1^{v_1},\ldots,\omega_{s_m}^1,\ldots,\omega_{s_m}^{v_1},\omega_{s_m+1}^1,\ldots,\omega_{s_m+1}^{v_2},\ldots,$$
$$\omega_{s_m+s_{m-1}}^1,\ldots,\omega_{s_m+s_{m-1}}^{v_2},\ldots,\omega_\ell^1,\ldots,\omega_\ell^{k_m-k_{m-1}+k+1},\ldots,\omega_P^1,\ldots,\omega_P^{k_m-k_{m-1}+k}].$$

Again, the congruences (21) require the existence of P-s_m-s_{m-1} generators such that

$$d\omega_i^{k_m-k_{m-1}+k+1} \equiv dt\wedge\omega_i^{k_m-k_{m-1}+k+2} \bmod w^{(k_m-k_{m-1})}, du_1,\ldots,du_{s_m+s_{m-1}} \quad , s_m+s_{m-1}+1\le i\le \ell$$

and

$$d\omega_i^{k_m-k_{m-1}+k} \equiv dt \wedge \omega_i^{k_m-k_{m-1}+k+1} \mod w^{(k_m-k_{m-1})}, du_1, \ldots, du_{s_m+s_{m-1}}, \quad \ell+1 \le i \le P.$$

Inductively, the set of generators

$$\begin{aligned} S = [&\omega_1^1, \ldots, \omega_1^{\nu_1}, \ldots, \omega_{s_m}^1, \ldots, \omega_{s_m}^{\nu_1}, \omega_{s_m+1}^1, \ldots, \omega_{s_m+1}^{\nu_2}, \ldots, \\ &\omega_{s_m+\ldots+s_2+1}^1, \ldots, \omega_{s_m+\ldots+s_2+1}^{\nu_{P-1}}, \ldots, \omega_P^1, \ldots, \omega_P^{\nu_P}] \end{aligned} \tag{23}$$

is obtained. This set of generators, ω_i^j, is adapted to the derived flag associated with the precompensator. Using these generators, the conditions for dynamic feedback linearizability can be stated as follows. We first require the following definition.

As in Gardner and Shadwick (1992), we identify a tower structure associated with the generalized controllability indices of the form

$$\begin{array}{cccccccc} \omega_1^1 & \omega_1^2 & \ldots & \omega_1^{\nu_1} & \ldots & \omega_P^1 & \ldots & \omega_P^{\nu_P} \\ . & . & & . & & . & & \\ \omega_1^1 & \omega_1^2 & & \omega_1^{\nu_1} & & \omega_P^1 & \omega_P^2 & \\ . & . & & . & \ldots & \omega_P^1 & & \\ \omega_1^1 & \omega_1^2 & & \omega_1^{\nu_1} & & & & \\ . & & & & & & & \\ \omega_1^1 & \omega_1^2 & & & & & & \\ \omega_1^1 & & & & & & & \end{array}$$

where the elements in the top row are generators of S. Generators in the second row generate $w^{(1)}$ and those in each successive row generate derived systems of the derived flag associated with a precompensator. Similar to Gardner and Shadwick, the set of integers

$$m_j = \dim(w^{(j)}/w^{(j+1)})$$

is defined which gives the number of towers with at least j+1 rows for $1 \le j \le k_m - k_1 + k + 1$. We now state the following theorem:

Theorem 2

A nonlinear control-affine system is dynamic feedback linearizable in the sense of Sluis (1993) if and only if there exists a feedback transformation $v=\alpha(x,u)$ and a set of generators adapted to the derived flag (19) associated with a precompensator which satisfy the following conditions:

i) the precompensator, **P**, belongs to the class described in Lemma 1,

ii) its generators satisfy the congruences

$$\begin{aligned} d\omega_{q+1}^{v_q - j} &\equiv dt \wedge \omega_{q+1}^{v_q - j+1} \\ &\vdots \\ d\omega_P^{v_{m_j} - j} &\equiv dt \wedge \omega_P^{v_{m_j} - j+1} \end{aligned} \qquad \mod w^{(j+1)}, dv_1, \ldots, dv_q \tag{24}$$

where $m_j = \dim(w^{(j)}/w^{(j+1)})$, $q = P - s_1 - \ldots - s_p$, $k_{p-1} - k_1 + 1 \le j \le k_p - k_1$ when $1 \le p < m$ and $k_m - k_1 + 1 \le j \le k_m - k_1 + k + 1$ when $p = m$.

Proof:

The conditions for dynamic feedback linearizability given in terms of the derived flag associated with the precompensator are closely related to the conditions of the GS algorithm. The construction is also very similar. As in Gardner and Shadwick (1992), a feedback invariant filtering of the Pfaffian system associated with a nonlinear system is considered, and the conditions for dynamic feedback linearizability are expressed in terms of congruences. The state-

space and feedback transformations required are obtained by transforming these congruences to equalities.

The main difference is that the construction implies the existence of a precompensator of the class described in Lemma 1.

Assume that the system is dynamic feedback linearizable. This naturally implies feedback linearizability of the extended system $\sum$=[S,P], and the generators of the derived systems of the Pfaffian associated with the extended system must fulfil the congruences (14) of the GS algorithm. Let the precompensator be represented by the indices $\{k_1, ..., k_m\}$ with multiplicities $\{s_1, ..., s_m\}$, $m \leq P$, $\sum_i s_i = P$. As shown in the proof of Lemma 1, fulfilment of congruences (14) is equivalent to fulfilment of congruences (24) for the derived flag associated with the precompensator. Fulfilment of these congruences therefore constitutes a necessary condition for dynamic feedback linearizability.

The sufficiency of this condition follows from the fact that, conversely, the fulfilment of the congruences (24) also corresponds to the fulfilment of the congruences (14) for the prolongated system. This can be seen directly by replacing the terms $dv_1,..., dv_q$ in Equation (24) by the generators associated with the prolongations of each input channel, given by

$$\left[dv_1 - v_1^{(1)}dt, \ldots, dv_1^{(j)} - v_1^{(j+1)}dt, \ldots, dv_q - v_q^{(1)}dt, \ldots, dv_q^{(j)} - v_q^{(j+1)}dt\right]$$

for $k_{p-1}-k_1+1 \leq j \leq k_p-k_1$, $q=P-s_1-...-s_p$ when $1 \leq p < m$ and $k_m-k_1+1 \leq j \leq k_m-k_1+k+1$ when $p=m$. From the fulfilment of congruences (14) it is therefore possible to construct the required state-space and feedback transformations by application of the GS algorithm to the tower structure of the prolongated system.■

Theorem 2 states that it is possible to construct precompensators from prolongations of

state-feedback transformations of the original system by studying the derived structure given in Definition 1. The conditions imposed on this structure by the GS linearizability conditions of the prolongated system provide a method to compute these feedback transformations. They also provides a necessary and sufficient condition for dynamic feedback linearizability by endogenous feedback.

In the general case, we consider dynamic feedback linearizability by prolongations of dynamic state feedback transformations of the form $v=\alpha(x,u,u^{(1)}, ..., u^{(\beta+1)})$, where $v\in\mathbb{R}^p$, $u^{(\beta)}$ denotes the set $\{u_1^{(\beta_1)}, ..., u_p^{(\beta_p)}\}$ and $\{\beta_1, ..., \beta_p\}$ is the degree of precompensation of u_i. In order to construct these feedback transformations we must consider fulfilment of Theorem 2 subject to the presence of a linear precompensator. That is, we apply the conditions of Theorem 2 to the Pfaffian system

$$S' = \left[w_1,\dots,w_N,\eta_1^1,\dots,\eta_1^{\beta_1},\dots,\eta_P^1,\dots,\eta_P^{\beta_P}\right]$$

subject to the precompensator

$$P' = \left[dv_1 - v_1^{(1)}dt,\dots,dv_1^{(\gamma_1)} - v_1^{(\gamma_1+1)}dt,\dots,dv_P - v_P^{(1)}dt,\dots,dv_P^{(\gamma_P)} - v_P^{(\gamma_P+1)}dt\right]$$

with degree of precompensation $\{\gamma_1, ..., \gamma_p\}$. Using this approach, the problem of dynamic feedback linearization can be solved by constructing the derived systems of S' associated the precompensator P' such that the conditions of Theorem 2 are met.

By construction, the degree of precompensation $\{\alpha_1, ..., \alpha_p\}$ of the resulting precompensator must be such that $\Sigma_i\alpha_i=\Sigma_i\beta_i+\Sigma_i\gamma_i=q$. Consequently, the dynamic feedback transformation must also be such that

$$\operatorname{rank}\left[\frac{\partial\alpha(x,u,\ldots,u^{(\beta+1)})}{\partial u^{(\beta+1)}}\right] = P.$$

The restrictions of the class of precompensators described in Lemma 1 are still applicable to the general case. To show this, consider an ordering of the inputs $\{v_1, \ldots, v_P\}$ with degree of precompensation $\{\gamma_1, \ldots, \gamma_P\}$, $\gamma_1 \leq \ldots \leq \gamma_P$, with multiplicities $\{s_1, \ldots, s_m\}$ and corresponding indices $\{k_1, \ldots, k_m\}$. From Lemma 1, we know that the class of admissible precompensators is given by

$$(N+\sum_{i=1}^{P}\beta_i)-(k_2-k_1)s_1-\ldots-(k_m-k_{m-1})(s_1+\ldots+s_{m-1})<0.$$

Since the system S′ is obtained by prolongation of the original system inputs, we know that its derived flag contains at least one generator that fulfils the required congruences. This generator can always be obtained from the prolongation of the input channel with the highest degree of precompensation and must therefore be such that $k \geq \max_i \beta_i$. The resulting class of precompensators can therefore be restricted to

$$(N+\sum_{i=1}^{P}\beta_i)-kP \leq (k_2-k_1)s_1+\ldots+(k_m-k_{m-1})(s_1+\ldots+s_{m-1})<N+\sum_{i=1}^{P}\beta_i-(k-1)P$$

or, equivalently, to

$$N-\sum_{i=1}^{P}(k-\beta_i) \leq (k_2-k_1)s_1+\ldots+(k_m-k_{m-1})(s_1+\ldots+s_{m-1})<N-\sum_{i=1}^{P}(k-\beta_i-1).$$

This identity, along with the identity $\Sigma_i\alpha_i=\Sigma_i\beta_i+\Sigma_i\gamma_i$, defines the class of admissible precompensators.

We can now state the following theorem:

Theorem 3

A nonlinear control-affine system is dynamic feedback linearizable if and only if there exists a dynamic feedback transformation $v=\alpha(x,u, ..., u^{(\beta+1)})$ and a set of generators from the ideal generated by the Pfaffian

$$S' = \left[w_1,\ldots,w_N,\eta_1^1,\ldots,\eta_1^{\beta_1},\ldots,\eta_P^1,\ldots,\eta_P^{\beta_P}\right]$$

adapted to the derived flag (19) associated with a precompensator which satisfies the following conditions:

i) the precompensator, **P**, belongs to the class described in Lemma 1

ii) its generators satisfy the congruences

$$\begin{aligned} d\omega_{q+1}^{\nu_q-j} &\equiv dt\wedge\omega_{q+1}^{\nu_q-j+1} \\ &\vdots \\ d\omega_P^{\nu_{m_j}-j} &\equiv dt\wedge\omega_P^{\nu_{m_j}-j+1} \end{aligned} \qquad \text{mod } w^{(j+1)}, dv_1,\ldots,dv_q \tag{24}$$

where $m_j=\dim(w^{(j)}/w^{(j+1)})$, $q=P-s_1-\ldots-s_p$, $k_{p-1}-k_1+1\le j\le k_p-k_1$ when $1\le p<m$ and $k_m-k_1+1\le j\le k_m-k_1+k+1$ when $p=m$.

Proof:

The proof is a direct consequence of Theorem 2.■

In the next section, we demonstrate the application of Theorem 2 to three examples.

5.3 Examples

Example 5.2 Counter-example of Charlet et al. (1989, 1991)

Consider the counter-example of Charlet *et al.* (1989, 1991)

$$\begin{aligned}\dot{x}_1 &= x_2 + x_3u_2\\ \dot{x}_2 &= x_3 + x_1u_2\\ \dot{x}_3 &= u_1 + x_2u_2\\ \dot{x}_4 &= u_2\end{aligned}$$

It is easily verified that this system is not feedback linearizable and that it does not fulfil the sufficient conditions of Charlet *et al.* (1989, 1991). This system does, however, fulfil the conditions of Theorem 2.

The Pfaffian system associated with this system is given by

$$\begin{aligned}I &= [dx_1 - (x_2 + x_3u_2)dt, dx_2 - (x_3 + x_1u_2)dt, dx_3 - (u_1 + x_2u_2)dt, dx_4 - u_2dt]\\ &= [w_1, w_2, w_3, w_4]\end{aligned}$$

Let us first construct the class of possible compensators for systems with 4 states and 2 inputs. This system has no Pfaffian subsystem which fulfils the congruences (14), and so we let k=0. From Lemma 1,

$$\begin{aligned}N - P \le (k_2 - k_1)s_1 < N,\\ 4 - 2 \le (k_2 - k_1)s_1 < 4,\\ 2 \le (k_2 - k_1)s_1 < 4\end{aligned}$$

or $(k_2-k_1)s_1=2$ or 3. Since $s_1=1$, $k_2-k_1=2$ or 3.

Upon relabelling the inputs to $\{v_1, v_2\}=\{u_2,u_1\}$, the precompensator can be defined by $\{\alpha_1,$

$\alpha_2\}=\{3, 0\}$, such that $\{s_1, s_2\}=\{1, 1\}$ and $\{k_1, k_2\}=\{0, 3\}$.

We now construct the derived flag associated with this precompensator. From

$$d\begin{pmatrix} w_1 \\ w_2 \\ w_3 \\ w_4 \end{pmatrix} \equiv dt \wedge \begin{pmatrix} 0 \\ 0 \\ 1 \\ 0 \end{pmatrix} dv_2 \mod I, dv_1$$

we obtain the first derived system as $w^{(1)}=[w_1, w_2, w_4]$. Proceeding, we obtain

$$d\begin{pmatrix} w_1 \\ w_2 \\ w_4 \end{pmatrix} \equiv dt \wedge \begin{pmatrix} v_1 \\ 1 \\ 0 \end{pmatrix} dx_3 \mod w^{(1)}, dv_1$$

Defining $w_5=v_1w_2-w_1$, we see that

$$dw_5 \equiv 0 \mod w^{(1)}, dv_1$$

and, consequently, the second derived system is generated by $w^{(2)}=[w_4, w_5]$. For the next step,

$$d\begin{pmatrix} w_4 \\ w_5 \end{pmatrix} \equiv dt \wedge \begin{pmatrix} 0 \\ v_1^3 - 1 \end{pmatrix} dx_2 \mod w^{(2)}, dv_1$$

such that $w^{(3)}=w_4$. This system fulfils the conditions of Theorem 2 and is therefore dynamic feedback linearizable. To see this, let $\omega_1^{\,1}=w_4$. From (19), we have that $\nu_1=1$ and $\nu_2=3$. Consequently, we let $\omega_2^{\,1}=w_5$. By exterior differentiation, we get

$$d\omega_2^1 \equiv dt \wedge (v_1^3-1)dx_2 = dt \wedge (v_1^3-1)w_2 = dt \wedge \omega_2^2 \mod w^{(2)}, dv_1.$$

and

$$d\omega_2^2 \equiv dt\wedge(v_1^3-1)w_3 = dt\wedge\omega_2^3 \mod w^{(1)}, dv_1.$$

According Theorem 2, the system is dynamic feedback linearizable and is therefore equivalent to a linear controllable system. Application of the GS algorithm to the extended system shows that the extended system is linearizable with controllability indices $\{\nu_1, \nu_2\}=\{4, 3\}$ and linearizing output functions

$$y_1 = x_4$$

$$y_2 = x_2u_2 - x_1.$$

Example 5.3 Dynamic feedback linearization of a system without drift

Consider the simple system

$$\dot{x}_1 = x_1x_2u_1 + x_2^2u_2$$

$$\dot{x}_2 = u_1$$

$$\dot{x}_3 = u_2$$

It can be easily verified that this system is not feedback linearizable. We now verify the dynamic feedback linearizability of this system. As before, we construct the class of possible precompensators. By Lemma 1,

$$N - P \le (k_2 - k_1)s_1 < N,$$

$$1 \le (k_2 - k_1)s_1 < 3.$$

and, therefore, $(k_2-k_1)s_1=1$ or 2. Taking $s_1=1$, we obtain $k_2-k_1=1$ or 2. Let us consider the precompensator $\{s_1, s_2\}=\{1,1\}$, $\{k_1, k_2\}=\{0,1\}$, where k_2 corresponds to the u_1 prolongation.

We now construct the derived flag associated with this precompensator. The first derived

system is obtained from

$$d\begin{pmatrix} w_1 \\ w_2 \\ w_3 \end{pmatrix} \equiv dt \wedge \begin{pmatrix} x_2^2 \\ 0 \\ 1 \end{pmatrix} du_2 \mod w_1, w_2, w_3, du_1.$$

Taking $w_4=x_2^2 w_3-w_1$, we obtain the derived system associated with the precompensator $w^{(1)}=[w_2, w_4]$. This system fulfils the conditions of Theorem 2. By exterior differentiation, the following generators of original Pfaffian system

$$\omega_1^1 = w_2$$

$$\omega_2^1 = w_4 = x_2^2 w_3 - w_1$$

$$\omega_2^2 = (x_2^3 u_1 + 2x_2 u_1) w_3$$

are obtained with generalized Kronecker indices {1,2}.

By the GS algorithm, the prolongated system is feedback linearizable with linearizing output functions

$$y_1 = x_2$$

$$y_2 = -x_1 + x_2^2 x_3$$

and Kronecker indices {2,2}.

Example 5.4 Dynamic feedback linearization in the sense of Sluis (1993)

To demonstrate the application of Theorem 2 to the more general precompensators described by Sluis, we consider the following example

$$\dot{x}_1 = x_2$$

$$\dot{x}_2 = u_1 \sin x_5 - u_2 \cos x_5$$

$$\dot{x}_3 = x_4$$

$$\dot{x}_4 = u_1 \cos x_5 + u_2 \sin x_5 - 1$$

$$\dot{x}_5 = x_5$$

$$\dot{x}_6 = u_2.$$

Inspection of the derived flag of the Pfaffian system associated with this nonlinear system indicates the existence of generators of the first derived system that fulfil the congruences of the GS algorithm. We therefore let k=1.

From Lemma 1,

$$N - (k+1)P \le (k_2 - k_1)s_1 < N - kP$$

or

$$2 \le (k_2 - k_1)s_1 < 4.$$

This gives k_2-k_1=2 or 3.Let k_2=2 and consider the feedback transformation $v_2=u_1-x_6^2$, $v_1=u_2$ with degree of precompensation $\{k_1, k_2\}=\{0,2\}$. The Pfaffian associated with this nonlinear system is given by

$$S = \begin{bmatrix} dx_1 - x_2 dt, dx_2 - (u_1 \sin x_5 - u_2 \cos x_5)dt, \\ dx_3 - x_4 dt, dx_4 - (u_1 \cos x_5 + u_2 \sin x_5 - 1)dt, \\ dx_5 - x_6 dt, dx_6 - u_2 dt] \end{bmatrix}.$$

The first derived system associated with the precompensator is obtained from the structure

equations:

$$\begin{aligned} dw_1 &\equiv 0 \\ dw_2 &\equiv -dt\wedge\cos x_5 du_2 \\ dw_3 &\equiv 0 \\ dw_4 &\equiv dt\wedge\sin x_5 du_2 \\ dw_5 &\equiv 0 \\ dw_6 &\equiv dt\wedge du_2 \end{aligned} \qquad \mod [w_1, w_2, w_3, w_4, w_5, w_6, dv_2]$$

Defining $w_7=\cos x_5 w_6+w_2$ and $w_8=\sin x_5 w_6-w_4$, it can be verified that

$$\begin{aligned} dw_7 &\equiv 0 \\ dw_8 &\equiv 0 \end{aligned} \qquad \mod [w_1, w_2, w_3, w_4, w_5, w_6, dv_2]$$

The structure equations of the first derived system are given by

$$\begin{aligned} dw_1 &\equiv -dt\wedge\cos x_5 dx_6 \\ dw_3 &\equiv dt\wedge\sin x_5 dx_6 \\ dw_5 &\equiv dt\wedge dx_6 \\ dw_7 &\equiv -dt\wedge x_6\cos x_5 dx_6 \\ dw_8 &\equiv dt\wedge x_6\sin x_5 dx_6 \end{aligned} \qquad \mod [w_1, w_3, w_5, w_7, w_8, dv_2]$$

Defining

$$
\begin{aligned}
w_9 &= \cos x_5 w_5 + w_1 \\
w_{10} &= \sin x_5 w_5 - w_3 \\
w_{11} &= x_6 w_1 - w_7 \\
w_{12} &= x_6 w_3 - w_8
\end{aligned}
$$

it can be verified that

$$
\begin{aligned}
dw_9 &\equiv 0 \\
dw_{10} &\equiv 0 \\
dw_{11} &\equiv 0 \\
dw_{12} &\equiv 0
\end{aligned}
\quad \mod [w_1, w_3, w_5, w_7, w_8, dv_2].
$$

The structure equations associated with the second derived system are given by

$$
\begin{aligned}
dw_9 &= 0 \\
dw_{10} &\equiv 0 \\
dw_{11} &\equiv dt \wedge \cos x_5 dv_2 + dt \wedge (x_6^2 \sin x_5 - (v_2 + x_6^2)\sin x_5) dx_5 \\
dw_{12} &\equiv -dt \wedge \sin x_5 dv_2 + dt \wedge (x_6^2 \cos x_5 - (v_2 + x_6^2)\cos x_5) dx_5
\end{aligned}
\quad \mod [w_9, w_{10}, w_{11}, w_{12}]
$$

Finally,

$$
\begin{aligned}
dw_9 &\equiv -dt \wedge x_6 \sin x_5 dx_5 + dt \wedge \cos x_5 dx_6 + dt \wedge dx_2 \\
dw_{10} &\equiv dt \wedge \cos x_5 dx_5 + dt \wedge \cos x_5 dx_6 + dt \wedge dx_2
\end{aligned}
\quad \mod [w_9, w_{10}].
$$

This system fulfils the conditions of Theorem 2 and is therefore dynamic feedback linearizable. The Kronecker indices of the precompensated system are $\nu_1=\nu_2=4$. The generalized Kronecker indices for the original system given by (20) are {2,4}.

6. Conclusions

In this chapter, the exact linearization problem of nonlinear control systems has been considered, using the exterior calculus framework of the GS algorithm. Using a bioreactor model as an example, it was shown how the GS algorithm can be used to derive state-space coordinate transformations and feedback transformations which exactly linearize a nonlinear system.

Using a CSTR example, it was shown how the GS algorithm can be used to uncover obstructions to the linearizibility of a nonlinear system. These obstructions are curvature-like functions which are invariant under state-space and state feedback transformations. Since elimination of these obstructions will provide an exactly linearizable control system, these feedback invariant functions provide a natural choice of geometric outputs for the system. More work is required to understand more completely the implications of these functions in controller design.

The problem of exact linearization by dynamic state feedback and state space transformation was also solved. A necessary and sufficient condition for the linearizibility of a control system by dynamic feedback was found by adapting the linearizability conditions of the GS algorithm to account for the presence of a precompensator. This condition provides an algorithm which generalizes the GS algorithm. For systems that are linearizable by static state feedback, the algorithm developed in this Chapter reduces to the GS algorithm.

Nomenclature

A N+q by N+q matrix

A Chemical species A

a Smooth function of **x** and **z**

a_i Batch reactor parameters

B N+q by P matrix

B Chemical species B

b Smooth function of **x** and **z**

b_i Batch reactor parameters

C Chemical species C

$C^k(M)$ Space of functions with k continuous derivatives

c Smooth function of **x** and **z**

c(s) Curve in M^*

d Smooth function of **x** and **z**

d Exterior derivative

e_i Basis vector of a vector space

f Smooth vector valued function of the drift vector field of a nonlinear system

I Pfaffian system

$\mathbf{I}^{(i)}$ i^{th} derived system of **I**

I Inhibitor concentration

K Field

K Saturation constant

K_I	Inhibition constant
k_i	Degree of differentiation of input channel(s) with multiplicity s_i
$k_i(x_3)$	Rate constant for reaction i
M	Differentiable manifold
M^*	Differentiable manifold ($=M\times\mathbb{R}^P\times\mathbb{R}$)
m_j	Number of towers with at least j+1 rows
N	State space dimension
P	Pfaffian system associated with a precompensator
P	Input space dimension
p	Maximum rate of product inhibition
S	Pfaffian system associated with a nonlinear system
S_f	Inlet substrate concentration
s_i	Multiplicity of input channels with degree of differentiation k_i
T	N+q by N+q invertible matrix
T_pM	Tangent space to M at a point p
T_p^*M	Cotangent space to M at a point p
t	Time
U_i	Open set on a manifold M
U	Open coordinate neighbourhood on a manifold M
u	Input variables
V	Vector space
V^*	Co-vector (or dual) space

$\mathbf{v}$ Feedback transformed input

v_i Vector of a vector space V

W Vector space

$\mathbf{w}$ Set of generators from the derived flag of the Pfaffian system **S**

w_i Generator from the set **w**

w Vector of the vector space W

$\mathbf{x}$ State variables

Y_i Yield of biomass for cells i

$\mathbf{y}$ Linearizing output variables

$\mathbf{z}$ Variables associated with a precompensator

Greek Letters

α Element of a field K

α_i Degree of differentiation of an input channel u_i

β Element of a field K

γ Set of generators from a Pfaffian system **I**

γ_i Batch reactor parameters

Δ Distribution on M

$\Lambda^P(M)$ Space of p-vectors on M

η Set of differential one-forms

Θ Codistribution on M

μ_i Specific growth of cells i

μ_{maxi} Maximum specific growth rate of cells i

ν_i Generalized Kronecker indices

ξ In Section 2, set of differential one-forms

ξ In Section 5, extended state-space coordinates

Σ Pfaffian associated with an extended system

$\Sigma^{(i)}$ i^{th} derived system of Σ

ϕ Vector valued function

ϕ_i i^{th} element of ϕ

$\Omega^p(M)$ Space of p-covectors on M

ω Set of differential one -forms and generators from a Pfaffian system

ω_i i^{th} element of ω

Symbols

$\wedge$ Wedge products

d Exterior derivative

$\mathbb{R}$ Space of real numbers

Chapter 6

Conclusions

The development of nonlinearity measures is of great interest in a number of areas of chemical engineering, especially in modelling, optimization and control of chemical processes. In the modelling and optimization of chemical processes, measurement of nonlinearity has important influence in parameter estimation (Bates and Watts, 1988) and in system identification (Nikolaou, 1993; Haber, 1985). The application of nonlinear measures in chemical process control, primarily motivated by the need for alternative nonlinear controller design methods, is recent (e.g., Ogunnaike *et al.*, 1993; Stack and Doyle III, 1995; Nikolaou, 1993). The assessment and compensation of nonlinearity is a complex problem that can be investigated using a wide variety of approaches spanning many research areas such as differential geometrical control, optimal control theory, system identification and statistical model development. This study extends the ability to detect and measure nonlinearity in steady-state and dynamic systems.

The main result of this thesis is the development of a framework for the assessment of nonlinearity in controlled processes. Assuming that the process can be represented by a twice differentiable process map, the extent of nonlinearity is measured by evaluating the induced local curvature of the process response. The magnitude of this curvature is assessed with respect to an appropriately chosen scaling region. This approach provides an effective methodology for the development of dimensionless curvature measures that can be used to characterize and quantify the nonlinear behaviour of steady-state and dynamic controlled processes.

In Chapter 2, the framework was applied to the assessment of steady-state process nonlinearity. A root mean squared measure of the deviation of the process behaviour from its

tangential approximation was proposed as a measure of nonlinearity. Using an orthogonal decomposition, the contributions of the tangential and normal components of the nonlinear terms to the nonlinearity measure were evaluated. It was demonstrated that the presence of tangential nonlinearity requires a change of input coordinates. Normal nonlinearity indicates the need for state-space and feedback transformations. The impact of steady-state curvature on controller performance using a bioreactor example. Gains in optimal performance were realized by using an input-output linearizing controller in comparison to two linear controllers (linear state-feedback and PI). A simple quadratic gain PI controller was also shown to improve the performance of the closed-loop process.

This methodology provides a simple approach for analyzing nonlinear control processes. It can be easily employed for preliminary process investigation using models that locally approximate the steady-state locus. It also provides a procedure for the computation of coordinate transformations that can be used in controller design to remove local effects of gain nonlinearity. Application of this framework in engineering practice requires a rigorous methodology for evaluating nonlinearity from plant data. Although this has been an important consideration in the scope of this thesis, additional research is still needed to develop an effective method. This method should also include provisions for sampling properties to enable assessment with statistical uncertainty.

The fundamental impact of nonlinearity on closed-loop steady-state process behaviour was studied. Using classical differential geometrical tools, a set of second order identities related to the invertibility of the nonlinear process were developed. Associated with these identities was the decomposition of closed-loop nonlinearity into mismatch terms and compensation terms. Root

mean squared measures of closed-loop nonlinearity were developed and it was demonstrated that they could be used together with individual contributions of the identities to describe the significance and sources of the nonlinear behaviour of a process.

The second order identities were also used to provide a nonlinear extension of the relative gain array (RGA). Their geometrical interpretation also provided a fundamental definition and a new interpretation of the RGA. Application of the identities to the assessment of higher order interaction was shown to be very similar to the analysis of the linear RGA. Higher interaction tables were constructed to measure the contributions of the nonlinear terms to interaction in a closed-loop process. Further work is required to understand the implications of these measures of nonlinear interaction in controller design.

The process map framework was also used to develop a general methodology for the assessment of dynamic nonlinearity in controlled processes. Using an operator-based approach, a measure of nonlinearity was developed for processes described by twice Fréchet differentiable nonlinear operators. As in the steady-state case, the magnitude of the measure was measured relative to regions of unit norm in the output space. Scaling of the output response signals was provided by linear invertible operators that mapped regions of interest in the output signal space to regions of unit L_p norm.

A potential application of the measure of dynamic nonlinearity to chemical processes was demonstrated. First and second order sensitivity equations of the output with respect to the inputs were used to evaluate the nonlinearity measures for continuous and batch chemical processes. The batch example was used to demonstrate how the measure can be used to evaluate the extent of nonlinearity in a closed-loop process. By scaling the process output with respect to the

controller operator, one obtains a measure of the extent of nonlinearity resulting from the combination of process output and controller response. In the example presented, it was shown that the mild nonlinearity of the process was increased by the presence of a linear PI controller as a result of considerable input saturation in the closed-loop system. From this point of view, the measure developed in this thesis is indeed a control-relevant measure (Stack and Doyle III, 1995). Through scaling, an appreciation of the process nonlinearity as seen from the controller, is obtained. The use of this measure may provide considerable insight into the relationship between linear controller performance and process nonlinearity. The measure can also potentially be used to develop alternative descriptions of process uncertainty with implications in robust controller design. Further work is needed to fully develop this approach.

In Chapter 5 of the thesis, the linearizability of control systems was studied. Analysis focused on exact linearization of control systems by state-feedback and coordinate transformations. The main tool employed was the linearization algorithm developed by Gardner and Shadwick (1992), called the GS algorithm. This algorithm, based on an exterior calculus setting, is an algebraically and computationally attractive way of solving exact feedback linearization problems for nonlinear systems. Potential extensions and applications of this algorithm were examined in this thesis.

It was shown that the GS algorithm can be used to characterize the set of linearizable systems for different classes of process models. Using this algorithm to uncover obstructions to linearizability of classes of models provides a systematic way of choosing appropriate model forms in process model formulation. Since the vanishing of these quantities provides a sufficient condition for linearizability, selection of model forms which satisfy this condition may lead to

simplification of controller design procedures based on feedback linearization for particular classes of processes.

Extension of this method to dynamic feedback linearization of control-affine processes was also considered. A necessary and sufficient condition for dynamic feedback linearizability of nonlinear control affine systems was developed. The linearizability conditions are based on a filtering of the Pfaffian system associated with a nonlinear system that take account of the presence of a specific precompensator. In this setting, a precompensator can be expressed by a set of nonlinear algebraic constraints that impact the structure of the derived flag of the system. This approach can be used to define all kinds of dynamic compensator. As demonstrated in this thesis, linear and nonlinear precompensators can be treated as well fully dynamic feedback transformations. The GS algorithm was used to show how one can restrict the class of suitable precompensators and design nonlinear precompensators. The conditions derived in Chapter 5 complement the sufficient conditions obtained by Charlet *et al.* (1989) and the necessary conditions of Sluis (1993). The formulation presented in this thesis provides a very general description of the problem of exact linearization that is closely related to the concept of differential flatness. This formulation may provide enhanced insight into the understanding of the geometric structure of nonlinear control system.

References

Aranda-Bricaire, E., C.H. Moog and J.-B. Pomet, 1995, A Linear Algebraic Framework for Dynamic Feedback Linearization, *IEEE Trans. Autom. Control.*, **40**, 127-132.

Aranda-Bricaire, E., C.H. Moog and J.-B. Pomet, 1993, Feedback Linearization: A Linear Algebraic Approach, in *Proc. 32nd IEEE Conf. Decision Control*, 3441-3446.

Atkins, R. and W. Shadwick, Invariant Functions of Control-linear Systems, *Syst. Con. Lett.*, **21**, 389-395 (1993).

Banaszuk, A. and J. Hauser, Approximate Feedback Linearization: A Homotopy Operator Approach, in *Proc. ACC*, Baltimore, MD (1994).

Bates, D.M. and D.G. Watts, *Nonlinear Regression Analysis and Its Applications*, John Wiley & Sons, New York (1988).

Bates, D.M. and D.G. Watts, Relative Curvature Measures of Nonlinearity (with discussion), *J. Roy. Stat. Soc.*, Ser. B. **42**, 1-25 (1980).

Bates, D.M. and D.G. Watts, Parameter Transformations for Improved Approximate Confidence Regions in Nonlinear Least Squares, *Ann. Stat.*, **9**, 1152-1167 (1982).

Bequette, B. W., Nonlinear Control of Chemical Processes: A Review, *Ind. Eng. Chem. Res.* **30**, 1391-1413 (1991).

Bristol, E.H. , On a New Measure of Interaction for Multivariable Process Control, *IEEE Trans. Autom. Control*, AC-**11**, 133-134 (1966).

Brockett, R.W., Feeback Invariants for Non-linear Systems, *IFAC Congress*, **6**, 1115-1120 (1978).

Brockett, R.W., R.S. Millman and H. Sussman eds., *Differential Geometric Control Theory*, Birkhauser (1983).

Charlet, B., J. Lévine and R. Marino, Sufficient Conditions for Dynamic State Feedback Linearization, *SIAM J. Control Optim.*, **29**, 38-57 (1991).

Charlet, B., J. Lévine and R. Marino, On Dynamic Feedback Linearization, *Systems Control Lett.*, **13**, 143-151 (1989).

Daoutidis, P. and C. Kravaris, Structural Evaluation of Control Configurations for Multivariable Nonlinear Processes, *Chem. Eng. Sc.*, **47**, 1091-1107 (1992).

Desoer, C.A. and M. Vidyasagar, *Feedback Systems: Input-Output Properties*, Academic Press, New York (1975).

Di Benedetto, M.D., J.W. Grizzle and C.H. Moog, Rank Invariants of Nonlinear Systems, *SIAM J. Cont. Optim.*, **27**, 658-673 (1989).

Doyle III, F.J. and M. Morari, Controller Design for Conic Sector Bounded Nonlinearity, in *Proc. ACC*, San Diego, CA (1990).

Fliess, M., J. Lévine, P. Martin and P. Rouchon, Nonlinear Control and Lie-Bäcklund Transformations: Towards a New Differential Geometric Standpoint, in *Proc. 33rd Conf. Decision Control*, 339-344 (1994a).

Fliess, M., J. Lévine, P. Martin and P. Rouchon, Flatness and Defect of Nonlinear Systems: Introductory Theory and Examples, to appear in *Int. J. Control* (1994b).

Fliess, M., J. Lévine, P. Martin and P. Rouchon, On Differentially Flat Nonlinear Systems, in *Proc. 2nd IFAC NOLCOS Symp.*, M. Fliess, Ed., Bordeaux, 408-412 (1992).

Fliess, M., Nonlinear Control Theory and Differential Algebra: Some Illustrative Examples, *Proc. 10th. IFAC World Congress*, Munich (1987).

Gardner, R., Invariants of Pfaffian Systems, *Trans. AMS*, **126**, 514-533 (1967).

Gardner, R., *The Method of Equivalence and its Applications*, SIAM-CBMS, **58** (1983).

Gardner, R.B. and W.F. Shadwick, The GS Algorithm for Exact Linearization to Brunovsky Normal Form, *IEEE Trans. Autom. Control.*, **37**, 224-230 (1992).

Gardner, R. and W.F. Shadwick, Symmetry and the Implementation of Feedback Linearization, *Syst. Cont. Lett.*, **15**, 25-33 (1990).

Georgiou, T.T., Remarks on Differential Stability of Nonlinear Systems, *Proc. 33rd Conf. Decis. Cont.*, Lake Buena Vista, Florida, 646-647 (1994).

Georgiou, T.T., Differential Stability and Robust Control of Nonlinear Systems, *Proc. 32nd Conf. Decis. Cont.*, Austin, Texas, 984-989 (1993).

Goldberg, M.L., D.M. Bates and D.G. Watts, Simplified Methods for Assessing Nonlinearity, *Am. Stat. Ass. Proc. Bus. Econ. Statistics Section*, 67-74 (1983).

Grosdidier, P. and M. Morari, The μ Interaction Measure, *Ind. Eng. Chem. Res.*, **26**, 1193-1202 (1987).

Guay, M., P.J. McLellan and D.W. Bacon, Measurement of Nonlinearity in Chemical Process Control Systems: The Steady-State Map, *Can. J. Chem. Engng.*, **73**, 868-882 (1995).

Guay, M. and D.D. McLean, Optimization Strategies for Parameter Estimation in Systems Described by Simultaneous Ordinary Equations, *Comput. Chem. Eng.*, **19**, 1271-1286 (1995).

Guzzella, L. and A. Isidori, On Approximate Linearization of Nonlinear Control Systems, *Int. J Rob. Nonlin. Cont.*, **3**, 261-276 (1993).

Haber, R., Nonlinearity Tests for Dynamic Processes, *IFAC Ident. Syst. Param. Estim. 1985*, 409-414 (1985).

Hamilton, D.C., D.G. Watts and D.M. Bates, Accounting for Intrinsic Nonlinearity in Nonlinear Regression Parameter Inference Regions, Ann. Stat. **10**(2), 386-393 (1982).

Henson, M.A. and D.E. Seborg, Nonlinear Control Strategies for Continuous Fermentors, *Proc. of the ACC*, San Diego CA (1990).

Hermann, R., The Theory of Equivalence of Pfaffian Systems and Input Systems under Feedback, *Math. Systems Theory*, **15**, 343-356 (1982).

Hermann, R., The Formal Linearization of a Semisimple Lie Algebra of Vector Fileds around a Singular Point, *Trans. Amer. Soc.*, **130**, 105-109 (1968).

Hirschorn, R.M., (A,B)-invariant Distributions and Disturbance Decoupling of Nonlinear Systems, *SIAM J. Cont. Optim.*, **19**, 1-19 (1981).

Hirschorn, R.M., Invertibility of Nonlinear Control Systems, SIAM J. Cont. Optim. **17**, 289-297 (1979).

Hoo, K.A. and J.C. Kantor, Global Linearization and Control of a Mixed-culture Bioreactor with Competition and External Inhibition, *Math. Biosc.*, **82**, 43-62 (1986).

Hunt, L.R., R. Su and G. Meyer, Global Transformations of Nonlinear Systems, *IEEE Trans. Autom. Cont.*, **28**, 24-31 (1983a).

Hunt, L.R., R. Su and G. Meyer, Design for Multi-input Nonlinear Systems, in *Differential Geometric Control Theory*, Brockett, R.W., R.S. Millman and H. Sussman Eds.,

Birkhauser, 268-298 (1983b).

Hunt, R. and J. Turi, A New Algorithm for Constructing Approximate Transformations for Nonlinear Systems, *IEEE Trans. Autom. Cont.*, **38**, 1553-1556 (1993).

Isidori, A., *Nonlinear Control Systems*, 2nd ed., Springer-Verlag, Berlin (1989).

Isidori, A, Control of Nonlinear Systems via Dynamic State Feedback, in *Differential Geometric Control Theory*, M. Hazewinkel and M. Fliess, eds., D. Reidel, Boston, 121-145 (1986).

Isidori, A., C.H. Moog and A. De Luca, A Sufficient Condition for Full Linearization via Dynamic State Feedback, *Proc. 25th IEEE Conf. Decis. Cont.*, Athens, 203-207 (1986).

Jakubczyk, B. and W. Respondek, On the Linearization of Control Systems, *Bull. Acad. Polon. Sci. Ser. Sci. Math. Astronom. Phys.*, **28**, 517-522 (1980).

Johansen, T.A. and B.A. Foss, Constructing NARMAX Models Using ARMAX Models, *Int. J. Cont.*, **58**, 1125-1153 (1993).

Kang, W., Approximate Linearization of Nonlinear Control Systems, *Syst. Cont. Lett.*, **23**, 43-53 (1994).

Khatskevich, V. and D. Shoiykhet, *Differentiable Operators and Nonlinear Equations*, Birkhauser Verlag, Berlin (1994).

Koung, C.-W. and J.F. MacGregor, Geometric Stability of Linear Inverse-Based Controllers for Bivariate Nonlinear Processes, *Ind.Eng.Chem.* **30**, 1171-1181 (1991).

Koung, C.-W. and J.F. MacGregor, Robustness of Multivariable Linear Controllers to Process Nonlinearities, *Ind.Eng.Chem.* **31**, 1085-1096 (1992).

Kravaris, C. and J.C. Kantor, Geometric Methods for Nonlinear Process Control. 1. Background, *Ind.Eng.Chem.* **29**, 2295-2310 (1990a).

Kravaris, C. and J.C. Kantor, Geometric Methods for Nonlinear Process Control. 2. Controller Synthesis, *Ind.Eng.Chem.* **29**, 2310-2323 (1990b).

Kravaris, C. and C.-B. Chung, Nonlinear State Feedback Synthesis by Global Input/Output Linearization, *A.I.Ch.E.J.*, **33**(4), 592-603 (1987).

Krener, A.J., Approximation Linearization by State Feedback and Coordinate Change, *Syst. Cont. Lett.*, **5**, 181-185 (1984).

Krener, A.J., S. Karahan, M. Hubbard and R. Freeza, Higher Order Linear Approximation of Nonlinear Systems, *Proc. 26th Conf. Decis. Cont.*, Los Angeles, CA (1987).

Krener, A.J., S. Karahan and M. Hubbard, Approximate Normal Forms of Nonlinear Systems, *Proc. 27th Conf. Decis. Cont.*, Austin, Texas, 1223-1229 (1988).

Krener, A.J. and W. Kang, Extended Normal Forms of Quadratic Systems, *Proc. 29th Conf. Decis. Cont.*, Honolulu, Hawaii, 2091-2096 (1990).

Lang, S., *Differentiable Manifolds*, Springer-Verlag, New-York (1985).

Leontaritis, I.J. and S.A. Billings, Input-Output Parametric Models for Non-Linear Systems, *Int. J. Control* **41**, 303-344 (1985)

Ljung, L., *System Identification: Theory for the User*, Prentice-Hall, Inc., Englewood Cliffs, New Jersey (1987).

Maner, B.R., F.J. Doyle III, B.A. Ogunnaike and R.K. Pearson, Nonlinear Model Predictive Control Scheme Using Second Order Volterra Models, *in the Proc. of the American Control Conf.*, Baltimore MD (1994).

Manousiouthakis, V. and M. Nikolaou, Analysis of Decentralized Control Structures for Nonlinear Systems, *A. I. ChE J.*, **35**, 549-558 (1989a).

Martin, P., A Geometric Sufficient Condition for Flatness of Systems with m Inputs and m+1 States, in *Proc. 32nd Confer. Decision Control*, 3431-3436 (1993).

McLellan, P.J., T.J. Harris and D.W. Bacon, Error Trajectory Descriptions of Nonlinear Controller Designs, *Chem. Eng. Sci.* **45**, 3017-3034 (1990).

Mijares, G., C.D. Holland, R.C. McDaniel, C.R. Dollar and S.E. Gallun, Analysis and Evaluation of the Relative Gains for Nonlinear Systems, *Comput. Chem. Engng.*, **9**, 61-70 (1985).

Morari, M and E. Zafiriou, *Robust Process Control*, Prentice Hall, New Jersey (1989).

Nett, C.N. and V. Manousiouthakis, Euclidean Condition and Block Relative Gain Array: Connections, Conjectures and Clarifications, *IEEE Trans. Autom. Control*, AC-**32**, 405-407 (1987).

Newell, R.B. and P.L. Lee, Applied Process Control: A Case Study, Prentice-Hall of Australia Ltd (1989).

Nijmeijer, H. and A. J. Van der Schaft, *Nonlinear Dynamical Control Systems*, Springer-Verlag, New York (1990).

Nikolaou, M., When is Nonlinear Dynamic Modelling Necessary?, in *Proc.of the American Control Conf,*, San Francisco, CA (1993).

Nikolaou, M. and V. Manousiouthakis, A Hybrid Approach to Nonlinear System Stability and Performance, **35**(4), 559-572 (1983b).

Ogunnaike, B.A., R.K. Pearson and F.J. Doyle, III, Chemical Process Characterization: With Applications in the Rational Selection of Control Strategies, *in Proc. Europ. Cont.Conf.*, June 28-July 1, Groningen, The Netherlands 1067-1071 (1993).

Piette, R., T.J. Harris and P.J. McLellan, Graphical Interpretations of Steady State Interaction Measures, submitted to *Ind. Eng. Chem. Res.* (1995).

Rouchon, P., Necessary Condition and Genericity of Dynamic Feedback Linearization, *J. Math. Syst. Estim. Contr.*, **4**, 1-14 (1994).

Shadwick, W.F., Differential Systems and Linearization for Aircraft Flight Control, *Proc. 32nd Conf. Decis. Cont.*, Austin, Texas, 3420-3424 (1993).

Shadwick, W.F., Absolute Equivalence and Dynamic Feedback Linearization, *Systems Control Lett.*, **15**, 35-39 (1991).

Shadwick, W.F. and W.M. Sluis, Dynamic Feedback for Classical Geometries, *Contemp. Math.*, **170**, 207-213 (1994).

Skogestad, S. and M. Morari, Implications of Large RGA Elements on Control Performance, *Ind. Eng. Chem. Res.*, **26**, 2323-2330 (1988).

Skogestad, S., M. Morari and J.C. Doyle, Robust Control of Ill-Conditioned Plants: High-Purity Distillation, *IEEE Trans. Autom. Control*, AC-**33**, 1092-1105 (1988).

Sluis, W.M., A Necessary Condition for Dynamic Feedback Linearization, *Systems Control Lett.*, **21**, 277-283 (1993).

Stack, A.J. and F.J. Doyle III, A Measure for Control Relevant Nonlinearity, *Proc. 1995 ACC*, Seattle, WA (1995).

Tchòn, K., Towards Robustness and Geneicity of Dynamic Feedback Linearization, *J. Math. Syst. Estim. Cont.*, **4**, 165-180 (1994).

Willems, J., Paradigms and Puzzles in the Theory of Dynamical Systems, *IEEE Trans. Autom. Control*, AC-**36**, 259-294 (1991).

Willems, J., *The Analysis of Feedback Systems*, M.I.T. Press, Cambridge, Massachusetts (1971).

Zames, G., On the Input-Output Stability of Time-Varying Nonlinear Feedback Systems, Part I: Conditions Derived Using Concepts of Loop Gain, Conicity and Positivity, *IEEE Trans. Aut. Cont.*, **11**(3), 228-238 (1966a).

Zames, G., On the Input-Output Stability of Time-Varying Nonlinear Feedback Systems, Part I: Conditions Involving Circles in the Frequency Plane and Sector Nonlinearities, *IEEE Trans. Aut. Cont.*, **11**(3), 465-476 (1966b).

VITA

Name:	Martin Guay
Place and Year of Birth:	Lévis, Québec, Canada May 13, 1966
Education:	University of Ottawa, Canada, 1984-1990 B.A.Sc. (Chemical Engineering, Biotechnology Option, COOP) Thesis: "Sensitivity Analysis in Systems of Ordinary Differential Equations"
	University of Ottawa, Canada, 1990-1992 M.A.Sc. Chemical Engineering Thesis: "Multiresponse Model Building in Systems Described by Ordinary Differential Equations with Application to Batch Culture Kinetics"
	Queen's University, Canada, 1992-1996 Current program, Ph.D. (Chemical Engineering)
Experience:	Research Scientist, 1995-Current Dupont Canada Inc. Kingston Research and Development Centre Kingston, Ontario, Canada
	Teaching Assistant, 1992-1995 Department of Chemical Engineering Queen's University, Canada
	Substitute Professor, 1991 Department of Chemical Engineering University of Ottawa, Canada
	Teaching Assistant, 1990-1992 Department of Chemical Engineering University of Ottawa, Canada
	Research Assistant 1990-1992 Department of Chemical Engineering University of Ottawa, Canada

VITA

Publications:

Guay, M., P.J. McLellan and D.W. Bacon, "Measurement of Nonlinearity In Chemical Process Control Systems: The Steady-State Map", *Can. J. Chem. Eng.*, **73**, 868-882 (1995).

Guay. M., P.J. McLellan and D.W. Bacon, " On a measure of Closed-Loop Nonlinearity and Interaction for Nonlinear Chemical Processes", submitted for review to *A.I.Ch.E. J.* (1995).

Guay, M. "Curvature Measures for Multiresponse Regression Models", *Biometrika*, **84**, 411-417 (1995).

Guay, M. and D.D. McLean, "Optimization Strategies for Multiresponse Parameter Estimation in Systems Described by Ordinary Differential Equations", *Comput. Chem. Eng.*, **19**, 1271-1286 (1995).

Guay, M., P.J. McLellan and D.W. Bacon, "A Necessary and Sufficient Condition for Dynamic Feedback Linearization of Control-Affine Systems", submitted for review to *Int. J. Contr.* (1995).

Guay, M. and P.J. McLellan, "Input-Output Linearization of General Nonlinear Control Systems", *Proc. of the 1994 American Control Conference Baltimore MD* (1994).

Awards:

Fonds pour la formation de chercheurs et l'aide à la recherche (FCAR) B1 Scholarship, 1994-1995

Queen's University Dean's Award, 1992-1995

Natural sciences and engineering research council of Canada PGS B Scholarship, 1992-1994

Ontario Graduate Scholarship, 1991-1992

University of Ottawa Entrance Scholarship, 1991-1992

Science and Engineering Dean's List, 1986-1990
University of Ottawa, Canada